UNIVERSIDADE DE LISBOA

INSTITUTO SUPERIOR TÉCNICO

Thermal, daylighting and energy performance of glazing systems with solar control films

Júlia Oliveira Pereira

Supervisor: Doctor Maria da Glória de Almeida Gomes
Co-supervisor: Doctor Maria Manuela de Oliveira Guedes de Almeida
Co-supervisor: Doctor António Heleno Domingues Moret Rodrigues

Thesis approved in public session to obtain the PhD Degree in

Civil Engineering

Jury final classification: Pass with Distinction and Honour

2022

UNIVERSIDADE DE LISBOA
INSTITUTO SUPERIOR TÉCNICO

Thermal, daylighting and energy performance of glazing systems with solar control films

Júlia Oliveira Pereira

Supervisor: Doctor Maria da Glória de Almeida Gomes
Co-supervisor: Doctor Maria Manuela de Oliveira Guedes de Almeida
Co-supervisor: Doctor António Heleno Domingues Moret Rodrigues

Thesis approved in public session to obtain the PhD Degree in

Civil Engineering

Jury final classification: Pass with Distinction and Honour

Jury

Chairperson: Doctor Jorge Manuel Caliço Lopes de Brito, Instituto Superior Técnico, Universidade de Lisboa
Members of the Committee:

Doctor Vasco Manuel Araújo Peixoto de Freitas, Faculdade de Engenharia, Universidade do Porto
Doctor Carlos Augusto Santos Silva, Instituto Superior Técnico, Universidade de Lisboa
Doctor Luís Paulo Lomelino Gomes Fernandes, Lawrence Berkeley National Laboratory, EUA
Doctor Maria da Glória de Almeida Gomes, Instituto Superior Técnico, Universidade de Lisboa

Funding Institutions: Fundação para a Ciência e Tecnologia

2022

Ao Álvaro, à minha irmã Rita e aos meus Pais.

Abstract

Façades of recent buildings, especially the commercial ones, have been built with a high window-to-wall ratio window-to-wall ratio, such as curtain walls, double-skin façades and skylights. Despite the appealing design from the aesthetic standpoint and allowing pleasant daylighting levels, this architectural trend can nevertheless give rise to thermal and luminous indoor discomfort problems. Solar gains through glazing systems, especially in climates with long and hot summers, contribute significantly to cooling loads and lead to overheating of indoor spaces and/or glare problems, disrupting users' productivity.

This work's main objective was to evaluate the thermal, luminous and energy performance of glazing façades with solar control films (SCFs) through an experimental study conducted in situ and a building energy simulation approach using experimentally calibrated models. For this purpose, several office rooms were selected from two different buildings, which constitute the present doctoral thesis's case studies. The first building has clear single glazing on the windows' façade and the second one has double-glazing systems with a solar control coating incorporated. In both buildings, adjacent office rooms were selected to be monitored, where SCFs were installed on the glazing except in one office left with the original window without SCFs, which serves as a basis for comparison (reference office). The selection of several office rooms with identical geometry, constitution, solar orientation, and occupancy characteristics, with and without SCFs installed on the glazing, allows to assess the existing thermal and visual comfort conditions without SCFs and to perform a comparative analysis of the effects of the SCFs application on the indoor conditions.

The experimental field data was also used to calibrate the geometrical models of the office rooms of both of the buildings in a well-established building energy simulation program (EnergyPlus) to perform a more comprehensive and thorough study on the impact of the window films' application in existing windows of office spaces.

An environmental and economic study was also performed for the three SCFs that showed the highest thermal, visual and/or energy performance. This study considered the application of the films as a retrofitting scenario of the existing glazing systems of the second building used as case study. The complete replacement of the existing windows with a new one was also analysed as an alternative scenario.

Finally, a parametric analysis was performed to evaluate the thermal, visual and energy performance and the global performance of a typical second case study building office for different solar orientations, types of glazing, climate, and glazing area on the façade.

KEY-WORDS: Window retrofitting; Solar control films; Visual performance; Thermal performance; Energy efficiency; Office buildings; *In-situ* measurements; Energy simulation.

Resumo

A utilização do vidro na construção tem tido uma expressão cada vez mais significativa, resultando em rácios de envidraçado na fachada muito elevados, especialmente em edifícios não residenciais. Esta tendência deve-se às boas características estéticas e óticas do vidro, que permitem a entrada de luz natural e visão para o exterior, podendo contribuir para poupanças de energia com iluminação. No entanto, os ganhos solares pelos envidraçados, especialmente em climas com verões quentes e prolongados, contribuem de forma significativa para as cargas térmicas de arrefecimento e podem originar problemas de sobreaquecimento e/ou encandeamento, perturbando o conforto e produtividade dos utilizadores.

O objetivo principal deste trabalho consistiu no desenvolvimento de campanhas experimentais *in-situ* e de modelos para simulação energética de edifícios, que permitem avaliar o desempenho térmico, lumínico e energético de envidraçados de fachadas com películas de controlo solar (PCS). Para tal, foram selecionados gabinetes de escritórios em dois edifícios, tomados como casos de estudo da presente tese, onde a janela da fachada de um dos edifícios é constituída por um envidraçado simples incolor e o segundo por um envidraçado duplo com película de proteção térmica incorporada. Em ambos os edifícios foram selecionados gabinetes adjacentes para monitorização experimental de diversas variáveis que permitem a análise do desempenho térmico e lumínico e onde um deles permaneceu sem PCS (gabinete de referência) e nos restantes gabinetes foram instaladas PCS. A seleção de diversos gabinetes com características de geometria, constituição, orientação solar e ocupação idênticas, com e sem PCS instaladas no envidraçado da fachada permite uma análise das condições existentes do conforto térmico e visual e uma análise comparativa do efeito da aplicação de PCS. Para além disso, os dados recolhidos nas campanhas experimentais permitem calibrar modelos de simulação dinâmica dos escritórios através de um programa de simulação energética de edifícios (EnergyPlus), com o objetivo de realizar um estudo mais abrangente e completo sobre o efeito da aplicação de diversas PCS em janelas existentes de escritórios.

Para além disso, foi analisado o desempenho ambiental e económico de três PCS diferentes que apresentaram o melhor desempenho na análise de simulação energética do ponto de vista térmico, lumínico e energético. Este estudo foi realizado considerando a aplicação destas PCS como um possível cenário de reabilitação na totalidade dos envidraçados do segundo edifício caso de estudo da presente tese. A mesma análise ambiental e económica foi também efetuada para um cenário de não reabilitação, mas de substituição total dos envidraçados existentes por um novo envidraçado com melhor desempenho térmico e lumínico.

Por fim, foi realizado um estudo paramétrico onde se avaliou o desempenho térmico, visual e energético, e o desempenho global, de um gabinete típico do segundo edifício caso de estudo para diferentes orientações solares, tipo de envidraçado, clima e área de envidraçado na fachada.

PALAVRAS-CHAVE: Reabilitação de envidraçados; Película de controlo solar; Conforto visual; Conforto térmico; Eficiência energética; Edifícios não residenciais; Medição in-situ; Simulação energética.

Acknowledgements

The author would like to thank all of those who somehow contributed to the execution of this thesis, namely:

Department of Civil Engineering (DECivil) - CERIS Research Institute -, Instituto Superior Técnico, Universidade de Lisboa, for providing the necessary resources to develop the work performed in the thesis.

To office occupants and the facility and logistics team of Instituto Superior Técnico and European Maritime Safety Agency, for providing the space and conditions for the installation of the experimental equipment and their patience and understanding.

To my colleagues MSc students *Ricardo Coelho*, *Duarte Oliveira*, and *David Lourenço* for their supporting in assembling the experimental equipment and in collecting the experimental data throughout the different periods of each experimental campaign.

To IMPERSOL company, in the name of *Guilherme Vendeirinho* and *Carlos Miguel*, for the technical support and for the assistance with the application of the films. Thank you for the patience in debating the various challenges that this work presented and for embracing new ideas with your good energy.

To the colleagues that became dearest friends, *Vera Durão*, *Ana Ferreira*, *André Quinhones*, and *Henriqueta Teixeira*. Thank you for your support and encouragement in these last four years.

A special thanks to Alexandra Baixo, for her company, support, and advice.

I would also like to thank and acknowledge the role of my supervisors, Profs. *Maria da Glória Gomes*, *António Moret Rodrigues* and *Manuela Almeida*, in my professional and personal development. Thank you for your guidance, support, and advice throughout my PhD research studies. It was a privilege to work and learn from your exceptional scientific knowledge, work ethics, and human qualities. It was four full years of hard work, dedication, and commitment. I learned a lot!

Last but not least, my deepest thanks to my family, for their support and understanding.

The author wishes to acknowledge the support of the FCT (Foundation for Science and Technology) PhD Grant FCT PD/BD/127848/2016 which has made this research possible.

Index

List of Figures

List of Tables

Acronyms

Abbreviations

ACCD	Andalusia Construction Cost Database
BES	Building energy simulation
C	Cooling
CED	Cumulative Energy Demand
CF	Carbon Footprint
CIE	Commission International de l'Eclairage
COP	Coefficient of performance
DF	Daylight Factor
DGI	Daylight Glare Index
DWC	Days without occupancy
D-HOT	Day with the Highest daily average Outdoor Temperature
D-LOT	Day with the Lowest daily average Outdoor Temperature
D-SS	Day with the highest sun's elevation angle – as close as possible to the Summer Solstice
D-WS	Day with the lowest sun's elevation angle – as close as possible to the Winter Solstice
EC	Economic Costs
EE	Embodied Energy
EER	Energy efficiency ratio
EU	European Union
FOV	Field of View
GHG	Greenhouse Gas
H	Heating
HVAC	Heating, ventilation, and air conditioning
IEA	International Energy Agency
IGDB	International Glazing Database
IPCC	Intergovernmental Panel on Climate Change
L	Lighting
LCA	Life Cycle Assessment
LCE	Life Cycle Energy
LCI	Life cycle inventory
LPD	Lighting Power Density
LSG	Light-to-solar gain ratio
MBE	Mean Bias Error
MDF	Medium Density Fiberboards
NU	Not Useful
NW	New window
ODH	Overheating or overcooling degree days
OE	Operational energy
PNEC	National Energy and Climate Plan (Plano Nacional de Energia e Clima)
PVB	Polyvinyl Butyral
PET	Polyethylene Terephthalate
PMMA	Polymethyl Methacrylate
RNC	Roadmap to Carbon Neutrality
SC	Shading coefficient

SCF	Solar Control Films
SGG	Saint Gobain Glass
TST	True Solar Time
U	Useful
UDI	Useful Daylight Illuminance
UV	Ultraviolet
VB	Venetian Blind
WWR	Window-to-Wall Ratios

Latin capital letters

C_e	Current value of the electricity cost for domestic consumers
$C_{v.RMSE}$	Coefficient of variation of the Root-Mean Square Error
Csa	Hot-summer Mediterranean climate, according to Köppen climate classification
Csb	Warm-summer Mediterranean climate, according to Köppen climate classification
$E_{ind,hor}$	Indoor horizontal illuminance
$E_{ind,vert}$	Indoor vertical illuminance
E_{mat}	Primary energy consumption of manufacture of the material
E_{trans}	Primary energy consumption of transport of the material
$E_{out,vert}$	Outdoor vertical illuminance
EC_{ini}	Initial cost with production and construction works of the retrofitting solution
EE_M	Embodied energy during the Product and Construction stages
EN_{cool}	Energy needs with cooling
EN_{heat}	Energy needs with heating
EN_{light}	Energy needs with lighting
$Glob_{solar}$	Global solar radiation on horizontal plane
I_{ind}	Indoor irradiance
$I_{ind,vert}$	Indoor vertical irradiance
I_{OE}	Conversion factor from electricity to carbon emissions in Portugal
I_{out}	Outdoor Irradiance
$I_{out,vert}$	Outdoor vertical irradiance
IS_i	Aggregated indicator for the i façade scenario
M	Mass of the constitutive materials
N	Life cycle period
N_{MBE}	Normalized Mean Bias Error
P_{EF}	Primary energy factor of electricity generation
R	Periodicity of the retrofitting scenario
R_a	General colour rendering index
R_{ij}	Simulation result of façade scenario i^{th} when is evaluated according to the j^{th} indicator
$\overline{R}_{ij}$	Normalised value of the j indicator for the façade scenario i^{th} when is evaluated according to the j^{th} indicator
R_j^*	Optimum value of the j^{th} indicator of performance (ideal value)
R_{*j}	Worst value achieved by the j^{th} indicator of performance (anti-ideal value)
$T_{i.exp}$	Experimental values of the indoor air temperature
$T_{i.sim}$	Simulated values of the indoor air temperature
T_{out}	Outdoor air temperature

U	Thermal Transmittance
W_j	Weight or relative importance of the performance indicator j

Latin lowercase letters

g	Solar Factor
low-e	Low emissive double glass
m	Total number of performance indicators j for the façade scenario i
n	Total number of façade scenarios

Greek lowercase letters

α	Discount rate based on a 10year government treasury yield
α_e	Solar absorptance
α'	Harmonized index of consumer prices
α_1	Absorptance of (front) pane
ε	Emissivity
ε_i	internal emissivity
ρ_e	Solar reflectance
$\rho_{b,vis}$	Visible (back) reflectance
$\rho_{f,sol}$	Solar (front) reflectance
$\rho_{f,vis}$	Visible (front) reflectance
$\rho_{v,e}$	Exterior visible light reflectance
$\rho_{v,i}$	Interior visible light reflectance
τ_e	Solar transmittance
τ_{sol}	Solar transmittance
τ_{vis}	Visible Light Transmittance
τ_{vis}	Visible transmittance

1. Introduction

1.1 Framework and motivation

Scientific evidence for rapid climate change resulting from human activities is unequivocal [1]. The increase of human-made emissions is very likely the primary driver for the global warming trend in the past decades. As a fact, the sixth warmest years on record occurred from 2014 onward (Figure 1).

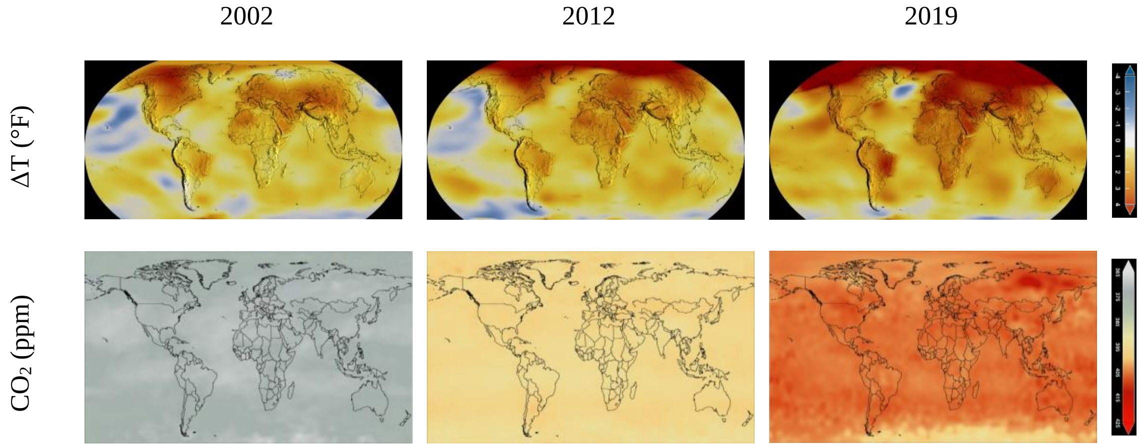

Figure 1. Progression of global surface temperature (dark blue and red indicate areas cooler and warmer than average, respectively) and concentration of CO_2 emissions at an altitude range of 3 to 12.87 km (red-to-yellow and green-to-blue areas indicate higher and lower concentrations of CO_2, respectively). Adapted from [2]

The Sixth Assessment Report (AR6) of the Intergovernmental Panel on Climate Change (IPCC) [1] establishes that global temperature has increased, oceans have warmed, glaciers are retreating, extreme weather events are getting more intense, and global sea level is rising. The concentration of CO_2 in the atmosphere is the highest of the last two million years, and the planet is 1.1ºC warmer than before the industrial revolution. This latest report outlines five scenarios to understand future planet conditions, ranging from a world where climate policy is rolled back to a world where very ambitious actions take place in the 2020s. The five possible future scenarios show that the next decades will be warmer than today; however, future actions to reduce CO_2 emissions will dictate different outcomes for the planet's living conditions by mid-century. If CO_2 emissions are reduced to net zero and the global temperature does not increase over 1.5ºC, global warming can be stabilized.

Several efforts have been made to tackle climate change and mitigate and adapt to its impacts over the last years. The Paris agreement established in the 21st Conference of Parties targets net-zero emissions by 2050 [3]. This agreement that includes more than 60 countries, further stipulates that all Parties are invited to submit their long-term development strategy by 2020, aiming to accelerate and intensify actions on a global scale to reduce greenhouse gas (GHG) emissions, and for that, it defines three comprehensive objectives:

- limit average global warming to below 2ºC since pre-industrial levels and encourage efforts to limit the average global temperature increase to 1.5 °C;
- increase the aptitude to adapt to the adverse impacts of climate change, increasing climate resilience and low carbon development;
- and align financial flows to be consistent with a more resilient and low carbon development path.

In the 2010s, GHG emissions on the planet were around 50 billion tonnes of carbon dioxide equivalent per year, and almost three-quarters come from energy use, around one-fifth from agriculture and land use, and the remaining 8% from industry and waste [1], [4], [5]. Identifying the most pollutant sectors is essential to reduce GHG emissions effectively. In 2016 in Portugal, 30% of the GHG emissions were mainly related to electricity and heat, manufacturing & construction energy, and buildings (Figure 2).

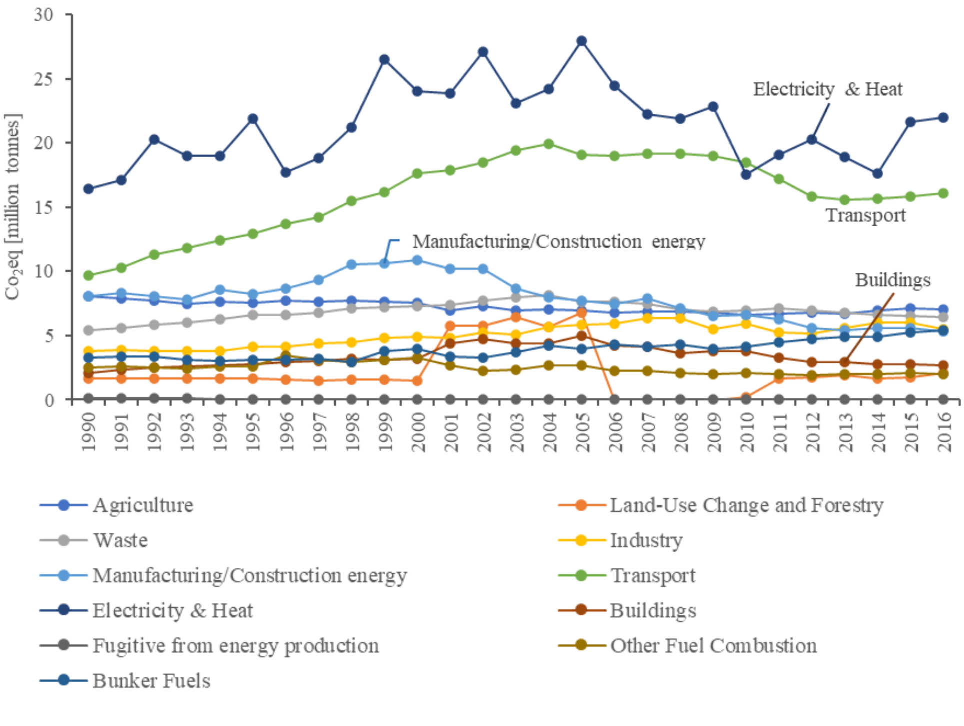

Figure 2. GHG emissions by sector in Portugal, in million tonnes of carbon dioxide equivalent, CO_2eq, from 1990 to 2016 [6]

With the global population growth trend, the increasing demand for higher standardized comfort levels, and the rise of active systems in buildings, a potential rise in total energy demand is expected [7]. These circumstances make the building sector a potential target to implement energy efficiency measures and to increase environmental sustainability on a global scale.

In the European Union (EU), Member States are being pushed by European directives to promote energy retrofit and decarbonize their building stock, disrupting the construction sector paradigm of the last decades [4-6]. This net-zero pathway reinforces the EU commitment with the Paris agreement in developing a more sustainable, competitive, secure, and decarbonized energy system by 2050.

In regards to the energy consumption of the building stock, the heating and cooling energy needs are highly related to the age of the building. The International Energy Agency (IEA) stated in their Energy Technology Perspectives 2020 report [7] that buildings prior to 1960 may require three times more heat loads than those constructed under current thermal regulations. In fact, while new buildings have improved their energy performance over time due to higher demanding regulations for thermal comfort levels (reports indicate an increase of energy efficiency and a reduction of energy needs of 20% globally and 30% in the USA and EU since 2000 [10]), older buildings still represent the vast majority of the building stock (Figure 3). In this context, and as part of a much-needed long-term national policy to enhance the market growth in the rehabilitation works' sector, there is a pivotal opportunity to create policies that decarbonize the building sector and promote nearly zero energy of new and existing buildings.

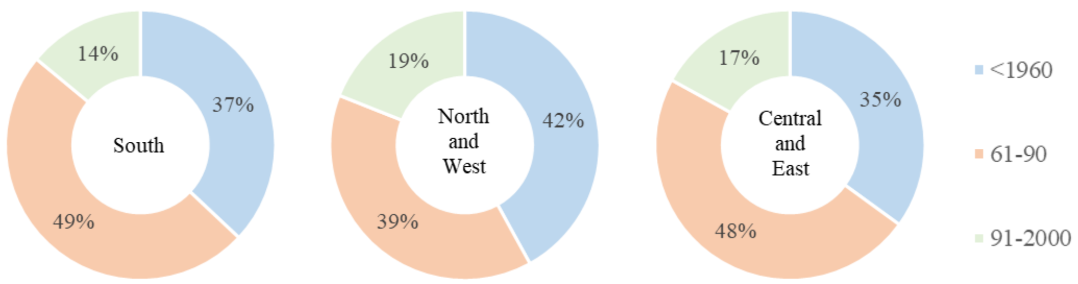

Figure 3. Age categorization of the residential building stock in Europe [11]

The European Directive of the European Parliament and of the Council of 2018/844 of 30 May 2018 [9] establish milestones for short (2030), medium (2040), and long (2050) terms through policies and investment decisions at a national level to decarbonize the energy supply and to reduce the final energy consumption. These ambitious and broad goals are very much linked to the rehabilitation and refurbishment of existing buildings, since almost 50% of the final energy consumption within the EU is related to heating and cooling, of which 80% is consumed in buildings (around 3 100 Mtoe [7]). When considering both the construction and operational use phases of the building, the sector's direct and indirect CO_2 emissions account for 9.8 $GtCO_2$ globally [7]. Materials' manufacture and construction buildings add more than 3.5 $GtCO_2$ of energy [7].

In order to support effective policies for the transition towards more energy-efficient buildings and to monitor whether new regulations for new and existing buildings are meeting the established goals of the EU, Portugal has developed a comprehensive plan for the long-term renovation of its national building stock (PNEC) [12], [13]. From the set of challenges that affect the energy performance of national buildings, besides natural ageing of materials and lack of maintenance, PNEC highlights the low thermal performance of building envelopes (inadequate thermal insulation of walls/roof and low energy-efficient windows) and the use of energy inefficient active systems. In fact, a considerable share of the national building stock precedes the first thermal regulation – about 70% [14] – creating a key opportunity to promote overall energy efficiency and decarbonize the building sector.

In what concerns the rehabilitation of the building envelope, windows are within the primary building elements to merit attention as regards the implementation of energy retrofitting measures due to the higher heat exchange between indoor and outdoor environments, when compared to the other components in the building envelope, and whose impact is proportional to the area they occupy in façades. Office buildings represent a case where thermal and visual comfort problems are more acute since the glazing areas are more significant in the façades than the opaque ones.

1.2 Objectives and methodology

This thesis presents a contribution to enlarge the knowledge of the thermal, daylight, and energy performance of solar control films (SCFs) as a retrofitting solution for glazing areas of existing buildings to enhance its energy efficiency and contribute to decarbonizing the building sector. In this context, this research aims to support decision-making for retrofitting existing windows through dynamic simulation with an added contribution of experimental analysis from *in-situ* field monitoring.

The methodology followed was based on a combined experimental and modelling analysis that focused specifically on two case study buildings located in Lisbon, capital of Portugal, one with single and the other with double-glazed windows. Both buildings were selected due to their large areas of glazing in the façade, poor thermal and visual performance, and high energy demand in the office areas.

The experimental field analysis involved monitoring and comparing data collected through extensive *in-situ* experimental campaigns using small-scale modelling and actual full-scale office spaces with similar characteristics (geometry, materials, solar exposition and orientation, and internal gains). In the two case study buildings of the present thesis, office rooms with and without solar control films were monitored during the summer and winter seasons. The objectives of this experimental analysis are:

- to assess the existing conditions of the office rooms without SCF – temperature, illuminance, and irradiance on the working plane area – and the share of the offices' thermal and visual comfort and energy demand attributed to the window systems. This is an introductory study that also helps identifying the film and its thermal and optical properties that could better improve the indoor comfort conditions and decrease the energy demand;
- to compare the thermal and visual differences and comfort characteristics of similar office rooms in actual occupancy conditions without and with SCFs under the existing windows' scenario;
- to calibrate a geometrical model of the office rooms in a well-established building energy simulation program (EnergyPlus) to perform a more comprehensive and thorough study on the impact of the window films' application in existing windows of office spaces.

Although it is time-consuming, model calibration is the most significant step when designing models in simulation programs that represent real case study rooms or buildings. The calibration process helps improving the agreement between the models' output and the actual conditions and thus is an important step for the purpose of predicting the building's performance for different retrofitting scenarios with an admissible and measurable accuracy. The calibration process developed in this thesis was conducted by comparing the predicted values of indoor temperature and other variables obtained through EnergyPlus with the ones obtained experimentally. With the calibrated models established, it was possible to estimate the energy performance and calculate comfort indexes based on an annual performance for different SCFs, solar orientation, and climate conditions.

The main aspects that contributed to the definition of this research study were the following:

- interest on the topics of thermal and visual comfort, energy efficiency and sustainability in the context of building rehabilitation;
- lack of consistent information regarding the thermal and visual performance of existing films for building rehabilitation and the corresponding optical and thermal properties of different glass substrates without and with films;
- address the gap in knowledge concerning the variation in energy needs between glazing systems without and with films, in the Portuguese context, characterized by the predominance of clear sky conditions;
- contribute to energy efficiency and sustainability in the building sector by predicting energy savings related to indoor temperature and lighting comfort levels in scenarios pre and post-rehabilitation of glazing systems with films;
- interest in developing experimental procedures to evaluate indoor spaces' thermal and visual performance and design energy simulation models that forecast energy performance of buildings.

1.3 Research questions

The specific research questions addressed by the present thesis are the following:

- Is there reliable information available for decision-makers and building professionals regarding the retrofit potential of SCFs (differences in type and application, and advantages and disadvantages)?

The decision of the films' selection often depends on the knowledge and experience of distributors and/or installers, which can be insufficient from a comfort standard or energy efficiency point of view. Taking into account the long-term goals related to sustainability and decarbonization in the construction sector and the wide spectrum of available retrofitting solutions for building envelopes, there is a need to develop available and useful information to support building professionals in the decision-making process for retrofitting of existing buildings.

- How do SCFs influence glass's thermal and optical properties in a window system?

Nowadays, there is a wide range of window films for retrofitting purposes with applications on both internal and external surfaces in glazed areas of buildings façades, appropriate for cold and hot climates. One of the most significant aspects of considering SCFs for rehabilitation purposes is assessing variations in the thermal and optical properties of existing glazing.

The optical properties of the individual films are not straightforward to assess through experimental or numerical analysis. Due to the films' composition and thickness, the optical properties can only be measured using a glass sample as a substrate, and then calculations and assumptions/simplifications must be performed to assess the individual properties of the films. This fact directly affects the scarce information concerning SCFs as an individual material.

The complete technical sheets of SCFs usually provide thermal and optical properties for single and double glazing without and with SCF for specific glass's thickness. This information allows for comparing the properties without and with SCFs when applied on generic glazing. Though this information may be beneficial, it falls short when considering the full range of different glazing currently manufactured and placed in existing buildings.

- How do Solar Control Films (SCF) influence the thermal and visual conditions and the energy performance of existing office buildings?

SCFs have gained popularity in commercial buildings as an effective means of lowering building energy costs by reducing excessive solar heat gain through windows while improving people's comfort. For comfort and energy efficiency purposes, it is essential to balance the daylight availability and the solar heat gains and losses throughout summer and winter. This balance can be very complex to achieve since it is dependent on many variables such as type of window, % of the glazed area in the façade, solar orientation, climate region, etc. For example, in Mediterranean climates, where most of the regions are characterized by relatively mild winters and very warm summers, it is critical to evaluate if the solar heat gain reduction due to the films' application is adequate to significantly decrease the cooling loads in the summer without increasing the heating loads substantially in the winter. Besides, in most situations, the application of the film reduces the daylight availability, and if the film is not correctly selected, it can increase the use of electric lighting and thus increase the energy consumption of the building.

- What are the environmental and economic impacts of this retrofitting solution?

The nearly zero-energy buildings defined in recent EU directives, as being high energy performance buildings with the low amount of energy demand being satisfied by renewable sources, are one of the long-term goals for the decarbonization of the buildings sector. Energy-saving policies and programs formulated for buildings at the national and international levels generally address the topics of energy efficiency and renewable energy sources during the operational stage of a building. The main reason for this relates to the fact that operational energy is the dominant energy share of the building's life cycle energy demand due to the long service life inherent in the structures. The operational energy typically accounts for the vast majority of a building's life cycle energy and GHG emissions, thereby offering significant energy and cost-saving potential. Nonetheless, as an intrinsic part of sustainable development of any country, energy-saving and efficiency of energy use should not be only focused on building's service life but regarded in a broader perspective by considering the entire life cycle of the construction. In this perspective, when studying a new material such as SCFs, not only the energy savings during the operational stage shall be accounted for but also the total energy required for the extraction, processing, manufacturing, and operation in buildings.

1.4 Outline of thesis

This thesis is structured in eight chapters and four appendixes.

Chapter 1 (current chapter) – *Introduction* – establishes the framework of the studies' field, presenting the motivation and objectives, specific research questions, methodology used, and the output contributions of the thesis.

Chapter 2 – *Glazing systems and solar control films: comfort, energy efficiency and sustainability* – presents an overview of the topics considered and a comprehensive state-of-the-art review concerning solar control films as a material and retrofitting measure for existing glazing systems.

Chapter 3 – *Experimental analysis of daylighting availability* – presents the methodology and the results obtained from a field experiment in a small-scale model to assess the influence of different SCFs on the indoor daylight illuminance levels and their spatial distribution on the horizontal plane (at work plane height) when applied on single glass. The experiment was performed with the glazing oriented to the South, in Lisbon, under clear sky conditions, during summer and winter solstices, and under overcast sky conditions.

Chapter 4 – *Performance of solar control films in single-glazed windows* – and Chapter 5 – *Performance of solar control films in double-glazed windows* – present the thermal, daylighting, and energy performance of office spaces that show thermal and/or visual discomfort conditions. Both these chapters investigate the thermal and luminous performance of windows of existing office rooms experimentally, without and with solar control films (SCFs), and use the experimental data to calibrate building simulation models and assess the energy performance of several SCFs with different thermal and optical characteristics. The main difference between the two chapters is based on the type of windows installed in the façade, Chapter 4 addressing clear single-glazed units and Chapter 5 double-glazed units with a solar coating.

Chapter 6 – *Energy, environmental, and economic analysis of windows' retrofit with solar control films* – examines through an energy, environmental, and economic standpoints over a defined life cycle period the impact of installing three different SCFs on the existing windows of a building. The complete replacement of the existing window with a new one is also analysed as an alternative retrofitting solution.

Chapter 7 – Thermal, daylighting and energy performance of glazing with SCFs – aggregated performance indicators – develops a parametric analysis to evaluate the performance of single and double glazing units of office rooms without and with two high-performing solar control films for different façade conditions and different locations on the mainland Portugal. This chapter consolidates and unifies the information of experimental and numerical conclusions of the previous chapters

Chapter 8 – *Conclusions and future work* – describes an overall conclusion of the work developed in the present thesis and describes possible lines of investigation for future research.

2. Glazing Systems and Solar Control Films: comfort, energy efficiency and sustainability

The topic of energy efficiency in buildings has been the centre of a broad technical and scientific discussion in recent years in what concerns decarbonization or carbon neutrality in the building sector. In that sense, several innovative materials for opaque and transparent components with application in the buildings' enclosure, high-performance lighting systems, and more efficient heating and cooling systems that maximize energy savings have been investigated and developed in the last decades.

Glazing systems are one of the most significant components concerning thermal and visual comfort and energy efficiency in buildings. The relevance of energy rehabilitation of existing buildings significantly impacts a country at several levels in both the final energy demand and GHG emissions. In this regard, research and development in glazing systems have experienced a rapid evolution with several innovative breakthroughs, such as laminated glass panes in the 1920s and coated products in the 1970s. Since then, the traditional clear single glass window has changed from single pane to low thermal transmittance and then to low-emissivity windows, vacuum glazing, electrochromic windows, thermotropic materials, silica aerogels, and transparent insulation materials. The development of transparent selective coatings and films provides a wide range of optical properties for glazing surfaces, allowing high daylight levels while preventing excessive heat gains throughout the glazing. In a report study, Bakker and Visser [15] demonstrated that a greater use of high-performance glazing systems with solar control coatings in residential buildings in EU countries could prevent up to 80 million tons of CO_2 emissions annually.

In Mediterranean climate regions, the problem of the high levels of energy consumption through glazing surfaces in building envelopes can be more acute, considering that the difficulties are not only related to the heat losses but also to the excessive passage of solar and visible radiation. Glare and overheating risks of the occupied spaces are more likely to occur and, as a result, the operational energy consumption to maintain the required comfort levels throughout both heating and cooling seasons can increase (air conditioning loads are as significant as the heating loads). Also, when considering the transparent components of the building's enclosure as opposed to the opaque ones, not only the mean thermal transmittance needs to be considered to assess the heat exchanges between the indoor and outdoor environments but also the solar and visible transmittance coefficients to evaluate the daylight availability and estimate the energy demand associated with artificial lighting loads.

Portugal's construction sector has evolved at different rates throughout the last decades. From the existing building stock, two-thirds were built prior to the first decree-law for energy efficiency requirements of new buildings in 1990 [16] – Decree-Law 40/90 of 2 June, meanwhile revoked. In the period between 2010 to 2014 – probably the most challenging due to stalled economic growth and extreme austerity measures that limited the access to public and private investments in the construction sector – rehabilitation works increased at a rate that was almost inversely proportional to that of new construction works (Figure 4a). Since then, with the economic recovery, rehabilitation works have decreased their pace and currently represent 24.4% of the total finished buildings in Portugal (approximately 6700 buildings), of which 28% was in the non-residential buildings (Figure 4b). While new buildings have improved their energy performance over time due to higher demanding regulations for thermal comfort levels, older buildings represent the vast majority of the building stock. In this context, and as part of a much-needed long-term national policy to enhance the market growth in the rehabilitation works' sector, there is a key opportunity to promote nearly zero-energy buildings.

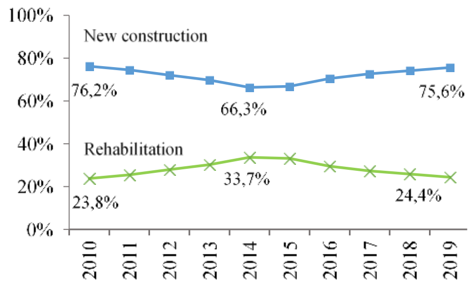

a.

b.

Figure 4. a. Share of new construction works and building rehabilitation in Portugal [16]; b. Rehabilitation by type of building (residential and non-residential in Portugal) [16]

Globally, a substantial share of the existing building stock is very likely to still be in use in 2050 as the average lifetime of modern residential construction and commercial buildings vary between 70-100 years and 30-50 years, respectively, and historic buildings can last more than 150 years.

For Portugal to achieve the energy and climate objectives proposed in the national energy and climate plan 2021-2030 (PNEC 2030) [17] and the roadmap to carbon neutrality (RNC2050) [18], it is essential to renew the energy efficiency of the existing building stock deeply. The rehabilitation of existing buildings brings multiple benefits at national and individual levels: reduction of energy consumption and therefore energy dependency and energy poverty, improvement of thermal comfort and indoor air quality and therefore labour productivity. These are strong arguments for investing in the rehabilitation of existing buildings [19]. Thus, prioritizing energy efficiency and promoting energy from renewable sources assumes particular relevance and priority.

In that respect, the Long-Term Strategy for the Renovation of Buildings in Portugal [12] provides an effective response to renovate the entire national buildings stock, establishing indicative goals for the horizons of 2030s, 2040s and 2050s, compared to the 2018 records:

- renovate the built area in the proportion of 363 680 501 m^2 until 2030, 635 637 685 m^2 until 2040 and 747 953 071 m^2 until 2050;
- increase by 11%, 27%, and 34%, the primary energy savings by 2030, 2040, and 2050, respectively;
- decrease the discomfort hours in buildings by 26%, 34%, and 56% by 2030, 2040, and 2050, respectively.

By means of theoretical and experimental work, the present thesis explores the use of SCFs as a rehabilitation material for existing buildings to enhance thermal and visual indoor comfort and increase energy efficiency and environmental sustainability in alignment with international and national goals to reduce GHG emissions. The following sections 2.1 and 2.2 describe the theoretical information concerning different glazing as a substrate for the application of window films (section 2.1) and rehabilitation material (section 2.2). The information and developed topics of the following sections are essential and relevant for the developed work throughout the present thesis.

2.1 Glazing System

Glass is manufactured from the fusion of inorganic substances, usually silica and metal oxides. Soda-lime silicate glasses, usually used in the construction industry, are made from a vitrified compound (silica) used in the form of sand, soda in the form of carbonate and sulphate, which acts as a melting compound, a drying agent (calcium oxide) in the form of limestone, and other metal oxides. The coloured features of tinted glass derives from this mixture, which improves the physical properties of glass, in particular its resistance to atmospheric agents.

The glass made for glazing is usually manufactured using the *float process.* This manufacturing process allows to obtain clear glasses with great optical quality (insignificant optical distortion) and perfectly flat surfaces. After being manufactured, glass may have heat treatment, generating tempered glass. In case of breakage, this heat treatment confers greater mechanical resistance, increasing the protection against injuries as glass breaks up into small non-cutting pieces. There are also laminated types of glazed glass, consisting of at least two glass panes fixed together by one or more polyvinyl butyral (PVB) films, which offer safety in case of impact since most shards remain adhered to the film, reducing the risks of injury. The level of safety of laminated glass varies according to the thickness and/or number of glass panes and lamination films.

Currently, there is a great variety of glass available on the market tailored to adapt to the different types of buildings and glazed façades to satisfy the desired functions of the glazed glass. The cost, configuration, thermal and optical properties vary depending on the type of glass. Amongst all the thermal and optical properties, the *Visible Light Transmittance* (τ_v) and the *Solar Factor* (g) properties, referred to in the European standards [20], [21], are highlighted as being the main properties of a glazed pane. In turn, the *Thermal Transmittance* (U) is also considered an important property because it represents the greater or lesser ease of the heat flows through the glazing. The selection of the most suitable glass to be employed depends on the properties mentioned above, which are essential for optimizing and sizing the glazed frame.

In the scope of the current study, the most common and significant types of existing glass are:

- clear or float glass: glass with high transmittance with both flat and parallel surfaces. It is the most common type of glass from which the other types of glass are manufactured;
- tinted glass: in this case, colour is added to the glass during the manufacturing process, which confers solar control properties by the absorption effect. This type of glass can be applied for aesthetics, privacy, or solar control purposes;
- reflective glass: glass resulting from the deposition of thin metal coats on a clear glass, which confers to the glass solar control properties by the reflection effect. This type of glass is recommended for glazed windows and façades with intense sun exposure;
- spectrally selective glass: glass with a deposited solar control coat that significantly reduces, by reflection or absorption, the solar gains of the thermal radiation while allowing high visible radiation transmittance levels;
- low emissivity: glass with a high thermal performance due to the deposition of a thin and transparent coat made of metallic materials on the glass that reduces its emissivity. It reflects the

long-wavelength infrared radiation, reducing thermal losses and gains by radiation through the glazed glass.

As a result of the combination of different types of glass mentioned above, with specific thicknesses and properties, it is possible to create multiple types of glazing suitable for different applications. Figure 5 shows the most common types of glazing for consideration as representative solutions for windows: single glazing, double glazing, and multilayer glazing. Single glazing has the lowest thermal performance but exhibits the highest visible and solar radiation transmission values. This characteristic, if manifestly excessive can cause visual discomfort to the occupants compared with other types of glass. Double glazed glasses with two glass panes and a gas filling chamber present not only a better thermal performance, namely the low emissive double glazing, but also a lower visible and solar transmission. Multilayer glasses consist of multiple glass panes and glass filling chambers that strongly impact the thermal and optical properties by increasing the thermal performance but at the expense of the luminous performance.

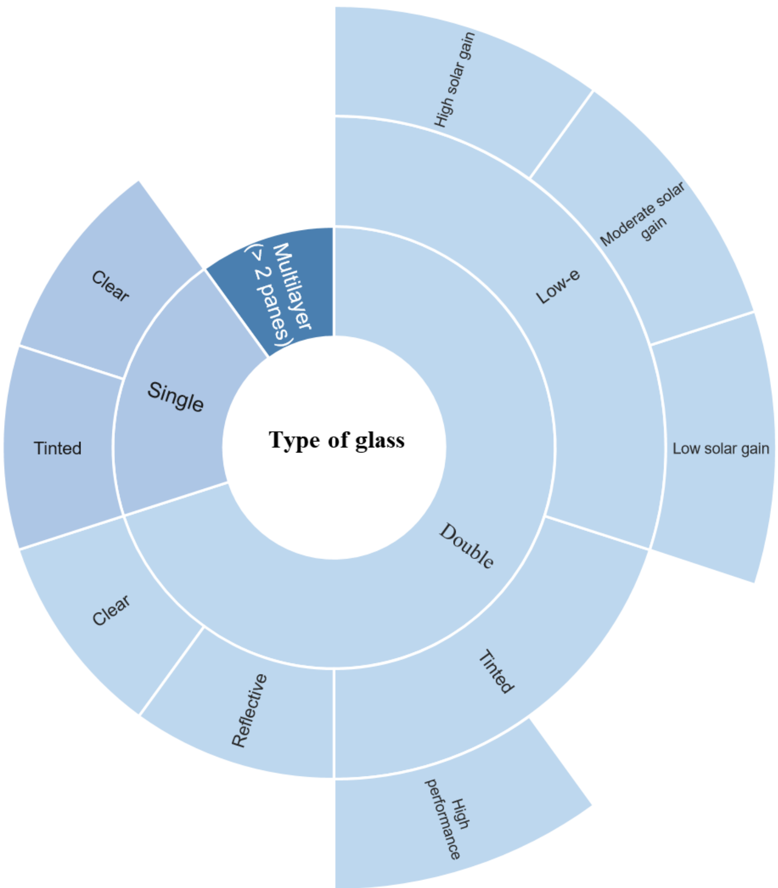

Figure 5. Types of glass for consideration as representative solutions for windows [20], [21]

The various types of glazing shown in Figure 5 and their main properties *(U, g,* τ_v) can be observed in Figure 6 to Figure 9. Moreover, the values of the properties shown in these figures correspond to average values of similar glazing from different manufacturers [22], [23]. It is also important to note that these values are only accurate for the centre of the glass and not for the total glazing area, as they depend on the glazed configuration and the materials and structure of the frame. Therefore, it is only possible to compare types of glazing and not windows.

Compared with other glasses, the *clear single glass* (Figure 6a) provides greater thermal energy and visible transmittance, ensuring greater solar gains and/or losses and greater availability of natural light.

Adding colour to the single glass manufacturing process leads to *tinted single glass* (Figure 6b), reducing its visible light transmittance (τ_v) value and the solar energy factor (*g)*, but does not modify the thermal transmittance (*U value)* when compared to the clear single glass. Tinted single glasses are mainly applied as a glare control solution. Absorptive glasses reduce the solar gains through glazed glasses by absorbing part of the incident radiation.

Figure 6. Thermal Transmittance, *U-value* [W/m^2.K], Visible Light Transmittance, τ_v [-], and Solar Factor, *g* [-], in the centre of single glasses: a. clear; b. tinted

The double-glazing gas filling chamber shown in Figure 7 is filled with atmospheric air mainly consisting of oxygen and nitrogen. The clear double glass (Figure 7a) has Visible Light Transmittance and Solar Factor values lower than the values of clear single glass. Within these two glass panes, there is a gas filling chamber that, when properly sealed, improves the thermal and acoustic insulation of the glass. The thermal transmittance value for this type of glass is approximately half of the clear single glass value.

The *tinted double glass* (Figure 7b) is usually applied when the main objective is to reduce the solar factor for thermal reasons, which has costs in terms of natural lighting since the colour of the glass penalizes its visible transmittance in relation to the clear double glass. The use of blue or green colours in double glazing tends to penalize less its visible light transmittance. This type of glass is available in the market in various colours, commonly bronze or grey, and one (exterior) or both panes can be tinted. As already concluded for the *tinted single glass*, the thermal transmission value does not change significantly in the *tinted double glass*.

The *high-performance tinted double glazing* (Figure 7c) has a higher visible light transmittance and a lower solar factor than the double-tinted glass, so a larger fraction of the visible solar spectrum radiation is transmitted, and most of the infrared radiation is absorbed.

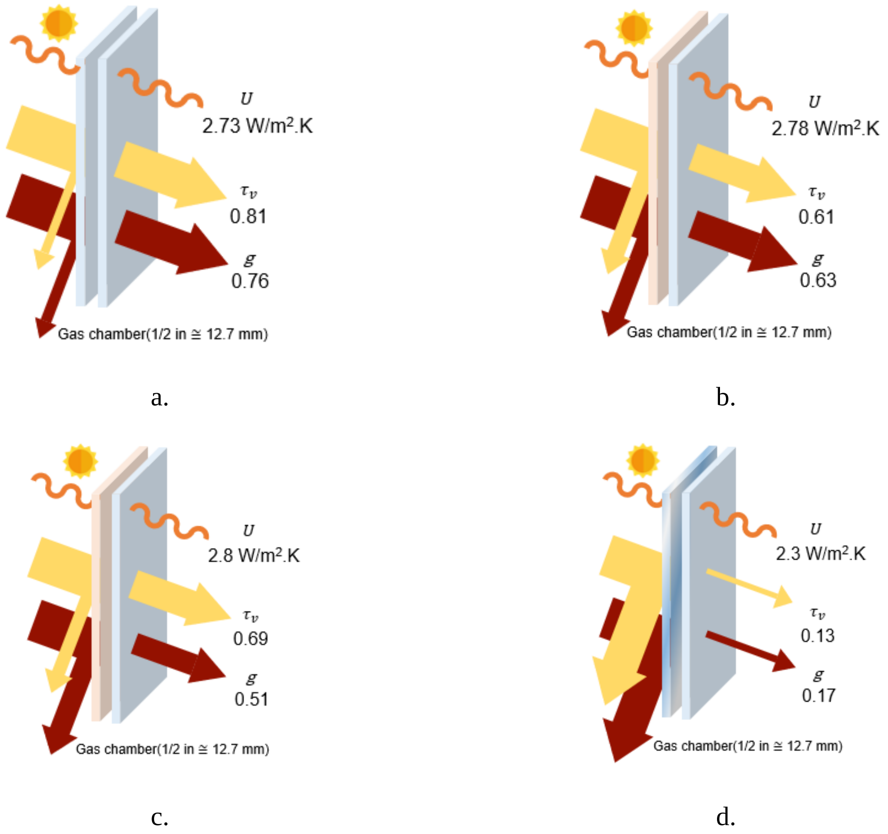

Figure 7. Thermal Transmittance, U [W/m^2.K], Visible Light Transmittance, τ_v [-], and Solar Factor, g [-], in the centre of double-glazing with an air filled chamber: a. clear; b. tinted; c. high-performance tinted and; d. reflective

The *reflective double glass* (Figure 7d) undergoes treatments based on metal oxides during its manufacturing process to increase the solar radiation reflection, thus reducing the heat transfer to the indoor environment. Throughout the sun hours, radiation reflection from the outdoors occurs while, at night, the radiation from indoors is reflected by the glass. The properties of this type of glass depend on different criteria such as location, reflectance of the metal layer, thickness of the glass and gas filling chamber. This type of glass is common in commercial and service buildings that present excessive solar gains due to their large glazed areas.

The *low emissive double glass* (*low-e)* incorporates low-emissive coating layers with low emissivity values and thermal radiation reflection (infrared and ultraviolet radiation). The presence of these low emissive layers enables the control of solar gains by reducing the solar factor of the glass without penalizing the transmission of visible radiation, thus avoiding the mirror effect observed in the case of reflective glasses. Thermal radiation from the outdoor and indoor environments is reflected by the low outer and inner emissive layers, which contribute to the rejection of long-wavelength outdoor radiation and the keeping of indoor thermal radiation.

Glasses with low emissive coating layers can be grouped according to the following solar gain levels: high solar gain, moderate solar gain, and low solar gain. The thermal transmittance value for the three types of glass with low-emissive coating layers is approximately the same. The values of some properties *(U,* g, τ_v) in the center of low-emissive double-glazing, with an argon chamber (1/2 in ≅12.7 mm), are associated with different solar gains (high, moderate, and low) and are shown in Figure 8.

The *low-emissive double glass* with high solar gain (Figure 8a) enables the reduction of thermal losses from the indoor environment and admits solar gains, and it is usually used in climates associated with high energy heating needs. The low-emissive layers included in these glasses are usually deposited by means of a pyrolytic treatment during the manufacturing process.

The *low-emissive double glass* with a moderate solar gain coefficient (Figure 8b) is considered spectrally selective since it reduces the solar heat gains and presents high values of visible radiation transmittance. This type of glass is suitable for temperate climates with both similar heating and cooling energy needs as it reduces the cooling needs without significantly increase the heating needs and by decreasing a little more than half the solar factor of the glazed glass. The low-emissive layers are commonly applied through a vacuum *sputtering* process during glass production.

The *low-carbon double-glazed glass* with a reduced solar gain coefficient (Figure 8c) is more spectrally selective than the double-glass with a moderate solar gain coefficient, significantly reducing solar gains and allowing high values of visible radiation transmittance. This type of glass has a greater visible transmittance level with a certain reduction of solar gains, than the tinted or reflective double glazing. It also reduces heat losses to levels as those observed in the case of low-emissive double-glazed glass. However, it leads to a significant reduction in solar gains, greater than that observed for the other low-emissive glasses. Therefore, this is a glass with a high application potential in climates with significant cooling energy needs. During glass manufacture, the low-emissive coating layers are typically applied using the *vacuum sputtering* process.

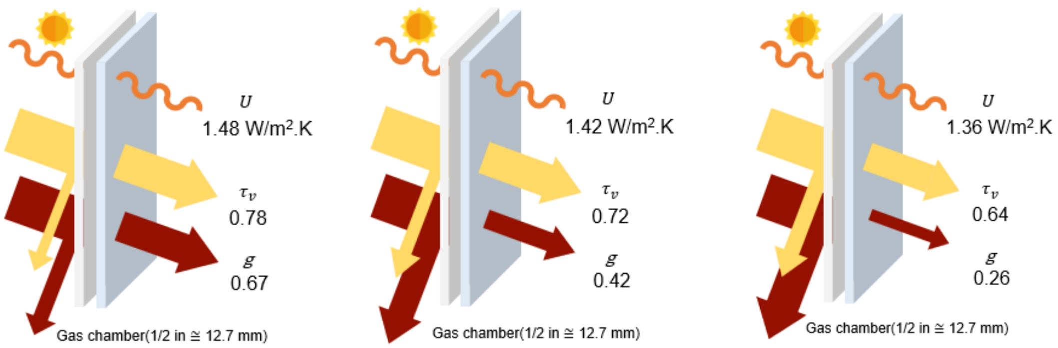

a. b. c.

Figure 8. Thermal Transmission, U [W/m^2.K], Visible Light Transmittance, τ_v [-], and Solar Factor, g [-], in the centre of low-emissive double-glazing with a glass filling chamber (1/2 in ≅12.7 mm): a. high solar gain; b. moderate solar gain; c. low solar gain

Incrementing the number of glass panes, generating multilayer glazing, increases the window's thermal insulation; however, this increase is not proportional to converging to a stabilized level. Despite reducing the thermal and optical properties of the glazed glass, each glass pane increases the thickness and weight of the glazed glass to a point where the addition of more glass panes becomes physically and economically unfeasible. A multilayer glass (clear triple glass) and its main properties (U, g, τ_v) values are displayed in Figure 9. Clear triple glass reduces the thermal transmittance to less than a third, compared to clear single glass.

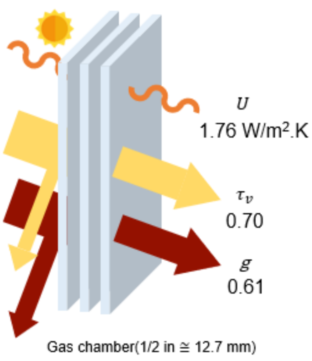

Figure 9. Thermal Transmission, U [W/m^2.K], Visible Light Transmittance, τ_v [-], and Solar Factor, g [-], in the centre of clear triple glass

Figure 10 shows the transmittance of UV, visible and infrared radiation of several glazing with 6 mm glass pane thickness and 12 mm air gap chambers thickness in the case of double and triple glazed glass. The transmittance values were determined using the *Optics* program [24]. It can be observed that the transmittance of visible radiation decreases with the glass thickness, and the transmittance value is higher for the *clear single glass*, followed by *clear double* and *clear triple glazing* (Figure 10).

When comparing the visible light transmittances of the tinted single and double glasses with the clear single and double glasses, it can also be concluded that the use of colouring (bronze colour) for tinted glasses reduces the visible transmittance. The low-emissive double glass with moderate solar gain allows a higher reduction of the thermal radiation transmission, thus exhibiting a visible light transmittance close to the triple glass value.

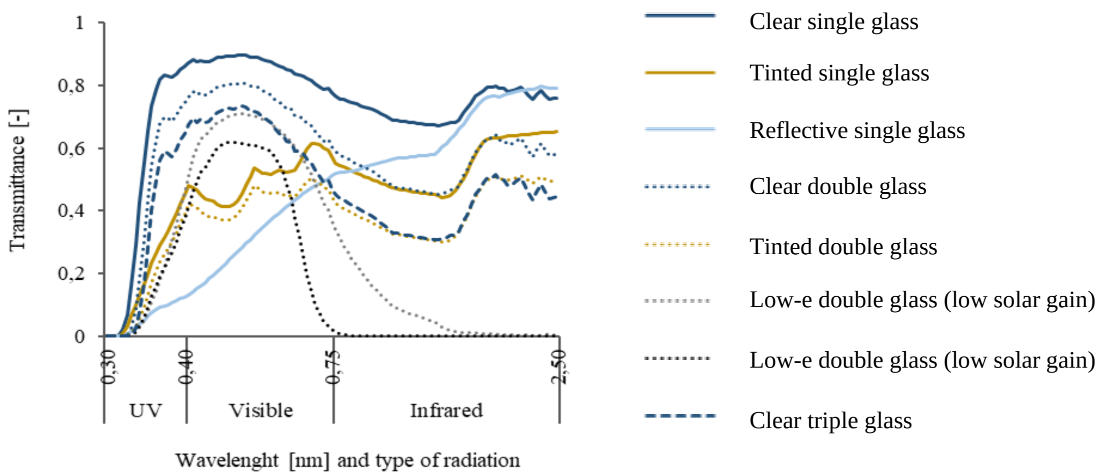

Figure 10. Transmittance of clear and tinted single-glazing with 6 mm glass panes thickness and double-glazing with 6 mm glass panes thickness with a 12 mm air filling chamber

2.2 Solar Control Films

2.2.1 Introduction to window films

Solar control film (SFC) is a thin laminate film material that can be applied to glass surfaces to modify their optical and thermal properties without having to change the type or structure of glazing systems in buildings façades. Nowadays, there is a wide range of window films for retrofitting purposes with applications on both internal and external surfaces in glazed areas of buildings façades, suitable for retrofitting purposes in cold and hot climates [25]. The efficiency of a film is directly related to the glass substrate, solar orientation, external and internal shading conditions, air-conditioning system and local climate. Films with external application on the glass surface present lower durability than those with internal application because they are exposed to weather elements and possible damages induced by people or objects for glazing surfaces at the ground level [26]. Also, inappropriate cleaning tasks or insufficient maintenance routines have proven to decrease the life span of the films [26].

The first window films were developed in the 1960s and had the primary purpose of balancing heat exchanges through glass surfaces by blocking radiation across the entire range of frequencies of the solar spectrum [27]. Although this was a significant discovery with a high potential to improve thermal and visual comfort in buildings, problems regarding the decrease of the external visibility (reductions in the visible range spectrum), excessive use of artificial light and heating loads motivated new research and product development.

In the 1970s, with the industrial revolution at its peak, new solutions and materials that improved thermal comfort and energy efficiency in buildings have been investigated and developed. The incorporation of polyester fibres in window films produced more energy efficient films for cold climates due to the increase of the absorption coefficient and reradiation of long wave in the infrared electromagnetic spectrum, thus reducing the heat losses to the outdoor environment without decreasing the visible solar transmittance through the glass surface [27].

2.2.2 Typical composition of window films

Existing window films are composed of several membranes of different intercalated materials that can reach up to eight different layers and undergo seven different manufacturing procedures [28]. Figure 11 shows a standard structure of a solar control film.

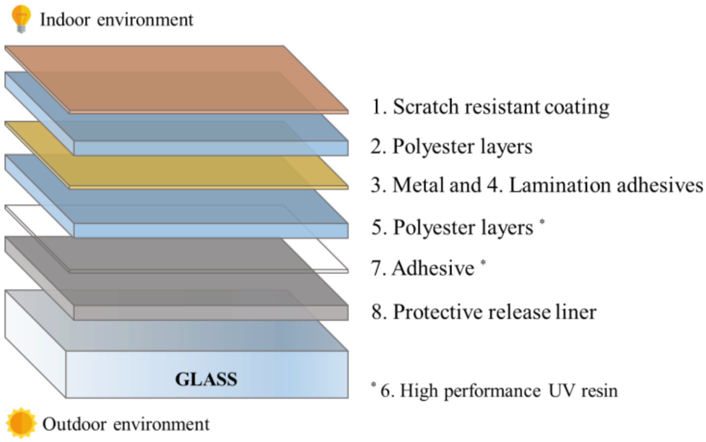

Figure 11. Standard structure of a solar control window film with internal application on the glass surface: 1. scratch resistant coating, 2. and 5. polyester layers, 3. lamination adhesive(s), 4. metal, 6. high performance UV resin, 7. adhesive and, 8. protective release liner

As shown in Figure 11, a typical layout of a solar control film with internal application on the glass surface can be constituted by eight different layers [27], [28], namely:

1. Scratch resistant coating: this hard acrylic coating finishing layer is in contact with the indoor environment of the building and its function is to protect the film from scratching and abrasion;

2. and 5. Polyester: the polyester membrane offers good optical, thermal, mechanical, physical and chemical characteristics to the film. It is very durable, resistant, flexible and withstands high and low temperatures. It can have different finish types, such as UV resin or adhesives. Incorporating several layers of polyester (multi-layered structure), connected through lamination adhesives, increases the absorption and solar (front) reflectance coefficients. Many films are made with metal deposits on their polyester substrate. This type of film is in the solar control series range due to the high solar (front) reflectance coefficient and is traditionally called reflective or metallized films;

3. Metal: the oxide metals presented in the solar control films are incorporated into the polyester membrane and has the function of reducing solar gains through glazing. The metal used is usually aluminum and can reduce solar gains by about 80% and reduce visible radiation between 15% to 70%. Recent films based on nanotechnology are produced without metal oxides, resulting in thin films with a combined high visible transmittance and low solar (front) reflectance coefficients;

4. Lamination adhesive: joins several layers of polyester through lamination processes. Sometimes they are embedded in the polyester membranes themselves;

6. High performance UV resin: blocks UV radiation and protects the polyester layers and lamination adhesives. This resin improves thermal performance by reducing the solar gains in the UV solar spectrum and protects the indoor environment content from early degradation by exposure to UV rays. It can be incorporated in the adhesives or in the polyester layer itself;

7. Adhesive: there are two types of adhesives in window films – pressure sensitive and water activated adhesives. The first one adheres to the glass surface through the application of pressure forces without the need to apply any type of solvent, water, or heat. On the contrary, water activated adhesives, as the name implies, needs water to ensure a correct adherence, forming chemical bonds with the glass surface, which guarantees higher durability and a more transparent appearance. However, its removal or replacement can be difficult;

8. Protective release liner: a polyester film that protects the adhesive from contamination before installation. It should only be removed before applying the film to the glass.

2.2.3 Types of window films

Films designed for use in glazing are composed of different polyester layers connected with pretreatment to ensure a correct adherence of adhesives and coatings to which a transparent, tinted or metallized polyester layer can be incorporated, thus contributing to a greater or lesser reduction of UV radiation flow (thermal, solar, and ultraviolet range spectrum) through the window by reflecting or absorbing part of the incident radiation.

As mentioned before, the performance of SCFs depends on the type and size of the glazing; the local weather conditions; the application of SCF on the interior or exterior glass surface; the façade orientation; the existing interior and exterior shading; the type of air conditioning system and the cleaning and maintenance of the building.

Currently, there is a wide range of films designed to be applied on the interior or exterior of glazed windows with different objectives. The most important types of window films identified in accordance with EN 15752-1 [20] and shown in Figure 12 are:

- solar control films (the focus of the current study): they decrease the solar gains by reducing the solar factor (g) of the glass substrate to which they have been applied. They can be applied on the interior or exterior surface of the glazing;

- low emissivity films: they promote thermal insulation by reducing the thermal transmittance (U value) of the glass pane, and should be applied on the exterior (hot climates) or interior (cold climates) surfaces that are in contact with the outdoor and indoor environments, respectively, in order to obtain a better performance when applied to double glazed windows;
- ultraviolet protection (UV) radiation films: they reduce the UV radiation transmittance through the glazing below 0.001, having a positive impact on the residents' health and the durability of material goods present in the indoor environment;
- privacy films: they reduce vision through the glass pane by decreasing its visible light transmittance, by increasing the visible light reflectance of the glass pane on the outside/public side or by applying opaque or decorative features to the glass;
- decorative films: they change the appearance of the glass pane to which they have been applied, and they may present different patterns, textures or colours;
- protection films: they increase the resistance of the glass pane to intentional or accidental impacts and reduce the amount and size of possible shrapnel, protecting residents and material goods while keeping most shards bonded to the film;
- safety films: while the previous films increase the resistance of the glass pane to impacts, these films can offer resistance to shock waves from explosions and/or ballistic attacks;
- protection of Radio Frequency and Electromagnetic Frequency films: they attenuate the transmittance of frequencies over the range of 30MHz to 15 GHz by $\geq$ 20 dB;
- anti-graffiti films: they protect the surface of the glass pane against scratching, graffiti, and painting, and can be easily removed. They present a resistant anti-scratch layer that prevents the glass from being replaced.

The presentation of window films by the industry, as shown in Figure 13 is different from that indicated in EN 15752-1 [20] (Figure 12). In fact, the industry has treated window films differently to allow a better perception of the films available in the market and a comparison between them by the customer.

Figure 12. Main types of window films according with EN 15752-1 [20]

Figure 13. Film solutions offered by the main industry players

2.2.4 Main properties of window films

The determination and knowledge of glazed systems' thermal and optical properties are essential to ensure a good thermal and energy performance in buildings, especially when the building has a high ratio of glazed to opaque areas in its envelope. An appropriate choice of the glazed system to be applied at the design stage enhances the thermal and visual comfort of the occupants and, consequently, the energy efficiency of the building.

The International Glazing Database (IGDB) [29] encompasses the most extensive collection of products used for the construction of windows, namely: different types of glass, films, lamination adhesives, window frames, and filling gasses. It also contains detailed optical and thermal information on these products, which determines the energy performance of glazed systems.

The addition of a new product into the IGDB database follows a set of standards issued by the National Fenestration Rating Council [30]. The incorporation of a new film into this database requires that manufacturers provide film samples applied to single uncoated glass substrates, with a solar and optical transmittance greater than 0.83 and 0.89, respectively, thus ensuring that the film will have transmittance values similar or lower than those of the glass on which it will be applied [31]. The glasses that meet these criteria are: 3 mm single glass; 3 mm single glass with low iron content, and 6 mm single glass with low iron content. Additionally, manufacturers must submit samples of the same glass, but without the film, so that this product's thermal and optical properties can be determined separately. Due to this requirement and given that the film works when applied on a glass substrate, the manufacturers' technical datasheets provide aggregate thermal and optical information of the film in single 3 mm and/or 6 mm glasses. Although the existing glasses on building windows are currently usually double glazing and not single glazing, it is still common to see technical data sheets containing information of films available in the market being applied to single 3mm or 6mm glasses.

According to EN 15752-1 [20], the definition of window films depends on their reflectance (interior and exterior) and their transmittance properties for the different radiation in each spectral range: solar, visible, UV and thermal ranges. Following the EN 12898 standard [32], thermal radiation refers to emissivity over long wavelength infrared radiation. The solar-optical properties for window films determined in accordance with EN 410 [33] and referred to in EN 15752-1 [20] are:

- solar transmittance (τ_e): fraction of solar radiation passing through the glass and film system;
- solar reflectance (ρ_e): fraction of solar radiation which is reflected by glass and film system;
- solar absorptance (α_e): fraction of solar radiation which is absorbed by the glass and film system;

- visible light transmittance (τ_V): fraction of visible radiation passing through the glass and film system;
- exterior visible light reflectance ($\rho_{V,e}$): fraction of visible radiation that is reflected by the exterior surface of the glass and film system;
- interior visible light reflectance ($\rho_{V,i}$): fraction of visible radiation that is reflected by the interior surface of the glass and film system;
- total solar energy transmittance factor or solar factor (g): relationship between the total amount of radiation (transmitted directly and after being absorbed) flowing into the interior environment and the global incident solar radiation on the glass and film system;
- total shading coefficient (SC): ratio between the gain of solar heat through a glass and film system and the gain of solar heat through a double-resistant transparent glass system;
- UV transmittance (τ_{UV}): fraction of UV radiation that runs through the glass and film system;
- general colour rendering index (R_a): degree of reliability of the light source that permeates the film revealing the colours of the illuminated objects compared to their appearance when illuminated by natural daylight.

The values of previous properties can be expressed in decimal or percentage except for the total shading coefficient (SC) and the general colour rendering index (R_a) [20]. In addition to the solar-optical properties listed above, the manufacturers' technical datasheets also usually contain thermal properties of the glass and film system such as:

- thermal transmittance, U [W/m^2.K]: quantifies the heat flow that passes in one hour through 1 m^2 of the glass and film system separating two environments (exterior and interior) with a temperature difference of 1 °C;
- emissivity, ε [-]: the relationship between the energy emitted by the glass pane and film system and the energy emitted by the blackbody at the same temperature.

The awareness of these properties is fundamental to evaluate the effective performance in each range: thermal, optical, and energy ranges. In fact, when exposed to solar radiation, I, the glazing system composed of glass and film exchanges heat between the indoor environment () and the outdoor environment (), as illustrated in Figure 14. This process involves three different heat transfer mechanisms: conduction through the glass, the film system, and the window frame; radiation through the glass and film system surfaces and gas convection in the filling chamber, in the case of double or multiple glazing windows. As regards the incident radiation on the glazed pane, a fraction is reflected directly to the outdoor environment (ρ_e, $\rho_{V,e}$); another fraction is transmitted directly to the indoor environment (τ_e, τ_V, τ_{UV}) and the remainder is absorbed by the glass (α_e). In terms of the absorbed radiation, part is subsequently re-radiated to the outdoor environment and another part to the indoor environment. Some of the properties described in this section are shown in Figure 14.

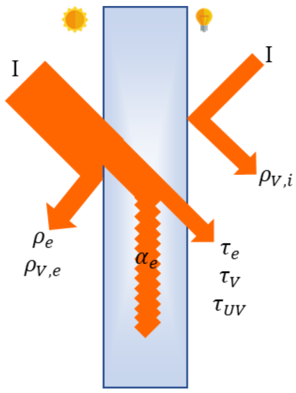

Figure 14. Heat transfer through a single glass: incident radiation, *I*; solar transmittance, τ_e, reflectance, ρ_e, and absorptance, α_e; visible light transmittance, τ_V; exterior, $\rho_{v,e}$, and interior, $\rho_{v,e}$, visible light reflectance; and UV transmittance, τ_{UV}

The characterization of the ranges for thermal and solar-optical properties of different types of Solar Control Films (SCFs), when applied to a clear single glass (6 mm), are shown in Figure 15.

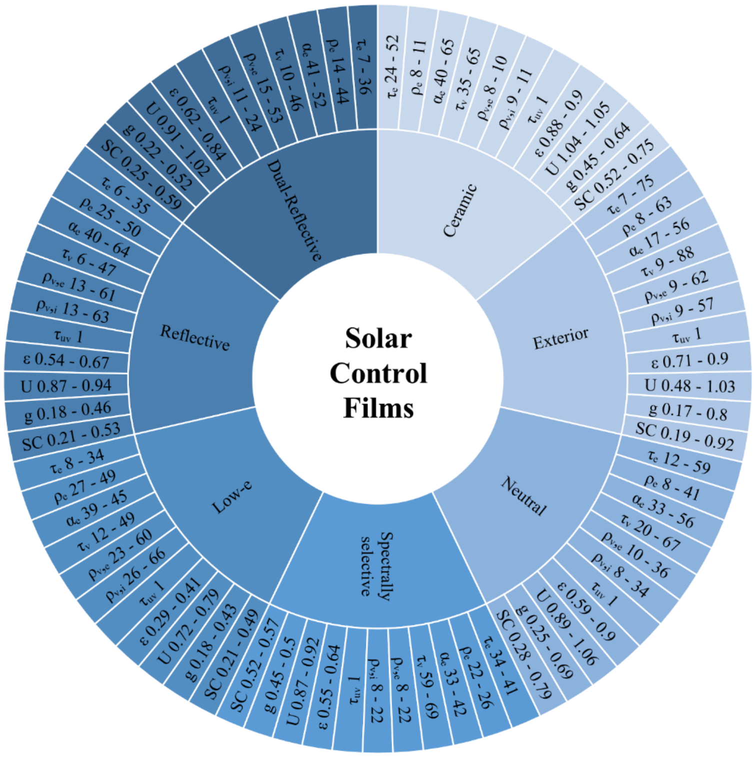

Figure 15. Characterization of the ranges for thermal and solar-optical properties of the different types of Solar Control Films (SCFs) when applied to a single clear glass of 6 mm: solar transmittance, τ_e, reflectance, ρ_e, and absorptance, α_e, visible light transmittance, τ_v, exterior, $\rho_{v,e}$, and interior, $\rho_{v,e}$, visible light reflectance, UV transmittance, τ_{UV}, emissivity, ε, thermal transmission, U [W/m^2.K], solar factor, g, and shading coefficient, SC

2.2.5 Influence of solar control films on different types of glass

The performance of SCFs depends on their thermal and optical properties as well as on the properties of the glass substrate to which they have been applied to, as referred to in EN 15755-1 [34]. To test the influence of a substrate (glass) on the thermal and optical properties of the glass and film system, a total of eight different glasses, two single and six double glazing panes were selected, which represent the most common types of glass referred to in section 2.2. The selected glasses, manufactured by *Saint Gobain Glass* (SGG), and used as a glass substrate to which the SCF will be applied, are composed of glass panes with a 6 mm thickness and gas filling chambers with a 16 mm thickness, in the case of double-glazing windows. The selected glasses and their main optical and thermal properties are shown in Table 1. The reflective and low-emissive double-glazed glasses have solar control coatings on the internal surface of the exterior glass, which is in contact with the gas filling chamber (surface 2), resulting in the most appropriate solar control solution suitable to the Mediterranean climate.

Table 1. Representative solutions of various types of common glazing (single and double) with 6 mm thickness glass panes and a 16 mm thickness glass filling chamber in the case of double glazing, and their main optical and thermal properties: solar transmittance, τ_e; visible light transmittance, τ_v; visible exterior reflectance, $\rho_{v,e}$; visible interior reflectance, $\rho_{v,i}$; external emissivity, ε_e; internal emissivity, ε_i; solar factor, g; and thermal transmittance, U [W/m^2.K]

Type of glazed glass	τ_e	τ_v	$\rho_{v,e}$	$\rho_{v,i}$	ε_e	ε_i	g	U
Single								
Clear	0.82	0.89	0.08	0.08	0.84	0.84	0.85	5.81
Tinted (Bronze)	0.50	0.49	0.05	0.05	0.84	0.84	0.64	5.81
Double								
Clear	0.68	0.80	0.15	0.15	0.84	0.84	0.75	2.69
Tinted (Bronze)	0.42	0.44	0.07	0.12	0.84	0.84	0.52	2.69
Reflective	0.39	0.29	0.54	0.46	0.84	0.84	0.45	2.69
Low-emissive high solar gain	0.49	0.79	0.12	0.12	0.05	0.84	0.54	1.72
Low-emissive moderate solar gain	0.34	0.70	0.32	0.13	0.04	0.84	0.38	1.70
Low-emissive reduced solar gain	0.26	0.60	0.16	0.17	0.04	0.84	0.30	1.70

After inspecting the *Optics6* tool library, the SCF of the leading manufacturers (3M, Hanita Coatings, Johnson Window Films, Llumar, Solar Gard) were compiled. Table 40 to Table 43 of Annex A show the list of films considered within the scope of this study and their main properties. Since the properties of films without a substrate are not available, the properties of the several films analysed in section 2 are shown when applied on clear glass with 6 mm in Annex A.

The following sections present the obtained results of applying the different films shown in Annex A in each of the types of glass presented in Table 1. The thermal and optical properties of the glazed systems and films were obtained by using *Optics6* and *Window7.6* tools. In the scope of this study, seven parameters were considered and analysed: solar transmittance, visible light transmittance, interior visible reflectance, exterior visible reflectance, emissivity, solar factor, and thermal transmittance. It is important to highlight that there are limitations when SCFs are applied to specific glazed glass due to glass ruptures by means of potential thermal break, usually promoted by the increased of the solar absorptance coefficient and, therefore, a careful analysis should be done before the application of the film.

- Single glazing

The main thermal and optical properties for clear and tinted single glass, without and with the various types of SCFs, are shown in Figure 16 and Figure 17, respectively. Annex B presents the mean and the coefficient of variation of these same properties for each film type applied to single glazed glass.

The application of SCFs to the internal surface of the glazed windows (Figure 16a and Figure 17a) likewise enabled a reduction of the solar (τ_e) and visible (τ_v) transmittance values on both single glasses. For a given exterior visible reflectance ($\rho_{v,e}$) value, the SCF caused a negligible increase in the reflective properties of the external surface of the single tinted glass, contrary to what was observed in the case of single clear glass. In the presence of SCF, the interior visible light reflectance ($\rho_{v,i}$), internal emissivity (ε_i) and solar factor (g) values are approximately the same between the two single glasses. The thermal transmittance (U) for each type of SCF is approximately the same for both single glasses. The most significant reduction in both glazed glasses is associated with the low-emissivity SCF.

Figure 16b and Figure 17b show the thermal and optical properties of single clear and tinted glass, without or with SCF, applied to the external surface of the glass. It is possible to observe that the effect of the films on the values (τ_e, τ_v, ε_i and g) are approximately the same for each type of SCF for both single glasses.

Each type of film has similar exterior visible light reflectance ($\rho_{v,e}$) values for both single glasses when applied externally, except for the case of the reflective SCF, which provides a negligible reduction when applied to a single-tinted glass. The reflective, protective and safety films considered in this study led to a significant increase in the interior visible light reflectance ($\rho_{v,i}$) values when applied to single tinted glass. The thermal transmittance (U) remained unchanged with the application of the SCF, except for reflective films applied to single tinted glass. In this case, a small reduction of these values was obtained.

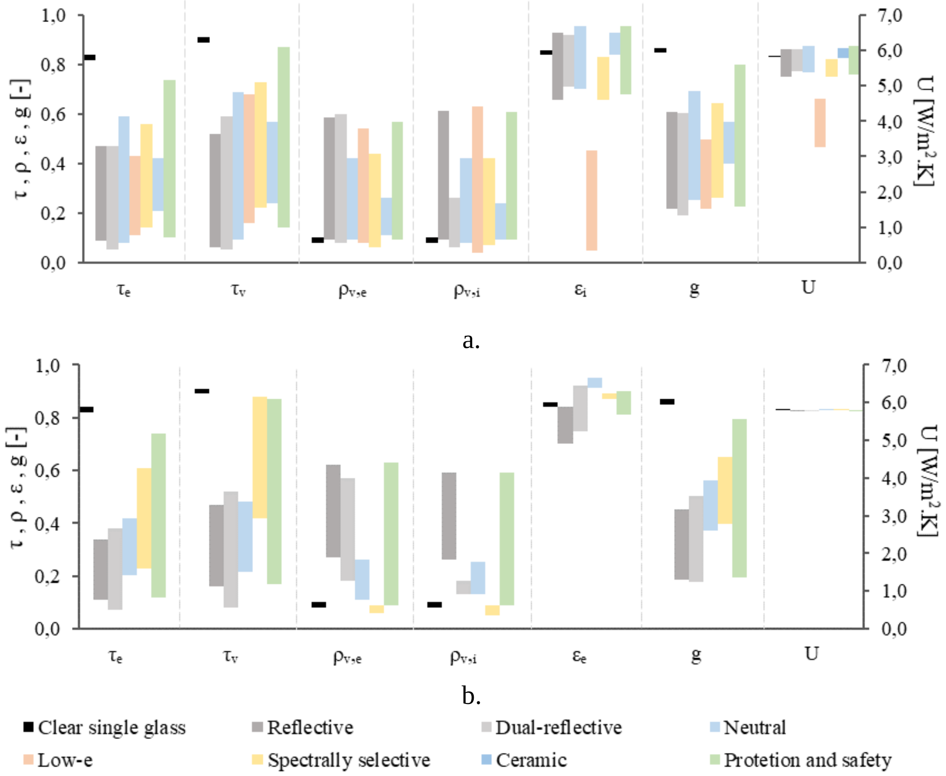

Figure 16. Ranges of the main thermal and optical properties (τ_e, τ_v, $\rho_{v,e}$, $\rho_{v,i}$, ε, g and U) of a single glass without and with SCFs applied to the a. internal and b. external surfaces

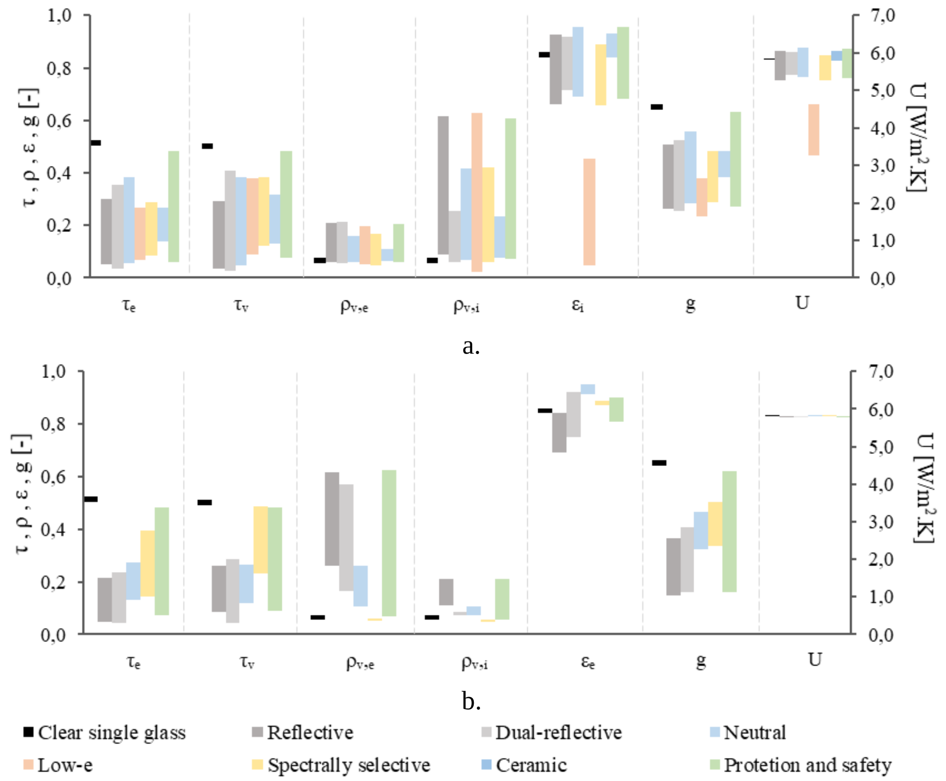

Figure 17. Ranges of the main thermal and optical properties (τ_e, τ_v, $\rho_{v,e}$, $\rho_{v,i}$, ε, g and U) of a (bronze) tinted single glass without and with SCFs applied to the a. internal and b. external surfaces

- Double glazing

The main thermal and optical properties of the double glass solutions, without or with the various types of SCF, which were selected previously in Table 3, will be analysed in this section. Annex B presents the mean and the coefficient of variation of these same properties for each SCF type applied to double glazed glass as well as the number of SCF of each type considered in this study.

Figure 18 shows the thermal and optical properties values for clear double-glazed glass without and with SCF. The SCF applied to the internal surface of the glazed glass (Figure 18a) allowed a reduction of the τ_e, τ_v, $\rho_{v,i}$, $\rho_{v,e}$, and ε_i values similar to those previously observed in the presence of these same films when applied to the single clear glazed glass. For a given solar factor (g), the SCF did not cause such significant reductions in this property value when compared to those obtained by the same films applied on single clear glass. A reduction of the thermal transmittance (U) was obtained like the one previously observed in the case of single clear glass.

In the presence of SCF applied to the external surface of the clear double glazed glass (Figure 18b), the reduction of the thermal and optical properties values, for each type of film, are approximately the same as those previously obtained for the single colorless glazing.

The ranges of the main thermal and optical properties for tinted double glazed glass, without and with SCF, are shown in Figure 19. SCF applied to the internal surface of the glazed glass (Figure 19a) caused a reduction of the values of the properties like the one previously obtained for the single tinted glazing. However, the SCF allowed a reduction of the solar factor (g) values like the one observed in the case of single tinted glass, contrary to what was observed for double and single clear glazed glass.

The application of films on the external surface of the tinted double glazed glass caused a reduction in thermal and optical properties like the one observed in the case of single tinted glass.

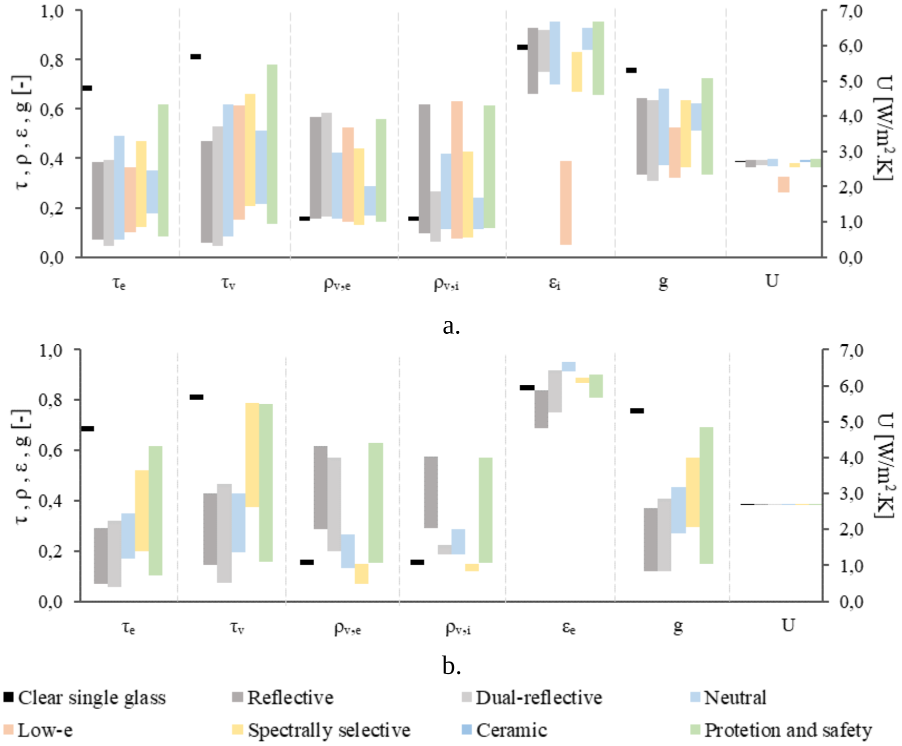

Figure 18. Ranges of the main thermal and optical properties (τ_e, τ_v, $\rho_{v,e}$, $\rho_{v,i}$, ε, g and U) of a clear double glass (6+16A+6 mm) without and with SCFs applied to the a. internal surface of the interior glass pane and b. external surface of the exterior glass pane

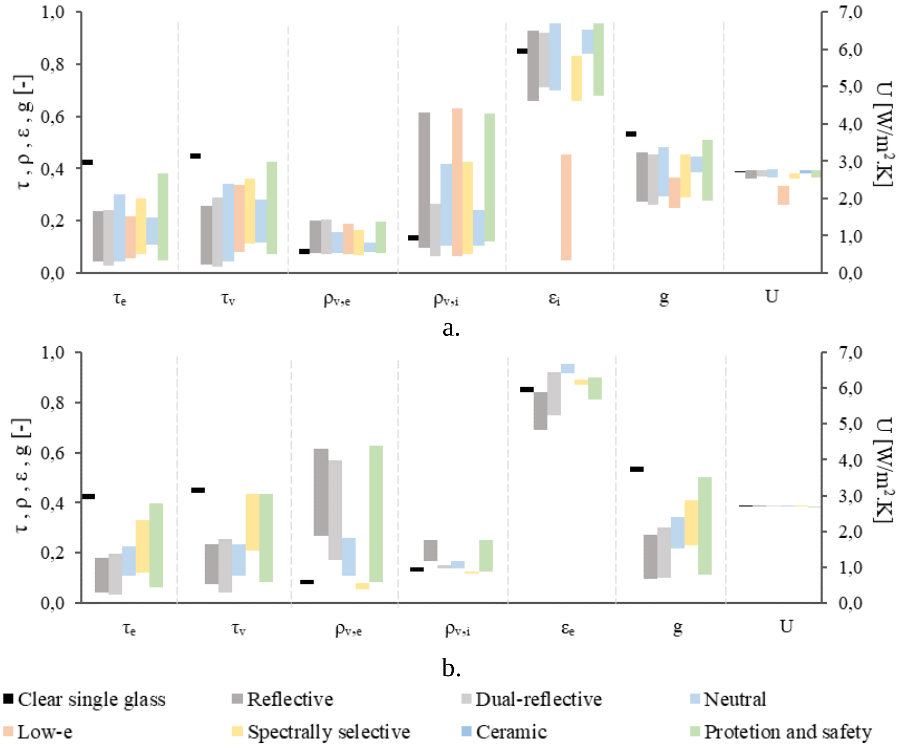

Figure 19. Ranges of the main thermal and optical properties (τ_e, τ_v, $\rho_{v,e}$, $\rho_{v,i}$, ε, g and U) of a (bronze) tinted glass (6+16A+6 mm) without and with SCFs applied to the a. internal surface of the interior glass pane and b. external surface of the exterior glass pane

Figure 20 shows the thermal and optical properties of a double reflective glazed glass without and with SCF. In the presence of SCF applied to the internal surface of the glazed glass (Figure 20a), the ranges of solar (τ_e) and visible light (τ_v) transmittance values are smaller than those obtained for the clear double glazing, because the reflective glass (without SCF) has significantly lower values of these properties. In the presence of these SCF and due to its high exterior visible light reflectance ($\rho_{v,e}$), the reflective glazed glass provides a negligible increase in the values of this property.

The remaining $\rho_{v,i}$, ε_i and U values are like those observed in the case of the clear double glaze for all types of SCF. However, the SCF allows to obtain lower solar factor (g) values than those obtained in the case of clear double glass as the reflective glass without film presents a low solar factor.

Figure 20b shows the properties in the presence of SCF applied to the external surface of glazed glass. Again, it is possible to observe that smaller ranges of τ_e, τ_v and g values are obtained, when compared to the clear double glass, which, in the absence of SCF, shows higher values of these properties. Contrary to what was observed in the case of clear double glazed glass, the application of SCF to the external surface of the reflective glass promoted the reduction of the exterior visible light reflectance and a negligible increase of the interior visible reflectance. In the presence of the same SCF, both the external emissivity and the thermal transmittance are approximately the same as those previously obtained for the clear double glass.

The ranges of the main thermal and optical properties of the low-e (high, moderate and low solar gain) glasses are shown in Figure 21, Figure 22, and Figure 23, respectively. The solar control films applied to the interior surface of a low-e (high solar gain) glazed glass (Figure 21a) allowed to obtain ranges of τ_v, $\rho_{v,e}$, $\rho_{v,i}$ and ε_i values like those previously observed in the case of clear double glazing, because these values are similar between both glazed glass in the absence of SCF. However, in the presence of these films, it is possible to observe a reduction in the ranges of τ_e, g, and U values, when compared to those obtained for the clear double glass, because the low-e glass has lower values than those observed in the case of clear glass. These relationships can also be analysed by comparing the ranges of most properties in the presence of SCF applied to the external surface of the low-emissive (high solar gain) double glasses (Figure 21b) and tinted double glasses (Figure 19b). The emissivity values of the external surface increase significantly in the presence of SCF, because the original low-e glass shows an extremely low external emissivity (0.05). The application of the SCF did not change the thermal transmittance of the glazed glass and film system.

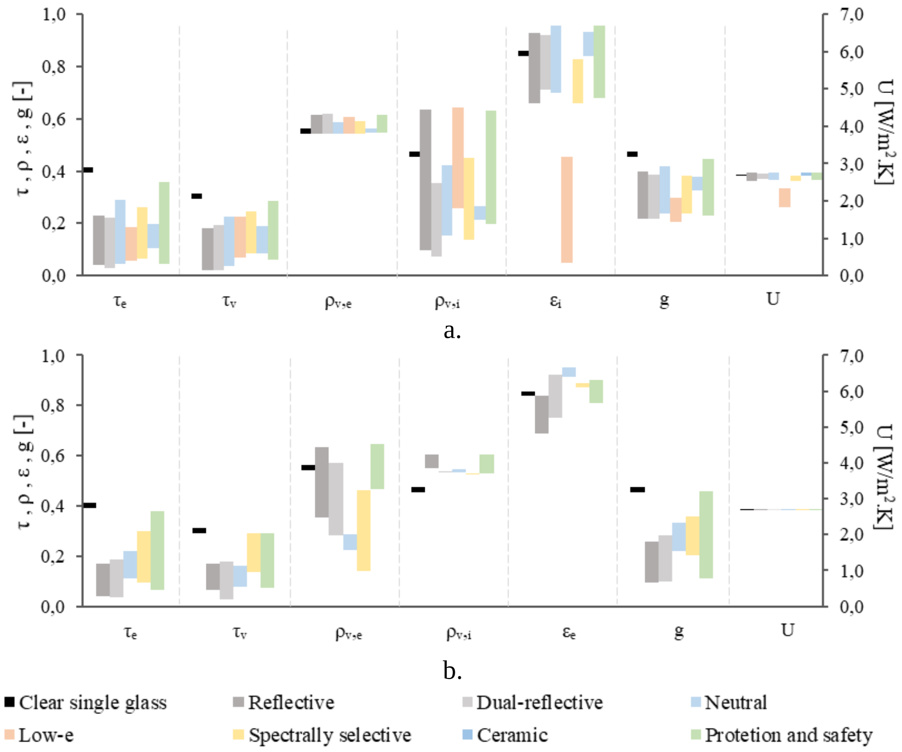

Figure 20. Ranges of the main thermal and optical properties (τ_e, τ_v, $\rho_{v,e}$, $\rho_{v,i}$, ε, g and U) of a reflective double glass (6+16A+6 mm) without and with SCFs applied to the a. internal surface of the interior glass pane and b. external surface of the exterior glass pane

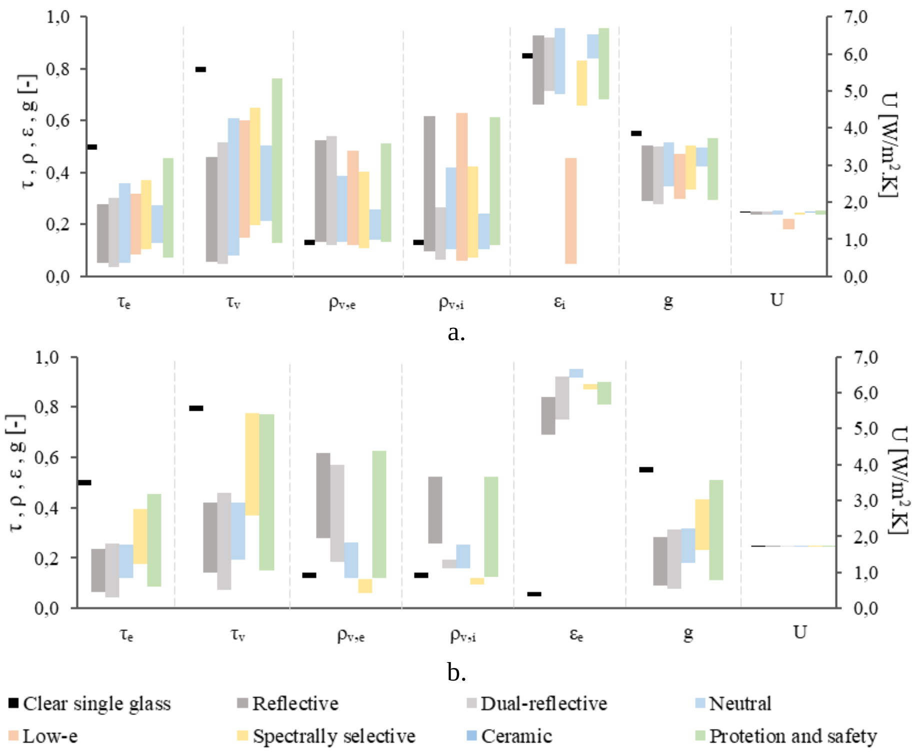

Figure 21. Ranges of the main thermal and optical properties (τ_e, τ_v, $\rho_{v,e}$, $\rho_{v,i}$, ε, g and U) of a low emissive double glazed glass (high solar gain) without and with SCFs applied to the a. internal surface of the interior glass pane and b. external surface of the exterior glass pane

The low-e (moderate solar gain) glazed glass shows $\rho_{v,i}$, ε, and U values like those observed in the case of a high solar gain glazed glass in the presence of SCF applied to the internal surface (Figure 22a). The ranges of solar (τ_e) and visible light (τ_v) transmittance values calculated for a moderate solar gain glazed glass are smaller than those obtained in the case of a high solar gain glazed glass, keeping the lowest values within the range, but reducing the maximum values. The exterior visible reflectance ($\rho_{v,e}$) value of a moderate solar gain glass is higher than that observed in the case of a high solar gain glass. Thus, in the presence of SCF, values are concentrated within smaller intervals. As a result, the maximum values of this property remain the same while minimum values are higher than those obtained in the case of high solar gain glass with SCF. This is because the solution adopted as representative of the low-e (moderate solar gain) glass (Table 1) shows solar control properties through high reflection of the solar radiation. The solar factor (g) values of a moderate solar gain double glazed glass are concentrated within smaller intervals, and thus show lower values than those observed in the case of high solar gain glazed glass in the presence of SCF, as one would expect. This is because the moderate solar gain glazed glass has a lower g value than that observed in the case of the high solar gain glazed glass before the application of the SCF.

The impact of the application of SCF to the external surface (Figure 22b) is similar to that described above for SCF applied to the internal surface of moderate solar gain glazed glass when compared to the impact of the same films applied to the high solar gain glass, except for the exterior visible light reflectance ($\rho_{v,e}$), which shows values concentrated within smaller intervals because the moderate solar gain glazed glass has a higher ($\rho_{v,e}$) value than the one in the case of the high gain glazed glass in the absence of SCF.

The impact of SCF applied to the internal (Figure 23a) and external surfaces (Figure 23b) of reduced solar gain glazed glass led to $\rho_{v,i}$, ε, U values similar to those previously obtained in the presence of the same SCF when applied to moderate and high solar gains glazed windows. In the presence of SCF applied either to the interior or exterior, the g, τ_e, and τ_v values show smaller intervals and lower values than those previously obtained when compared to those obtained for the same properties in the case of a moderate solar gain glazed glass. In the presence of SCF applied to the internal surface, the exterior visible light reflectance ($\rho_{v,e}$) shows larger intervals while values are slightly lower than those obtained in the case of the moderate solar gain glazed glass in the presence of the same SCF. As the reduced solar gain glazed glass, without SCF, has a $\rho_{v,e}$ value lower than that of the moderate solar gain glazed glass, the presence of external SCF led to larger intervals of values of this property having reached lower values when compared to the moderate solar gain glazed glass.

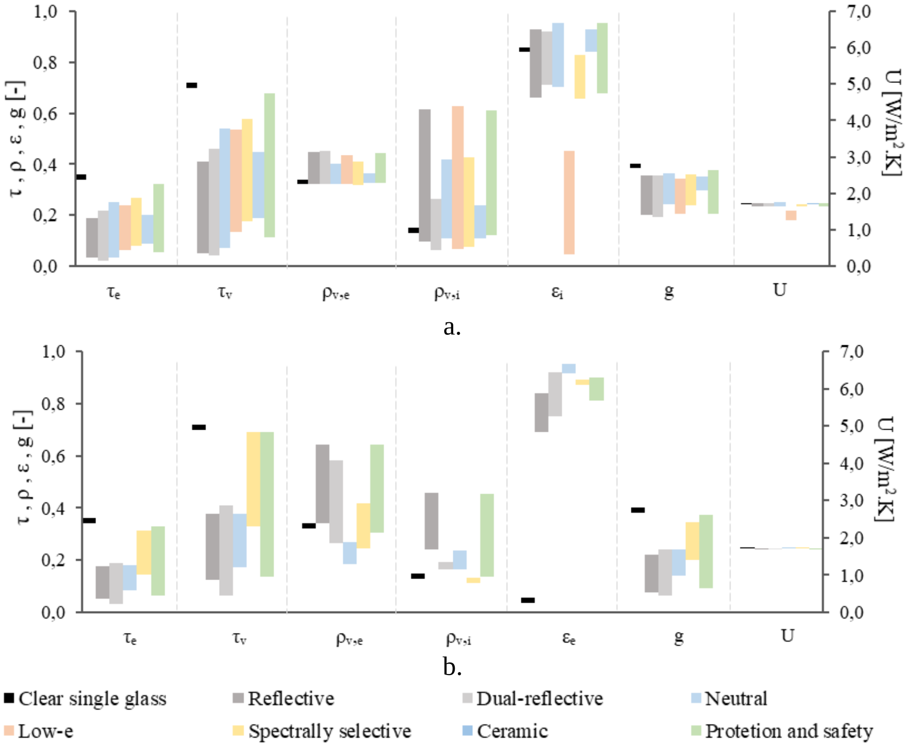

Figure 22. Ranges of the main thermal and optical properties (τ_e, τ_v, $\rho_{v,e}$, $\rho_{v,i}$, ε, g and U) of a low emissive double glazed glass (moderate solar gain) without and with SCFs applied to the a. internal surface of the interior glass pane and b. external surface of the exterior glass pane

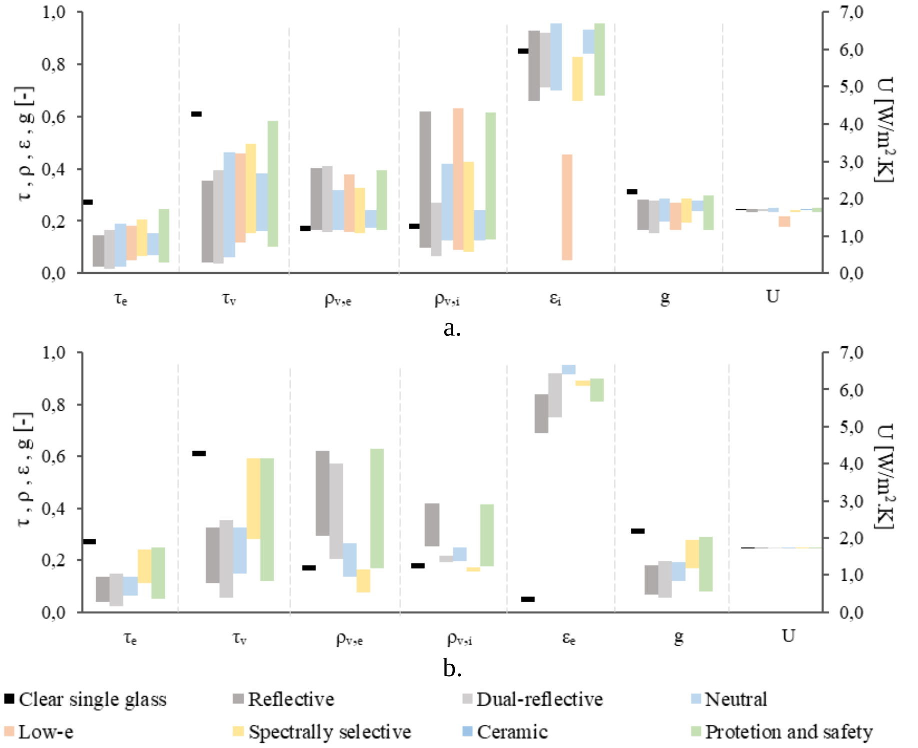

Figure 23. Ranges of the main thermal and optical properties (τ_e, τ_v, $\rho_{v,e}$, $\rho_{v,i}$, ε, g and U) of SCFs when applied to the a. interior and b. exterior surfaces of a of 6+16A+6 mm low-emissive and spectrally selective double glass (low solar gain)

2.2.6 Existing studies

The world's population growth and the improvement of people’s living conditions have caused a significant increase in global energy needs. Exploring non-renewable fossil fuels, which are the most consumed energy sources globally, is highly harmful to the environment. Thus, increased society awareness is needed for a more efficient and sustainable energy consumption aimed at reducing energy needs and reduce social inequalities.

The energy consumption by the building sector worldwide has increased and, currently, accounts for 40% of the world's energy consumption. It also accounts for approximately 36% of the greenhouse gases emissions [8], [35], [36] . Several studies have been conducted to find solutions that improve buildings' energy performance, which also contributes to countering and reversing this trend. Virtual modelling; optimization studies; methods of application and maintenance, from the materials to the building and city dimensions, are examples of increasingly frequent practices that help and promote sustainability in the construction sector.

However, the study of the energy performance at the building level implies the knowledge of numerous physical, social, economic, and political variables combined with building users’ behavior and climatic variables, which makes this topic a complex area of research.

Glazed surfaces of the external envelopes, for originating overheating and glare occurrences and an increase of the building’s energy consumption, are one of the main parts of the building where refurbishment is strongly recommended. Installing solar control films (SCFs) can be considered as an alternative and effective solution in reducing heat gains through window systems by changing the reflecting and absorbing solar radiation coefficients. Beyond being of easy application and not requiring façade alteration, also contribute to improve thermal, luminous and energy performance of buildings, while reducing glare and UV penetration, and further provide fade protection for furniture. In addition, spectrally selective films can provide a wide range of optical properties for glazing surfaces, making them appropriate for cold and warm climates. Although the number of studies about the effect of Solar Control Films (SCF) on the performance of buildings is still relatively small, they generally conclude that the presence of these films increases the energy efficiency of buildings and improves the thermal and visual comfort of occupants as they reduce extreme solar gains and tackle glare discomfort conditions.

Very scarce studies have investigated the impact of SCFs on buildings performance either using numerical simulation [37]–[40] or the experimental approach [41]–[43].

Yin et al. [37] modelled and simulated a commercial building in Shanghai (China) with double low-e glazing systems for two different SFCs and obtained an average value of 50% reduction in the cooling loads. Despite the heating loads have increased, the overall performance of the building resulted in an energy efficiency improvement. An evaluation of a double-glazing unit, with and without SCF, was performed by Xamán et al. [38], [39] for both warm and cold climates. Results showed that, for warm climates, the application of SCF could reduce the energy gains up to 52% when compared to the case without SCF. Other study, performed by Chaiyapinunt et al. [40], deeply investigated thermal comfort and heat transmission for different types of glass with and without SCF for Bangkok climate. The results indicated that the glass with SCF lead to a reduction in the heat gain due to solar radiation in the same amount of the optical properties of the film and have a minimal effect in heat gain by thermal conduction

Regarding experimental research and product development, Nagahama et al. [41] developed a new SCF that decreased the solar transmittance by 51% on a float glass with 8 mm. Moretti et al. [42] carried out an experimental and a numerical analysis in two similar offices in Italy, on a double pane window in the South-West façade, one with and the other without SCF. In the office with SCF applied the incoming solar radiation showed a reduction of the mean and peak values in a range of 46-66%, while the reduction in illuminance was quite constant and consistent with the optical properties of the SCF. As a result, the glass surface temperature decreased 10ºC and the indoor air temperature 2ºC in sunny days, approximately. The authors concluded that, in general, the application of SCF decreases the cooling energy demand and the indoor temperature in the cooling season and, inversely, increases the heating energy demand and the energy consumption with artificial light in the heating season. Li et al. [43] conducted an experimental study in Hong-Kong in two test cells with glazing systems facing the South-Southwest direction. Different combinations of glass and SCF were evaluated. The authors reported that film applications on single glass windows induce higher indoor glass surface temperatures for clear glass than for tinted or laminated glass, proving the higher ability of solar films in absorbing and reflecting radiation when applied on clear glazing. Also, a dynamic simulation through EnergyPlus was used by the same authors to evaluate the annual energy saving potential for different typical built environments in Hong Kong, the results showing a significant reduction in energy consumption per unit window area of SCF.

As noticed in the above literature review, the impact of solar films on the performance of the buildings' transparent elements is a recent subject of study with different topics of interest and that still have a large potential of research, as are the different types of impact (thermal, luminous and energy performance), the factors of which the impacts depend on (film properties and film positioning, glazing characteristics, type of building, climate parameters, façade orientation) and the study approach (experimental, numerical).

As it so possible to conclude from the existing studies, the topic of SCFs for glazing rehabilitation is disperse in terms of methodology followed and studied variables or indexes to assess the film's performance. Moreover, most of the existing studies are located in Europe and the East and South-East Asia, corresponding to temperate and subtropical climate areas, respectively, according to the Köppen-Geiger classification (Figure 24) [44]. This fact justifies the need of further studies and more extensive result sets to get deeper into the subject.

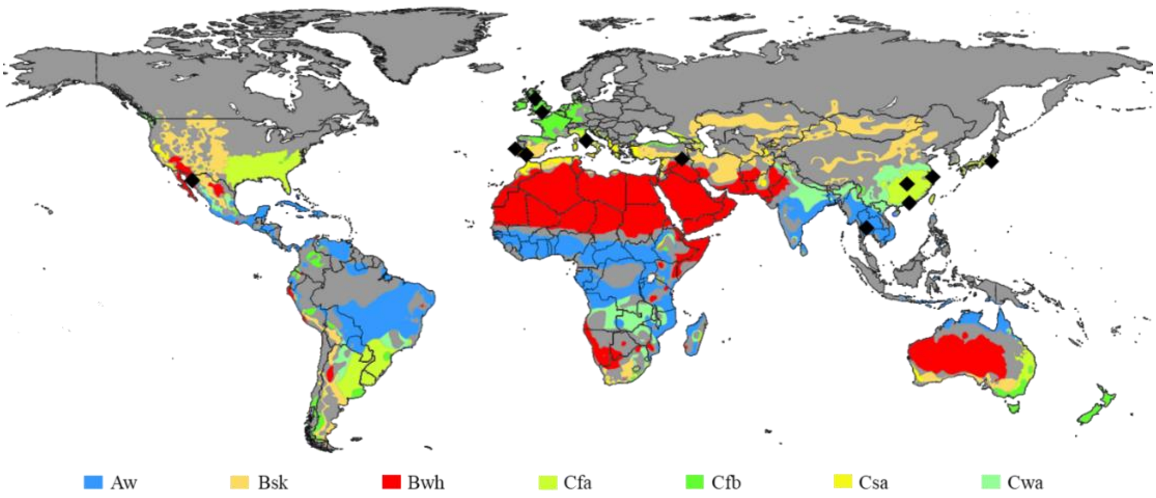

Figure 24. Studies on the performance of solar control films distributed according to their climate (Köppen-Geiger climate classification [44]): wet tropical climate in dry season (Aw); cold semi-arid climate (Bsk); hot arid desert climate (Bwh), humid subtropical climate in hot and long summer (Cfa); long and cool summer oceanic temperate climate (Cfb); Mediterranean dry summer climate, hot and long (Csa), humid subtropical climate in dry winter, hot and long summer (Cwa)

Table 2 presents the main characteristics of the existing studies that address the topic of solar control films.

Table 2. Main type of performed analysis and several research characteristics of existing studies in solar control films (organized by type of climate, according to Köppen-Geiger climate classification)

Glazing		Numerical analysis	Experimental analysis			Simulation analysis				Economic analysis	Ref.
Single	Double		Thermal	Visual	Energy	Model calibration	Thermal	Visual	Energy		
				x	x						[45]
				x	x	x		x	x		[46]
x	x		x			x			x		[43]
x	x	x									[40]
x		x	x	x	x						[47]
x			x		x					x	[48]
	x					x			x		[37]
x		x									[41]
	x	x									[49]
x	x	x									[38]
	x	x									[39]
x			x		x						[50]
	x		x	x	x		x	x	x		[42]
	x					x	x	x	x		[51]
x						x			x	x	[52]
	x					x			x		[53]
x		x							x		[54]
x			x	x		x	x		x		[55]
	x			x				x	x		[56]
	x		x	x		x		x	x	x	[57]
	x					x			x	x	[58]

Cwa   Aw   Cfa   Cfb   Bwh   Bsk   Csa

3. Experimental analysis of daylight availability

The daylight illuminance level and their spatial distribution are important design elements to achieve indoor visual comfort conditions and sustainability in buildings during its operational stage. While a proper daylighting scheme increases the efficiency of the building, the excessive use of glazed surfaces can contribute to thermal and visual discomfort, hence increasing the cooling demand and the artificial lighting. This section analyses experimentally the impact of single glazing with different SCFs on the indoor illuminance levels and the respective distribution on horizontal plane (height of the working plane) by comparing the measured absolute values and by examining them according to the useful daylight illuminance metric. Field experiments in a small-scale model with the glazing oriented to the South, in Lisbon, were performed for a clear glass (with 6 mm) without and with 4 different SCFs applied on the external surface of the glass, under clear sky conditions during summer and winter solstice at 9h00, 12h00 and 15h00 and under overcast sky conditions.

Even though this thesis analyses different SCFs with application on external and internal of single glazing, SCFs *A* to *M* (Table 7, section 4), and on external pane of double glazing, SCFs *A* to *G* (Table 14, section 5), this current section intends to perform a preliminary assessment of the daylight availability on horizontal plane for two types of films – two reflective and two spectrally selective films. The work presented in this chapter/section was published in [28].

3.1 Introduction

Daylighting has played an essential role in the history and evolution of architecture. While the lack of natural light is known to cause negative effects on humans' health and mood [59], an appropriate strategy between lighting design and building project can improve the visual comfort and indoor environmental quality and the energy efficiency through the optimization of artificial lighting, cooling and heating energy needs [60], [61]. In a study conducted by Klepeis et al. [62] showed that people spent more than 85% of their time in enclosed buildings and that daylighting is a fundamental functioning resource to be taken into account in buildings.

Computer simulations and scale models are two different approaches that can be used to tackle accurately daylighting systems in buildings exposed to lighting conditions. Both approaches can be evaluated under real sun and sky conditions or under artificial sun and sky conditions [60]. Software-based approaches broadened conventional practices of how daylight modelling was being performed. In early years, this type of analysis was very time-consuming, computationally demanding and not easily to handle. Faced with the emergence of computational modelling based on the mastery of physics involved, but not yet fully experimentally tested, building designers initially showed some reservations in integrating into their practices tools that did not allow the use and modelling by hand the real materials involved in the lighting study as scale models did [60], [63]. Nowadays with higher computer power and more advanced simulation tools through the evolution of specialized hardware and development of complex algorithms [63], [64], the use of computer modelling to predict illuminance levels in early stages of the building design has gained attention from professionals in the building sector. Different methodologies and tools to predict daylight behaviour in indoor environments have emerged, supported by sophisticated light transport algorithms that allowed more accurate results in acceptable timeframes and the possibility to optimize the design of simple or complex design façades to promote the visual comfort and the energy efficiency of the building.

The use of scale models is widely accepted as an adequate method for daylight assessment of indoor environments of buildings [65]. While this method allows to predict the daylight performance in early stages of the design process or in pre-refurbishment interventions, scale models, particularly small-scale ones, tend to overestimate the illuminance values on horizontal and vertical plane when compared to full-size buildings [66]. Studies comparing illuminance performance on horizontal plane measured in small-scale models and full-size buildings demonstrate that small-scale models out-perform by 10-30% the real scenario or building they represent, under overcast sky conditions [67]–[69]. According to Cannon-Brookes [69], errors in the physical representation of the indoor environment and difficulties in accurately defining photometric properties of materials can justify this discrepancy as well as other physical parameters as maintenance and dirt in the building. As underlined by Boccia & Zazzini [65], experimental tests performed under real sky conditions produce a more realistic representation of the daylight performance when compared with tests conducted under artificial sky using sky simulators. Moreover, the study developed by Kesten [66], highlights that model scale factor is a function of the daylighting design purpose, where greater scales within 1:10 to 1:1 are appropriate to accurately assess more critical or advanced daylighting devices and useful for detailed building façades and rooms.

This section presents a study of daylight availability using a small-scale model (1:10) approach to test various SCFs with different optical properties to assess their performance on a horizontal plane at 0.8 m (at full scale) when applied in single-pane glass units. This study increases the existing research on solar control films (SCFs) by studying the indoor illuminance performance of office rooms with single-pane glass units without (reference scenario) and with 4 different solar control films (SCFs) – 2 spectrally selective and 2 reflective – for retrofitting purposes of existing buildings. This approach can be useful for refurbishment purposes of buildings with single-glazed windows in Mediterranean climates, Csa and Csb Köppen-Geiger climate classification [44], as it is the case of Portugal, to increase visual comfort without having to activate shading devices or other solutions that can compromise the view to the outside [70], [71]. The illuminance levels were measured under overcast sky conditions and under real sky conditions during summer and winter solstice. An analysis and discussion based on the registered absolute illuminance values and the useful daylight illuminance was performed and SCFs that presented the most suitable illuminance values to perform office activities (e.g. writing, typing, reading, data processing) were identified.

3.2 Small-scale model definition and experimental procedure

To evaluate the daylight illuminance levels and the spatial distribution of solar control films (SCFs) applied in single-pane glass, *in-situ* measurements of indoor illuminances on a horizontal plane were carried out in a small-scale model on the rooftop of DECivil building in Instituto Superior Técnico in Lisbon, Portugal. Taking advantage of the modularity of the model, 5 different glazing systems were tested: a single-pane clear glass, SG, with 6 mm, taken as the reference scenario, and 4 different solar control films applied on the external surface of a 6 mm single-pane glass (designated as SG_SCF B, SG_SCF D, SG_SCF F, and SG_SCF G). Tests were conducted with the glazing system oriented to South under:

- overcast sky conditions;
- clear sky conditions during the summer and winter solstice when the sun's elevation angle is at its highest and lowest, respectively, with respect to the annual solar dynamic behaviour in three periods of the day 09h00, 12h00 and 15h00 (True Solar Time – TST).

The definition for both the overcast and clear sky days was considered as defined in ISO 15469:2004 for CIE (Commission International de l'Eclairage) standard overcast and clear sky [72].

Figure 26 (a) and (b) show a photo and a 3D representation of the small-scale model used in this study, respectively. The model was built with 30 cm high, 40 cm wide and 70 cm long (as interior measurements) in compliance with the daylighting rule of thumb where the depth of the daylight area of an indoor environment is between 1 to 2 times the size of the window-head-height [64] combined with the typical geometrical representation of office rooms in buildings. The surfaces were constructed using medium density fiberboards (MDF) and, except for the floor, all surfaces have white melaminic finishing. During the construction of the model, special attention was given to possible openings in the structure that could allow the entrance of radiation other than from the fenestration system and therefore interfere with the results. For this reason, silicone sealant was applied in some parts of the model as a precaution. In addition, to enable a swift exchange between different glass substrates and minimize the time interval between successive measurements, the model fenestration wall was designed to be completely filled with glass, without any other parts that could make glass assembly difficult. For the tests, the model was placed over a black plastic to decrease the influence of the solar reflection from the ground and to protect the materials from the floor's humidity.

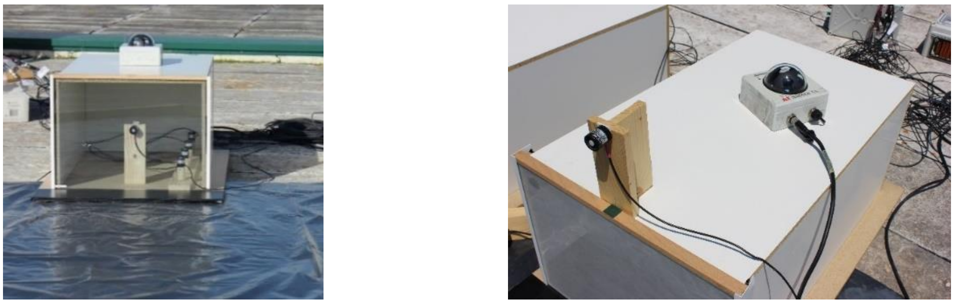

Figure 25. Small scale model (1:10) on the rooftop of DECivil building in IST, Portugal

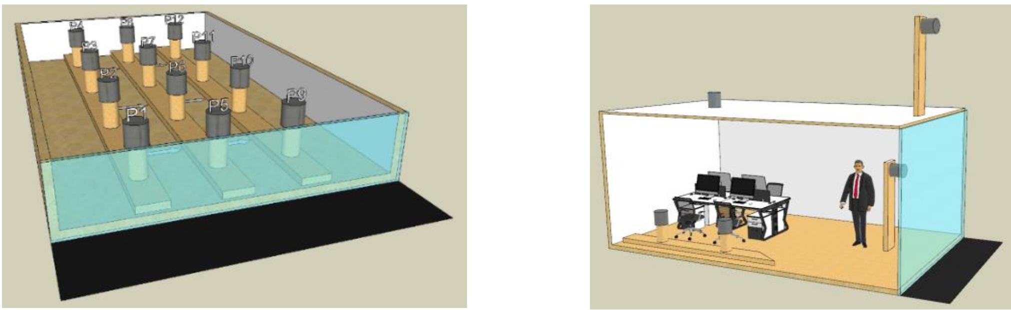

a. b.

Figure 26. 3D representation of the small-scale model: (a) position of the indoor lxmeter sensors on horizontal plane (12 points), (b) and position of the indoor and outdoor lxmeter sensors on vertical plane

Illuminance values were measured with lxmeter LI-COR LI200 sensors (± 5% accuracy) over a grid of 12 points on a horizontal plane at 0.08 m (0.8 m at full scale) above the floor, corresponding to the common height of the working plane (Figure 26a). In the small-scale model, a wooden ruler with 4 lxmeter sensors fixed on stoppers (Figure 25 and Figure 26b) was placed in three different positions (right, central and left) during the measurements. The right, central and left illuminance points were measured in different moments in time, taking about 2 minutes to record all the 12 illuminance values on the horizontal plane for each glass substrate. This timeline was tested on the rooftop in one pilot day previously to the first real measurement during the summer solstice to test the facility and understand the logistics of the tasks involved. Details regarding the timelines and steps of each measurement were registered and as a result, all the measurements were established to start 20 minutes before and end about 20 minutes after the schedule time (09h00, 12h00 and 15h00, TST), with the following sequence being adopted: 1º SG_SCF B, 2º SG_SCF D, 3º SG_SCF F, and 4º SG_SCF G, and 5º SG. Outdoor illuminance on horizontal planes were measured in one point in the model's exterior in each of the three periods of the day. Also, photos were captured inside the model for all the 5 tested fenestration systems.

3.3 Glazing solutions

Table 3 shows the main thermal and optical properties of the analysed solutions. These properties were obtained using Window and Optics tools [73] which allow to calculate spectral data of combined layers of glass with applied films. While SCFs *F* and *G* are spectrally-selective films and can be identified by their high visible transmittance (*SCF B*: τ_{vis}= 16%; *SCF D*: τ_{vis}= 35%, *SCF F*: τ_{vis}= 66%; *SCF G*: τ_{vis}= 39%), SCFs *B* and *F* are reflective films and show higher values of solar (front) reflectance (*SCF B*: $\rho_{f,sol}$= 58%; *SCF D*: $\rho_{f,sol}$= 37%, *SCF F*: $\rho_{f,sol}$= 27%, *SCF G*: $\rho_{f,sol}$= 25%).

Table 3. Thermal and optical characteristics of 5 different glazing solutions: solar transmittance, τ_{sol}, solar (front), $\rho_{f,sol}$, and (back), $\rho_{b,sol}$, reflectance, absorptance, α, visible transmittance, τ_{vis}, visible (front), $\rho_{f,vis}$, and (back), $\rho_{b,vis}$, reflectance, thermal transmittance, *U*, and solar factor, *g*

	τ_{sol}	$\rho_{f,sol}$	$\rho_{b,sol}$	α	τ_{vis}	$\rho_{f,vis}$	$\rho_{b,vis}$	U [W/m^2.K]	g
SG	0.85	0.08	0.08	0.08	0.90	0.08	0.08	5.73	0.88
SG_SCF *B*	0.11	0.58	0.55	0.30	0.16	0.58	0.58	5.63	0.23
SG_SCF *D*	0.25	0.37	0.38	0.36	0.35	0.33	0.37	5.63	0.41
SG_SCF *F*	0.35	0.27	0.14	0.36	0.66	0.12	0.14	5.62	0.51
SG_SCF *G*	0.22	0.25	0.13	0.52	0.39	0.7	0.12	5.62	0.44

3.4 Results and discussion

The daylight performance was evaluated through the absolute values of indoor illuminance on horizontal plane considering 500 lx as the recommended value for comfortable daylighting illumination for office room activities (e.g. writing, typing, reading, data processing) according to EN 12464-1 of 2014 [74] and considering the illuminance range values defined in the Useful Daylight Illuminance (UDI) metric [75]. The UDI metric considers that values below 100lx are insufficient and can contribute to increase the energy needs with artificial lighting, values between 100-300lx require supplementary artificial lighting and values above 3000lx can cause thermal and/or visual discomfort and therefore values in these illuminance ranges are not considered useful. On the contrary, values between 300-3000lx are considered useful and desirable for indoor environments. This section presents the experimental data of indoor illuminance on horizontal plane collected under overcast and clear sky conditions. The 12 individual data points with experimental measured illuminance values for each tested fenestration system were interpolated and extrapolated for mapping the illuminance distribution along the entire horizontal working plane area. Accompanying each graph, a digital photo taken before the measurements from the interior of the small-scale model with a Canon EOS 600D camera, controlled remotely, is shown.

Table 4 shows the outdoor illuminance on horizontal plane, E_{out}, registered at 09h00, 12h00 and 15h00 for the three measured days.

Table 4. Outdoor illuminance values [klx] on horizontal plane, E_{out}, measured at 09h00, 12h00 and 15h00, for clear sky conditions and overcast sky conditions

Illuminance values [klx]	09h00	12h00	15h00
Clear sky			
Summer solstice	72	104	116
Winter solstice	29	59	36
Overcast sky			
Low direct and global radiation		24	

3.4.1 Overcast sky conditions

In this section, the distribution of the illuminance levels at the work plan was evaluated through the absolute values of daylighting and the Daylight Factor (DF). The experimental procedure was performed during one day of February at 11h00 with predominance of overcast sky conditions where the average of outdoor global and diffuse radiation on horizontal plane during the data collection period were 281W/m^2 and 274W/m^2, respectively, and the outdoor illuminance on horizontal plane was ~26klx (Table 4).

- Solar and visible transmittance

Visible transmittance, τ_{vis}, is a fraction of the visible spectrum of daylight (380 to 720 nanometers) and the optical property that allows characterizing the "attenuation" of daylighting due to the presence of a glazing. The definition of this parameter through experimental methods uses illuminance measurements during an overcast day according to the following equation:

$$\tau_{vis} = \frac{E_{Vind}}{E_{Vout}} \tag{3.1}$$

where

E_{Vind}: indoor illuminance on vertical plane, measured closer to the inner pane of the glass and with the sensor facing the outdoor environment (vertical pyranometer attached to a vertical wood inside the small-scale model in Figure 25);

E_{Vout}: outdoor illuminance on vertical plane, measured closer to the outer pane of the glass and with the sensor facing the outdoor environment (vertical pyranometer attached to a vertical wood outside the small-scale model in Figure 25).

Figure 25 shows the results of the visible transmittance values for the five scenarios of the glazing systems, from the higher to the lower value of visible transmittance.

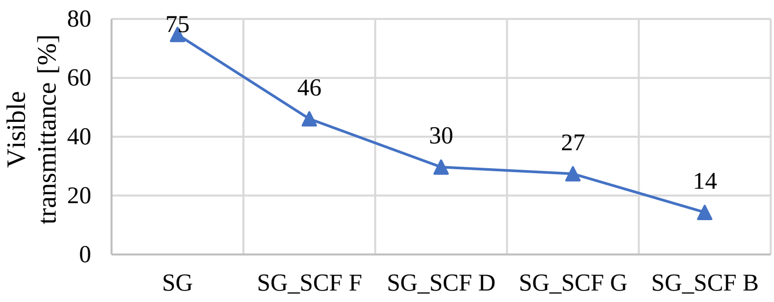

Figure 27. Visible transmittance values of the five glazing systems

The comparison between the transmittance values obtained from the Window and Optics tools (Table 3) and the experimental measurements ((Figure 27) show that the later ones are lower than expected. Since this difference is observed for all the scenarios, one reason could be that the substrate (single clear glazing with 6 mm, SG) used in the experimental procedure, for all the glazing scenarios, has a lower visible transmittance value than the observed for the same type of glass in the IGBD database of Window and Optics tools. Another reason could be associated with the distance between the gazing substrate and the sensor; due to the continuous replacement of the different substrates of this experiment and the sensor cable, the sensor could not be placed precisely after the glass substrate.

- Daylight Factor (DF) and Uniformity (Unif) on horizontal plane

Daylight availability can vary significantly throughout the days and seasons of the year, for both clear and overcast skies. However, assessing and characterizing daylight availability in indoor spaces can be a difficult task for overcast skies due to the high variability of daylighting associated with cloudy unpredictability and variability. For this reason, the assessment of daylight availability is not quantified nor evaluated by the absolute values of illuminance but rather by the proportion of the indoor and outdoor illuminance values, as follows:

$$DF = \frac{E_{Hind}}{E_{Hout}} \tag{3.2}$$

where

DF: Daylight Factor;

E_{Hind}: indoor illuminance value on horizontal plane;

E_{Hout}: outdoor illuminance value on horizontal plane.

The uniformity, Unif, is also an important quality parameter for the evaluation of indoor daylight since it quantifies the contrast in illuminance values and it is calculated as follows:

$$Unif = \frac{E_{Hmin}}{E_{Haver}} \tag{3.3}$$

where

$Unif$: Uniformity;

E_{Hmin}: minimum indoor illuminance value on horizontal plane;

E_{Haver}: average illuminance value on horizontal plane.

The assessment of daylighting levels under overcast conditions is usually carried out with the primary objective of quantifying the distribution of illuminances through the Daylight Factor (DF). The DF presents a significant advantage over other concepts or methods for characterizing the daylight availability in indoor environments under overcast sky conditions [76], since, in principle, it should not vary with the outdoor conditions. As the outdoor daylight availability varies due to cloudy unpredictability, so thus the indoor daylight availability, keeping the DF at constant values.

CIE recommends this method to analyze indoor daylighting conditions in buildings [76] under overcast sky conditions. This type of sky is not representative of the average climatic conditions occurring in

Portugal; however, it is useful for establishing minimum daylight conditions since it represents the worst-case scenario in terms of daylight availability [76].

Figure 28 shows the DF and Unif values on horizontal plane at 0.8 m height (working plane) in a scale ranging from 0 to 26 % under overcast sky for the 5 scenarios of the fenestration system: SG; SG_SCF B; SG_SCF D; SG_SCF F, and SG_SCF G. Due to technical difficulties it was not possible to take digital photos from the interior of the small-scale model in overcast sky conditions.

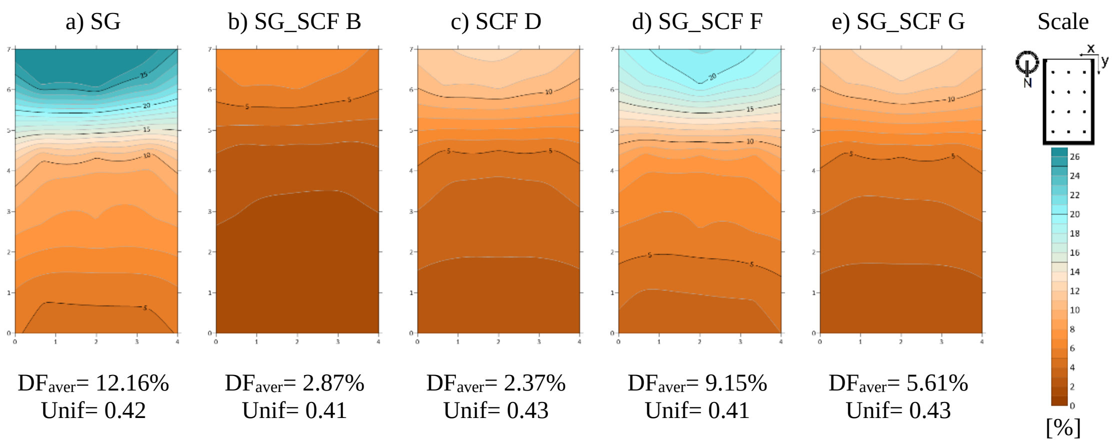

Figure 28. DF on horizontal plane under undercast sky conditions

3.4.2 Clear sky conditions

Figure 29 and Figure 30 show the digital photos and the indoor illuminance values on horizontal plane at 0.8 m height (working plane) in a scale ranging from 0 to >10 klx at 9h00, 12h00 and 15h00 under clear sky conditions in both summer and winter solstices, respectively, for the 5 scenarios of the fenestration system: SG; SG_SCF B; SG_SCF D; SG_SCF F, and SG_SCF G. The photos were taken from the interior of the small-scale model with a Canon EOS 600D camera, controlled remotely.

During both summer and winter seasons, all SCFs significantly reduced the indoor illuminance values, showing in the summer solstice lower illuminance values than those obtained in the winter solstice. This can be explained by the higher summer sun angles and thus lower values of incident direct radiation on a façade South oriented in the summer period when compared to the winter period [77]. This effect is also noticed in the photos captured inside of the small-scale model (see photos of the *SG* in Figure 29 and Figure 30, as an example).

In the summer solstice, illuminance values on a horizontal plane for the glass with SCFs vary between 0-1000 lx in a significant area of the horizontal working plane at 0.8 m, except for *SG_SCF F*, which is the film with the higher value of the solar transmittance. While the *SG* and *SG_SCF F* showed values higher than 500-1000 lx in almost all of the total area of the working plane, SCFs *SG_SCF B*, *D* and *G* showed illuminance values between 500-1000 lx in more than 50%, which results in a better visual performance by preventing possible glare situations. The *SG* and *SG_SCF B* scenarios showed the highest and the lowest range of illuminance values, varying between 0.33-10 klx and 0.34-2.11 klx, respectively, which results in a higher and lower daylight availability asymmetry throughout the horizontal working plane. Analyzing the experimental results in the summer solstice through the range values defined in the UDI metric, it is possible to conclude that the reference scenario, *SG*, showed the highest area of illuminance values outside the useful range (>3 klx), which indicates that this scenario shows a high risk of causing visual discomfort conditions to perform any type of work activity. In the summer solstice, *SG_SCF A* and *B* showed a high area of the working plane within the useful illuminance range value, however in the winter solstice almost all the illuminance values are above the useful range. The most reflective film, *SG_SCF C*, showed values within the useful range throughout the day in all the area of the working plane, except during the winter solstice at 12h00. *SG_SCF D* showed medium values between the two spectrally selective *SG_SCF A* and *B.*

In the winter solstice, as expected, the illuminance values were higher for the *SG* since it is the fenestration scenario with the highest solar factor, showing illuminance values higher than 500 lx in all the horizontal working plane area and above 10 klx in 50% of the horizontal working plane area. The *SG* scenario's results indicate that visual discomfort through the influence of glare situations can occur, making this space unpleasant or even impossible to work on it without the activation of complementary shading devices. *SG_SCF A*, *B* and *D* also showed values well above the recommended values of 500 lx to perform office tasks while the reflective *SG_SCF C* showed illuminance values closer to those recommended during the morning and afternoon periods. The results of the reference scenario, *SG*, showed illuminance values outside the useful range in almost all the working plane area, which indicates that from 09h00 to 15h00 the illuminance levels are so high that visual discomfort associated with glare is very likely to occur. Spectrally selective *SG_SCF A* and *B* showed, during the morning and afternoon periods, small areas within the useful range of illuminance values (0.3-3 klx) in the working plane area. The reflective *SG*_SCF *C* and *D* exhibited a higher area of the grid within the useful illuminance values, especially *SG_SCF C* with more than 50% of the grid area within the useful values during the morning and afternoon periods. In fact, when compared to the other films, *SG_SCF C* (τ_{sol}= 11%, τ_{vis}= 16%) provides the highest decrease of the illuminance values and thus is the most appropriate retrofitting scenario to prevent possible glare situations during both summer and winter seasons.

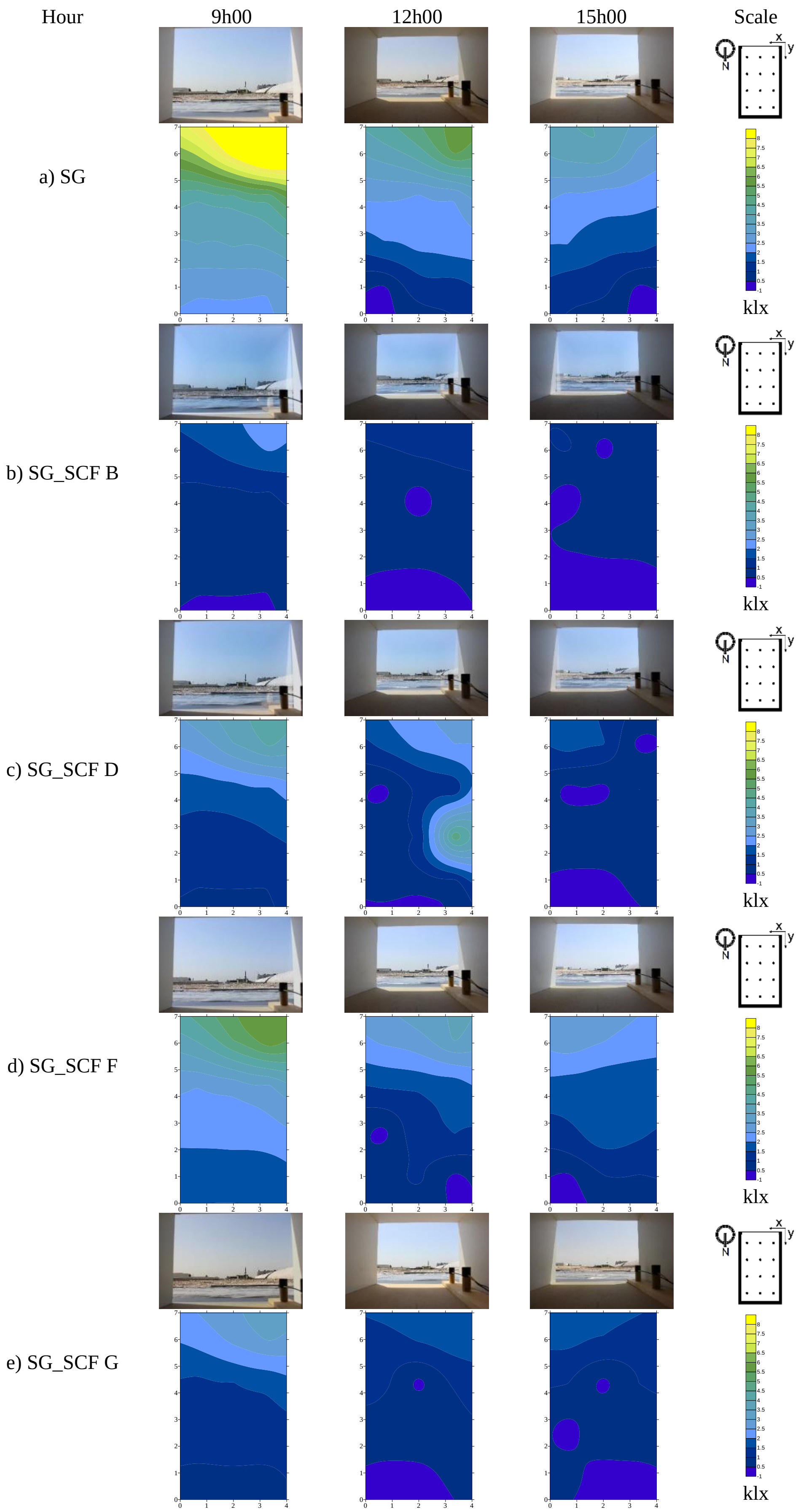

Figure 29. Photos and illuminance levels on horizontal plane in the summer solstice under clear sky conditions

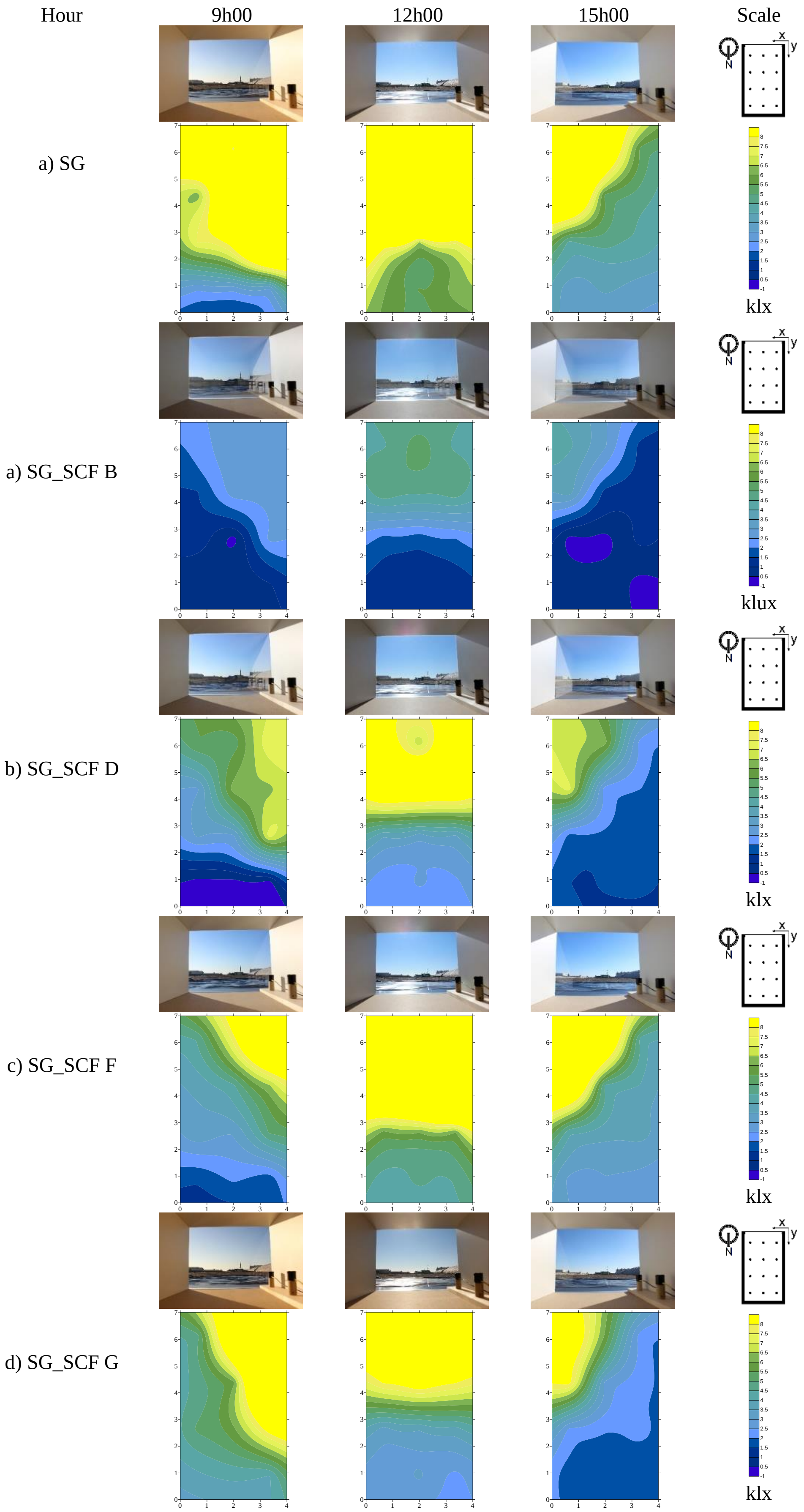

Figure 30. Photos and illuminance levels on a horizontal plane in the winter solstice under clear sky conditions

3.5 Conclusion and perspectives

In this study, the indoor illuminance distribution on the horizontal working plane at 0.8 m was measured under clear sky conditions in the summer and winter solstice using a small-scale model for 5 different glazing systems. A single pane clear glass with 6 mm was tested and taken as the reference scenario. Furthermore, four different solar control films, two spectrally selective and two reflective, were applied to the external surface of a 6 mm single-pane clear glass and tested.

The results show that for single-pane glass systems, SCFs can significantly decrease the indoor daylight illuminance levels likely to cause glare problems (≥ 3 klx), which is a relevant issue in locations with predominant clear sky conditions. The application of SCF in glazing showed a greater performance in summer, when compared with single glazing without SCF, not only in decreasing the illuminance levels below the critical values (3 klx), but also in promoting a more extensive spatial distribution of acceptable levels of daylight availability (0.3 – 3 klx). In winter, the performance of these films was not as noticeable as in summer, due to the lower sun's height and greater perpendicularity of the sun's rays to the glazing surface.

The application of reflective SG_SCFs B and D and spectrally selective SG_SCF F and G on a 6 mm single-pane glass decreased the illuminance indoor values throughout the working plane, which had a positive effect in lessening possible glare situations due to the high illuminance levels, in both summer and winter seasons.

The highly reflective film, SG_SCF C, which has the lowest solar and visible transmittance, was found to be the best retrofitting scenario in providing illuminance values within the useful range (0.3 – 3 klx) according to the UDI metric ranges in clear sky days. Therefore, this film has the highest potential to increase the visual comfort conditions in office rooms with single pane clear glass oriented to South, showing illuminance values closer to 0.5 lx in a higher area of the working plane and preventing possible glare situations when compared to the other films, during sunny days in both summer and winter seasons. In fact, except SG_SCF C, for which the area with acceptable values of illuminance during the winter is considerable, the other three SCFs lead to higher risk of glare occurrences in the whole room extension. During the winter solstice when compared to the summer solstice under clear sky conditions, SG_SCF C showed higher illuminance values across the working plane. On the one hand, this film decreased the daylight availability reducing the risk of glare occurrences during both summer and winter seasons and, on the other hand, as the results showed, it did not decrease the daylight values to a point where supplementary artificial lighting is required for office work activities. Nevertheless, to overcome the problem with glare occurrences, movable shading devices might be considered as a feasible complementary solution, especially during the winter period under clear sky conditions.

This section focused the analysis on visual comfort and under clear sky conditions, which are typical of Southern countries, where summer is the dominant season, and under overcast sky conditions, which can be considered as the worst scenario for cloudy days. Window films when compared to shading solutions decrease the solar and visible transmittance of glazing systems without compromise the view to the outside, which, alongside the ease of maintenance (same as the glass without SCF) and flexibility in application, is an advantage. As a possible drawback of the films studied, which may cause suspicion in the use of window films, the less durability of this solution is pointed out when compared to traditional ones. Depending on the type of application (on the internal or external side of the glass), the service life of these films can vary between 6 and 12 years and thus require frequent replacements to maintain the same performance throughout the building operation stage, which can be a disadvantage of SCFs when compared to shading solutions. Other potential drawback is the decrease of the daylight availability and the heat gains during the winter season, which can lead to higher energy demand with electric lighting and heating loads. Therefore, although these films proved to be appropriate when the aim is to minimize the risk of visual discomfort, it is recommended in the design to extend the analysis to overcast sky conditions and to thermal comfort, even if these are not the prevailing climate conditions in European Southern countries such as Portugal.

The results of this study show that SCFs have a high influence in the indoor illuminance levels and therefore the studies on visual comfort metrics and on thermal and energy efficiency indicators should not be considered separately but instead in an integrated approach enabling to better understand the trade-offs between the variation of solar and visible transmittance and the heat gain/losses coefficients derived from the application of the film. Also, a combined approach between SCFs and other shading devices should be considered to increase the visual comfort conditions when higher illuminance levels are registered.

4. Performance of solar control films in single-glazed windows

This section examines the thermal and luminous performance of single-glazed windows of an existing building without and with solar control films (SCFs) and a venetian blind for comparison purposes in actual working conditions. An experimental campaign was carried out simultaneously in both cooling and heating seasons in two similar office rooms, one with a SCF applied on the internal surface of the glass and the other without any SCF. The experimental data was used to calibrate a simulation model in EnergyPlus and assess the energy performance of several SCFs with different thermal and optical characteristics for different orientations of the façade. A decision-making framework was applied to identify the potential use of SFCs as retrofitting solutions for single-glazed windows based on energy performance criteria. The investigation developed in this section give rise to the publication [25].

4.1 Methodology

Thermal, luminous and energy performance of the glazing system of two similar offices in Lisbon (38°7′N, 9°1′W), one with a solar control film (SCF) – retrofitted office – and the other without – reference office –, were investigated through combined experimental and modelling approaches. The methodology showed in Figure 31 comprises the following steps:

a. experimental campaign carried out simultaneously in both offices during the cooling and heating seasons and included temperature, illuminance, and irradiance measurements;

b. calibration of the reference office through a building energy simulation model using SketchUp and EnergyPlus modelling software [78]. The model calibration was based on the use of the statistical indices Mean Bias Error – *MBE* – and Coefficient of variation of the Root-Mean Square Error – $C_{v,RMSE}$ –, which are found to adequately measure the level of approximation between numerical and experimental results [79]–[81];

c. simulation of the reference office to assess the current conditions of the heating, cooling, and lighting energy needs;

d. definition of the different configurations of the glazing system of the office using Window and Optics tools [73] to calculate glazing system optical and thermal metrics: without SCFs and with different types of SCFs (SG_SCFs *A* to *G* designed for application on the external side of the glass and SG_SCFs *H* to *M* designed for application on the internal side) and with a venetian blind (VB) for North (N), South (S), East (E) and West (W) solar orientations;

e. using hourly weather data, annual energy use was estimated and analysed for different configurations of the glazing system of the office. The energy performance of the case study was estimated and compared for all solar control solutions – SCFs and venetian blind – and a decision-making framework was designed to select a trade-off solution according to the defined objective.

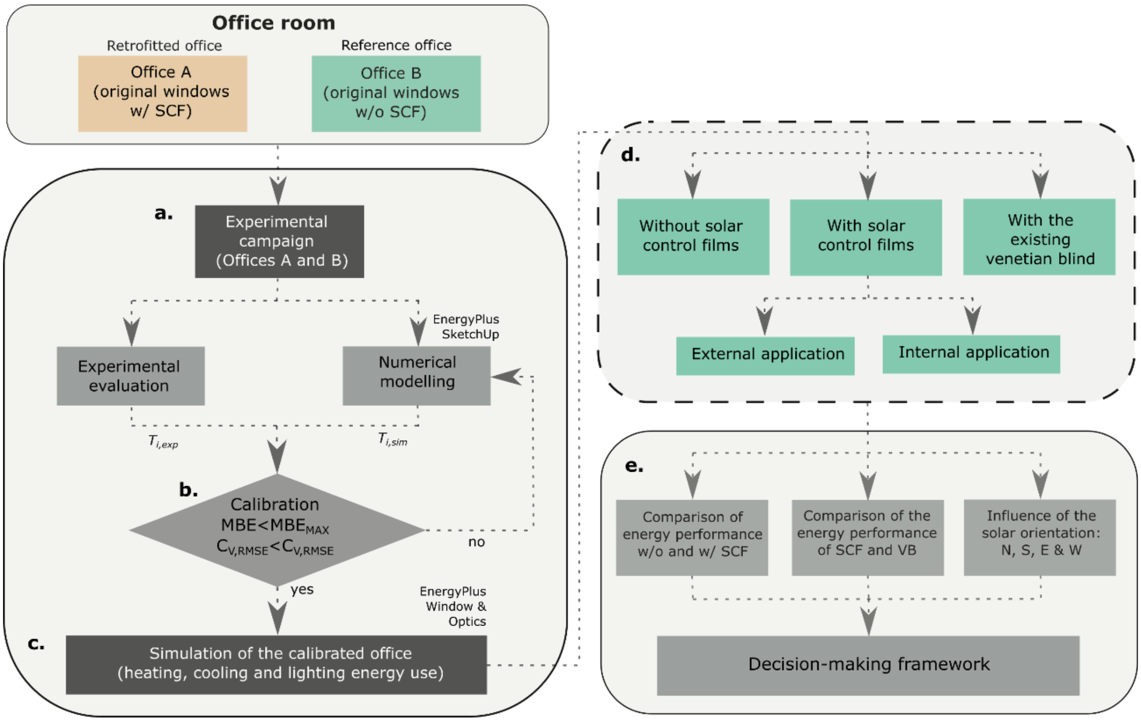

Figure 31. Methodology flowchart

4.2 Case study

Field experiments were carried out in two office rooms oriented East on the second floor of the DECivil building in Instituto Superior Técnico of Lisbon, Portugal (Figure 32a). The building, located in the city center, has a rectangular shape with four floors above ground: both the ground and the first floor consist essentially of classrooms and the second and third floors of office rooms. The façades have large areas (Figure 32b) of single clear glazed windows with 6 mm thickness and thermo-lacquered aluminium frames without thermal break.

By aiming to rehabilitate the glazing system via the decrease of the solar gains through the windows without compromising daylighting, the unit responsible for the building maintenance decided to make a pilot test in one office by installing a spectrally selective SCF on the glazing – office I – and observe the corresponding impact on comfort, namely during the summer season. The applied SCF is a commercial metal-free film with an almost clear colour and 38 µ thickness. In view of making the installation easier and cheaper, the film was applied on the internal side of the glass, although a later analysis of the technical sheet of the film recommended its application by the external side.

In this study the impact of this SCF under the actual installation conditions was assessed by confronting the experimental results obtained in the retrofitted office with those collected in the reference office – taken as basis for comparison – with the original glazing. The analysis of the same film but under the recommended installation conditions – application on the external side of the glass –, together with similar analyses of other films, is made through dynamic simulation of a calibrated model of the same typical office, allowing for comparative assessments and providing insight into the potential of thermal, luminous and energy improvement of SCFs as a retrofitting measure.

The offices I and II, where the experimental campaign took place, have a total area of 13.5 m^2 and 3.15 m height and a window area of 3.5x2.1 m^2 (Figure 32c). The façade oriented to the East is the only surface in contact with the outdoor environment and is exposed to direct solar radiation during the morning period. The office rooms have the same opaque and transparent components and the same configuration of the walls, ceiling, and floor.

Table 5 shows the main characteristics of the glazing system with and without SCF (office rooms I and II, respectively) and Figure 33 the full spectrum graphics for the Solar Control Film (SCF), the glazing system with and without SCF.

a. b. c.

Figure 32. Case study: (a) location of the building in the Faculty Campus; (b) East oriented façade and; (c) office rooms

Table 5. Thermal and optical characteristics of the glazing system of office I and II: visible transmittance, τ_{vis}, visible (front) reflectance, $\rho_{f,vis}$, visible (back) reflectance, $\rho_{b,vis}$, solar transmittance, τ_{sol}, solar (front) reflectance, $\rho_{f,sol}$, solar (back) reflectance, $\rho_{b,sol}$, absorptance, α, thermal transmittance, U, (W/m^2.K), solar factor, g

	τ_{vis}	$\rho_{f,vis}$	$\rho_{b,vis}$	τ_{sol}	$\rho_{f,sol}$	$\rho_{b,sol}$	α	U	g
Office I (w/ SCF)	0.66	0.12	0.14	0.35	0.27	0.14	0.36	5.80	0.46
Office II (w/o SCF)	0.89	0.08	0.08	0.77	0.07	0.07	0.16	5.91	0.82

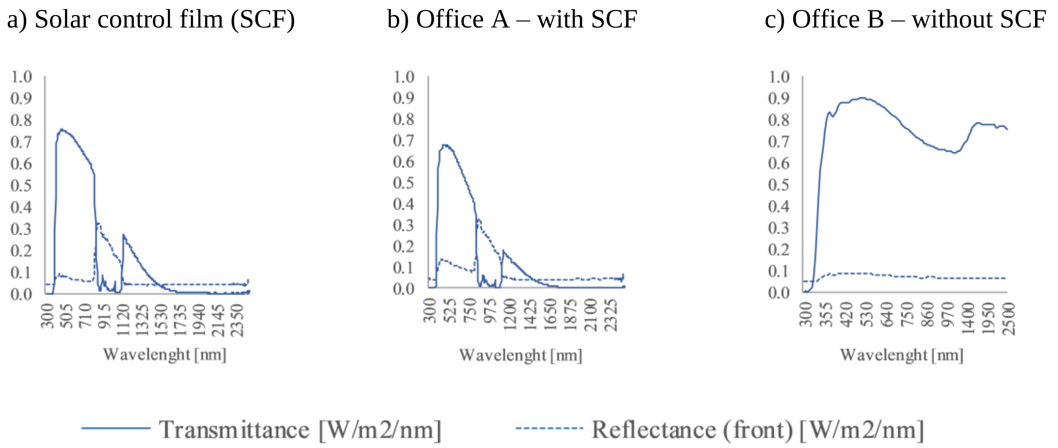

Figure 33. Transmittance and (front) reflectance of: a) solar control film (SCF), b) SCF in the internal side of the glass and, c) glass without SCF

Both offices have an internal venetian blind (VB) with vertical cream-coloured slats with 10 cm width, 8 cm distance between slats, 0.25 cm thickness and material conductivity of 0.2 W/m.K. During the data collection period, the VB was kept at the same position in both offices and outdoor obstacles, such as trees and overhangs, were flagged for further use in the modelling study. Internal gains were considered the same for the two offices due to the similarities in the schedules and characteristics of occupancy, electric equipment and lights. The HVAC system of both offices is a multi-split unit with COP= 3.0 and EER= 3.4. To simplify the modelling in the simulation study, the HVAC system was assumed to start operating when the indoor temperature is out of the thermal comfort range according to the Portuguese Regulation of the Energy Performance of Buildings (18ºC to 25ºC) [82].

4.3 Experimental set-up

The experimental campaign took place from 24th to 30th of November (heating season – winter) and from 25th to 31st of July (cooling season – summer). The following parameters were measured: i) indoor and outdoor temperature; ii) internal and external glass surface temperatures; iii) indoor and outdoor illuminance and irradiance on vertical plane and; iv) global solar radiation on horizontal plane. The internal (and external) glass surface temperatures were measured by securing thermocouples to the glass surfaces using overlapping layers of transparent tape to ensure the isolation from the indoor (and outdoor) environment. Field measurements are illustrated in Figure 34 and the main information about the equipment used can be found in Table 6. All measuring devices or sensors were connected to two data acquisition systems (one in each office room), data logger Campbell CR10X and DeltaT DL2 that recorded the data in ten minutes averages from one-minute records.

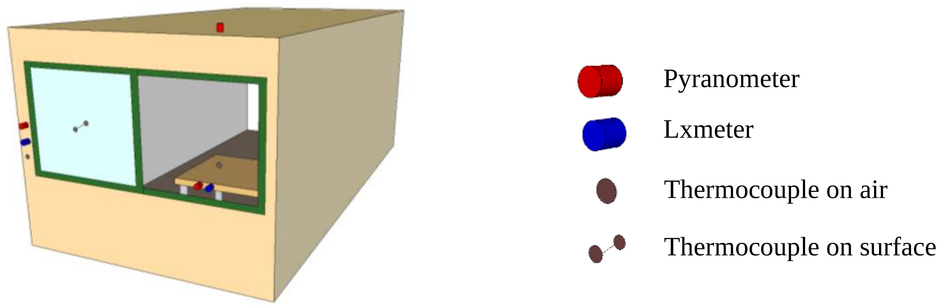

Figure 34. Layout of the instrumentation of a typical office room

Table 6. Equipment and measurements used in the experimental campaign

Equipment	Parameter	Model	Number	Precision	Name	Location
Thermocouple	Temperature	Type-T	7	±0.2ºC at 100ºC	T_{si}, T_{se} T_i, T_{out}	Internal and external surface of the glass Indoor and outdoor environments
Pyranometer	Global radiation	LI-COR LI210R	2	±3%	$I_{out,vert}$ $I_{out,hor}$	East façade's plane Roof
		Kipp & Zonen CMP3	2	±5% from -10ºC to 40ºC	$I_{i,vert}$	Side of the desk (15 cm away from the window)
Lxmeter	Illuminance	LI-COR LI200	3	±5%	$E_{i,vert}$ $E_{out,vert}$	Side of the desk (15 cm away from the window) East façade's plane

4.4 Simulation modelling

To evaluate the thermal and energy performance of different SCFs for several solar orientations, a building energy simulation model was performed in EnergyPlus software and calibrated by using the experimental data of the indoor temperature of the reference office. Due to very limited information available on SCFs, this study tested various SCFs with different thermal and optical characteristics to assess their performance and different applications on the glass substrate (internal and external application).

Table 7 lists different SCFs applied on a 6 mm clear glass (the same glass of the reference office) either on the external or the internal side and correspondent thermal and optical properties, in a descending order of solar (front) reflectance, $\rho_{f,sol}$. These properties were determined using Window and Optics tools [73], which are computer programs designed to deal with glass and glazing systems. For comparison purposes, the internal venetian blind existing in the offices was also implemented in the simulation model and its energy performance assessed considering full activation (whole window area covered by the device) and a constant 10º angle between slats. It is important to notice that SCFs *I* (U = 3.3 W/m^2.K) and *L* (U = 3.5 W/m^2.K) are the only films that decrease significantly the thermal transmittance, which is a result of their low-emissivity properties.

Table 7. Thermal and optical characteristics of a 6 mm glass, SG, with solar control films (SCFs) applied on the external and internal side, arranged in a descending order of solar (front) reflectance: solar (front) reflectance, $\rho_{f,sol}$, solar transmittance, τ_{sol}, visible transmittance, τ_{vis}, absorptance, α, emissivity, ε, thermal transmittance, U [W/m^2.K], solar factor, g, and light-to-solar gain ratio, *LSG*

	$\rho_{f,sol}$	τ_{sol}	τ_{vis}	α	ε	U [W/m^2.K]	g	LSG[2)]
External application								
SG_SCF A	0.64	0.10	0.15	0.26	0.87	5.64	0.20	0.75
SG_SCF B	0.59	0.10	0.16	0.31	0.70	5.64	0.23	0.70
SG_SCF C	0.50	0.17	0.26	0.33	0.87	5.64	0.30	0.87
SG_SCF D	0.37	0.23	0.34	0.40	0.84	5.64	0.39	0.87
SG_SCF E	0.34	0.29	0.43	0.37	0.76	5.63	0.44	0.98
SG_SCF F^{+} [1)]	0.27	0.33	0.65	0.40	0.87	5.63	0.50	1.30
SG_SCF G	0.25	0.21	0.38	0.54	0.87	5.63	0.43	0.88
Internal application								
SG_SCF H	0.53	0.14	0.18	0.33	0.71	5.30	0.21	0.86
SG_SCF I	0.46	0.22	0.34	0.32	0.04	3.30	0.26	1.31
SG_SCF J	0.27	0.36	0.47	0.37	0.79	5.50	0.45	1.04
SG_SCF K	0.26	0.21	0.23	0.53	0.90	5.80	0.33	0.70
SG_SCF L	0.19	0.47	0.70	0.34	0.10	3.50	0.52	1.35
SG_SCF M	0.16	0.36	0.39	0.48	0.93	5.80	0.46	0.85
Slats of the VB	0.75	0.10	0.50	0.15	0.90	-	0.45-0.56	1.00

[1)] corresponds to the spectrally selective film applied in office I under the recommended installation conditions – application on the external side of the glass

[2)] LSG = τ_{vis}/g

To assess the accuracy of the calibration model two commonly used statistical indices are employed [79]–[81]: the Mean Bias Error, *MBE*, which measures how close the simulation values are from the experimental values, and the Coefficient of variation of the Root-Mean Square Error, $C_{v,RMSE}$, which is a normalized measure that determines how well the simulation values fit the experimental ones considering both positive and negative differences. Lower values of $C_{v,RMSE}$ indicate a lower dispersion between simulation and experimental data. *MBE* and $C_{v,RMSE}$, written as percentage errors, were calculated through equations (4) to ().

$$MBE_n(\%) = \frac{\sum_{i=1}^{n}(X_{sim,i} - X_{exp,i})}{\sum_{i=1}^{n}(X_{exp,i})} \times 100\% \tag{4.1}$$

$$C_{v,RMSE}(\%) = \frac{\mathrm{RMSE}_n}{\bar{X}_{exp}} \times 100\% \tag{4.2}$$

$$\mathrm{RMSE}_n = \sqrt{\frac{\sum_{i=1}^{n}(X_{sim,i} - X_{exp,i})^2}{n}} \tag{4.3}$$

$$\bar{X}_{exp} = \frac{\sum_{i=1}^{n}(X_{exp,i})}{n} \tag{4.4}$$

where $X_{sim,i}$ and $X_{exp,i}$ are the simulated and the experimental data for the *i* period, respectively, $\bar{X}_{exp}$ is the experimental mean value and *n* the number of input data.

4.5 Experimental results

In this section, two comparable days for each summer and winter measuring periods are analysed in detail regarding the thermal, energy and luminous performance. These days were selected in periods without occupancy in both offices and no HVAC operation during both summer (*DwC-S*, 27th and 28th of July) and winter (*DwC-W*, 24th and 30th of November) seasons to minimize the influence of the different occupant behaviour in the results.

Table 8 presents the average and maximum outdoor temperature for the sun-hours period and the incident global solar radiation on vertical plane for those selected days.

Table 8. Average and maximum outdoor temperature (T_{out} and $T_{out,max}$), and incident global solar radiation on vertical plane ($I_{out,vert}$ and $I_{out,vert,max}$), for summer (*DwC-S*) and winter (*DwC-W*) representative days for the sun-hours period

	T_{out} [ºC]	$T_{out,max}$ [ºC]	$I_{out,vert}$ [W/m^2]	$I_{out,vert,max}$ [W/m^2]
DwC-S (27th/28th of July)	22.66/22.00	34.12/26.10	192/112	577/317
DwC-W (24th/30th of Nov)	11.21/10.63	13.90/12.89	164/148	553/550

4.5.1 Indoor and surface temperatures

Figure 35 shows the indoor, outdoor, and internal and external glazing surface temperatures, along with the incident solar radiation on vertical plane in the selected summer and winter days. It can be observed that the indoor temperature has the highest increase during the morning period, between 06h00 and 12h00, evidencing the strong influence of the direct solar radiation on the indoor environment of the offices.

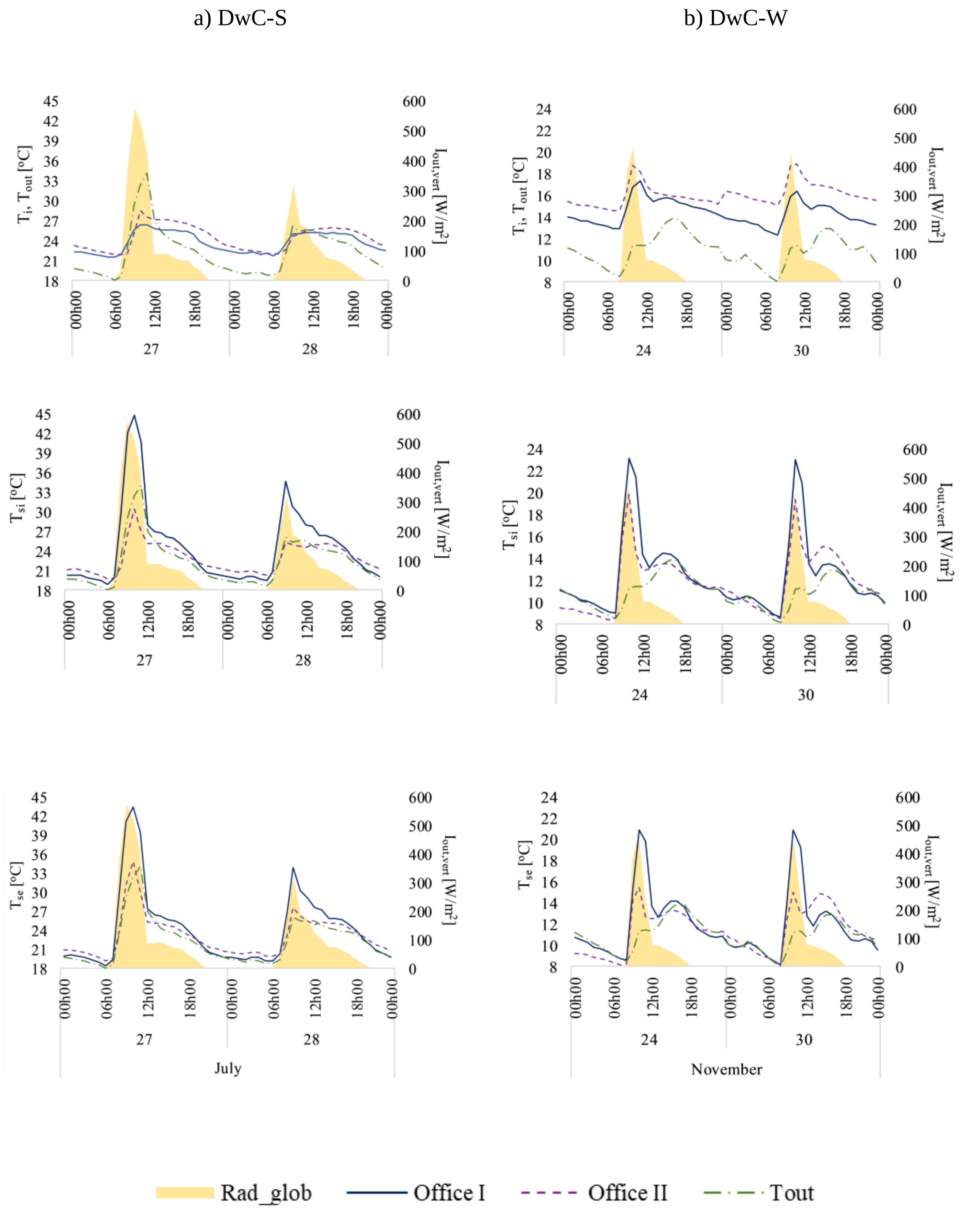

Figure 35. Indoor, T_i, and outdoor, T_{out}, temperatures, internal, T_{si}, and external, T_{se}, surface temperatures, and global solar radiation on vertical plane, $I_{out,vert}$, in office I (w/ SCF) and office II (w/o SCF) for: a) DwC-S and; b) DwC-W

By comparing the daily values of the indoor temperature of office I (w/ SCF) with office II (w/o SCF), an average daily (and peak) reduction during working hours (from 9h00 to 18h00) in office I of 0.92ºC (and 2.03ºC) and 0.47ºC (and 0.76ºC) is observed on the 27th and 28th of July and of 1.06ºC (and 1.94ºC) and 2.31ºC (and 2.57ºC) on the 24th and 30th of November, respectively. It is interesting to note that the level of irradiance in the two winter days is almost similar to that of summer day July 27th (Table 8) but induces a higher temperature reduction between offices I and II. This may be due to the lower winter sun angles and corresponding higher glass solar transmittances, which highlights the effect of the SCF in office I [77], [83], [84].

Regarding the surface temperatures, when the offices are directly exposed to solar radiation, the internal surface temperature of the glass is higher in office I (w/ SCF) than in office II (w/o SCF), reaching peak values in office I of 44.8ºC and 34.6ºC in the two summer days respectively, and 23.1ºC in both winter days. The external surface temperature of the glass in office I (w/ SCF) is also higher than in office II (w/o SCF) when the offices are exposed to direct solar radiation, reaching peak values in office I of 43.4ºC and 34.9ºC in the summer days, and in office II of 20.9ºC and 15.5ºC in the winter days. The higher surface temperatures of the glass with SCF (office I) are due to the increase of the absorption coefficient with the application of the film (α_I = 0.36 and α_{II} = 0.16). Moreover, when the offices are not directly exposed to solar radiation, the surface temperatures of the glass in both offices approximate each other and the outdoor temperature ($T_{si,I} \approx T_{se,I}$ and $T_{si,II} \approx T_{se,II}$).

Regarding the performance of the applied SCF (office I), the results did not meet the expectations since the reduction in indoor temperature of the office was low (less than 1ºC on average on a daily sun-hours basis during the summer days) when compared to office II (w/o SCF). This can be explained by the low reflective coefficient of the glass w/ SCF (Table 5) and by the fact that the film was applied to the wrong side of the glass. In fact, the correct application of the SCF in office II should be on the external surface of the glass and not on the internal surface as it was done. As a consequence of the incorrect application of the film in the glazing, the absorptance and (front) reflectance coefficients are operating to the indoor environment, which may contribute to increasing the indoor and internal glass surface temperatures. Also, the fact that the internal partition/wall between the offices in not adiabatic may increase the heat exchanges between the office areas and lessen the difference in indoor temperature.

4.5.2 Indoor vertical irradiance and illuminance

Figure 36 and Figure 37 show the indoor and outdoor irradiance and illuminance on vertical plane, respectively, in both offices I and II.

During insolation hours, the indoor irradiance (I_i) and illuminance (E_i) on vertical plane are higher in office II (w/o SCF) than in office I (w/ SCF) for the summer and winter days.

The use of the SCF produced an average daily reduction in indoor irradiance on vertical plane of 48-55% on the 27th and 28th of July and 49-50% on the 24th and 30th of November. These results are in accordance with the lower values of the solar factor of the glazing system with SCF (Table 5). As expected, the use of SCF decreases the solar gains through windows, which in general has a positive effect in summer, in terms of thermal comfort and energy savings, but a negative one in winter, where solar gains are welcome for naturally increasing the indoor temperature. Regarding the illuminance levels, the average daily reduction in indoor illuminance on vertical plane due to SCF use in office I, compared with office II, was 14-15% on the 27th and 28th of July and 49-50% on the 24th and 30th of November. It is possible to note that the daily reduction in indoor illuminance on vertical plane was higher in the winter than in the summer days. Moreover, an analysis using the UDI concept (Useful Daylight Illuminance) [75] was performed (Table 9). Daylight illuminance values below 100 lx can contribute to increasing energy consumption with artificial lighting and above 3000 lx can induce thermal and/or visual discomfort and lead occupants to activate shading devices.

Table 9. Useful daylight illuminance for office I and II during summer and winter periods

		Useful daylight illuminance (%)		
		$UDI_{<100}$	$UDI_{100\text{-}3000}$	$UDI_{>3000}$
DwC-S (27th/28th of July)	Office I (w/ SCF)	6.5	32.3	61.3
	Office II (w/o SCF)	6.5	29.0	64.5
DwC-W (24th/30th of Nov)	Office I (w/ SCF)	15.4	61.5	23.1
	Office II (w/o SCF)	15.4	34.6	50.0

It is possible to conclude that the $UDI_{100\text{-}3000}$ increases with the use of SCF in the glazing system by 3.2% and 26.9% for the summer and winter periods, respectively, and the $UDI_{<100}$ is the same in both offices for both the winter and summer periods.

The ratio of the measured indoor, E_i, and outdoor, E_{out}, illuminance on vertical plane allows to estimate the visible transmittance of the glass which, according to the measured data is 0.71 and 0.82 for offices I and II, respectively, in the summer days and 0.65 and 0.89 for offices I and II, respectively, in the winter days. By comparing these results with those of the simulation programs Window and Optics ($\tau_{vis,I}$= 0.66 and $\tau_{vis,II}$= 0.89, Table 5) it is possible to conclude that the experimental and simulation results are closer to each other during the winter days, which is a consequence of the lower sun angles in the winter days being closer to a normal incidence (optical properties of the glazing in the simulation programs are calculated at normal solar incidence), when compared to the summer days.

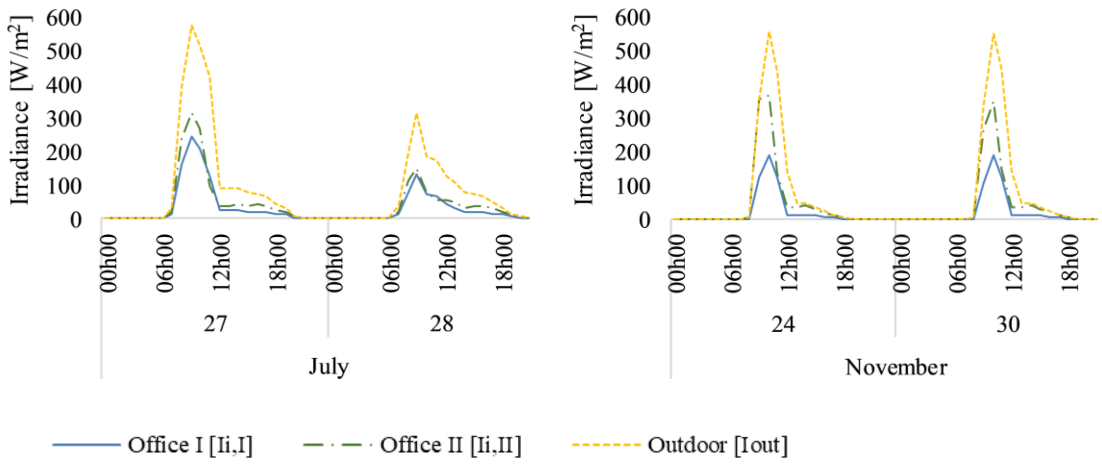

Figure 36. Indoor irradiance on vertical plane in office I, $I_{i,I}$, office II, $I_{i,II}$, and outdoor irradiance on vertical plane, I_{out}

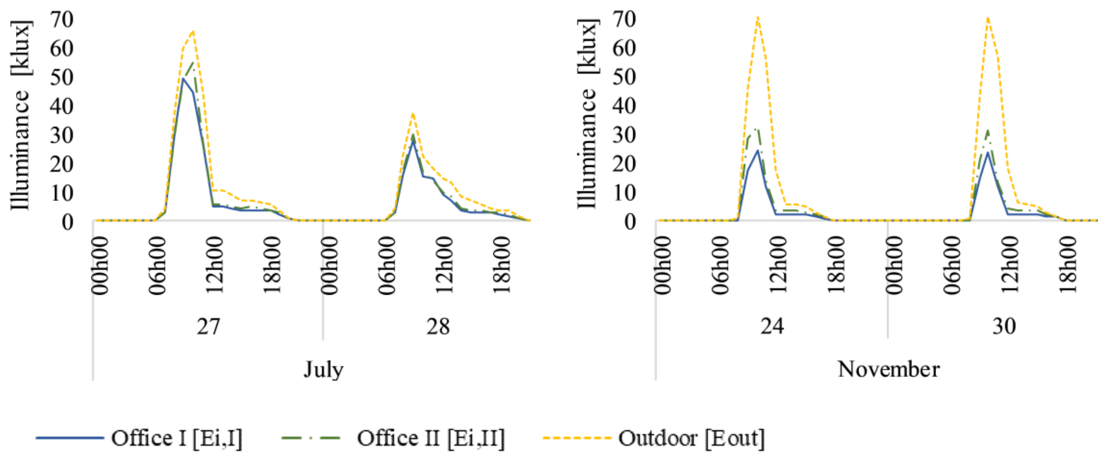

Figure 37. Indoor illuminance on vertical plane in office I, $E_{i,I}$, office II, $E_{i,II}$, and outdoor illuminance on vertical plane, E_{out}

4.6 Simulation results

4.6.1 Model calibration

The data collected in the experimental campaign, the indoor temperature and the climate data (outdoor temperature and global solar radiation on horizontal plane), was used to calibrate a computational model of the reference office built into the EnergyPlus building simulation program. The model calibration is important to minimize the difference between predicted simulated and measured experimental values and was performed for indoor temperature during one week of the cooling (25th to 31st of July) and of the heating (24th to 30th of November) seasons.

Figure 38 shows the experimental and simulated values of indoor temperature along with the outdoor temperature and incident global solar radiation on horizontal plane. Table 10 presents, by its turn, the error values for the heating and cooling periods calculated through equations (4.1) to (4.4).

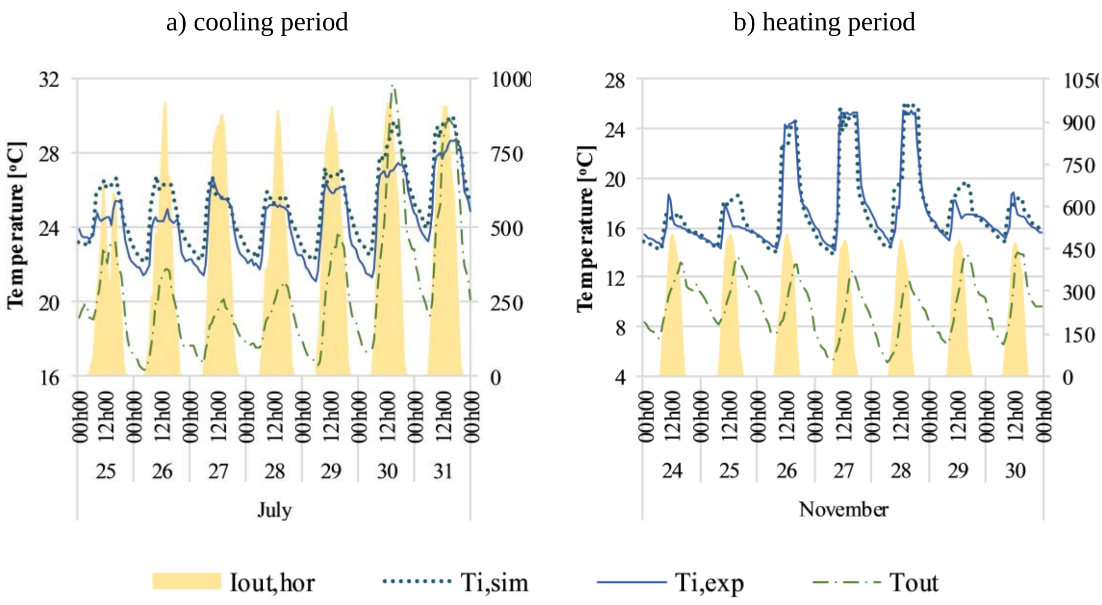

Figure 38. Computed and experimental indoor temperatures along with outdoor temperature and solar radiation on horizontal plane from: a) 25th to 31st of July (cooling period) and; b) 24th to 30th of November (heating period)

Table 10. Threshold limits and indices of the manual hourly calibration of the reference office

	Reference office calibration		Maximum values		
	Cooling period	Heating period	[79]	[80]	[81]
MBE	-0.86	1.18	±10	±5	±10
$C_{v,RMSE}$ (%)	6.10	6.22	30	20	30

It can be observed from Figure 38 that, although the experimental and the simulated values present some differences, the general trend is apprehended by the simulated model for both cooling and heating periods. It is worth highlighting that in the cooling period the difference between experimental and simulated values, $T_{i,exp}$ and $T_{i,sim}$, is higher during non-working hours on workdays. This means that the outputs obtained by the simulation model during working hours (from 9h00 to 18h00) have a lower error value associated in the cooling period. As referred to before, the modelling error was evaluated by two statistic indices, the Coefficient of variation of the Root-Mean Square Error ($C_{v,RMSE}$) and the Mean Bias Error (MBE). To validate the calibration, both indices were compared with threshold limits given by the Standard/Protocol presented in Table 10 [79]–[81]. As it can be observed in Table 10, MBE and $C_{v,RMSE}$ indices calculated for the reference office are both much lower than the threshold limits admitted in the literature for model calibration. Therefore, the simulation model can be considered sufficiently accurate to reproduce the thermal and energy performance of the reference office of the case study and thus appropriate to perform simulations for different scenarios, such as glazing systems with different types of solar control films, as described in the following section.

4.6.2 Impact of SCF

In order to assess the impact of several solar control films (SCFs), seven different SCFs with application on the external side of the glass (SCFs *A* to *G*) and six with application on the internal side of the glass (SCFs *H* to *M*) were selected and the respective performance evaluated by computational simulation using the EnergyPlus office model calibrated as described in section 6.6.1. The optical and thermal characteristics of the glazing system with these SCFs were calculated through Window and Optics programs (Table 7) and then used to define different transparent materials in EnergyPlus. The SCF selected for the simulation study also included the film existing in office I and simulations were performed for the internal and external surface positioning on the glass. The first case corresponds to the actual case study of incorrect application, with solar and optical characteristics given in Table 1 and identified in simulations as case *F-*. The second case corresponds to the application on the correct side of the glass and is assigned with the reference symbol *F+* in Table 3. Moreover, the existing venetian blind in the reference office was also modelled in EnergyPlus (Table 7) for comparison purposes.

In a first stage, some simulations were carried out without HVAC system in EnergyPlus to infer the influence of SCFs and the existing venetian blind on the thermal behaviour of the office and to assess the indoor thermal comfort conditions. With this purpose, the indoor temperature was simulated and analysed for two days, the coldest and the warmest day of the year using synthetic data of weather conditions based on thirty years of meteorological data (weather file) for Lisbon, Portugal. The coldest day was registered on the 31st of January with an average outdoor temperature during working hours (from 9h00 to 18h00) of 8.74ºC and global solar radiation on horizontal plane of 245W/m^2. The warmest day was registered on the 29th of August with an average outdoor temperature during working hours of 32.41ºC and global solar radiation on horizontal plane of 426W/m^2. Figure 39 presents the global solar radiation on the façades' plane, $I_{out,vert}$, indoor temperature of the office for the warmest and coldest days of the year for 5 different scenarios of the glazing system: without SCF (*Glass*), with the original SCF applied on the wrong side of the glass (SCF *F*-), with the same film but applied on the correct side (SCF *F*+), with the SCF with the highest solar (front) reflectance coefficient (SCF *A*) and with the venetian blind (*VB*).

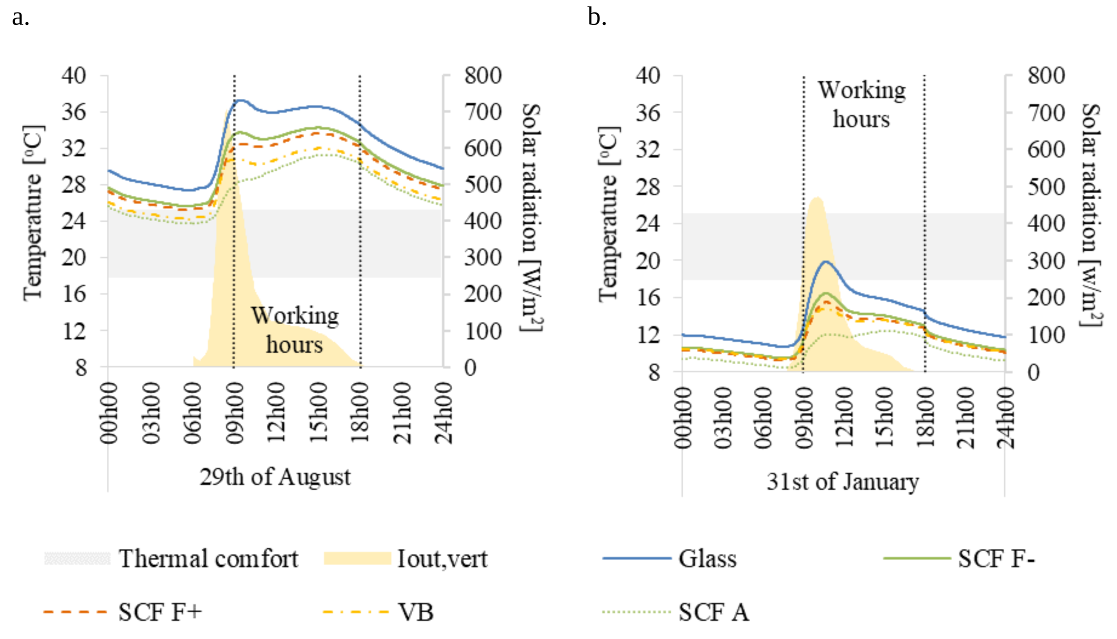

Figure 39. Global solar radiation on the façades' plane, $I_{out,vert}$, indoor temperature of the office for the glazing system without SCF (*Glass*), with SCF *F*- (wrong side of the glass), with SCF *F*+ (correct side of the glass), with SCF *A* (highest solar front reflectance coefficient) and with *VB* (venetian blind), for: a) warmest day and; b) coldest day

In the warmest day of the year: i) for all the cases analysed in Figure 39a, the indoor temperature during working hours is above 25ºC, which is the summer reference comfort temperature for Portugal according to Portuguese legislation [82]; ii) SCF *F*-, SCF *F*+, SCF *A* and the *VB* reduced the peak indoor temperature of the office at 9h30, when compared with the case without SCF (*Glass*) in 3.0ºC, 4.8ºC, 8.9ºC and 6.5ºC, respectively; iii) SCF *F*-, SCF *F*+, SCF *A* and the *VB* reduced the daily average indoor temperature in the office, when compared with the case without SCF (*Glass*) in 2.2ºC, 2.8ºC, 4.1ºC and 2.9ºC, respectively; iv) in the warmest day of the year, SCF *A* presents the highest thermal performance when compared to the cases analysed in Figure 39a for this summer day, which can be explained by the low value of solar transmittance and high value of solar (front) reflectance when compared to the other SCFs and the *VB* (Table 7).

In the coldest day of the year: i) for all the cases analysed in Figure 39b, the indoor temperature during working hours is below 18ºC except for the case of the office without SCF (*Glass*) from 10h00 to 12h00, which is the winter reference comfort temperature for Portugal according to Portuguese legislation [82]; ii) SCF *F*-, SCF *F*+, SCF *A* and the *VB* reduced the peak indoor temperature in the office at 10h40, when compared to the case without SCF (*Glass*) in 3.4ºC, 4.4ºC, 7.8ºC and 5.0ºC, respectively; iii) SCF *F*-, SCF *F+*, SCF *A* and the *VB* reduced the daily average indoor temperature in the office, when compared with the case without SCF (*Glass*) in 1.7ºC, 2.1ºC, 3.3ºC and 2.1ºC, respectively; iv) in the coldest day of the year, the office without SCF had the best thermal performance when compared to the cases analysed in Figure 39b, as expected, since a solution of the glass without SCFs or the VB presents the highest solar transmittance.

It should be noted that the application of SCFs *F+* and *A* showed a higher reduction of the peak indoor temperature in the warmest day than in the coldest day of the year. Although these films did not provide indoor temperatures within the reference comfort temperature range of 18-25ºC during working hours, the decrease in the peak indoor temperature in the hottest day of the year suggests that these films may have an important contribution in reducing the cooling energy needs and thus improving the energy efficiency of the office during the summer season.

To enhance the knowledge of the thermal comfort conditions provided by the application of SCFs and use of a venetian blind the number of working hours in a year for every temperature for the office without SCF (*Glass*) with SCFs *F*-, *F+* and *A* and the venetian blind *VB* were determined, as illustrated in Figure 40.

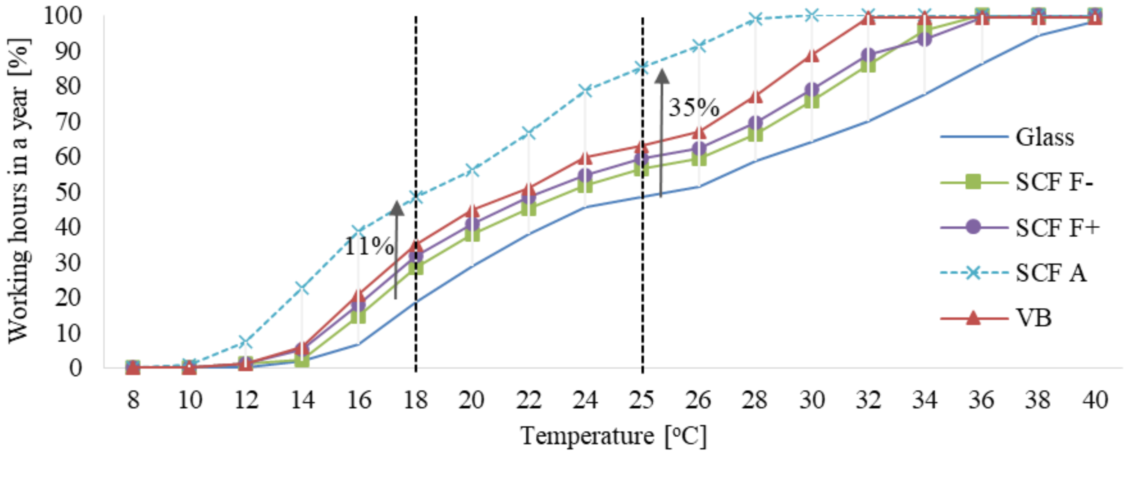

Figure 40. Number of working hours (from 9h00 to 18h00) in a year (%) for: Office w/o SCF (*Glass*), with SCF *F*- (wrong side of the glass), with SCF *F+* (correct side of the glass), with the SCF with the highest solar (front) reflectance coefficient (SCF *A*), and with the venetian blind (*VB*)

As it can be observed in Figure 40, the current glazing system of the typical office room (*Glass*) located in DECivil building in Instituto Superior Técnico do not provide thermal comfort for occupants, showing more than 50% of the working hours of the year above 25ºC and 19% below 18ºC, and 25% within the thermal comfort temperature.

It is also found that the use of SCF *F-* applied in the glazing of the office presents an improvement of the indoor thermal comfort conditions for the summer season, but not as high as the SCF *F+*, which represents the situation of the glazing with the same SCF but applied on the correct (outer) side of the glass. These results show that an incorrect application of the film can compromise the thermal performance of the office since the (front) reflectance coefficient is working towards the indoor environment and the absorptance coefficient is increasing the indoor temperature as the internal surface temperature of the film grows.

The venetian blind (*VB*) and SCF *F+* presented similar values of the number of working hours within the thermal comfort zone. Optical properties of the VB are dependent on solar incident angles, slat's material optical and thermal properties (Table 7) and slate's angle. With the use of a VB in the glazing, part of the solar radiation passes through the window without hitting the slats and the other part passes indirectly through reflections between slats and transmissions through the slats [85]. The results indicate that the existing VB in the office of the case study, with a constant 10º angle between slats and with the thermal and optical characteristics of the material indicated in Table 7, provide an annual indoor temperature closer to the SCF *F+* case than to the SCF *A* one (Figure 40).

SCF *A* improved the thermal comfort of the office during the summer season, presenting the highest decrease of the discomfort hours above 25ºC from 50% (office without SCF) to 15%, when compared to the other analysed solutions. Although this film did not improve substantially (12%) the percentage of hours throughout a year within the thermal comfort zone (from 25% in the office without SCF to 37% with SCF *A*), it improved considerably the number of hours above 25ºC, resulting in a more comfortable and energy efficient environment in the summer season.

In a second stage, simulations with HVAC system were conducted to analyse the impact on the energy performance of the different types of SCFs and the venetian blind listed in Table 7 for different façade solar orientations (North, N, East, E, South, S, and West, W). The simulation model was calibrated using EnergyPlus program (Figure 38 and Table 10) to analyse the energy performance of the office. SCFs with application on the external side (SCFs *A* to *G*) and on the internal side (SCFs *H* to *M*) of the glass were studied. Simulations without SCF (*Glass*) and with the venetian blind (*VB*) were also carried out for comparison purposes. The energy use for cooling, heating, and lighting is presented in Figure 41 and Figure 42, respectively, for external and internal application SCFs, respectively.

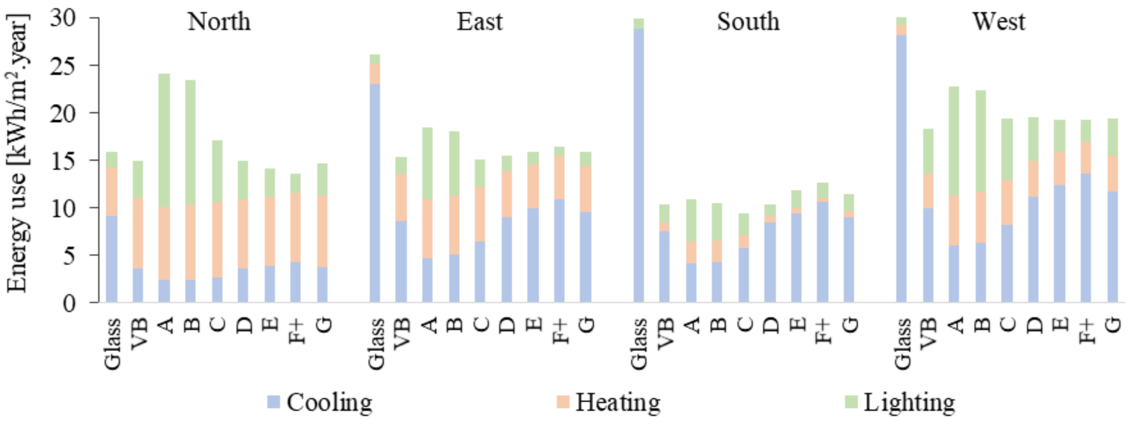

Figure 41. Annual energy use for different configurations of the glazing system: without any solar control solution (*Glass*) with a venetian blind (*VB*) and with SCFs on the external surface of the glass (*A* to *G*)

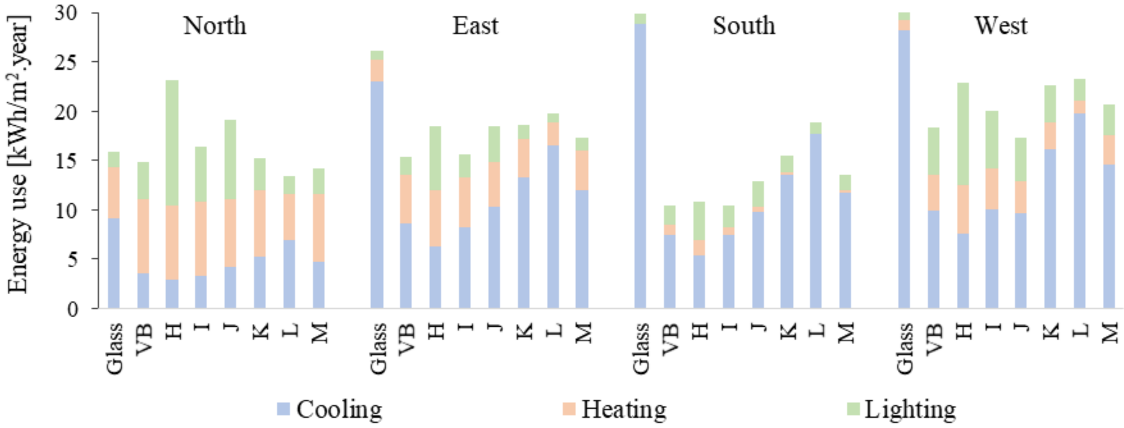

Figure 42. Annual energy use for different configurations of the glazing system: without any solar control solution (*Glass*) with a venetian blind (*VB*) and with SCFs on the internal surface of the glass (*H* to *M*)

The results show that all SCFs reduced the cooling and annual energy use when compared to the solution of single clear glass for all solar orientations. As expected, the cooling energy use shows the dominant share of the total energy use of the building of the case study due to Lisbon's Mediterranean climate characteristics (dry and hot summers and mild to cool wet winters, according to the Köppen-Geiger climate classification).

SCF *A* with external application (Figure 41) and SCF *H* with internal application (Figure 42) show the highest reduction in the cooling energy use for all solar orientations, varying between 74-86% and 69-82%, respectively, when compared to the other solutions. However, an increase in the heating and lighting energy use is noticed when compared to the case of single clear glass (*Glass*), which is due to the lower solar and visible transmittance coefficients of the glazing with those two SCFs.

On the other hand, SCF *F+* with external application (Figure 41) and SCF *L* with internal application (Figure 42) show the lowest reduction of the cooling energy use, varying between 52-63% and 25-39% for SCFs *F+* and *L*, respectively. Also, these films present the lowest increase in the heating and lighting energy use. Figure 43 presents the annual energy use savings (%) associated with the different SCFs (*A* to *M*) and the venetian blind (*VB*) when compared to the situation of the office without solar control solutions for different solar orientations, North, East, South and West.

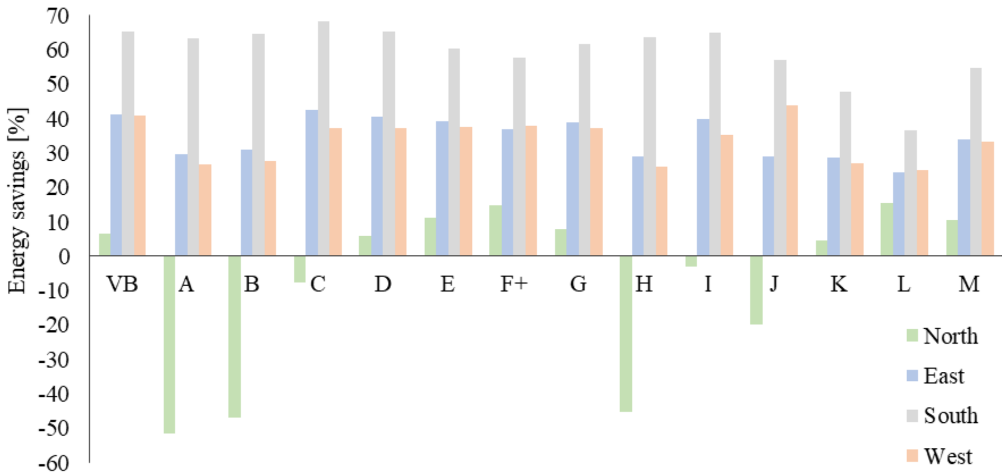

Figure 43. Energy use savings of the office with the venetian blind (*VB*), with external (*A* to *G*) and internal (*H* to *M*) solar control films

As it can be seen in Figure 43, when the façade is South oriented a significant reduction of the total energy use between 37-68% is found with the use of the venetian blind (*VB*) and with SCFs *A* to *M*. The offices oriented West and East have similar reductions in the energy use with VB and SCFs *H* to *M* with internal application, which vary between 24-47%. For the North oriented façade, almost half of the films (SCFs *A*, *B*, *C*, *H*, *I* and *J*) increase the energy use between (9-52%) and therefore are not recommended for thermal and energy retrofitting of single glazing systems with North solar orientation.

SCF *C* has one of the highest performances in reducing the energy use for East (savings of 42%), West (savings of 37%), and South (savings of 68%) solar orientations. This can be explained by the low solar transmittance (τ_{sol}= 0.17) and high solar (front) reflectance ($\rho_{f,sol}$= 0.50) coefficients of this film, which reduces the cooling energy use in the summer season, and by its medium light-to-solar gain ratio (*LSG*= 0.87), which reduces the lighting energy use, especially during the winter season.

From the obtained results, Table 11 shows for the SCFs presented in Table 7 a decision-making framework based on different performance criteria, cooling (C), heating (H), lighting (L) and combinations deriving therefrom (C+H, C+L, H+L and C+H+L) for all façade orientations (N+E+S+W). The corresponding solar transmittance, (front) reflectance and absorption coefficients of the glazing system with SCFs *A* to *M*, SCF *K-* and without SCF (*Glass*) are presented in Figure 44.

Table 11. Decision-making framework based on energy performance criteria for different solar orientations

Performance criteria	Orientation				
	North (N)	East (E)	South (S)	West (W)	N+E+S+W
Cooling (C)	A	A	A	A	A
Heating (H)	L	L	L	L	L
Lighting (L)	L	L	L	L	L
C+H	A	A	A	A	A
C+L	F	C	C	J	C
H+L	L	L	L	L	L
C+H+L	F	C	C	J	D

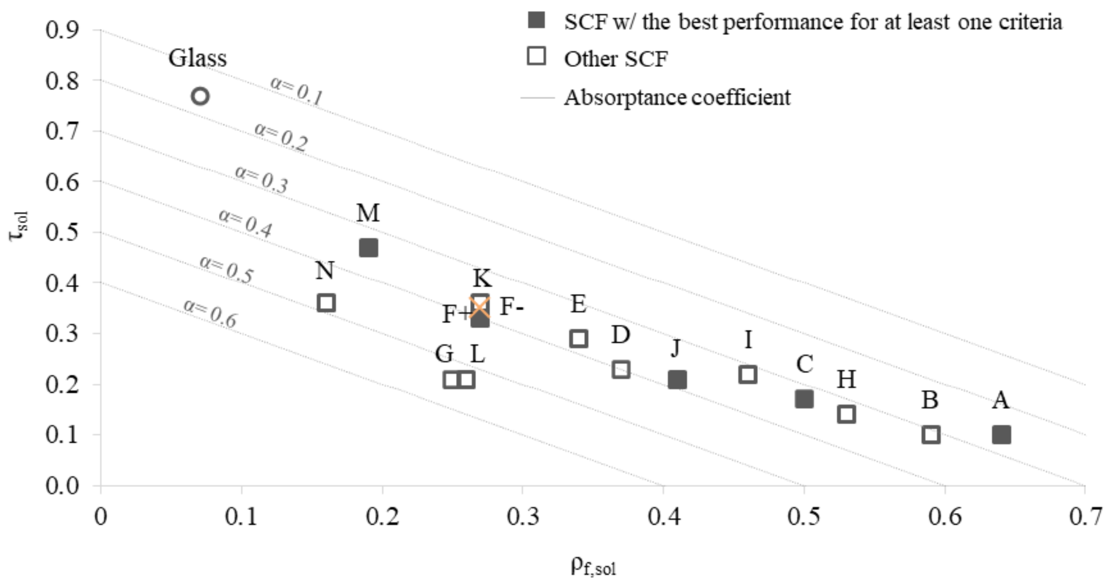

Figure 44. Optical properties of SCFs *A* to *M*, SCF *K-*, and without SCF, *Glass*

From Table 11 it is possible to conclude that SCFs *A* have the best energy performance for cooling, and *L* for heating and lighting performance criteria, for all solar orientations and for the combination N+E+S+W. This is due to the fact that SCF *A* has the highest solar (front) reflectance coefficient ($\rho_{f,sol}$= 0.64) and SCF *L* the highest visible transmittance and light-to-solar gain ratio (τ_{vis}= 0.70, LSG= 1.35), as described in Table 7. It is important to notice that the SCFs with applications on the external surface of the glass had a better performance in reducing the energy needs when the analysis takes into account the cooling performance criteria for almost all solar orientations.

For the C+H combination, SCF *A* has the best energy performance for all solar orientations. In this combination, the reduction in the cooling energy use (C) has a higher influence since the HVAC efficiency is lower for the cooling (COP= 3.0) than for the heating (EER= 3.4) energy supply and the cooling demand of the office is much higher than the heating demand, especially for South, East and West orientations. Therefore, the most energy efficient SCF for the cooling performance criterion (C) was expected to be the same for the C+H combination in orientations with high solar gains, such as, East, South, and West directions and in this study in was also the best solution for the North orientation.

For the C+L combination, all solar orientations show a different type of SCF that minimizes the energy use of the office. This may be related to the fact that SCFs with higher performance for the cooling energy use are associated with higher values of the solar (front) reflectance coefficient and, consequently, lower values of the visible transmittance, which increase the lighting energy use.

For the H+L combination, SCF *L* has the best energy performance for all solar orientations. This film has the highest solar transmittance (τ_{sol}= 0.47) and the highest solar factor (g= 0.52), resulting in a decrease of the heating energy use. Also, this film has the highest visible transmittance (τ_{vis}= 0.70), which leads to a decrease of the lighting energy use in both heating and cooling seasons.

For the C+H+L combination, SCF *F* has the best energy performance for North solar orientation (orientation with lower annual irradiation values) which can be explained by the higher values of solar factor (g= 0.5) and visible transmittance (τ_{sol}= 0.65) when compared to the other SCFs. SCF *C* shows the best performance for East and South solar orientations due to the high value of solar (front) reflectance ($\rho_{f,sol}$= 0.50) and lower values of solar factor (g= 0.30) and visible transmittance (τ_{sol}= 0.26), decreasing the solar gains and the total energy needs with cooling, heating, and lighting. Even though SCF *J* showed the best energy performance for West solar orientation, SCFs *C* to *G* with external application on the glass surface ($\rho_{f,sol}$ and τ_{vis} varying between 0.25-0.50 and 0.26-0.65, respectively) showed similar performances.

Finally, it is worth referring that the last column of Table 11 shows the SCF with the lowest energy use for each performance criteria considering all solar orientations at the same time. This is particularly important when the uniformization of the visual aspect of façades of the building is a requirement. SCF *D* has a low solar transmittance (τ_{sol}= 0.23) and medium values of visible transmittance (τ_{vis}= 0.34) and solar (front) reflectance ($\rho_{f,sol}$= 0.37), when compared to the other SCFs. This balanced combination of properties results in a combined reduction of the three performance criteria – cooling (C), heating (H) and lighting (L) – which explains the lower value of the annual energy use.

4.7 Conclusions and perspectives

In this section, an experimental campaign and a simulation study concerning an existing building were described and analysed to evaluate the thermal, luminous and energy performance of offices with single-glazed windows for different scenarios of the glazing system: without solar control solutions (only glass) and with solar control films (glass with SCFs) applied either to the internal or the external glass surface. From the experimental campaign, carried out simultaneously on two similar offices, one with the SCF applied to the internal surface of the glass (retrofitted office A) and the other without any film (reference office B), the following main conclusions can be drawn for representative selected days (offices not climate controlled) of the summer and winter periods:

- when compared to the single clear glass alone (office B), the glass with the SCF (office A) reduced the average indoor temperature during working hours (from 9h00 to 18h00) both in the winter and summer days, with the maximum percent reduction in the summer days (14.7%) being approximately the double of the winter days (7.1%);
- during working hours (from 9h00 to 18h00), the percent reduction achieved with the installed solar control film in the indoor irradiance on vertical plane was approximately the same in the summer (48-55%) and winter (49-50%) days, whereas in the indoor illuminance on vertical plane a lower difference was noticed, 14-15% and 49-50% in the summer and winter days, respectively.

From the computational study, conducted through a calibrated model of the typical office, the following main conclusion can be drawn for the energy performance associated with the different SCFs tested:

- all SCFs increased the heating and lighting energy use but reduced the cooling energy use of the typical office for East, South and West solar orientations;
- SCFs with low solar transmittance and high solar (front) reflectance, such as SCFs *A* and *H*, induced higher reductions of the cooling energy use and higher increases of the heating and lighting energy use;

- SCFs with high solar (front) reflectance and low solar and visible transmittance, as are SCFs *B* and *I*, led to the best energy performance for the criterion accounting for the cooling, heating, and lighting energy use for all solar orientations (N, E, S and W);
- when an uniformisation of the visual aspect of the building is required, SCF *B* revealed to be the most energy-efficient, reducing 16%, 47%, 68% and 44% of the annual energy use for North, East, South and West solar façade orientations, respectively. This film has a low solar transmittance coefficient (τ_{sol}= 0.22) and medium values of visible transmittance (τ_{vis}= 0.34) and solar (front) reflectance ($\rho_{f,sol}$= 0.46), when compared to the other SCFs;
- the analysis also showed the importance of applying the films to the correct side of the glass; incorrect applications result in unsatisfactory performances that unfairly contribute to product discredit.

This study expands the existing knowledge on SCFs by experimental and modelling approaches for a temperate Mediterranean climate, presenting a decision-making framework based on an energy performance criterion. Future work should consider thermal and lighting comfort indicators and the economic and environmental assessment of SCFs as a rehabilitation solution for glazing retrofitting of existing buildings.

5. Performance of solar control films in double-glazed windows

This section examines the thermal, daylighting, and energy performance of double-glazed windows of office spaces of a building located in Lisbon, without and with solar control films (SCFs) in actual working conditions. The building of the case study has large areas of glass in the façades and reveals thermal and visual discomfort conditions in the office spaces due to excessive solar gains and illuminance levels. To increase the comfort conditions, a SCF was applied previously to this study to decrease the solar gains through the windows without compromising the view. However, the SCF has reached its end of life and needs to be removed. The current section aims to analyse experimentally the thermal and daylight conditions of the office areas without and with SCFs. In this experiment, there was also the opportunity to monitor the performance of a SCF in new conditions (new film) and installed according to good application rules and other in an advanced stage of use and installed under poor applications, providing interesting elements of comparison on the in-service degradation of films and the importance of the quality of materials and installers. Based on the collected experimental data, a building energy simulation is modelled to assess the energy performance of different scenarios of the window with SCFs. Such an approach can be useful to support the definition of energy improvement strategies on office buildings with low thermal and/or visual comfort conditions and high glazing areas in temperate Mediterranean climates.

5.1 Case study

The building considered in this study is in the south area of Lisbon (38°7′N, 9°1′W), in Portugal, in front of the Tagus river (Figure 45). The city experiences a temperate Mediterranean climate (Köppen-Geiger: Csa/Csb) [44] with an average annual temperature of 16ºC and minimum and maximum temperatures occurring from December to February and from July to September, respectively.

Figure 45. External view of the building of the case study – main entrance

The building is divided into three main areas: an area consisting of halls, security rooms and a conference room (area A, Figure 46 a.) and two areas of office spaces, one with south-north oriented façades and three floors and the other with east-west oriented façades and four floors (areas B and C, Figure 46 a.).

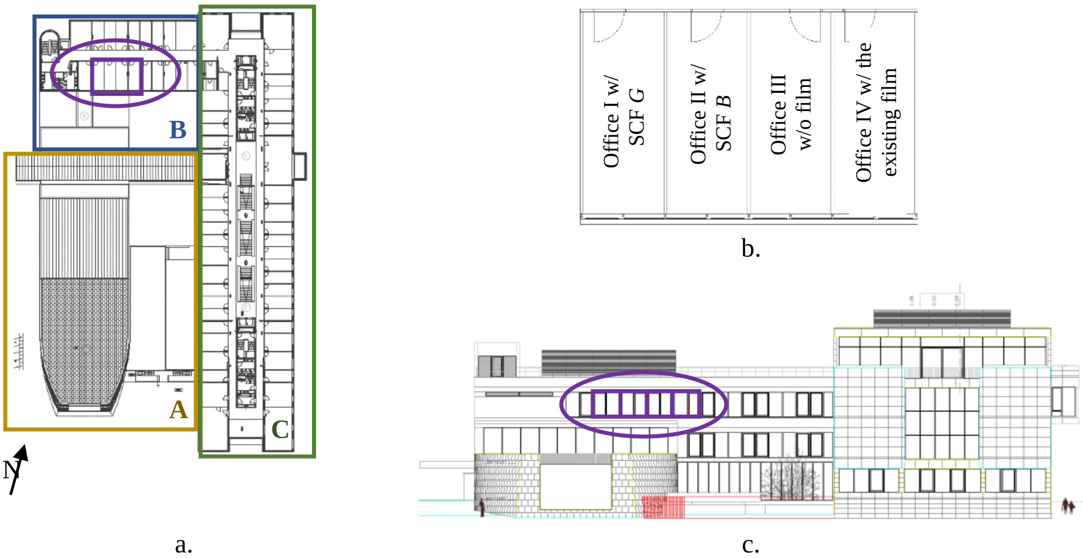

Figure 46. Location of the four offices: a. main floor plane; b) disposition and; c) front South elevation

Exterior walls are double brick (11 + 11 cm) with an air gap of 7 cm partially filled with extruded polystyrene (4 cm) and floor slabs are in reinforced concrete (20 cm). The original windows have argon filled double glazed units with a 14 mm argon chamber (from the outer to the inner panes of the glass: 8 mm low-ε glass, 14 mm argon, 8+8 mm laminated glass with a polyvinyl butyral coating) and due to thermal discomfort associated with overheating in the office spaces, a SCF was applied to the external surface of the outer pane in all the glass area of the façade.

Before the present study, a SCF has been applied before this study to the building, with the purpose of decreasing the solar gains through the windows without compromising the view (highly reflective film). The film has reached its end of life and revealed several problems regarding its integrity as shown in Figure 47. As a result, the optical and thermal properties of the film were seriously affected, losing homogeneity throughout the glass area, and showing differences from window to window depending on the type of problem and the level of deterioration of the film.

Figure 47. Examples of windows of the second case study building with the damaged SCF: a. tears; b. cracks; c. blistering; d. lack of transparency; e. detachment and; f. deterioration of the external layers of the film

5.2 Methodology

To assess the thermal, daylight, and energy performance of double-glazing units of offices areas without and with SFCs, four similar offices of the building were selected to be investigated. A spectrally selective and a highly reflective film were applied in office I and office II (retrofitted windows), respectively, to the external surface of the windows. In office III, the damaged SCF was removed, and the window was left without any SCF (original window). This latter scenario is considered in this study as the reference office. In office IV the damaged film was kept on the window (current window) in order to analyse the existing conditions of the office areas of the building.

The methodology showed in Figure 48 includes the following steps:

a. removal of the damaged film in offices I, II and III and application of the new SCFs *B* and *G* in offices I and II, respectively;

b. experimental campaign conducted simultaneously in the four offices during summer and winter periods that include measurements of indoor and outdoor temperature, illuminance, and irradiance;

c. modelling the four office areas using SketchUp, Window and Optics, and EnergyPlus software [78];

d. assessment of the quality of the simulation model of the offices based on the collected experimental data by using the statistical indices Mean Bias Error – *MBE* – and Coefficient of variation of the Root-Mean Square Error – $C_{v,RMSE}$ –, which are found to adequately measure the level of approximation between numerical and experimental results [79]–[81]. For assessing the model performance, the generic hourly weather file of Lisbon's city was used, but the outdoor related variables of temperature, humidity, radiation, and wind were replaced with the ones measured during the experimental campaign;

e. using the synthetic hourly weather file of Lisbon's city and the simulation model of the offices, the annual energy use related to heating, cooling, and lighting was estimated for the retrofitted and the original windows of the office areas as well as for different types of SCFs (SCFs *A* to *G* designed for application to the external side of the glass) for North (N), South (S), East (E), and West (W) solar orientations. The energy performance was estimated and compared for all the glazing options and a decision-making framework was designed to select a trade-off solution according to a specific defined objective.

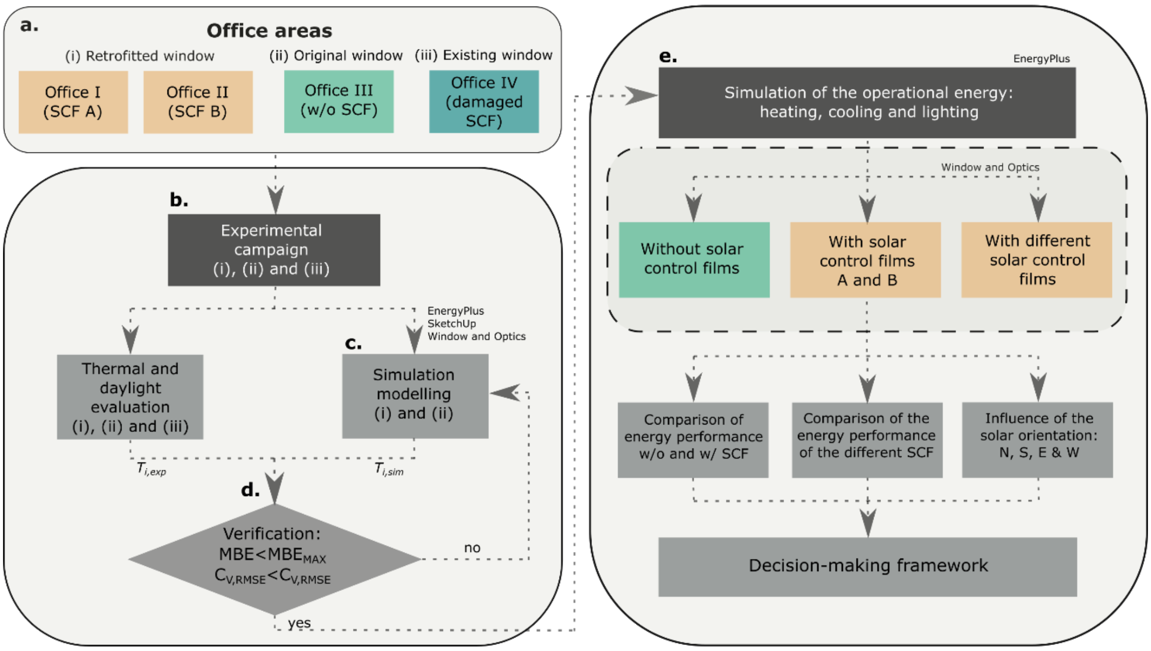

Figure 48. Methodology flowchart

5.3 Experimental procedure

The experimental campaign was performed simultaneously in the four offices I, II, III, and IV from the 1st of August of 2017 until the 31st of January of 2018. All the four offices are located on the 2nd floor

(Figure 46) and have a floor area of 2.4x6.0 m^2 and a south oriented window with 2.4x2.2 m^2 (width × height). The four office areas can be considered similar to each other in what regards the construction materials, geometrical and layout characteristics, occupancy schedule, lights, electric equipment and HVAC system, which are very similar to other office spaces of the building.

The existing damaged SCF was removed from the windows of offices I, II, and III previously to the experimental procedure (Figure 49 a.) and the new SFCs *G* and *B* were installed in offices I and II, respectively, on the external side of the glass (Figure 49 b.). Figure 50 and Figure 51 show an inner and outer view of the final appearance of the glazing systems in the offices, respectively. It is interesting to observe that the installation of the films changed the outer and inner colour of the original window and that the different daylight availability in each office is perceptible to the naked eye (see Figure 50 and Figure 51).

a. b.

Figure 49. a) Removal of the existing damaged SCF on the external surface of the glass (external view); b) Installation of SCF on the external surface of the glass (internal view)

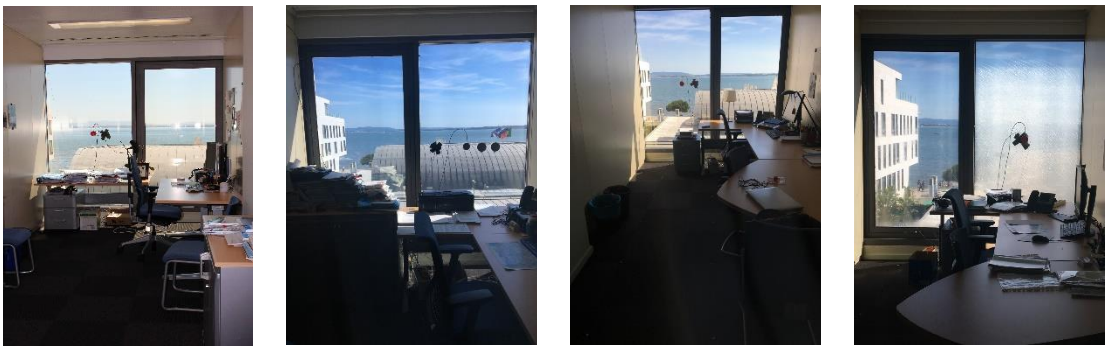

a. b. c. d.

Figure 50. Monitored office areas (inner view): a. Office I; b. Office II; c. Office III and; d. Office IV

a. b.

Figure 51. Monitored offices (outer view) before (a) and after (b) the installation of the films

Table 12 shows the main properties of the glazing systems of offices I (w/ SCF *G*), II (w/ SCF *B*), and III (w/o film). The properties of the original window of office IV were not assessed due to the difficulties of accurately modelling a damaged material in a simulation program.

Table 12. Thermal and optical characteristics of the glazing system of offices I (with SCF *G*), II (with SCF *B*) and III (without film): transmittance, τ, (front) reflectance, ρ_f, (back) reflectance, ρ_b, absorptance, α, thermal transmittance, U, [W/m^2.K], and solar factor, g

	Visible (%)			Solar (%)				U (W/m^2)	g (%)
	τ	ρ_f	ρ_b	τ	α_1	α_2	ρ_f		
Office I (w/ SCF *G*)	24	8	12	12	62	1	25	1.423	23.4
Office II (w/ SCF *B*)	11	58	30	6	35	1	59	1.424	12.1
Office III (w/o film)	56	14	10	37	41	6	16	1.430	48.0

The following physical parameters were continuously monitored in each office: indoor and outdoor temperatures, internal and external glass surface temperatures, and indoor and outdoor illuminance and irradiance on horizontal and vertical plane. The sensors were connected to dataloggers Delta T DL2, positioned in each office room and another in the roof, all programmed to record averages every 10 minutes from 1 minute's readings. The weather data was collected on the rooftop through a weather station and additional pyranometers.

Table 13 summarises the experimental equipment used, the respective location and equipment's accuracy, and measured variables. Figure 52 shows some pictures of the equipment installed in the office spaces and the rooftop. One important thing to highlight in this experimental procedure is that the equipment is distributed amongst the four offices and the roof (see Table 13 and Figure 52), and the data acquisition is independent from office to office. All it takes is one piece of the experimental equipment to fail to record the data, to not be possible to perform an analysis based on variables' comparison between the four offices.

For this reason, the decision of selecting several consecutive days, without data gaps, from all the days of the experimental campaign was taken in the current study. This decision allows a timeline analysis and variable comparison of representative days of summer and winter seasons: from the 14th to the 27th of August and from the 6th to the 13th of January.

Table 13. Experimental equipment and respective measured variables

Equipment	Model	Variable	Name	Accurancy	Location
Thermocouples	T-type	Temperature	T_{si}, T_{se} T_{ind}, T_{out}	±0.2ºC at 100 ºC	Internal and external surface of the glass Indoor and outdoor environment
Pyranometer	LI-COR LI200R	Global radiation	$E_{out,vert}$ $E_{ind,vert}$	±3%	South façade Vertical side of the work table
	Kipp&Zonen			5 to 20μV/W/m^2	Roof
		Global radiation	$E_{out,vert}$	±5 W/m^2 ±12%	
	BF5 Delta T	Difuse radiation	$E_{out,vert}$ (diffuse)	±20 W/m^2 ±15%	Roof
Luxmeter	LI-COR LI210R	Illuminance	$I_{out,vert}$ $I_{ind,vert}$	±5%	South façade Vertical side of the working table

a. b. c. d.

Figure 52. Experimental equipment installed in the office rooms and in the rooftop: a. pyranometer and luxmeter on vertical plane; b. thermocouples on the windows' glass surface; c. pyranometers on horizontal and vertical planes and; d. weather station

5.4 Simulation modelling

A numerical model of the office rooms was created to evaluate the thermal and energy performance of the office areas of the building. The geometrical characteristics were designed in SketchUp 3D Design Software, and the envelope properties, internal gains, HVAC thermostat temperatures, and schedules were specified using EnergyPlus software. The glazing properties of the original window of office III, the retrofitted windows of offices I and II, and other different SCFs applied to the original window were determined using Window and Optics tools [73] from Lawrence Berkeley National Laboratory. Figure 53 shows the 3D geometric BES model of the three offices I, II, and III of the building.

The modelling parameters and the assumptions of the simulation model regarding the internal gains were defined by examining occupants behaviour during the different days of the week (working days and weekends) or assumed as close to reality as possible and compared with values presented in the literature for office buildings [86], [87]. The infiltration rate was considered of 0.6 and 1.0 air changes per hour during non-working hours and working hours, respectively [82], for both heating and cooling periods.

Regarding the installed lighting power density (LPD), which depends on lamps' efficiency and control gear, it was assumed to be 3.33 W/m^2 for office spaces [88]. These values are compatible with the benchmark and maximum values for LPD defined in the Energy Consumption Guide 19 [89] and in ASHRAE Standard 90.1-2007 [90], respectively. Also, the lights were programmed to switch on during working hours when the minimum recommended values of illuminance levels for office areas (500 lux) was reached [74]. The office electrical equipment heat gains were considered 15 W/m^2 during working hours, and it was assumed that 20% of the equipment was left on during the night period (standby mode). Offices' occupancy was considered to be of 1 person per office in office areas during working hours.

The existing HVAC system of the building starts to work at 05h00 and is programmed to maintain the indoor temperature of the building at 21 ºC and the occupants can manually program the thermostat in each office room by ±3 ºC (18ºC to 24ºC). In the simulation model of the current study, the HVAC system was set to turn on when the indoor temperature is outside the thermal comfort range of temperatures for Portugal (18 ºC to 25 ºC), according to the Portuguese Regulation of the Energy Performance of Buildings [82].

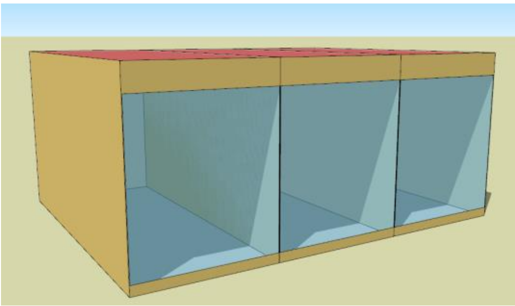

Figure 53. Geometrical model of the office areas built in SketchUp 3D modelling program

The performance of the model was assessed by comparing the values of the indoor temperature and the internal and external glass surface temperatures of offices I, II, and III obtained through simulation and experimentally during both the heating and cooling periods in which the experimental campaign took place. To evaluate the agreement between experimental and simulation results, the standardized statistical indexes – Mean Bias Error (*MBE*) and Coefficient of variation of the Root-Mean Square Error, ($C_{v,RMSE}$) [79]–[81]

– defined in equations (4.1) to () in section 4 were used. They provided a quantitative assessment of the model capability in predicting the existing conditions of the office spaces. The experimental collected values of outdoor temperature, relative humidity, global and diffuse radiation, and wind speed were set under the weather data file format of EnergyPlus (epw file) for the verification simulations.

Once the performance of the model is checked, the original synthetic weather data of Lisbon's city [78] is used in the subsequent performance simulation study. Therefore, the model's predictions could represent an annual performance of a typical meteorological year in Lisbon's city. Assessment of the quality of the model is an essential step of this evaluation, as it minimizes the difference between predicted numerical and measured experimental values. The verification process was not performed in office IV (with the current damaged SCF), as stated before, due to the difficulties of accurately modelling a damaged material in a simulation program.

To perform a comprehensive study on the energy performance of SCFs in double-glazed windows, several films with different optical properties – besides the SCFs *B* and *G* installed for the experimental analysis – were selected to be analysed using the original window of the building of the case study (without the damaged film) as a substrate. The energy performance of the glazing solutions was assessed for the different solar orientations and a decision-making framework based on energy performance criteria was elaborated, identifying the potential use of SFCs as an energy retrofitting solution for double-glazed windows. Table 14 lists the different SCFs with application on the external side of the back pane glass, when applied on the original glazing window (office III) and the correspondent thermal and optical properties determined using Window and Optics tools.

Table 14. Thermal and optical characteristics of the original double-glazed window with different *SCF*s applied on the external side of the back pane glass: solar (front) reflectance, $\rho_{f,sol}$, solar transmittance, τ_{sol}, visible transmittance, τ_{vis}, (front) absorptance, α, thermal transmittance, U [W/m^2.K], solar factor, g, and light-to-solar gain ratio, LSG

SCF (external application)	$\rho_{f,sol}$	τ_{sol}	τ_{vis}	α	U [W/m^2.K]	g	LSG=τ_{vis}/g
Original Window	0.16	0.37	0.56	0.41	1.43	0.48	
A	0.56	0.06	0.10	0.33	1.42	0.12	0.83
B – Office II	0.59	0.06	0.11	0.35	1.42	0.12	0.92
C	0.44	0.10	0.17	0.45	1.42	0.18	0.94
D	0.37	0.13	0.22	0.48	1.42	0.22	1.00
E	0.35	0.16	0.28	0.48	1.42	0.25	1.12
F	0.28	0.19	0.42	0.51	1.42	0.29	1.45
G – Office I	0.25	0.12	0.25	0.62	1.42	0.23	1.09

From the group of external SCFs studied in the current section (Table 14), SCFs *A* to *C* are highly reflective films and SCF *D* to *G* are highly absorbing films. According to the United States Department of Energy [91], the window with SCF *F* is the only spectrally selective solution since it shows a Light-to-Solar Gain ratio, *LSG*, higher than 1.25. It is important to notice that none of the SCFs changed the thermal transmittance, *U*, of the window due to the films' low thickness. In the previous section 4, [55] has identified that within the films in the category of solar control films, only the low-ε films change significantly the thermal transmittance of the window. In the current analysis, none of the selected external SCFs show low-ε properties since these types of films are mostly used on internal applications.

5.5 Experimental results

In the following sections, the experimental results obtained in the four offices that allow assessing the thermal, luminous, and energy performance without and with occupancy are analysed in detail. First, the indoor temperature of the four offices and the internal and external surface temperatures of the different offices are analysed for a selection of consecutive days of both the summer – 14th to the 27th of August – and winter – 6th to the 13th of January – periods of the experimental campaign that lasted from August to January (six full months). Then, for the same summer and winter periods, the indoor and outdoor irradiance and illuminance at the working plane (desk height of ~0.8cm) are analysed, and the results discussed. Finally, four reference days with specific outdoor weather conditions – highest and lowest outdoor temperature and sun's elevation angle – are selected to be analysed in greater detail.

The measured outdoor conditions from the 14th to the 27th of August (two weeks of the cooling season) and from the 6th to the 13th of January (one week of the heating season) are graphically depicted in Figure 54 and Figure 55. Due to technical problems related to the experimental equipment, it was not possible to measure the diffuse and direct solar radiation on horizontal plane and the global solar radiation on vertical plane in the winter period. At this stage, the analysis of the outdoor variables allows to understand and foresee the weather conditions that impact the indoor environment of the office spaces in the summer and winter periods.

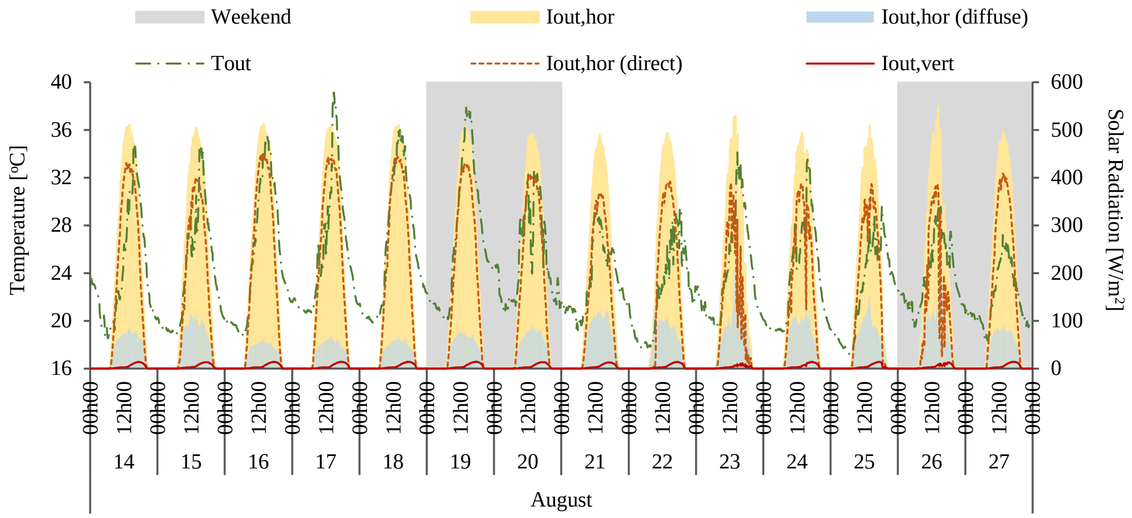

Figure 54. Outdoor conditions in the summer period: global, $I_{out,hor}$, diffuse, $I_{out,hor}$ *(diffuse)*, and direct, $I_{out,hor}$ *(direct)*, solar radiation on horizontal plane, global solar radiation on vertical plane, $I_{out,vert}$, and outdoor temperature, T_{out}

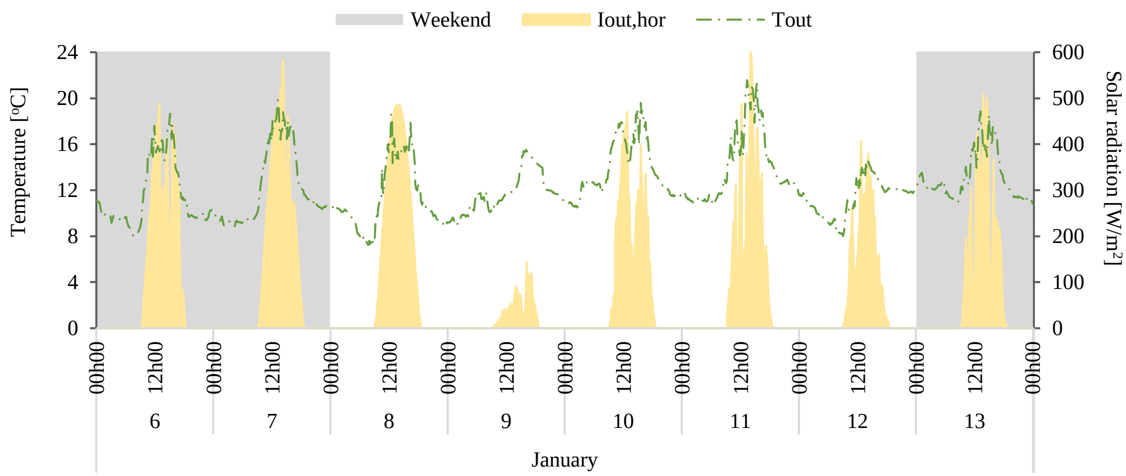

Figure 55. Outdoor conditions in the winter period: global solar radiation on horizontal plane, $I_{out,hor}$, and outdoor temperature, T_{out}

The summer period results show higher values of outdoor temperature and global solar radiation on horizontal plane, evidencing higher values of direct radiation (peak value of ~450 W/m^2) and lower values of diffuse radiation (peak value of ~233 W/m^2). These results point out a predominance of clear sky over intermittent or overcast sky conditions [92]. The measured global solar radiation shows a similar trend throughout the different days, reaching peak values ~500-550 W/m^2.

It is possible to observe a high variation of solar radiation during the winter period, with predominance of CIE clear and overcast sky conditions throughout the day. Moreover, it is observed that CIE intermittent sky conditions were predominant, and subsequently, global solar radiation on horizontal plane showed a higher variation of the average and the maximum values throughout the measuring days. In days characterized by CIE overcast sky conditions – as was the case of the 7th of January – the registered values of global solar radiation on horizontal plane (peak value of ~145W/m^2) and outdoor air temperature (varying between 9.0-15.5ºC) were much lower than those observed for intermittent CIE sky conditions (~145W/m^2 and 7.3-21.6ºC). The outdoor temperature shows a similar trend throughout the winter days except on the 9th of January, showing, as expected, lower peak values due to the lower global solar radiation.

In the obtained results of the different outdoor weather variables, it is possible to notice several days with higher values of peak and average solar radiation and outdoor temperature in summer and lower ones in winter (particularly on the 7th of January), which potentiate higher and lower heat gains in summer and winter seasons, respectively. Given these potential adverse effects, the outdoor conditions of the two summer and winter periods can be seen as representative design scenarios of summer and winter periods and, as a result, appropriate to evaluate the indoor thermal and luminous performance of indoor office spaces.

Table 15 shows the average and maximum outdoor temperatures and the incident global solar radiation on vertical plane during the sun-hours period in the summer and the winter days within which the experimental campaign took place.

Table 15. Average and maximum outdoor temperatures ($T_{out,aver}$ and $T_{out,max}$), and incident global solar radiation on vertical plane ($I_{out,vert,aver}$ and $I_{out,vert,max}$), for summer and winter days during sun-hours

	$T_{out,aver}$ [ºC]	$T_{out,max}$ [ºC]	$I_{out,vert,aver}$ [W/m^2]	$I_{out,vert,max}$ [W/m^2]
Summer (14th to the 27th of August)	26.39	39.14	286.30	549.10
Winter (6th to the 13th of January)	14.80	21.57	211.64	619.01

5.5.1 Indoor and surface temperatures

The thermal performance of the office areas was evaluated by examining the indoor temperature profiles, T_{ind}, which constitute the offices' thermal response to the external actions of temperature, T_{out}, and solar radiation, $I_{out,hor}$. The internal, T_{si} and external, T_{se}, surface temperatures of the glass façade are also examined to complement and support the information provided by the indoor temperature profile and assess the SCFs performance in terms of absorbed heat in both the inner and outer window panes. The obtained results are shown in Figure 56 to Figure 59 for the summer period and in Figure 60 to Figure 63 for the winter period, for offices I, II, III and IV.

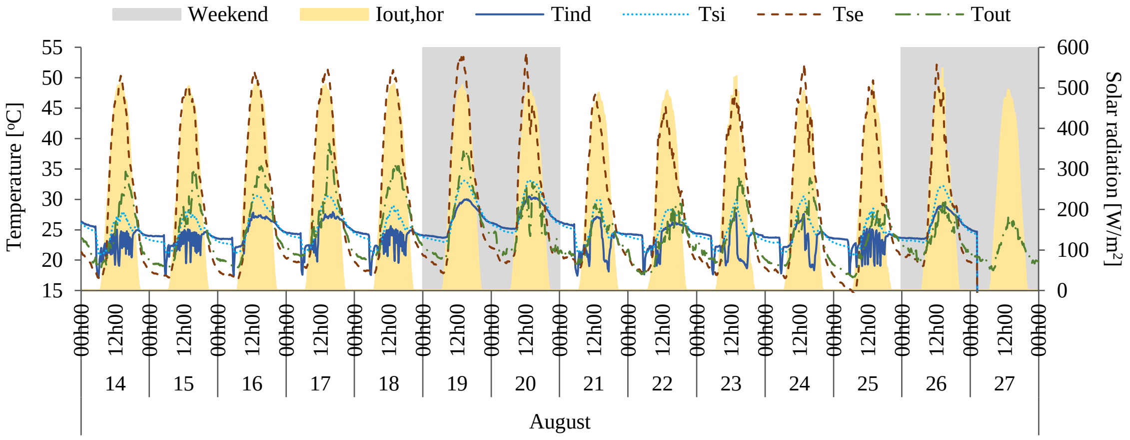

Figure 56. Thermal performance of office I in the summer period: indoor temperature, T_{ind}, and internal, T_{si}, and external, T_{se}, surface glass temperatures, as well as global solar radiation on horizontal plane

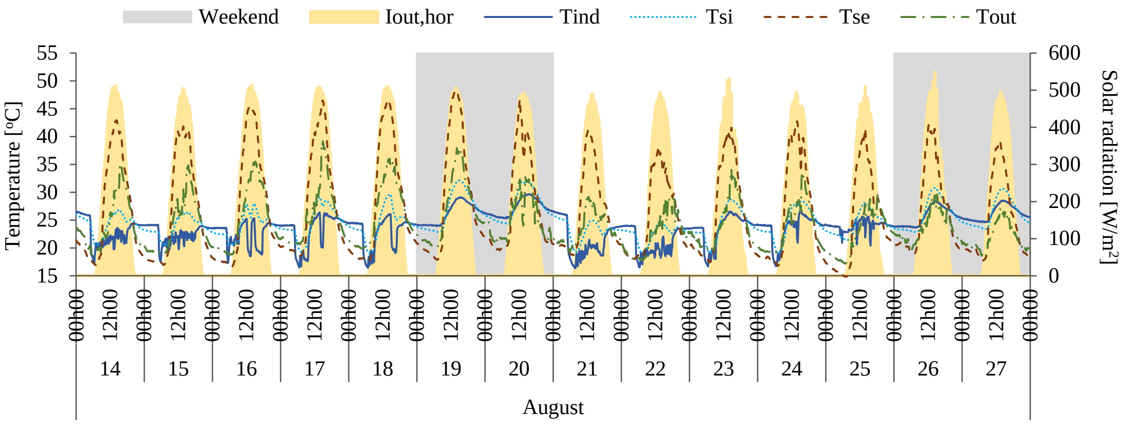

Figure 57. Thermal performance of office II in the summer period: indoor temperature, T_{ind}, and internal, T_{si}, and external, T_{se}, surface glass temperatures, as well as global solar radiation on horizontal plane

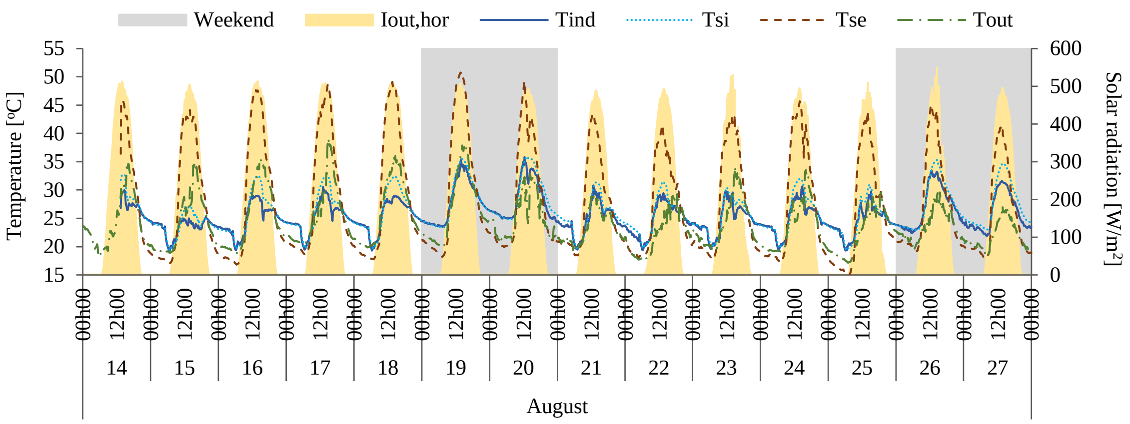

Figure 58. Thermal performance of office III in the summer period: indoor temperature, T_{ind}, and internal, T_{si}, and external, T_{se}, surface glass temperatures, as well as global solar radiation on horizontal plane

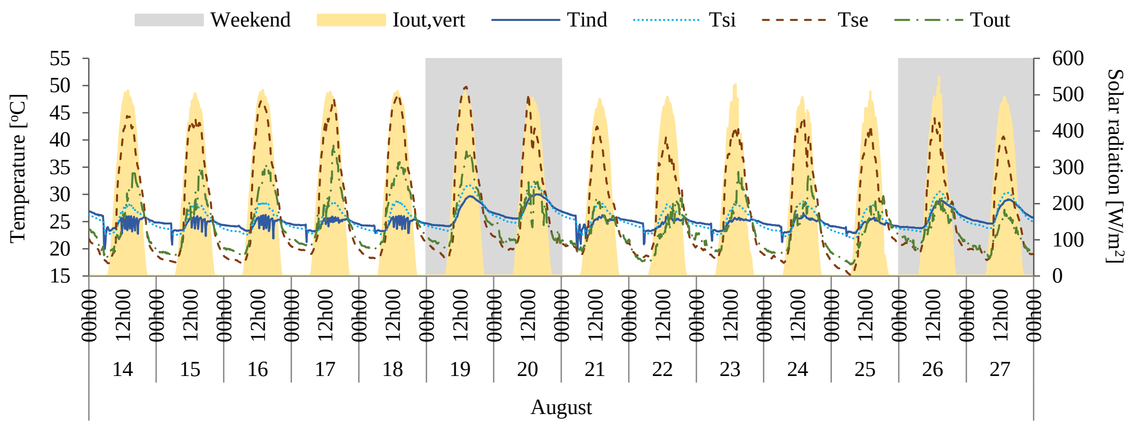

Figure 59. Thermal performance of office IV in the summer period: indoor temperature, T_{ind}, and internal, T_{si}, and external, T_{se}, surface glass temperatures, as well as global solar radiation on horizontal plane

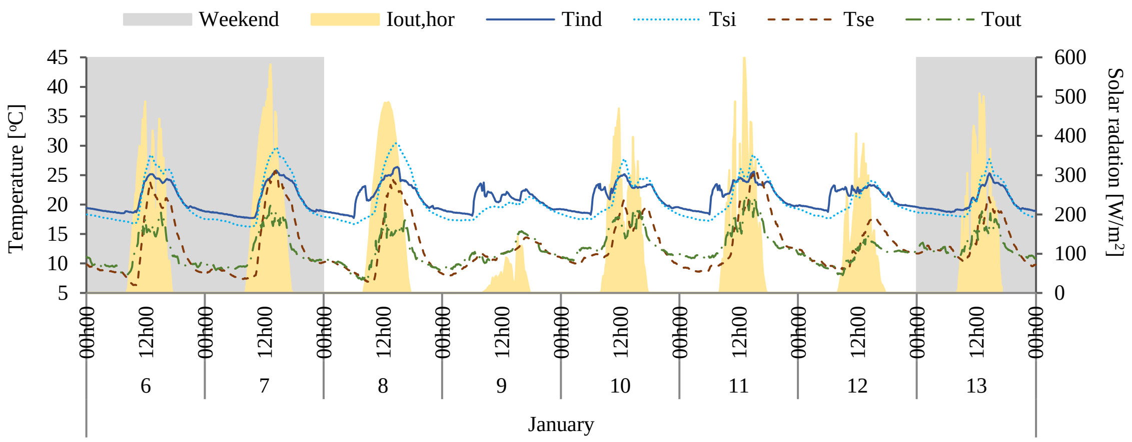

Figure 60. Thermal performance of office I in the winter period: indoor temperature, T_{ind}, and internal, T_{si}, and external, T_{se}, surface glass temperatures, as well as global solar radiation on horizontal plane

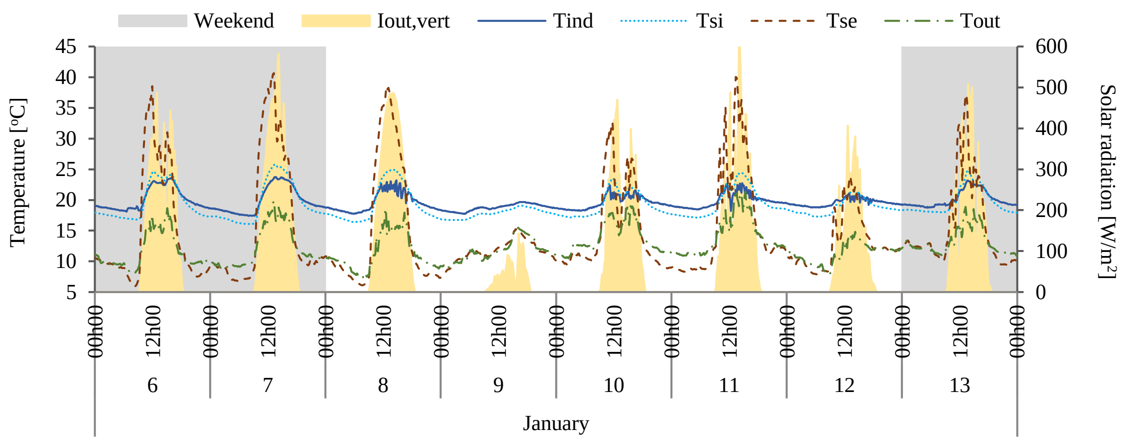

Figure 61. Thermal performance of office II in the winter period: indoor temperature, T_{ind}, and internal, T_{si}, and external, T_{se}, surface glass temperatures, as well as global solar radiation on horizontal plane

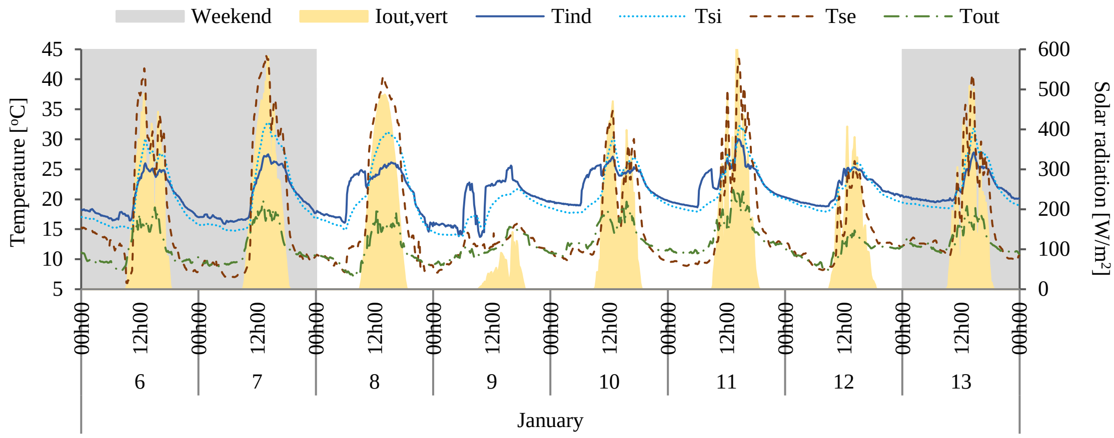

Figure 62. Thermal performance of office III in the winter period: indoor temperature, T_{ind}, and internal, T_{si}, and external, T_{se}, surface glass temperatures, as well as global solar radiation on horizontal plane

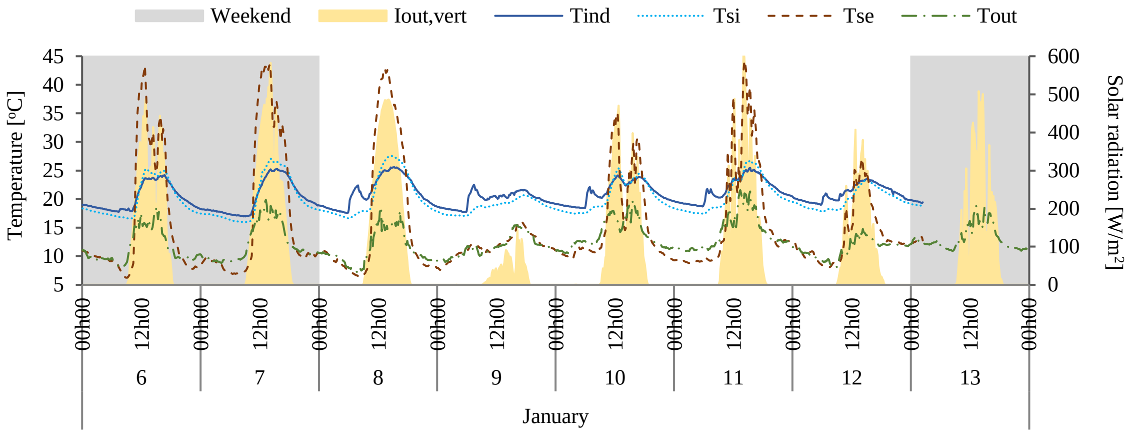

Figure 63. Thermal performance of office IV in the winter period: indoor temperature, T_{ind}, and internal, T_{si}, and external, T_{se}, surface glass temperatures, as well as global solar radiation on horizontal plane

In the summer period during working hours, the HVAC system keeps the indoor temperature between 17-28 ºC, 16-27 ºC, 19-31 ºC, and 20-27 ºC in offices I, II, III, and IV, respectively. When the HVAC system is turned off on weekends, the indoor temperature in homologous working hours ranges between 23-31 ºC, 24-30 ºC, 22-36 ºC, and 24-30 ºC in offices I, II, III, and IV, respectively, indicating that offices I and II with the new SCFs *G* and *B* show lower average and peak indoor temperature values. The offices with SCFs show lower indoor temperature ranges and temperature averages when compared to office III (reference office – original window without SCF), as expected, on all days of the summer period. It is possible to notice that peak indoor temperatures are ~3ºC higher in offices with SCFs and ~5 ºC higher in the reference office during weekends when compared with week days, indicating that the HVAC consumption is higher in the reference office to keep the indoor temperature within the comfort temperature values (18-25ºC).

In the winter period during working hours, when the HVAC system is turn-on by default, the indoor temperature ranges between 17-26 ºC, 18-23 ºC, 14-30 ºC, and 17-25 ºC in offices I, II, III, and IV, respectively. It is noteworthy that the reference office shows the highest (30ºC) and lowest (14ºC) indoor temperature and the highest indoor range of temperatures during the winter period compared to the other three offices. This fact is significant from a thermal comfort and energy efficiency standpoints as the indoor temperature displays higher periods outside the comfort range (18-25ºC) according to the Portuguese regulations [82], increasing the energy consumption due to higher heating and cooling loads. On weekends, when the HVAC system is turned off, the indoor temperature values in homologous hours (working hours) are very similar to those obtained during working days in the reference office, showing a range temperature difference lower than 1ºC. These results are justified by the fact that the occupant of this particular office does not acclimate the ambient air, turning off the climate control of the office when the HVAC system is activated automatically.

The internal surface and indoor temperatures show a similar profile shape, with the internal surface temperature showing higher range values. The maximum, minimum, and average internal temperature of the inner surface of the glass during working hours in working days are similar or higher than the indoor temperature (in most of the working hours, the difference is less than 1ºC) during both summer and winter periods, except on the 9th of January (which corresponds to the day with the lowest outdoor temperature and global solar radiation). When the solar radiation and outdoor temperatures begin to decrease during the afternoon period, the internal surface temperature of the glass begins to decrease due to lower radiative solar heat gains. This decrease occurs at higher rates than the decrease of the indoor temperature, and when the radiation approximates null values (and there are no radiative solar heat gains), the internal temperature is lower than the indoor temperature of the offices. The observed discrepancy between indoor and internal surface temperatures results from the windows thermal and optical properties. Low *U*- and *g*- values prevent the penetration of high values of incoming solar radiation during sun hours and less heat escape during night-time, decreasing the radiative solar heat gains during sun hours as well as the conduction heat losses during the night periods (or when the outdoor temperature is lower than the indoor temperature).

In the summer season during working hours, the external surface temperature of the outer glass surface shows a higher temperature range than the internal surface temperature in all offices, varying from 15-54ºC, 15-48ºC, 15-51ºC, and 15-51ºC in offices I, II, III, and IV, respectively. In the winter season, the external surface temperature also shows a higher temperature range than the internal surface temperature in all offices, varying from 7-25ºC, 6-40ºC, 6-44ºC, and 6-44ºC in offices I, II, III, and IV, respectively. All offices show similar minimum external surface temperatures during low insolation periods (15ºC for summer and 6/7ºC for winter) and different maximum values (48-54ºC for the summer and 25-44ºC for the winter periods). These results indicate that the external surface temperature is more dependent on the outdoor conditions (e.g. radiation, outdoor temperature, wind velocity and direction) than on the indoor conditions (e.g. indoor temperature, ventilation). On the other hand, the absorption coefficient also plays a significant role in the external surface temperature values: the higher this coefficient is, the higher the external temperature.

For those reasons, it was possible to identify wrong measurements of the external surface temperature in office I during the winter period. Since this office shows the highest absorption coefficient (office I: α_1=0.62; office II: α_1=0.35; office III: α_1=0.41) and the four offices were exposed to the same weather conditions, it was expected that the external surface temperature of office I would be the highest one when compared to the other offices. A comprehensive analysis of the recorded data during the winter period showed that the external surface temperature values increasingly approximate the outdoor temperature throughout the last days of the experimental period. It was theorised that these results could be related to a higher degradation of the insulation material (tape) that prevented this specific thermocouple from contacting the outdoor environment.

In conclusion, the results show that the absorption and the (front) reflective coefficients play a significant role in the thermal performance of the glazing. The higher the absorption coefficient of the external film is, the higher the external surface glass temperature will be. On the other hand, the higher the reflective coefficient, the lower are the solar gains and the indoor and internal and external glass surface temperatures. A careful selection of these coefficients can effectively reduce indoor temperature and mitigate possible thermal asymmetries on days with high solar radiation levels (higher temperatures near the window and lower ones on the opposite space).

5.5.2 Indoor vertical irradiance and illuminance

Figure 66 (summer) and Figure 67 (winter) show the outdoor and indoor irradiance on vertical plane for all the offices. In the graphics depicted on those figures, the vertical axis on the left side represents the indoor measurement and on the right side, the outdoor measurement. Although the two vertical axis show the same parameter (irradiance), it was impossible to show the indoor and outdoor values on the same axis due to scale compatibility, as the outdoor irradiance is 5 to 6 times higher than the indoor irradiance.

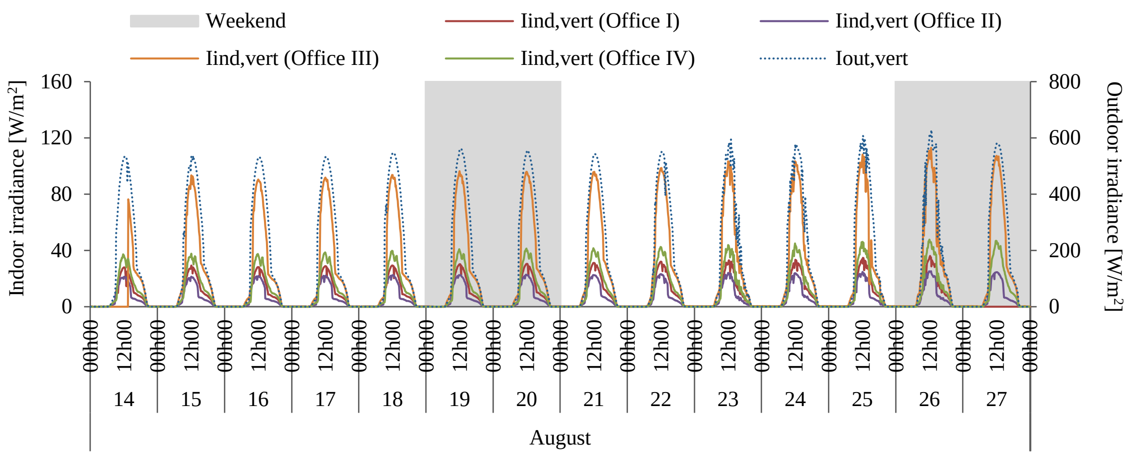

Figure 64. Indoor irradiance on vertical plane, $I_{ind,vert}$, in offices I, II, III, and IV and outdoor irradiance on vertical plane, $I_{out,vert}$, during the summer period

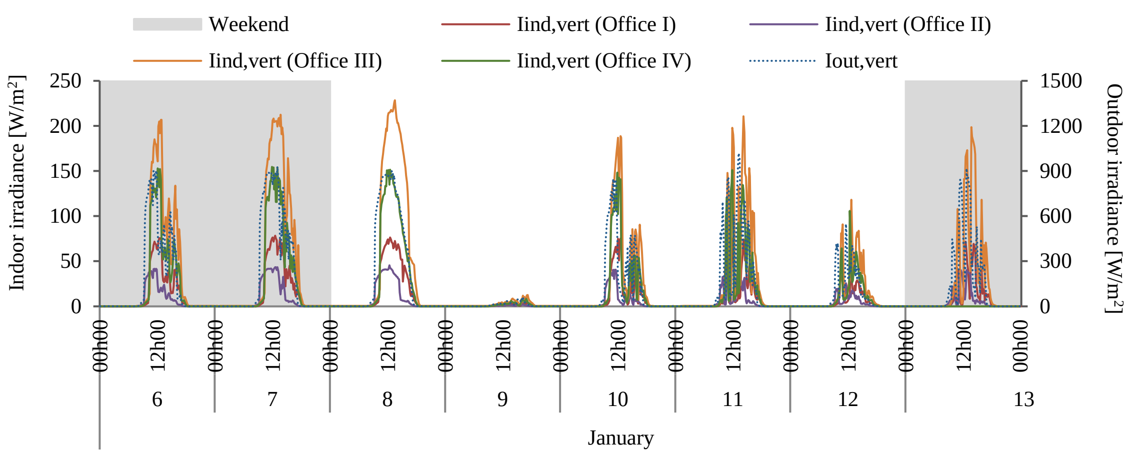

Figure 65. Indoor irradiance on vertical plane, $I_{ind,vert}$, in offices I, II, III, and IV and outdoor irradiance on vertical plane, $I_{out,vert}$, during the winter period

Outdoor irradiance maximum values occur around 12h00-13h00 as expected, due to the façades' South solar orientation, showing peak values of 530-630 W/m^2 in summer and 750-1000 W/m^2 in winter (except on the 9th of January and 12nd of January with lower values of solar radiation and a predominance of overcast and intermittent sky conditions, respectively). Table 16 sums the indoor irradiance maximum values, and the reduction in relation to the outdoor environment and to the reference office.

Table 16. Maximum irradiance and reduction in relation to the outdoor environment and to the reference office during days without occupancy in the summer and winter periods

Period	Office	Maximum [w/m^2]	Reduction in relation to the outdoor environment [%] [1)]	Reduction in relation to the reference office [%] [1)]
Summer	I	36	95.2	64.5
	II	25	96.4	75.6
	III	113	85.2	-
	IV	48	91.8	45.0
Winter	I	78	92.6	66.2
	II	42	95.9	81.5
	III	229	78.0	-
	IV	151	86.3	38.3

1) Calculated using trapezoidal numerical integration

Office III (original window) shows an indoor irradiance reduction on vertical plane of 85.2% in summer and 78.0% in winter in relation to the outdoor irradiance on vertical plane. These are very significant reductions and are exclusively related to the glazing system (without SCF), which shows that the original window already delivers by itself reasonable protection against solar heat gains. Nonetheless, solar heat gains are still at high levels and do not assure thermal comfort without resorting to the HVAC system (indoor irradiance peak values of 113 W/m^2 in summer and 229 W/m^2 in winter).

The application of SCFs in offices I and II resulted in decreased indoor irradiance on vertical plane of 64.5% and 75.6% in the summer days and 66.2% and 81.5% in the winter days compared to the reference office III. Given the fact that SCFs reduced the windows' g-value (office I: g=0.23; office II: g=0.12; office III: g=0.48), it was expected a decrease of the solar gains with a beneficial effect in summer periods in terms of thermal comfort and energy savings and a detrimental one in winter (as solar gains are desirable for naturally increasing the indoor temperature). However, it should be noticed that the minimum indoor temperature values registered in the winter period, during working hours, are very close to the minimum comfort temperature of 18ºC in the winter season, indicating that the solar heat gains in this period correspond, approximately, to the minimum values to ensure thermal comfort in the office areas.

Office IV (with the damaged SCF) shows higher peak vertical irradiance values (45 W/m^2 in summer and 151 W/m^2 in winter) than offices I and II with the new films. As the building management team reported, the damaged film is a reflective film with an approximate value of the (front) reflectance coefficient of SCF *B*. However, the obtained results do not show high similarity between irradiance values of offices II and IV, evidencing the already predicted variation of the optical and thermal properties of the film between the moment of its application and the moment of this study. To quantify the variation of the optical properties, the ratio of the measured indoor (I_{ind}) to outdoor (I_{out}) irradiance, which allows estimating the solar transmittance of a window, was calculated. Measurements during the winter days usually are closer to the values given in windows and films technical sheets due to the lower sun angles during this season being closer to a normal incidence of the solar rays. According to the experimental results, office IV has a solar transmittance of ~0.09 in summer (when the sun angles are higher) and ~0.20 in winter (when the sun angles are lower). When comparing the calculated value of solar transmittance of office IV at normal incidence (τ_{sol}=0.20) with the one of office II (τ_{sol}=0.06) it is possible to observe a variation of 70%.

Indoor horizontal and vertical illuminance are important indicators of the daylight availability in both the office area and the occupant's field of view (FOV), having a significant impact on the adaptation levels of the eye. Currently, office work activities involve the use of visual display units (computer, monitors, etc.) that are typically located at short distances (<1m) from the occupant's eye, promoting intense accommodation of the eye for prolonged hours a day. Frequently, due to office spaces' configuration (partitions, walls, etc.), far and near vision is confined to the latter, increasing the risk of developing ocular motility (abnormal eye alignment or difficulty in controlling eye movements) and binocularity functions (maintain visual focus on an object with both eyes, creating a single visual image) [93].

More recent glare indexes to predict visual discomfort conditions related to excessive luminance values are dependent on luminance ratios between glare sources and background surfaces in the occupants' FOV. These new indexes incorporate vertical illuminance in the viewer's FOV, which indicates the light availability that effectively reaches the occupant's eyes. Verdes et al. acknowledge in one study [94] that there is a high correlation between glare ratings and measured vertical daylight at the viewers' eyes when the occupant faces directly the window or walls that are perpendicular to the window, in a scenario without blinds. Also, the author states that vertical illuminance measurements near the window can effectively record the illuminance entering the room through the glass façade and therefore, it allows to estimate the visible transmittance of the glazing for different sun angles.

Apart from visual comfort, it is also important to evaluate the daylighting conditions in order to increase energy efficiency in buildings. Visual discomfort associated with excessive daylighting can trigger the activation of shading devices that too often remain in a "closed" position even after the discomfort conditions are no longer in place, ultimately increasing the electric light consumption [95].

Several studies [96], [97] suggest that workstations should be placed perpendicularly to the daylight sources – as is the case of windows – so that the line of sight would be parallel to the light source. This preferred workspace configuration is proven to reduce the risk of reflections in visual display units, such as monitors and computer screens, and the excessively bright light in the occupants' FOV. Guidelines or instructions to achieve comfortable indoor lighting conditions are varied and disperse in literature, as underlined by Jae Suk [98]. Even though visual comfort is not a new research topic, recommended threshold values are wide-ranging and too often applied to a restricted set of luminous conditions [98].

Different studies identify luminance thresholds of 2000-2800 cd/m^2 for visual comfort [99]–[103] and 2740-6000 cd/m^2 [99]–[101] for visual discomfort in the FOV, for a viewer's direction parallel to the light source (cd/m^2: candela per square metre is the SI unit of illuminance and luminous emittance and equals to 1 lx). Lower threshold values were found for a viewer's direction perpendicular to the light source (workstations placed parallel to daylight sources). Moreover, vertical illuminance at the occupants' eye between 875-2000 lx was found to provide visual comfort, whereas threshold values between 1250-3000 lx were found to cause visual discomfort conditions.

Figure 66 and Figure 67 show the outdoor, $E_{out,vert}$, and indoor, $E_{ind,vert}$, vertical illuminance for all offices in summer and winter periods, respectively. Just as the graphics depicted in Figure 64 and Figure 65, the two vertical axis present the same variable (illuminance), as it was impossible to present the indoor and outdoor values on the same axis due to scale compatibility, as the outdoor illuminance is almost two times higher than the indoor illuminance.

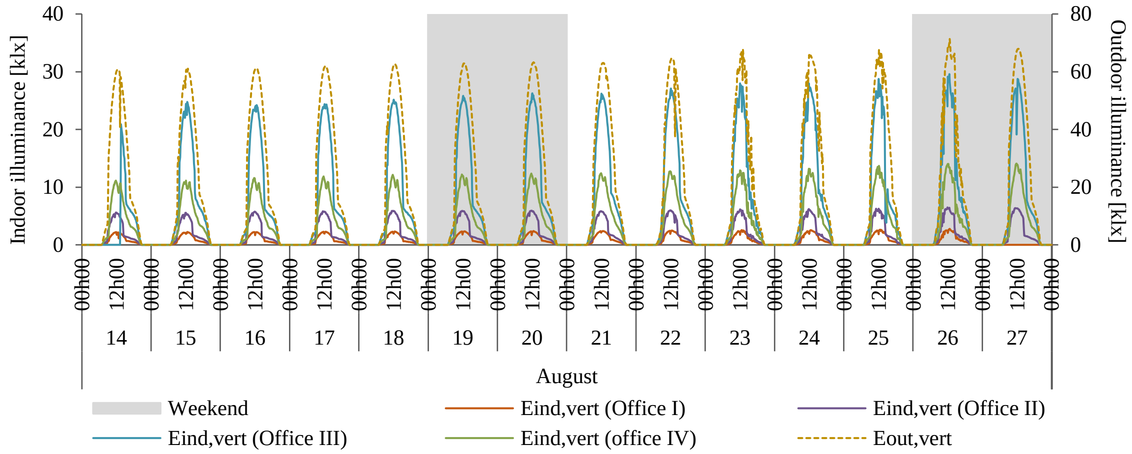

Figure 66. Indoor illuminance on vertical plane, $E_{ind,vert}$, in office I, II, III, and IV and outdoor illuminance on vertical plane, $E_{out,vert}$, during the summer period

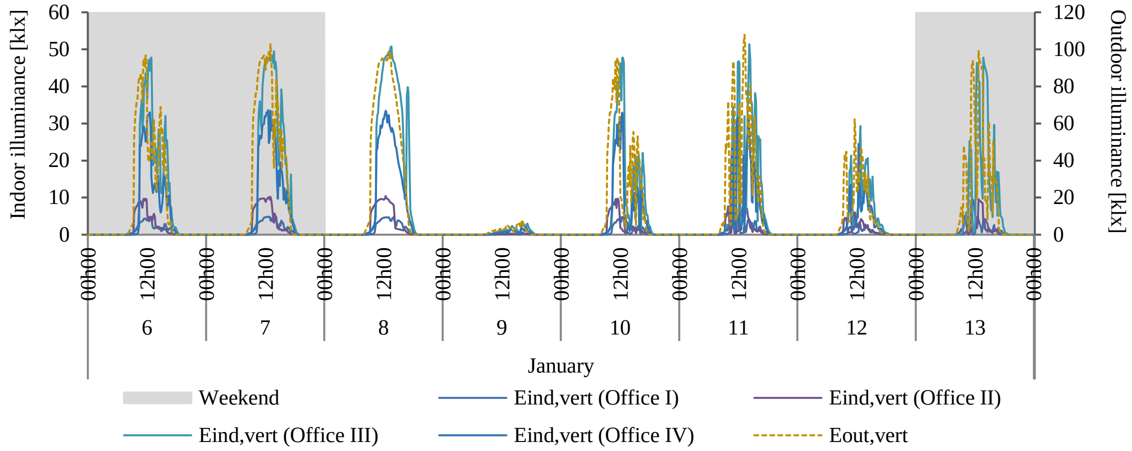

Figure 67. Indoor illuminance on vertical plane, $E_{ind,vert}$, in office I, II, III, and IV and outdoor illuminance on vertical plane, $E_{out,vert}$, during the winter period

As it was also noticed in the vertical irradiance analysis, the outdoor illuminance maximum values occur around 12h00-13h00 as expected due to the façades' South solar orientation, showing peak values of 61-69 klx in the summer and 95-108 klx in the winter periods (except on the 9th of January and 12nd of January with peak values ~6.5 klx and ~62 klx due to the predominance of overcast and intermittent sky conditions). Table 17 sums the obtained indoor illuminance peak values and the reduction in relation to the outdoor environment and to the reference office.

Table 17. Peak and reduction of indoor illuminance values in the four offices during days without occupancy in the summer and winter periods

Period	Office	Indoor peak [klx]	Reduction in relation to the outdoor environment [%] [1)]	Reduction in relation to the reference office [%] [1)]
Summer	I	28.1	96.8	89.8
	II	6.5	92.2	77.2
	III	29.6	65.7	0.0
	IV	14.1	82.7	49.7
Winter	I	5.0	95.6	90.2
	II	10.1	91.6	81.5
	III	50.2	48.5	0.0
	IV	32.7	72.5	39.3

[1)] Calculated using trapezoidal numerical integration

Office III (original window) shows a peak illuminance value of 29.6 klx in summer and 50.2 klx in winter and an indoor illuminance reduction on vertical plane in relation to the outdoor illuminance of 65.7% in summer and 48.5% in winter. This significantly reduces the indoor illuminance levels and is exclusively related to the original glazing system (without SCF). The original window already delivers by itself reasonable protection against visible gains. Nonetheless, illuminance peak values are still very high in this office, showing that visual discomfort through the influence of glare situations are very likely to occur, making this area unpleasant or even impossible to work on without the activation of complementary shading devices.

The application of SCFs resulted in the decrease of indoor illuminance on vertical plane in 89.8% (office I) and 77.2% (office II) in summer days and of 90.2% (office I) and 81.5% (office II) in winter days, respectively, when compared to the reference office (original window). Given the fact that SCFs reduced the windows' visible transmittance (office I: τ_{vis}= 0.25; office II: τ_{vis}= 0.11; office III: τ_{vis}= 0.56), it was expected a decrease of the visible gains with a beneficial effect in both summer and winter periods by reducing possible glare situations due to high illuminance levels. Although there is a significant reduction of indoor illuminance values with the application of SCFs *G* and *B*, the maximum values of 28.1 klx (office I) 6.5 klx (office II) in summer days and 6.5 klx (office I) and 10.1 klx (office II) in winter days are still high and do not ensure that glare situations do not occur (recommended values in literature: for office and computer work are of ~0.5 lx and for high-precision work of ~1.5-2.0 lx).

Office IV (with the damaged SCF) shows higher peak illuminance values in winter (32.7 klx) than offices I and II and higher peak values in summer (14.1 klx) than office II. The ratio of the measured indoor, $E_{ind,vert}$, to outdoor, $E_{out,vert}$, illuminance on vertical plane allows estimating the visible transmittance of the glass. According to the experimental results, office IV has a visible transmittance of ~0.22 in summer (when the sun angles are higher) and ~0.34 in winter (when the sun angles are lower). When comparing the calculated value of visible transmittance of office IV at normal incidence (τ_{sol}=0.34) with office II (τ_{sol}=0.11) it can be noticed a variation of 68%. This result is very similar to that obtained for the solar transmittance, proving that the initial properties of the damaged film were seriously affected since its application.

Nabil & Mardaljevic [75] developed a new concept to assess daylighting in buildings through the Useful Daylight Illuminance (UDI) metric. The UDI considers the number of hours of daylighting availability within defined ranges values categorized as useful (U) and not useful (NU):

- values below 0.1 klx are insufficient and can contribute to increase the energy needs with artificial lighting (NU);
- values between 0.1-0.3 klx may require supplementary artificial lighting (NU);
- and values above 3 klx can cause thermal and/or visual discomfort, and therefore values in this illuminance range are not considered useful (NU);

- on the contrary, values between 0.3-3 klx are considered useful and desirable for indoor environments (U).

Table 18 shows the daylight analysis using the UDI metric for weekend Days (Without Occupancy), *DwO*, of summer, *-S*, and winter, *-W*, periods. The selected days, *DwC-S* and *DwC-W*, ensure that artificial lighting was deactivated in all offices and that the indoor illuminance values are only dependent on the daylight availability related to the windows of each office area.

Table 18. Useful daylight illuminance, *UDI*, for office I, II, III, and IV during the summer, *DwC-S*, and winter, *DwC-W*, days without occupancy

		Useful daylight illuminance [%]			
		$UDI_{<0.1}$	$UDI_{0.1\text{-}0.3}$	$UDI_{0.3\text{-}3}$	$UDI_{>3}$
DwC-S	Office I (w/ SCF *G*)	12.2	12.2	75.6	0.0
	Office II (w/ SCF *B*)	5.5	7.3	50.9	36.4
	Office III (w/o SCF)	0.0	3.6	23.6	72.7
	Office IV (w/ damaged SCF)	1.8	5.5	30.9	61.8
DwC-W	Office I (w/ SCF *G*)	22.9	11.4	48.6	17.1
	Office II (w/ SCF *B*)	22.9	8.6	31.4	37.1
	Office III (w/o SCF)	17.1	0.0	17.1	65.7
	Office IV (w/ damaged SCF)	17.4	4.3	13.0	65.2

Office III has the lowest performance of the UDI metric, showing a high percentage of hours above 3 klx in summer (72.7%) and in winter (65.7%). These results combined with the high maximum illuminance values in summer (29.6 klx, Table 17) and winter (50.2 klx, Table 17) indicate that visual discomfort associated with glare is almost certain to occur without the activation of shading devices.

In line with the literature [55], [57], it can be concluded that the daylight availability below 3 klx has increased with the application of SCFs on the glazing system. In the summer period, office I shows the highest number of hours (75.6%) within the useful range of 0.3-3 klx, followed by office II (50.9%), office IV (30.9%) and office III (23.6%).

In the winter period, the useful daylighting availability, $UDI_{0.3\text{-}3}$, in the offices was not as high as in summer, showing a substantial decrease in the number of hours inside the useful range. A possible explanation is the lower sun's elevation and greater perpendicularity of the sun's rays to the glazing surface in the winter, increasing the incident direct radiation around 10h00-14h00 (façade South oriented) but decreasing enormously in the remaining hours due to higher shading effects derived from the windows' boundaries and surrounding buildings.

Compared to the other glazing solutions, SCF *G* (τ_{sol}= 12%, τ_{vis}= 25%) shows the highest increase of the useful daylight illuminance, $UDI_{0.3\text{-}3}$, and is the most appropriate retrofitting scenario to prevent possible glare situations during both summer and winter seasons, within the SCFs studied experimentally.

5.5.3 Summary of the experimental results

The data collected in the experimental campaign in August and January, considered in this study as representative of summer and winter periods, yielded a set of results described in sections 7.5.1 and 7.5.2 and summarised in Table 19. It should be noted that the parameters analysed with regard to thermal performance were obtained through data collected on days when the air conditioning was not working to evaluate the impact of the different glazing systems without having the interferences from the thermal control of the indoor environment.

Office III (original window) presents the lowest thermal, luminous, and energy performance for the summer season, reaching indoor temperature maximum values of 35.82ºC and presenting the highest indoor average temperature of 27.18ºC. This office shows the highest indoor illuminance, reaching maximum values of 29 619 lx in summer and 50 219 lx in winter, increasing the need of activating the shading device to control the transmitted solar radiation. However, it does not prevent excessive solar gains and the consequent risk of indoor overheating. These conditions are very likely to induce thermal and visual discomfort conditions for the occupants and reduce the satisfaction with the working space, especially during high insolation periods. Also, the daily range of indoor temperature throughout the days is very high in this office – with temperature varying between 21.88ºC and 35.82ºC in the summer period and between 15.89ºC and 27.81ºC in the winter period –, which contributes to occupants' thermal perception and awareness and increasing thermal discomfort in the office.

When comparing the results of the retrofitted offices, it can be noticed that the glazing system of office II is more effective in reducing the indoor temperature. In fact, SCFs *G* (office I) and *B* (office II) are both solar control films that alter the windows' properties by decreasing the solar gains through absorption (office I: $\rho_{f,sol}$= 0.25; α_1= 0.62) and reflection (office II: $\rho_{f,sol}$= 0.59; α_1= 0.35) processes, respectively [104]. These properties justify the higher external surface temperatures of the outer pane of the glass in office I compared to office II.

From the existing literature of SCFs, the thermal performance of offices I and II was expected since office II has a higher reflective coefficient than office I. Also, it should be noted that the minimum value registered during the winter campaign is very close to the minimum comfort temperature of 18 ºC for the winter season, according to the Portuguese regulation [82]. From a thermal standpoint, different studies emphasize that the application of SCFs is usually beneficial in summer and disadvantageous in winter due to the reduction of the solar gains [55], [57]. In the experimental study developed in section 4 [43], it was concluded that the application of a low reflective coefficient film in single glass windows with an East solar orientation resulted in a short and insufficient decrease of the indoor temperature (less than 1 °C on average on a daily sun-hours basis during the summer days). In the same study, a further investigation through a numerical analysis concluded that highly reflective films could decrease the discomfort hours above 25 °C by ~35% in the cooling season and increase the annual percentage of comfort hours by ~12%. Another study [57] compared two office areas located in a Mediterranean climate with double glazing units without and with a highly reflective external SCF with a Southeast solar orientation. In this study, the authors concluded that a higher reduction of the indoor temperature in the cooling than in the heating season resulted in an increase of the annual working hours within the comfort temperature range, according to the Portuguese regulations [82]. In terms of energy performance and aligned with literature findings, office II shows the highest irradiance reduction on vertical plane in relation to the outdoor environment (~96% for summer and winter) and in relation to the reference office III (75.6% for summer and 81.5% for winter), reaching maximum irradiance values of 25 W/m^2. The results indicate that this glazing is the most energy effective solution in reducing the solar gains in the summer and winter seasons (highest reduction in relation to the outdoor environment and the reference office).

The luminous performance analysis revealed that office I shows the lowest indoor illuminance peak value on vertical plane and consequently the highest illuminance reduction in relation to the outdoor environment and the reference office in both seasons, and office II the second-highest reduction. Even though the illuminance reduction levels are high, the absolute values of indoor illuminance indicate that offices I and II still show daylight illuminance values above the recommend ones to perform office activities during working hours (0.5 lx according to [74]).

A comprehensive analysis of the results obtained in office IV with the damaged SCF, which is a highly reflective film comparable to SCF *B*, showed that the level of deterioration of the film (tears, cracks, blistering, lack of transparency, detachment, and deterioration of external layers) seriously affected its optical and thermal properties. The calculated optical properties showed a variation of 70% of the visible and solar transmittance, having a high impact on the thermal and visual performance of the office space with this film.

Table 19: Monthly results of the experimental campaign yielded during both summer and winter periods: thermal, luminous, and energy performance of offices I, II, III, and IV

		Thermal performance									Luminous performance			Energy performance [w/m²]		
		T_{ind} [ºC]			T_{si} [ºC]			T_{se} [ºC]			$I_{ind,vert}$			$E_{ind,vert}$		
	Office	Min	Aver	Max	Min	Aver	Max	Min	Aver	Max	Max [lx]	Reduction in relation to outdoor environment[2] [%]	Reduction in relation to reference office[2] [%]	Max [W/m²]	Reduction in relation to outdoor environment[2] [%]	Reduction in relation to reference office[2] [%]
summer	I	23.46	26.53	30.49	22.90	27.07	33.20	17.85	29.22	54.16	2810	96.8	89.8	36	95.2	64.5
	II	23.64	26.28	29.65	22.84	26.58	32.13	17.65	26.97	48.16	6483	92.2	77.2	25	96.4	75.6
	III[3]	21.88	27.18	35.82	22.92	27.91	35.89	17.86	27.87	50.80	29619	65.7	0.0	113	85.2	0.0
	IV	23.80	26.61	30.02	23.19	26.72	31.74	17.95	27.50	49.76	14112	82.7	49.7	48	91.8	45.0
winter	I	17.72	20.55	25.8	16.26	20.43	29.74	6.33	13.05	25.66	5035	95.6	90.2	78	92.6	66.2
	II	17.41	19.91	23.73	16.09	19.43	25.8	5.95	15.30	40.66	10082	91.6	81.5	42	95.9	81.5
	III[3]	15.89	20.61	27.81	14.77	20.64	32.81	6.01	17.12	44.08	50219	48.5	0.0	229	78.0	0.0
	IV	16.96	20.15	25.28	15.98	19.80	27.05	6.24	16.49	43.6	32678	72.5	39.3	151	86.3	38.3

[1] Based on experimental data from days when the HVAC system was turned off
[2] Calculated using trapezoidal numerical integration
[3] Office III (without SCF)

Legend:

T_{ind}: indoor temperature

T_{si}: internal surface temperature of inner surface the glass

T_{se}: external surface temperature of outer surface of the glass

Max: maximum value

Min: minimum value

Aver: Average value

highest value for the parameter

lowest value for the parameter

5.5.4 Reference days

A comprehensive study on the thermal and visual performance of SCFs on glazed façades is carried out by analysing four reference days with extreme and opposing characteristics. The selected reference days were selected from the six months of the experimental campaign, comprising two days with the highest and lowest outdoor temperatures to analyse the thermal behaviour and two days with the highest and lowest sun's elevation to analyse the daylight availability at the working plane, as follows:

- Day with the Highest daily average Outdoor Temperature (D-HOT): 19th of August (T_{out}= 26.73ºC);
- Day with the Lowest daily average Outdoor Temperature (D-LOT): 6th of January (T_{out}= 11.48°C);
- Day with the highest sun's elevation angle – as close as possible to the Summer Solstice (D-SS): ~21st of June;
- Day with the lowest sun's elevation angle – as close as possible to the Winter Solstice (D-WS): ~21st of December.

It should be noted that the selected reference days, subject of study in this section, do not necessarily follow within the selected consecutive days analysed in both section 5.5.1, 5.5.2, and 5.5.3. The reference days were selected from the several days of the experimental campaign (full months from August to January) for displaying extreme climate conditions (outdoor temperature and sun's elevation) that directly influence the thermal and luminous performance and, consequently, the energy performance of the office areas. The selected days and the following analysis aim to contribute to the comprehensive knowledge of the influence of SCFs on the thermal and visual conditions of existing office buildings with double-glazed windows by analysing its impacts over the full spectrum of outdoor temperature and the sun's elevation possibilities.

5.5.4.1 D-HOT and D-LOT

Figure 68 shows, for the four offices, the values of indoor temperature, T_{ind}, internal, T_{si}, and external, T_{se}, surface temperatures, outdoor temperature, T_{out}, and global solar radiation on vertical plane, $I_{out,vert}$. The outdoor temperature, T_{out}, is the same in the three graphics depicted in D-HOT and D-LOT in Figure 68 and provide a reference for visual comparison of the three different temperatures depicted T_{ind}, T_{si}, and T_{se}. The vertical axis on the left and right show temperature and radiation values, respectively.

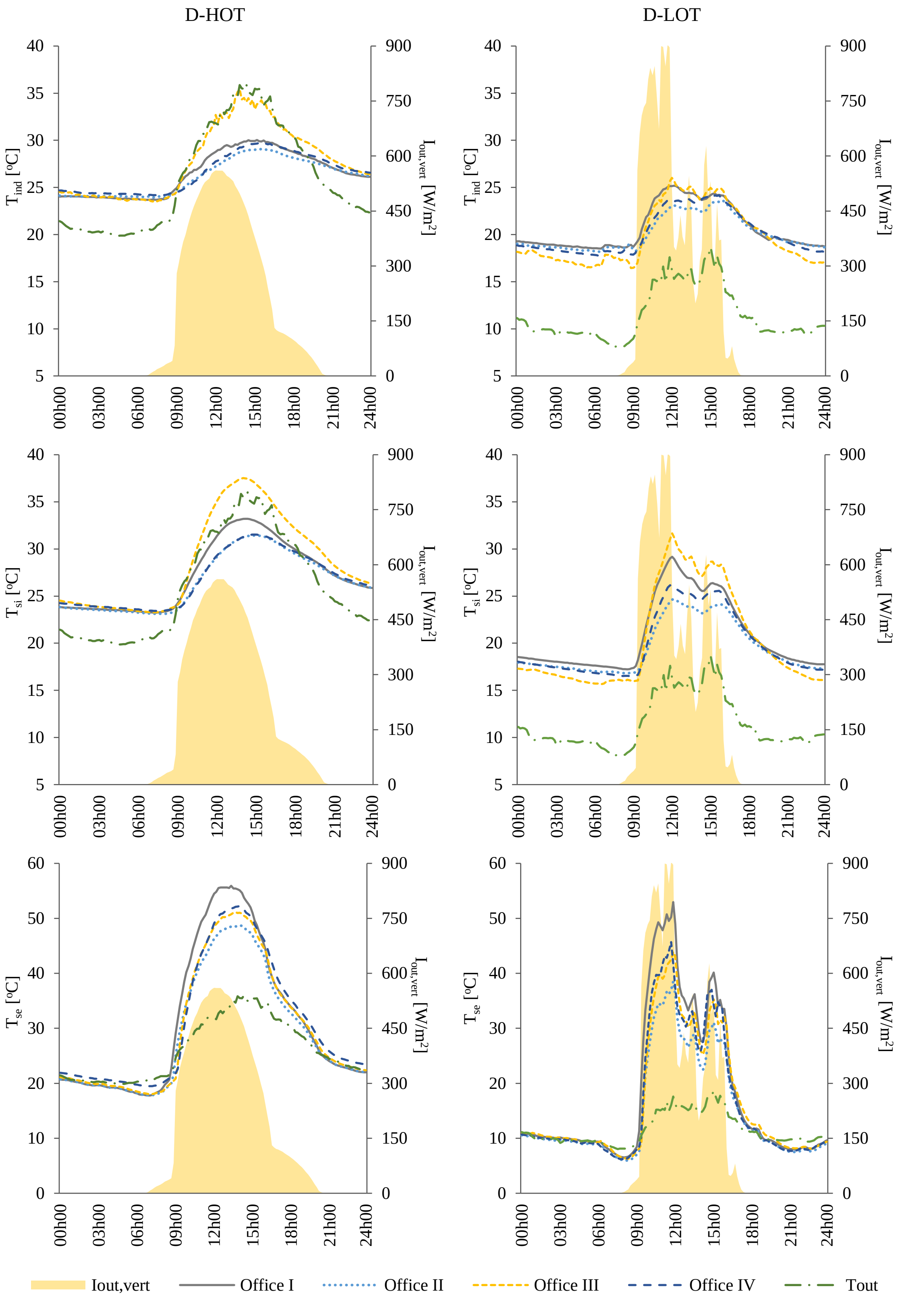

Figure 68. Thermal performance of the four offices in D-HOT (19th of August) and D-LOT (6th of January): indoor temperature, T_{ind}, and internal, T_{si}, and external, T_{se}, surface temperatures along with outdoor temperature, T_{out}, and global solar radiation on vertical plane, $I_{out,vert}$

In D-HOT it can be noticed that from 09h00 to 18h00, offices II and III show the lowest (24-29ºC) and the highest (25-36 ºC) range of indoor temperature, respectively, and offices I, II, III, and IV show maximum indoor temperature values of approximately 30 ºC, 29 ºC, 36 ºC, and 30 ºC, respectively. In D-LOT it can be noticed that from 09h00 to 18h00, offices II and III also show the lowest (18-24 ºC) and the highest (16-26 ºC) daily range of indoor temperature, respectively, whereas offices I and IV show indoor temperature ranges between 19-25 ºC and 18-24 ºC. In D-LOT it is important to notice that office III shows indoor temperatures that exceed the maximum comfort range of 25 ºC according to the Portuguese thermal regulation [57]. This is a crucial observation. If office III (original window) shows overheating hours in the day with the lowest daily outdoor temperature, then overheating hours will likely occur on all the other days with higher outdoor temperatures. In non-working hours, the indoor temperature is similar for the four offices in D-HOT and for the three offices with SCFs on D-LOT. These results support the conclusion that SCF *B* (film with the highest reflective coefficient) installed in office II has the best thermal performance in days with the highest and the lowest outdoor temperature since this office shows the highest percentage of the working hours within the comfort range of temperatures.

It can be concluded that thermal discomfort due to overheating of indoor spaces occurs during the entire working hours of D-HOT in all the offices and in some hours of D-LOT in office III. This fact underlines and justifies the relevance of this study since both the retrofitting SCFs *B* and *G* studied increased the thermal comfort conditions and therefore reduce the need to activate climatization systems.

The internal surface temperature of the glass, T_{si}, in the four offices have a similar behaviour throughout D-HOT. First, the temperature starts to increase after 09h00 following the increase of the global solar radiation on the façade. Then, T_{si} increases until 14h00 and then starts to decrease until 09h00 of the next day. However, the maximum values vary from office to office, reaching values of between 49-56 ºC in office III. The external surface temperature, T_{se}, shows higher values than T_{si} for the same hours of the day, ranging between 56 ºC and 49 ºC in office I and in office II, respectively, at around 14h00. Offices III and IV show similar values of T_{se} throughout the day, presenting a peak value of 52 ºC. By comparing the values of T_{se} and T_{si} at 14h00 in D-HOT it can be noticed that the difference in the surface temperatures (T_{se}-T_{si}) is around 22 ºC in office I, 17 ºC in office II, 15 ºC in office III and 21 ºC in office IV. Office III shows the lowest difference of the surface temperatures (T_{se}-T_{si}) and office I the highest. This was expected since office III shows the highest indoor and internal surface temperatures (decreasing the difference of T_{se}-T_{si})

and office I exhibits the highest absorption coefficient among the four glazing systems, consequently increasing the T_{se} values (office I: α_1=0.62; office II: α_1=0.35; and office III: α_1=0.41).

Figure 69 shows the profiles of indoor and outdoor temperatures, T_{ind} and T_{out}, and internal and external surface temperatures, T_{si} and T_{se}, in offices I, II, III, and IV for D-HOT.

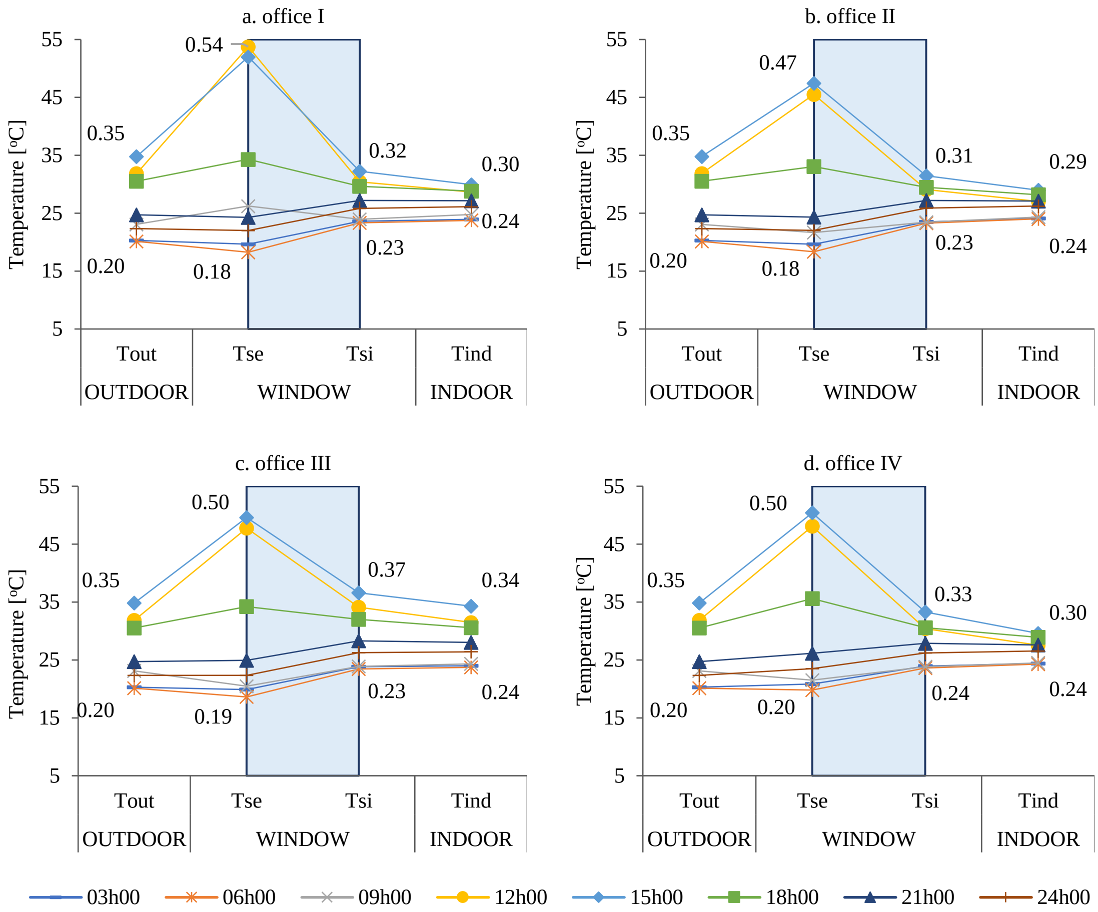

Figure 69. Horizontal temperature profile in D-HOT: indoor, T_{ind}, and outdoor, T_{out}, temperatures and internal, T_{si}, and external, T_{se}, surface temperatures at different hours for: a. office I, b. office II, c. office III and, d. office IV

The values of outdoor temperature, T_{out}, are the same in the graphics depicted in Figure 69 because T_{out} is not dependent on the type of office but rather on weather conditions. At 12h00, 15h00, and 18h00, T_{out} varies between 30.5ºC and 34.8ºC and in the other hours varies between 20.2ºC and 24.7ºC. It was expected that at 09h00, T_{out} could show higher values than those effectively observed (closer to those observed at 15h00, due to the façades South solar orientation). However, due to the building's "L shape" (zone B of the building identified in Figure 46a), there is a shading effect in the first hours of the morning period. This shading in the morning period can also be noticeable on outdoor vertical solar radiation levels, as solar radiation increases at a higher rate straight after 09h00 (see Figure 68 for example).

In the hours with higher solar radiation values (12h00 and 15h00), the external surface temperature, T_{se}, is higher than the outdoor temperature, T_{out}, and the difference between the two temperatures (T_{se}-T_{out}) is more noticeable in office I and less noticeable in office II. At 12h00 and 15h00, office I shows T_{se} values of 54ºC and 52ºC and office II of 46ºC and 48ºC. These differences are related to the different absorptance coefficients of the external surface of the window – which in offices I and II are related with the films and in office III with the outer glass layer of the window (office I: α_1= 0.62; office II: α_1= 0.35; office III: α_1= 0.41). The higher the absorptance coefficient and the solar radiation levels, the higher the values of T_{se}.

Regarding the internal surface, T_{si}, and indoor, T_{ind}, temperatures, T_{si} is higher than T_{ind} at 12h00 and 15h00 in all offices, and office III shows the highest T_{si} value (office I: T_{si}= 32.24ºC, office II: T_{si}= 31.44ºC, office III: T_{si}= 36.58ºC, and office IV: T_{si}= 32.28ºC). The difference between the two surface temperatures is more pronounced in office III than in the other offices. A higher gradient temperature between the inner surface of the glass and the indoor environment (T_{si}-T_{ind}) increases the heat transfer by convection and radiation, increasing the indoor temperature of the office, especially in locations nearby the window.

When comparing the T_{ind} at all hours, as concluded before, all offices show T_{ind} outside the comfort temperature according to the Portuguese thermal regulations (between 18 ºC and 25 ºC) [105]. However, it is essential to emphasize that office III showed the highest range of T_{ind}, varying between 24ºC and 34ºC, and office II, the lowest range of T_{ind}, varying between 24ºC and 29ºC. These results indicate that office III without SCF shows a higher heat exchange between indoor and outdoor environments when high solar radiation values are observed. This fact is crucial for the office space's thermal comfort and energy efficiency, as it indicates that greater use of the HVAC system is needed when there is no SCF that could avoid the temperature to reach the maximum thermal comfort temperature of 25ºC.

Figure 70 shows the profiles of indoor and outdoor temperatures, T_{ind} and T_{out}, and internal and external surface temperatures, T_{si} and T_{se}, in offices I, II, III, and IV for D-LOT.

At 12h00 T_{out} varies between ~18ºC and at all the other hours it varies between 9ºC and 11ºC. On this day, it is also noticeable that T_{out} at 18h00 is closer to the temperature values observed during the night period since there is no solar radiation at this hour.

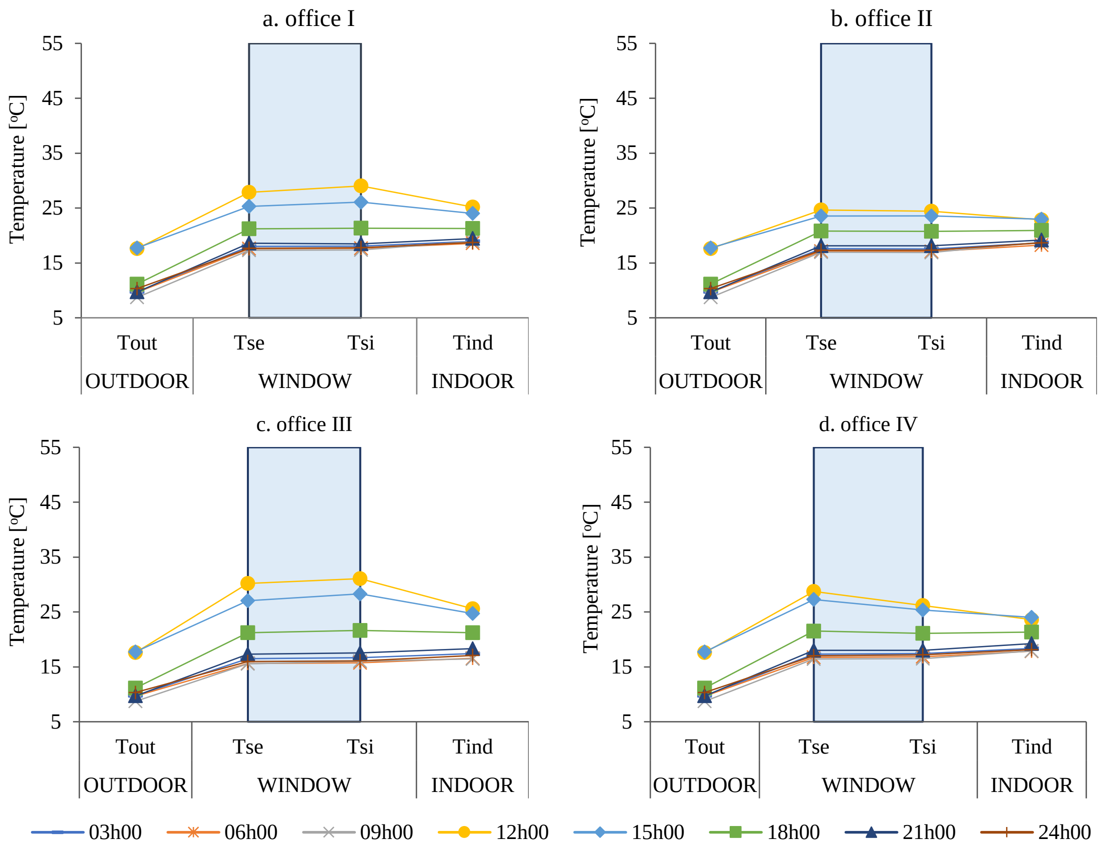

Figure 70. Horizontal temperature profile in D-LOT: indoor, T_{ind}, and outdoor, T_{out}, temperatures and internal, T_{si}, and external, T_{se}, surface temperatures at different hours for: a. office I, b. office II, c. office III and, d. office IV

During insolation hours, T_{se} is higher than T_{out} in all offices. The difference between these two temperatures is more pronounced in office III and less pronounced in office II. At 12h00 and 15h00, office III show values of T_{se} of 30ºC and 27ºC and office II of 25ºC and 24ºC, respectively.

In D-LOT, the values of T_{se} and T_{si} at the same hour are comparable with each other in all offices as opposed to the values recorded in D-HOT. Similar values demonstrate a lower heat transfer between the different layers of the window, resulting in lower heat exchange between the inner surface of the glass and the indoor environment. Regarding the internal surface, T_{si}, and indoor, T_{ind}, temperatures, T_{si} is higher than T_{ind} at 12h00 and 15h00 in offices I and III, and similar to each other in offices II and IV. In the remaining hours, with lower or no radiation levels, T_{se}, T_{si}, and T_{ind} show similar temperature values.

The T_{ind} of the offices varies between 19-25ºC, 18-23ºC, 17-26ºC, and 18-24ºC, in offices I, II, III, and IV, respectively. According to the Portuguese thermal regulation [105], offices I, II and IV show approximately T_{ind} within the comfort range of temperatures. Office III displays the highest range of T_{ind} with recordings of ~16ºC at 09h00 and ~26ºC at 12h00, which means that in those three hours it was observed the highest increase of T_{ind}, changing from being below the minimum thermal comfort temperature of 18ºC to being above the maximum thermal comfort temperature of 25ºC [105]. This rapid increase of T_{ind} can cause thermal discomfort as it goes from being too cold to being too warm in three hours, increasing occupants' thermal perception and awareness and very likely increasing the activation of shading devices or climatization systems.

Figure 71 and Figure 72 show, for each office, the values of outdoor and indoor vertical illuminance, $E_{out,vert}$ and $E_{ind,vert}$, and indoor horizontal illuminance, $E_{ind,hor}$. Indoor vertical illuminance was measured at 0.70m height and 0.10m distance away from the window. This sensor was placed in the same position in all four offices. The indoor horizontal illuminance was measured at the desk plane height (~0.70m) and placed next to each computer in each office, thus preventing measurements that encompassed light from the electrical equipment. However, during some visits to the office areas, it was often observed misplaced sensors (near the window or in front of the computer). The new misplaced positions were considered to be associated with occupants reorganizing the desks' materials or cleaning tasks. In a future investigation, it is recommended that sensors placed on the work desk should be fixed, for instance, with double-sided tape, preventing possible shifting/positioning of the sensor.

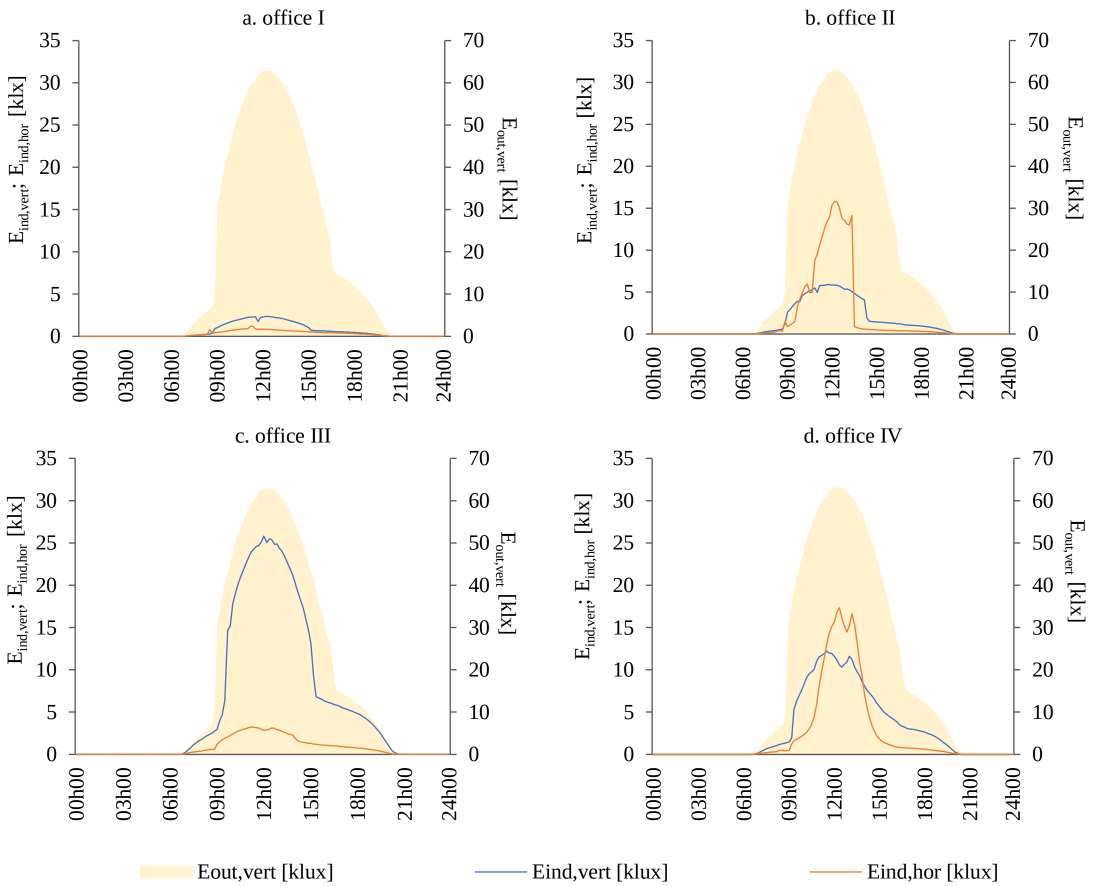

Figure 71. Illuminance levels during D-HOT: outdoor and indoor vertical illuminance, $E_{out,vert}$ and $E_{ind,vert}$, and indoor horizontal illuminance, $E_{ind,hor}$, at different hours for: a. office I, b. office II, c. office III and, d. office IV

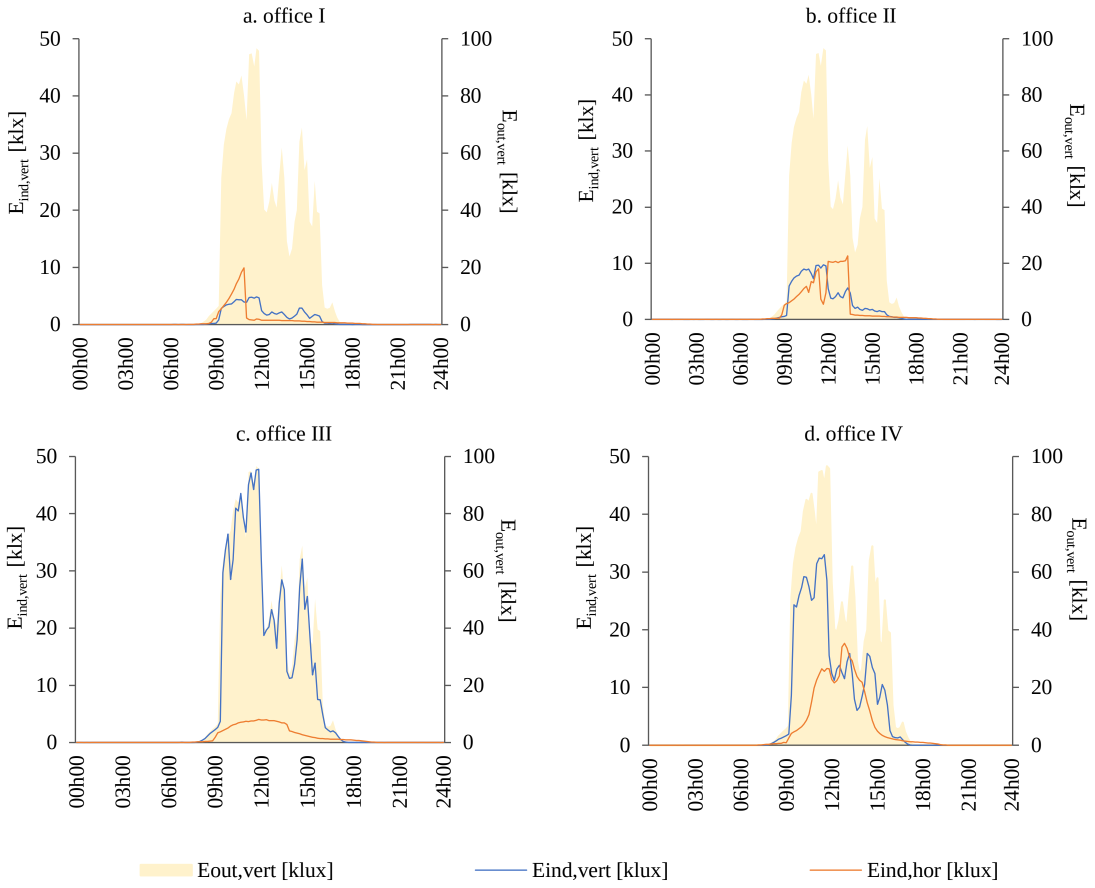

Figure 72. Illuminance levels during D-LOT: outdoor and indoor vertical illuminance, $E_{out,vert}$ and $E_{ind,vert}$, and indoor horizontal illuminance, $E_{ind,hor}$, at different hours for: a. office I, b. office II, c. office III and, d. office IV

In the D-HOT, the outdoor vertical illuminance, $E_{out,vert}$, (vertical axis on the right side of the graph in Figure 71) in the four offices are similar in shape and maximum values (~63klx), as expected, since the offices have the same Southside solar orientation. Also, it shows a considerable difference in the indoor horizontal, $E_{ind,hor}$, and vertical $E_{ind,vert}$, illuminance (both on the vertical axis on the left side of the graph) in offices I, II and III. During the insolation hours in the D-HOT, $E_{ind,vert}$ shows a mean (and maximum) value of 1.1klx (2.4klx), 2.5klx (5.9klx), 11.1klx (25.8klx), and 5.3klx (12.2klx), in offices I, II, III, and IV, respectively. The results indicate that the maximum values are higher than twice the mean values in each office and that office III and office I show the highest and the lowest mean indoor vertical illuminance. Indoor horizontal illuminance showed a daily mean (and maximum) value of 0.5klx (1.2klx), 3.3klx (15.8klx), 1.5klx (3.2klx), and 4.1klx (17.3klx), for offices I, II, III, and IV, respectively. It was expected that horizontal illuminance values in office II could be lower than those in offices I and III due to the higher visible transmittance of the glazing in office II; however, this was not the case. These results can only be justified due to offices' occupants changing the sensors arrangement on the desk tables.

According to the Useful Daylight Illuminance (UDI) range values – that consider daylight horizontal values within 0.3-3klx to be useful and values >3klx to cause thermal and visual discomfort – it can be concluded that offices III and IV are likely to show visual discomfort in sunny summer days in almost all the working hours.

Regarding D-LOT (Figure 72), the outdoor vertical illuminance, $E_{out,vert}$, in the four offices is similar in shape and show the same maximum value ~96.6klx (~35% higher than the $E_{out,vert}$ peak recorded in D-HOT). As stated before, this was expected since the offices have the same Southside solar orientation. During insolation hours, the indoor vertical illuminance shows a mean (and maximum) value of 0.8klx (4.8klx), 1.5klx (9.7klx), 7.6klx (47.8klx), and 4.8klx (33.0klx), for offices I, II, III, and IV, respectively. Vertical illuminance values show that the SCF *G* in office I is the most suitable in reducing the indoor illuminance, followed by the SCF *B* in office II. Finally, office III presents the highest values of indoor vertical illuminance, which potentiate visual discomfort conditions.

Figure 73 and Figure 74 show, for each office, the values of indoor (vertical axis on the left side of the graph) and outdoor (vertical axis on the right side of the graph) vertical irradiance, $I_{out,vert}$ and $I_{ind,vert}$. The indoor irradiance was measured at 0.70m height and 0.10m distance from the window. The outdoor irradiance was measured on the south façade.

The maximum outdoor and indoor irradiance on vertical plane occurs around 12h00, as previously observed with the outdoor and indoor illuminance results. In D-HOT, the outdoor irradiance on vertical plane in the four offices is similar in shape and maximum values, ~830W/m^2, since all the offices have the same south solar orientation.

In the D-HOT, office II with SCF *B* shows the lowest maximum and average indoor irradiance values, showing a maximum of 25W/m^2 and an indoor irradiance reduction of 96% in relation to the outdoor environment and a reduction of 76% in indoor irradiance on a vertical plane when compared to the reference office. Office I with SCF *G* shows a maximum value of indoor irradiance of 36W/m^2 and an indoor irradiance reduction of 95% in relation to the outdoor environment. Comparing the solution of the glazing system in office I with the reference office III, it can be noticed a reduction of 65% in indoor irradiance on a vertical plane. Office IV exhibits a maximum irradiance value of 48W/m^2 and an irradiance reduction of

92% in relation to the outdoor environment. Comparing the solution of the glazing system in office IV with the reference office III, it can be noticed a reduction of 45% in indoor irradiance on a vertical plane.

In the D-LOT, it can be noticed that indoor irradiance on vertical plane, $I_{int,vert}$, shows daily mean values of 21W/m^2, 9W/m^2, 48W/m^2, and 34W/m^2, approximately, and maximum values of 65W/m^2, 36W/m^2, 182W/m^2, and 135W/m^2, in offices I, II, III, and IV, respectively.

The results in both the D-HOT and D-LOT show that the SCF *G* in office II is the most effective in reducing indoor irradiance, followed by the SCF *B* in office I.

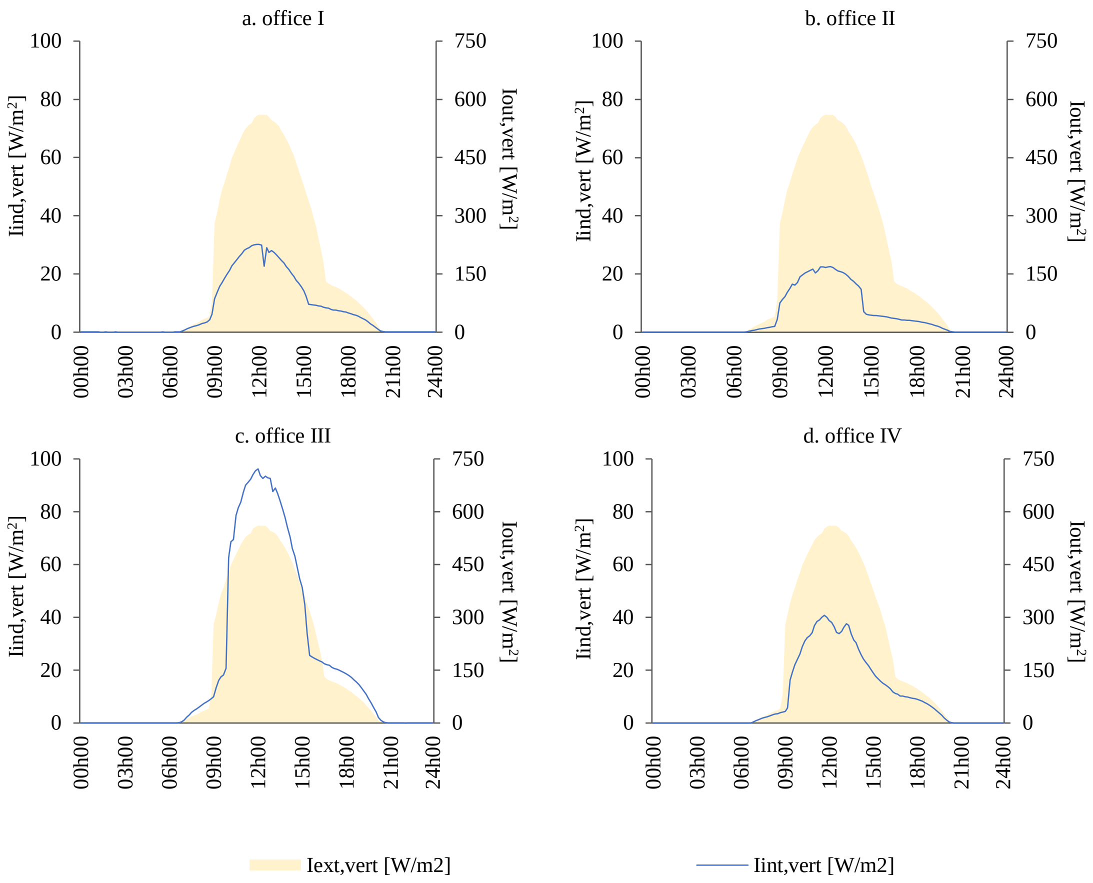

Figure 73. Irradiance levels during D-HOT: outdoor and indoor vertical irradiance, $I_{out,vert}$ and $I_{ind,vert}$, at different hours for: a. office I, b. office II, c. office III and, d. office IV

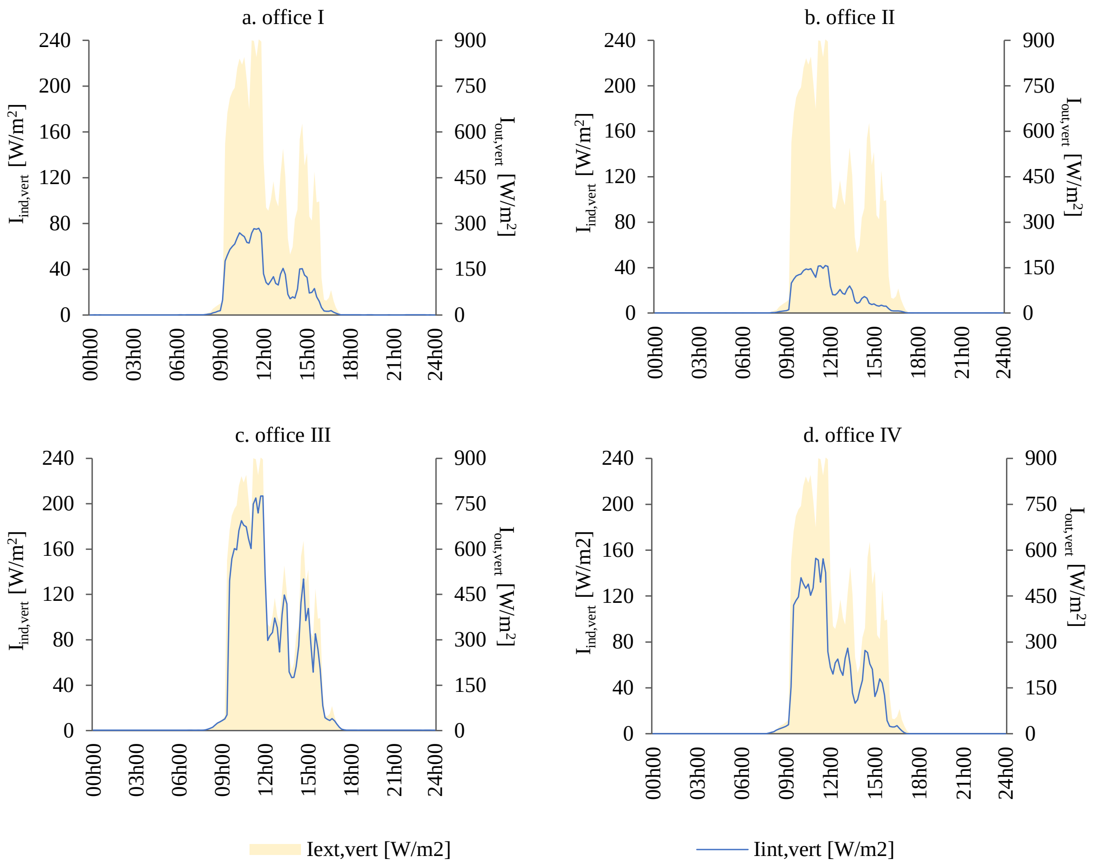

Figure 74. Irradiance levels during D-LOT: outdoor and indoor vertical irradiance, $I_{out,vert}$ and $I_{ind,vert}$, at different hours for: a. office I, b. office II, c. office III and, d. office IV

5.5.4.2 Summer and winter daylight availability

The daylight availability was evaluated through the absolute values of the indoor illuminance on horizontal plane (h=0.8m) considering 0.5klx as the recommended value for comfortable daylighting illumination for office room activities (e.g. writing, typing, reading, data processing) according to EN 12464-1 (2014) [74]. The evaluation was performed under clear sky conditions in days closer to the summer and winter solstice when the sun's elevation angle is at its highest and lowest level, respectively, concerning the annual solar dynamic behaviour. For each day, the illuminance values were measured at three different hours 09h00, 12h00, and 15h00 in 27 different points in each office as illustrated in Figure 75.

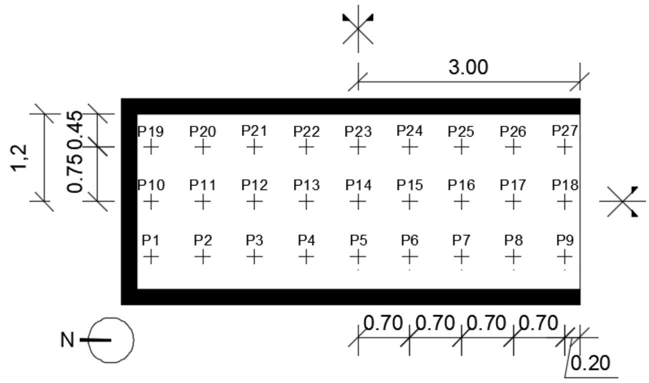

Figure 75. Illuminance measurement points in one office room

Figure 76 and Figure 77 show the obtained results of illuminance values on the working plane in the summer and winter days, respectively, for the four offices.

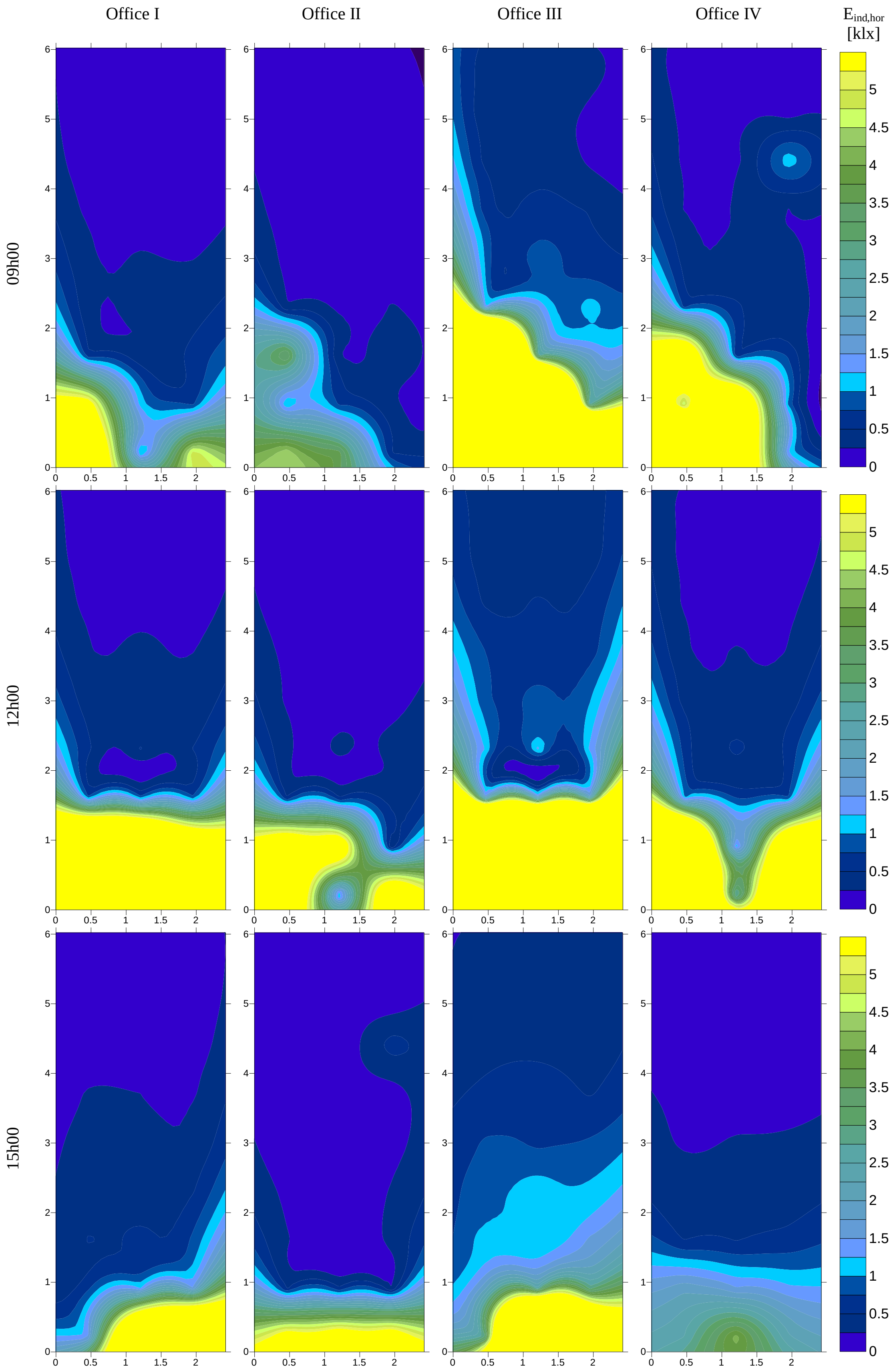

Figure 76. Horizontal illuminance distribution, $E_{ind,hor}$, at the working plane at 09h00, 12h00, and 15h00 in summer

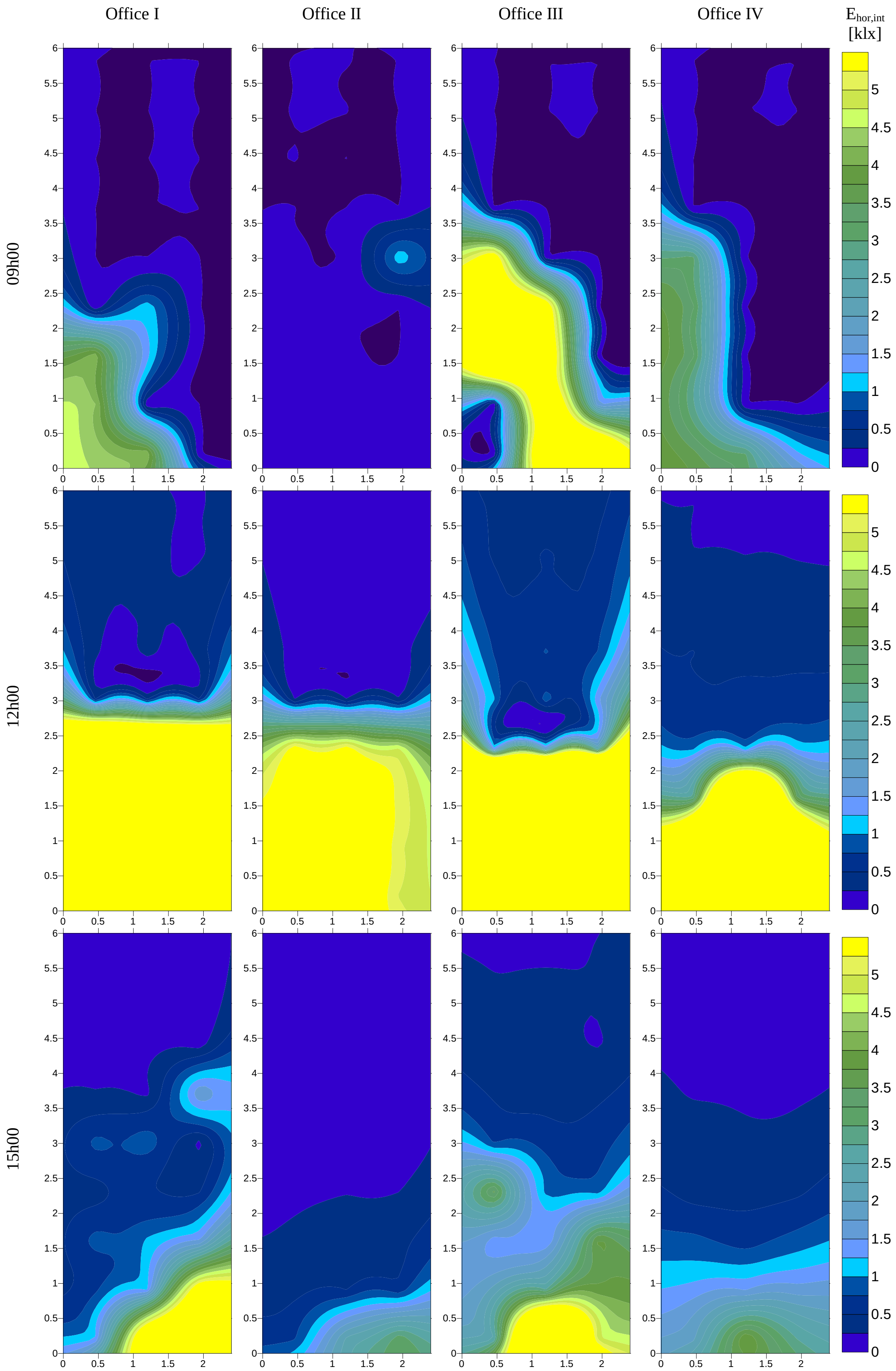

Figure 77. Horizontal illuminance distribution, $E_{ind,hor}$, at the working plane at 09h00, 12h00, and 15h00 in winter

The results of indoor illuminance on the working plane on the summer day demonstrate that all four offices show a significant area of the office room within the illuminance values of 0.2-0.5klx, which are close to the recommended value of 0.5klx for comfortable daylighting illuminance to perform office activities (e.g. writing, typing, reading, data processing), according to EN 12464-1 (2014) [74]. On the winter day, the illuminance values are higher than in the summer, especially at 12h00, due to the lower winter sun angles and higher values of incident direct radiation when compared to the summer period.

From the obtained results, it can be concluded that, in all the offices, the region near the window (~1-2 and ~1-3 meters away in summer and winter, respectively) is the one that presents higher illuminance values (>5klx) and a higher risk of visual discomfort conditions. Furthermore, it is the region where office occupants like to place their desk, as it provides a view to the outside while they are working. In this sense, the illuminance distribution of the office spaces will be analysed in greater detail for the three meters closer to the window (identified in Figure 76 and Figure 77 on the vertical axis on the right).

On the summer and winter days at 09h00 and 15h00, offices I, II, and IV with SCFs show lower illuminance values than office III, especially near the window. It can be noticed that offices I and II significantly reduced the area near the window with illuminance values above 0.5klx. At 12h00 on both days, all offices show similar illuminance results. On the summer day, offices I, II, and IV showed lower illuminance values; however, office II with the highly reflective SCF *B* showed similar values to office III on the winter day.

Analysing the results in the summer and winter days, SCF *B* showed the highest reduction of the indoor illuminance on horizontal plane near the window except in the winter day at 12h00. In this specific hour, the sun's height is at its lowest level and there is a greater perpendicularity of the sun's rays to the glazing surface. On sunny winter days, for all the analysed glazing scenarios without and with SCFs, visual discomfort through the influence of glare is very likely to occur in the region near the window. To prevent visual discomfort associated with the high levels of daylighting availability, it is recommended to place the desk table two to three meters away from the window or to activate existing shading devices.

5.6 Simulation results

5.6.1 Model calibration

The data gathered in the experimental procedure, namely the indoor temperature, the internal and external surface temperatures of the inner and outer surface of the windows' glass, and the weather data were used to design and check the accuracy of a computational model in the EnergyPlus simulation program considering offices I, II, and III. Figure 78 and Figure 79 show for the summer – 14th to the 27th of August – and winter – 6th to the 13th of January – periods, the experimental and simulated values of indoor air temperature, T_{ind}, and internal, T_{si}, and external, T_{se}, surface temperatures of the reference office. The same results for offices I and II are provided in Annex C. The error values of the simulation model for all the days of the experimental procedure are presented in Table 20 to Table 25 for offices I, II, and III.

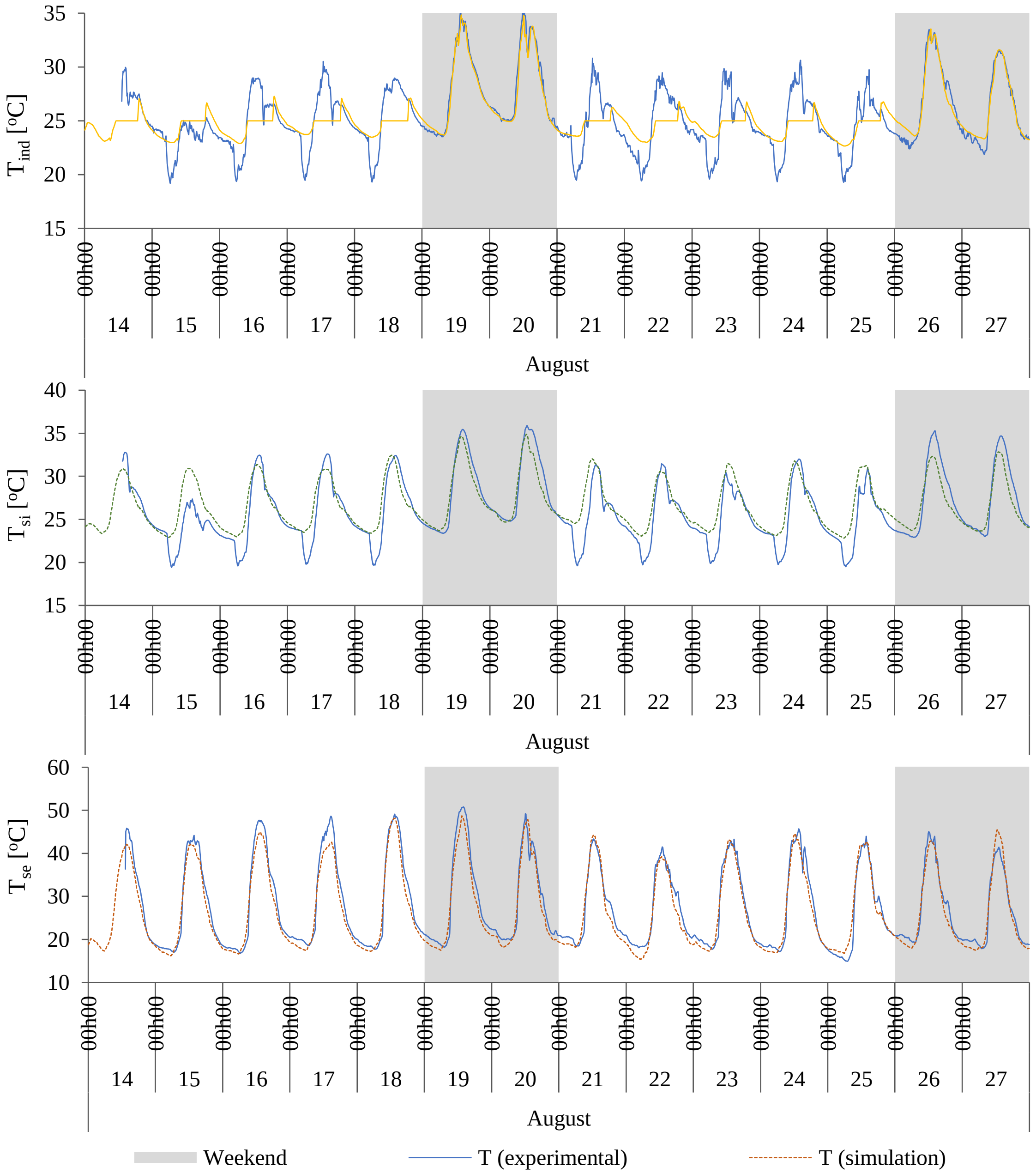

Figure 78. Experimental (plain lines) and simulated (dashed lines) values of indoor temperature, T_{ind}, and internal, T_{si}, and external, T_{se}, surface temperatures of office III in the summer period

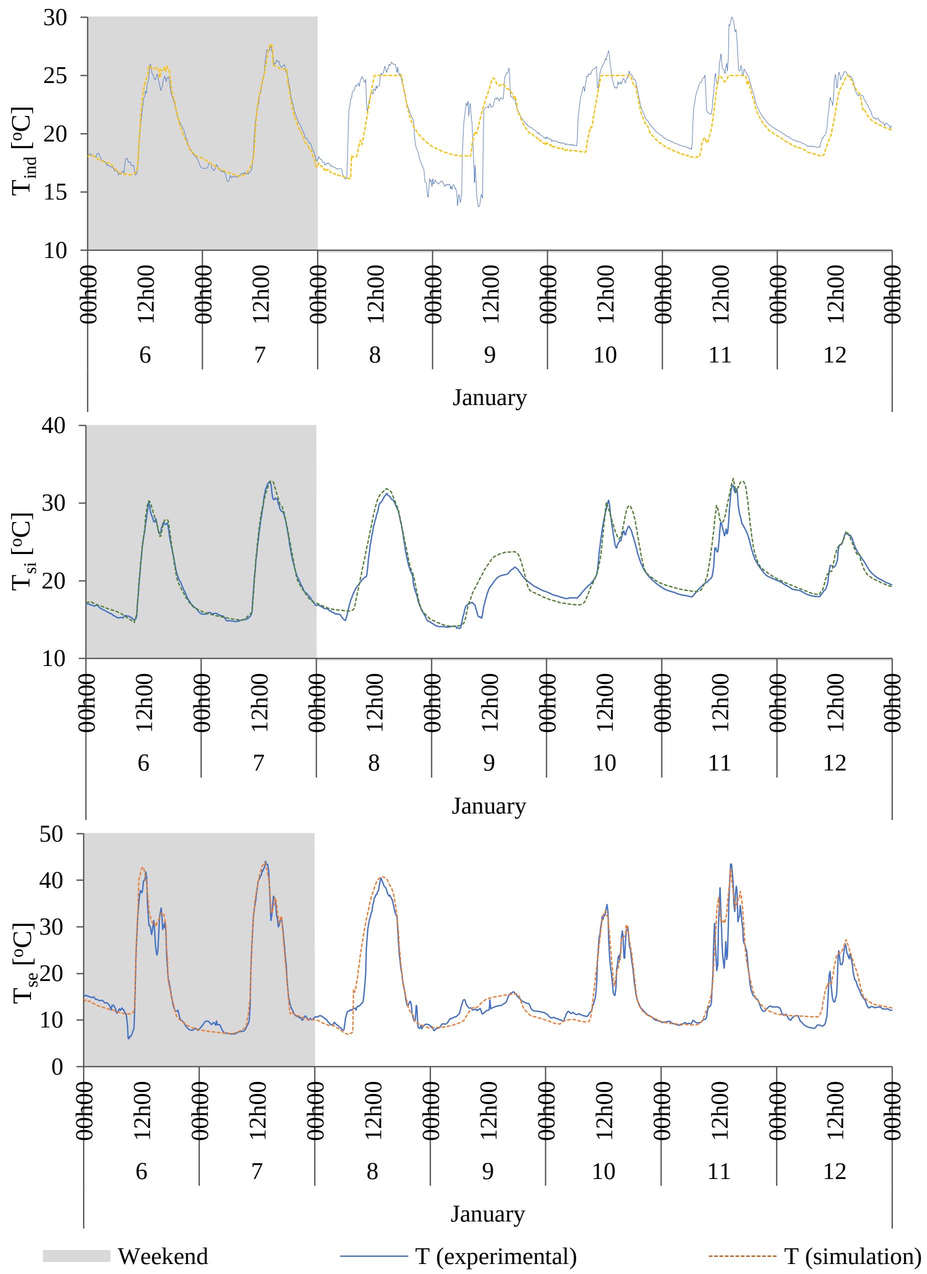

Figure 79. Experimental (plain lines) and simulated (dashed lines) values of indoor temperature, T_{ind}, and internal, T_{si}, and external, T_{se}, surface temperatures of office III in the winter period

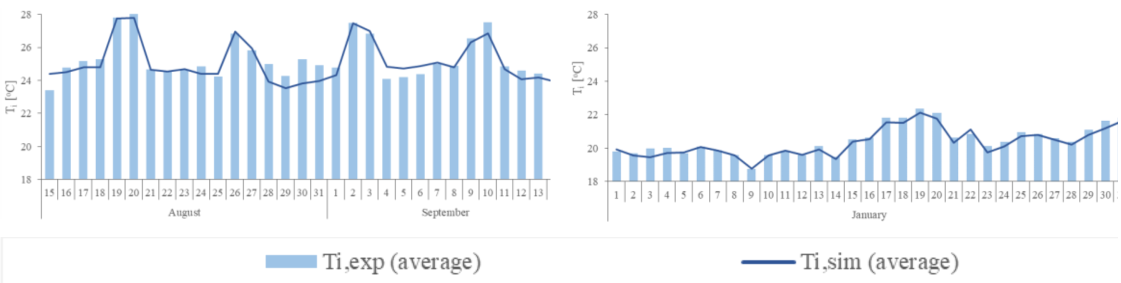

Figure 80. Monthly average verification of the experimental, $T_{i,exp}$, and simulated, $T_{i,sim}$, values of the indoor temperature

Table 20. Hourly calibration of office I in the summer period: simulated values and threshold limits

	Weekend			Working days			All days			Maximum values		
	T_{ind}	T_{si}	T_{se}	T_{ind}	T_{si}	T_{se}	T_{ind}	T_{si}	T_{se}	[79]	[80]	[81]
MBE [ºC]	-0.18	0.06	-0.84	0.92	1.36	-0.64	0.66	1.05	-0.69	±10	±5	±10
RMSE [ºC]	0.49	0.98	2.11	2.16	1.90	2.14	1.90	1.73	2.13	-	-	-
NMBE [%]	-0.02	0.01	-0.10	0.16	0.22	-0.08	0.11	0.16	-0.08	-	-	-
C_v(RMSE) [%]	1.86	3.61	7.21	9.12	7.68	7.52	7.81	6.83	7.45	30	20	30

Table 21. Hourly calibration of office II in the summer period: simulated values and threshold limits

	Weekend			Working days			All days			Maximum values		
	T_{ind}	T_{si}	T_{se}	T_{ind}	T_{si}	T_{se}	T_{ind}	T_{si}	T_{se}	[79]	[80]	[81]
MBE [ºC]	-0.12	-0.13	-0.71	1.26	1.27	-0.72	1.22	1.23	-0.62	±10	±5	±10
RMSE [ºC]	0.41	0.93	1.76	2.47	2.05	1.90	2.47	2.06	1.83	-	-	-
NMBE [%]	-0.02	-0.02	-0.10	0.22	0.21	-0.10	0.22	0.20	-0.09	-	-	-
C_v(RMSE) [%]	1.58	3.50	6.54	10.34	8.24	7.02	10.40	8.33	6.88	30	20	30

Table 22. Hourly calibration of office III in the summer period: simulated values and threshold limits

	Weekend			Working days			All days			Maximum values		
	T_{ind}	T_{si}	T_{se}	T_{ind}	T_{si}	T_{se}	T_{ind}	T_{si}	T_{se}	[79]	[80]	[81]
MBE [ºC]	-0.06	-0.57	-1.04	-0.12	1.10	-1.05	-0.11	0.60	-1.05	±10	±5	±10
RMSE [ºC]	0.68	1.44	2.14	2.08	2.06	2.13	1.79	1.89	2.13	-	-	-
NMBE [%]	-0.01	-0.07	-0.13	-0.02	0.17	-0.14	-0.02	0.04	-0.14	-	-	-
C_v(RMSE) [%]	2.52	5.15	7.69	8.43	8.11	7.73	7.02	7.25	7.72	30	20	30

Table 23. Hourly calibration of office I in the winter period: simulated values and threshold limits

	Weekend			Working days			All days			Maximum values		
	T_{ind}	T_{si}	T_{se}	T_{ind}	T_{si}	T_{se}	Ti_{ind}	T_{si}	T_{se}	[79]	[80]	[81]
MBE [ºC]	0.03	0.29	0.35	-0.81	0.07	-0.01	-0.57	0.14	0.09	±10	±5	±10
RMSE [ºC]	0.36	0.91	1.35	1.65	0.91	1.20	1.40	0.91	1.25	-	-	-
NMBE [%]	0.01	0.07	0.21	-0.18	0.02	-0.01	-0.13	0.03	0.05	-	-	-
C_v(RMSE) [%]	1.75	4.46	10.57	7.76	4.47	9.35	6.68	4.47	9.71	30	20	30

Table 24. Hourly calibration of office II in the winter period: simulated values and threshold limits

	Weekend			Working days			All days			Maximum values		
	T_{ind}	T_{si}	T_{se}	T_{ind}	T_{si}	T_{se}	Ti_{ind}	T_{si}	T_{se}	[79]	[80]	[81]
MBE [ºC]	-0,16	-0,29	0,80	-0,24	-0,36	-0,49	-0,22	-0,34	-0,12	±10	±5	±10
RMSE [ºC]	0,40	0,65	3,18	0,75	0,74	2,57	0,67	0,71	2,76	-	-	-
NMBE [%]	-0,04	-0,08	0,33	-0,06	-0,10	-0,24	-0,06	-0,09	-0,06	-	-	-
C_v(RMSE) [%]	1,80	4,69	8,69	8,45	4,82	8,46	7,16	4,78	8,54	30	20	30

Table 25. Hourly calibration of office III in the winter period: simulated values and threshold limits

	Weekend			Working days			All days			Maximum values		
	T_{ind}	T_{si}	T_{se}	T_{ind}	T_{si}	T_{se}	Ti_{ind}	T_{si}	T_{se}	[79]	[80]	[81]
MBE [ºC]	0.04	0.16	0.16	-0.61	0.66	0.61	-0.42	0.51	0.48	±10	±5	±10
RMSE [ºC]	0.51	0.47	1.68	2.19	1.57	2.65	1.87	1.35	2.41	-	-	-
NMBE [%]	0.01	0.04	0.05	-0.13	0.15	0.26	-0.09	0.12	0.19	-	-	-
C_v(RMSE) [%]	2.55	2.35	9.63	10.18	7.60	17.18	8.86	6.59	15.09	30	20	30

It can be observed in Figure 78 and Figure 79 that the highest difference between the experimental and the simulated values of office II is related to the unpredictability of the usage of the HVAC system associated with the occupant's behaviour or preference on those specific days (working days). Although the building has a centralised program system to maintain a set point temperature during working hours (21ºC ±3ºC), occupants can manually regulate indoor temperature through dedicated fan coils in their offices. Moreover, at ~05h00, it is possible to observe a sudden drop of the indoor temperature in office II to ~18ºC in all the working days of the summer period and a sudden rise of the indoor temperature to ~23ºC on the 9th of January. The fact that it is not possible to identify evident periods during the working hours with constant indoor temperature in the office (Figure 78 and Figure 79) shows the inconsistency of occupant's individual behaviour in the HVAC usage, observing even cases where no HVAC is used. Indeed, intermittent periods of the use of the HVAC system are common in Mediterranean climates. On the weekend days, when there is no occupancy and the HVAC is turned off, a minor discrepancy between experimental and simulation results is observed. The statistical indexes *MBE* and $C_{v.RMSE}$ (Table 20 to Table 25) support these conclusions, and during the weekend, the values of $C_{v.RMSE}$ are ~ 70-78%, 79-85%, and 70-75% lower in offices I, II, and III, respectively, than those observed during the working days. It can be observed that the calculated values of the statistical indexes for the indoor temperature of the offices model are both lower than the threshold limits for model calibrations [79]–[81], which indicates a good fit between simulation and experimental data. The differences in N_{MBE} and $C_{v.RMSE}$ were considered satisfactory for subsequence comparative analyses of different solutions for the glazing façade such as glazing systems with different types of solar control films.

In the present study, the model calibration was performed for the indoor temperature and the internal and external surface temperatures variables for being the most straightforward way to conduct the experimental procedure. In fact, some factors related to the building of the case study did not make it possible to use energy to calibrate the model. First, it would be necessary to have knowledge of the individual consumption regarding the heating, cooling, and lighting energy needs of each office space to analyse the influence of SCFs on the office's energy performance. Measurements of individual energy consumption of office spaces or measures of energy consumption of the building by type of end-use (lights, electric equipment, HVAC system, electric vehicles, and data centres) are not implemented in the building of the case study, and therefore the share of electric consumption associated with heat gains and losses due to the façade's characteristics is not possible to be deducted from the electric bills. In this case study, a high amount of data centre is present in the building and the energy consumption with the HVAC system to maintain the indoor temperature of those dedicated spaces is unknown. And second, due to the building construction configuration, it was not possible to experimentally measure isolated parts of the electric energy associated with energy consumption (and after convert the results into energy needs) without damaging existing materials or the structure of the building.

Although the calibration procedure did not use the energy consumption as a comparative analysis between experimental and simulated values, the simulated energy needs are only dependent on the indoor temperature and not on the type and characteristics of the HVAC system of the building. By choosing the indoor temperature and the internal and external temperatures of the glass as a term of comparison between predicted and experimental results in office spaces, if there is a close agreement between both, it is expected that a reasonably good agreement could also be found between what would be the estimated energy needs and what would be the real energy needs associated with the different glazing alternatives. Furthermore, the calibration study carried out had the main purpose of assessing the suitability of the data used related to the construction (building geometry, building orientation, materials properties) – actual characteristics of the building –, and which are invariable parameters through the simulation analysis. Once this calibration is achieved, the subsequent simulation to predict the results of the different retrofitting solution was carried in nominal conditions, which do not have necessarily to match with real conditions. For example, the existing HVAC system was not used in the model and instead a generic HVAC template with efficiency values of COP=3.0 and EER=3.4 as expressed in the Portuguese regulations were adopted. The results of energy needs obtained through the simulation model may not be the real ones because nominal conditions were used instead, but they are credible and comparable since the same basis of comparison was used.

5.6.2 Impact of SCFs in operational stage: thermal and visual comfort, and energy performance

To assess the impact of different SCFs on thermal and visual comfort, and energy performance of office spaces with double glazing systems, the SCFs that exhibited a higher energy performance in section 4 – SCFs with external application (SCFs *A* to *G*) – are numerically analysed in the current section 5 considering the building of the case study with double-glazing units (described in section 5.1). The calibrated computational model built in the EnergyPlus simulation program (section 5.4) and the Lisbon's city generic hourly weather file were used to estimate the indoor temperature, the daylighting availability, and the energy needs of the office spaces for different solar orientations.

5.6.2.1 Thermal comfort

To analyse the thermal performance of the office spaces without and with SCFs, several simulations were conducted in EnergyPlus considering a free float mode scenario (offices without HVAC system). The indoor temperature of the office spaces with the different glazing alternatives was analysed for the days of the year with the highest, 29th of August (warmest day), and the lowest, 31st of January (coldest day), average outdoor temperature, according to the generic data of weather conditions for Lisbon's city, for different solar orientations (Figure 81 and Figure 82). The warmest day shows average values during working hours (from 9h00 to 18h00) of the outdoor temperature of 32.41ºC and global solar radiation on a horizontal plane of 426W/m^2 and the coldest day shows, for the same parameters, 8.74ºC and 245W/m^2, respectively.

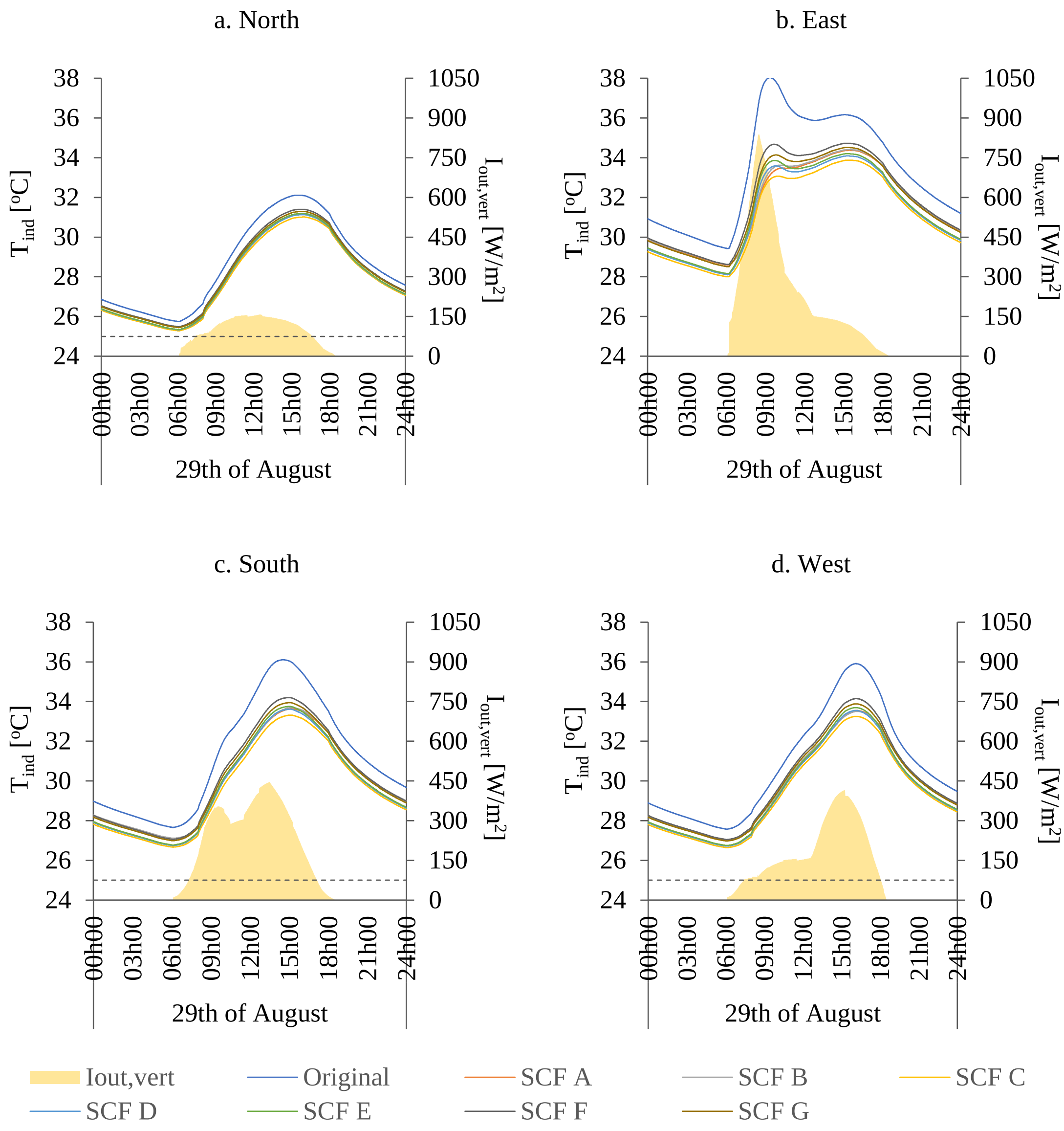

Figure 81. Solar radiation on the façade, $I_{out,vert}$, and indoor temperature, T_{ind}, of the office area for the different glazing: original window without SCF, *Original*, and with SCFs *A* to *G* on the day with the highest average outdoor temperature for: a. North, b. East, c. South and d. West solar orientations

On the warmest day of the year, all the glazing systems analysed in Figure 81 show indoor temperature values in working and non-working hours above the upper limit of 25ºC of comfort temperatures for Portugal [82]. For all solar orientations, the glazing with SCFs decrease the indoor temperature compared to the original window, and the highest decrease was observed for the glazing solution with SCF *C*.

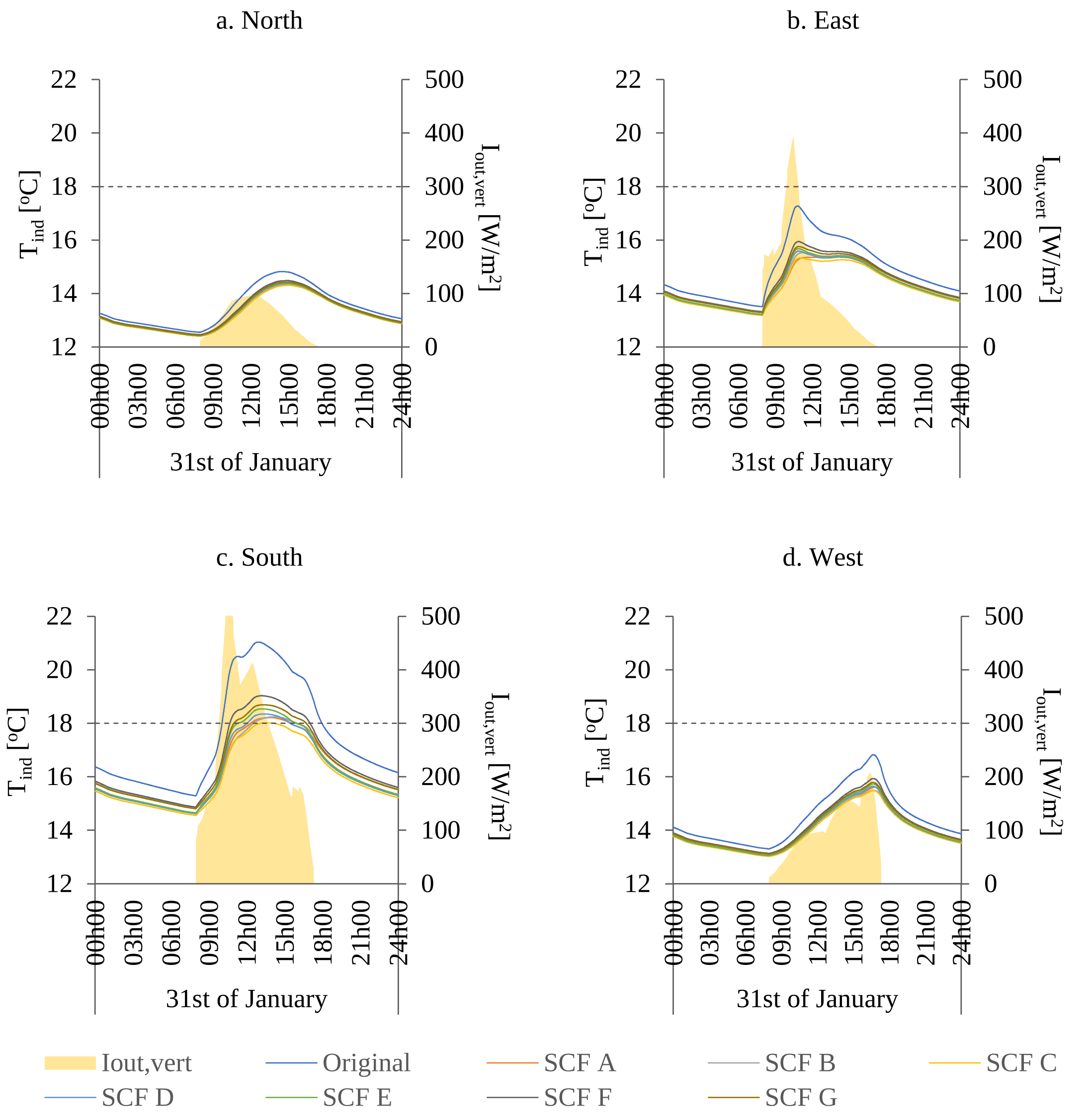

Figure 82. Solar radiation on the façade, $I_{out,vert}$, and indoor temperature, T_{ind}, of the office area for the different glazing: original window without SCF, *Original*, and with SCFs *A* to *G* on the day with the lowest average outdoor temperature for: a. North, b. East, c. South and d. West solar orientations

On the coldest day of the year, all the glazing systems analysed in Figure 82 show for North, East and West solar orientations indoor temperature values in working and non-working hours below the lower limit of 18ºC of comfort temperatures in Portugal [82]. The original window generates indoor temperature values above 18ºC during 90% of the working hours for the South solar orientation, whereas the glazing systems with SCFs show values between 17 % (SCF *C*) and 85 % (SCF *F*). It can be concluded that on days with extreme outdoor temperatures, the office spaces do not present thermal comfort conditions for occupants during the working hours for all the analysed solutions of the glazing system without and with SCFs, except for South facing offices during extremely cold days. It should be noted that the application of the SCFs significantly decreased the indoor temperature during the warmest day, especially for East, South and West solar orientations, which indicates that during the summer period, the glazing solutions with SCFs should have a higher decrease of the discomfort hours above 25ºC.

Table 26 presents the annual percentage of working hours inside and outside the comfort range of temperatures according to the Portuguese regulation [82] as well as the annual overheating ($ODH_{<18}$) and overcooling ($ODH_{>25}$) degree hours calculated according to the following equations (5.1) and (5.2):

$$ODH_{<18} = \sum |T_{ind} - 18| \times \delta \tag{5.1}$$

$$ODH_{>25} = \sum |T_{ind} - 25| \times \delta \tag{5.2}$$

where

δ is the counter of the number of hours below 18ºC for $ODH_{<18}$ and above 25ºC for $ODH_{>25}$. It equals zero if T_{ind} is above 18ºC in the equation (5.1) and below 25ºC in the equation (5.2).

Table 26. Thermal comfort indexes: discomfort working hours below 18ºC and above 25ºC, and overheating, $ODH_{<18}$, and overcooling, $ODH_{>25}$, degree hours

		Discomfort working hours below 18ºC [%]	$ODH_{<18}$ [ºC.h]	Discomfort working hours above 25ºC [%]	$ODH_{>25}$ [ºC.h]
North	*Original Window*	35,9	3716	37,6	4674
	SCF *A*	39,5	4368	33,7	3481
	SCF *B*	39,5	4348	33,7	3506
	SCF *C*	40,1	4445	33,3	3287
	SCF *D*	39,5	4341	33,7	3441
	SCF *E*	39,2	4303	33,8	3506
	SCF *F*	38,6	4174	34,7	3767
	SCF *G*	38,9	4247	34,2	3640
East	*Original Window*	22,1	1413	52,1	12432
	SCF *A*	28,4	2361	45,8	8308
	SCF *B*	28,0	2264	46,0	8390
	SCF *C*	29,6	2518	44,6	7596
	SCF *D*	28,8	2362	45,5	8052
	SCF *E*	28,5	2305	46,0	8291
	SCF *F*	27,1	2069	47,6	9232
	SCF *G*	27,6	2179	46,8	8765
South	*Original Window*	4,3	196	63,1	10561
	SCF *A*	11,8	556	46,3	6149
	SCF *B*	12,0	572	46,6	6194
	SCF *C*	14,5	723	44,3	5670
	SCF *D*	12,6	620	45,8	6094
	SCF *E*	11,5	574	46,9	6299
	SCF *F*	8,8	423	49,8	7031
	SCF *G*	10,0	484	48,3	6629
West	*Original Window*	27,5	2288	47,2	9126
	SCF *A*	32,7	3132	41,5	6003
	SCF *B*	32,8	3163	41,3	6004
	SCF *C*	33,3	3304	40,2	5602
	SCF *D*	32,8	3170	40,9	5967
	SCF *E*	32,7	3110	41,4	6149
	SCF *F*	31,6	2906	42,8	6769
	SCF *G*	32,2	3007	42,2	6431

According to the results of Table 26, the application of SCFs increased 3-10 % the discomfort hours below 18ºC and decreased 3-20 % the discomfort hours above 25ºC. Moreover, SCF *C* showed the lowest value of the overcooling hours compared to the other films, showing reduction values of the $ODH_{>25}$ of 33%, 39%, 46%, and 39% for North, East, South, and West solar orientations.

5.6.2.2 Visual comfort

To analyse the visual comfort of the office spaces without and with different SCFs with external application, several simulations were conducted in Energyplus. The daylight availability was analysed in one point of the office space corresponding to the seating position recommended in the experimental analysis of section 7.5.4 – at the desk plane height of 0.8 m and two meters away from the window. The calculated daylight glare index was analysed at the same point position but at 1,0 m height for a viewer's direction parallel and perpendicular to the lighting source. The light source corresponds, in this case, to the glazing system.

First, the daylight availability and the daylight discomfort glare of three typical days with different outdoor conditions – summer (Figure 83) and winter (Figure 84) solstice under clear sky conditions and one typical day under overcast sky conditions (Figure 85) – were analysed for the original glazing without and with SCFs *A* to *G*. The clear sky days were selected by analysing days closer to the summer and winter solstice that showed both higher values of global solar radiation and lower values of diffuse radiation (21st of June and 19th of December, respectively), and for the overcast sky day, , the day of the year with the lowest values of global and diffuse radiation (17th of January) was selected. The analyses of these three days allow assessing the visual performance of the office for different and opposite climate conditions and for different glazing solutions.

The clear sky days in the summer and winter solstices show during the working hours (from 9h00 to 18h00) average outdoor temperatures of 25.87ºC and 14.10ºC and global solar radiation on horizontal plane of 725W/m^2 and 236W/m^2, respectively. The overcast day shows averages of 13.22ºC and 22.68W/m^2.

Second, the annual daylight availability and the daylight discomfort glare were analysed according to the Useful Daylight Illuminance metric, UDI (useful range of 0.3-3klx [75]) and the Daylight Glare Index, DGI (considering comfort range values below the value of 22 [106]).

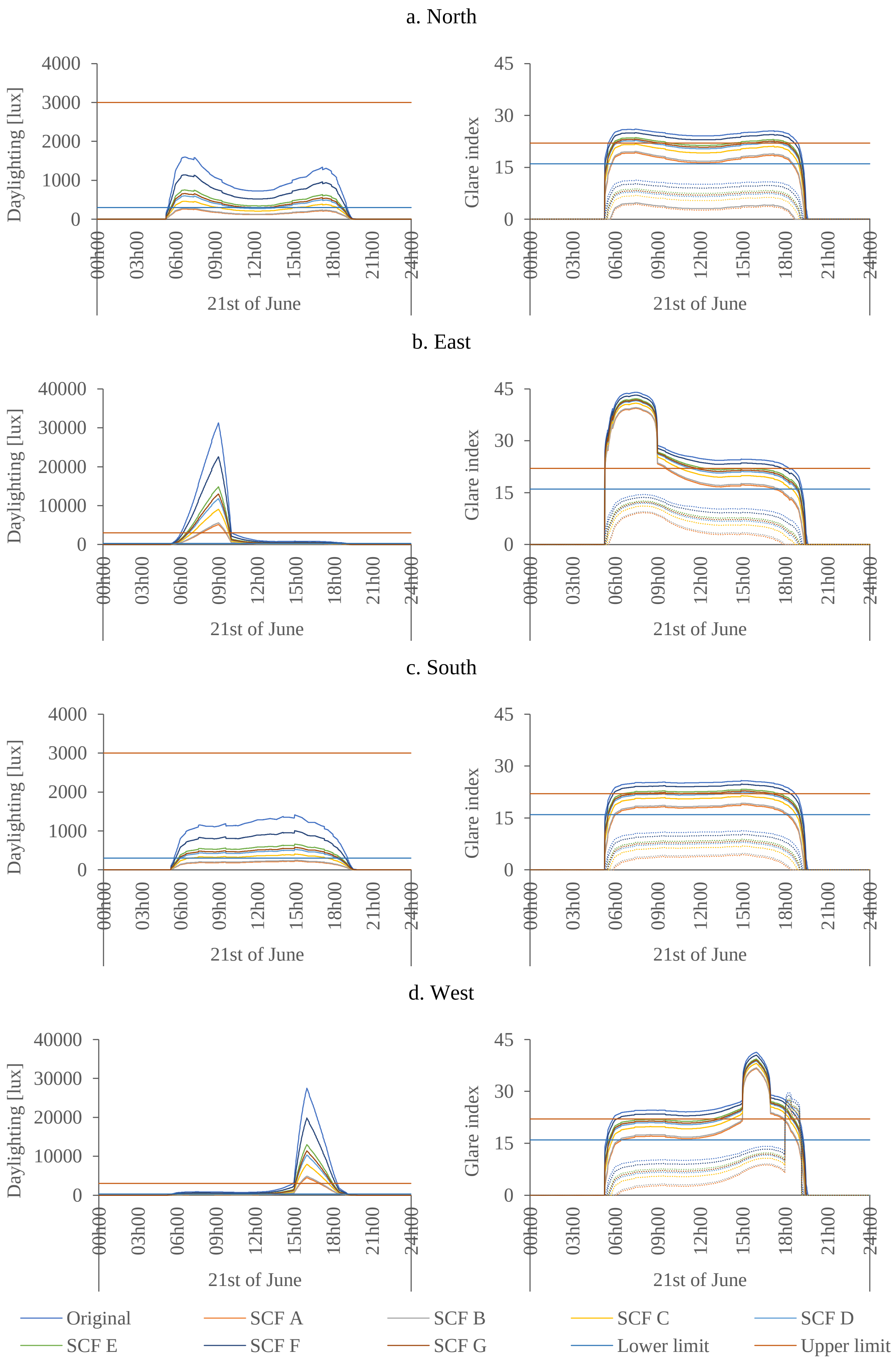

Figure 83. Daylight illuminance and glare index for a viewer's direction parallel (dotted lines on the right) and perpendicular (straight lines on the right) to the light source on the summer solstice for the original window without SCF, *Original*, and with SCFs *A* to *G* for: a. North, b. East, c. South and d. West solar orientations

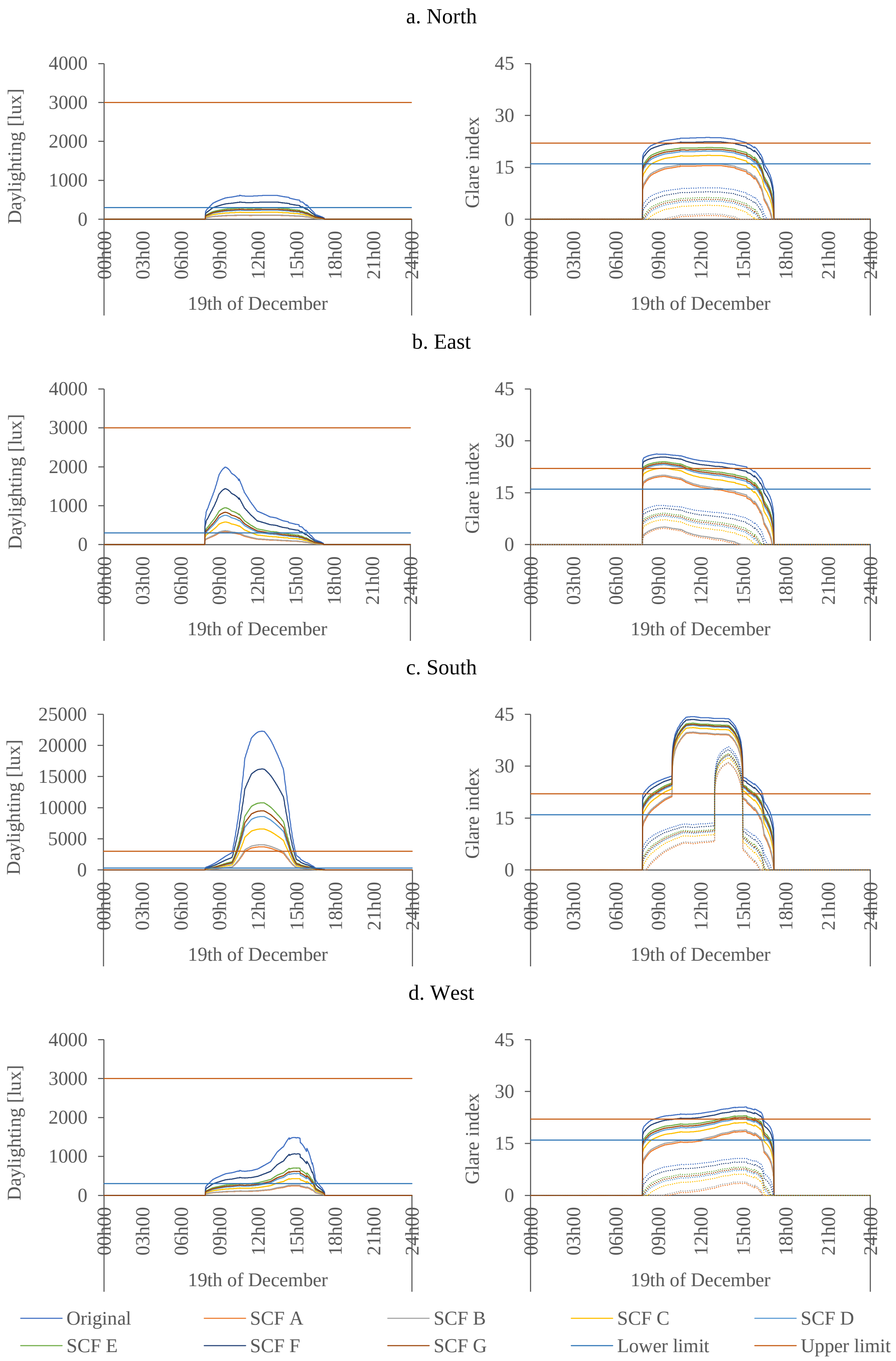

Figure 84. Daylight illuminance and glare index for a viewer's direction parallel (dotted lines on the right) and perpendicular (straight lines on the right) to the light source on the winter solstice for the original window without SCF, *Original*, and with SCFs *A* to *G* for: a. North, b. East, c. South and d. West solar orientations

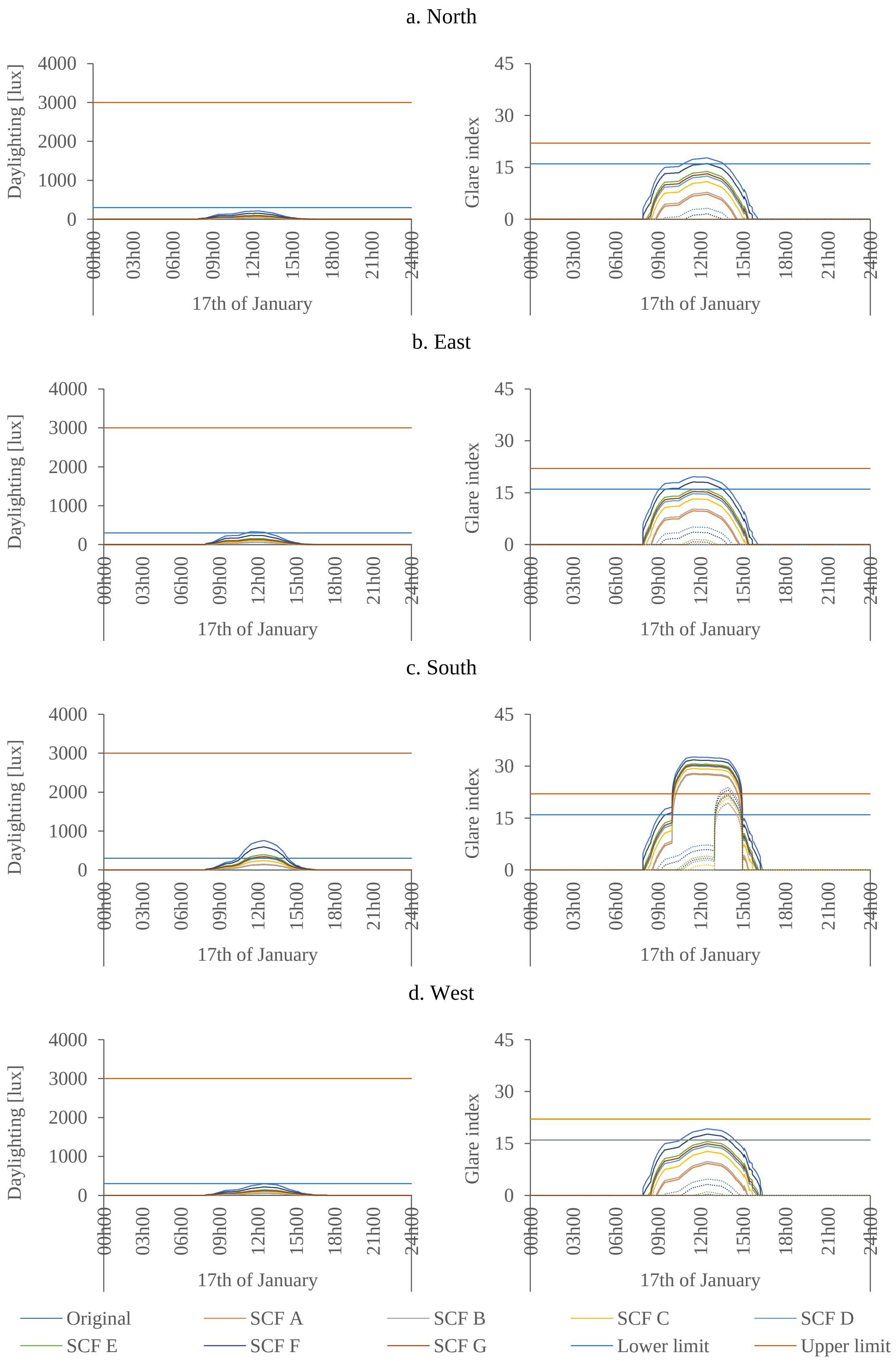

Figure 85. Daylight illuminance and glare index for a viewer's direction parallel (dotted lines on the right) and perpendicular (straight lines on the right) to the light source on one day with overcast sky conditions for the original window without SCF, *Original*, and with SCFs *A* to *G* for: a. North, b. East, c. South and d. West solar orientations

Figure 86 presents the annual percentage of the working hours of different daylighting range values for the original window, *original*, and for SCFs *A* to *G*, for all solar orientations.

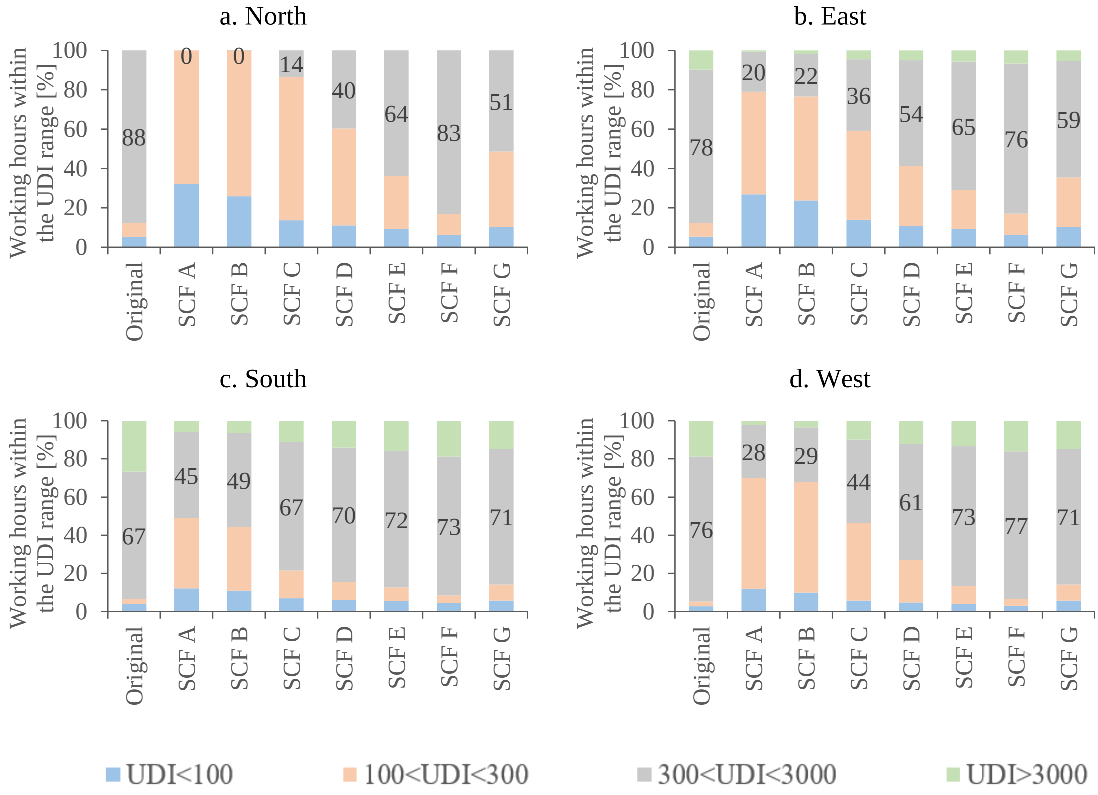

Figure 86. Annual percentage of the working hours of different UDI range values in the office area for the original window without SCF, *Original*, and with SCFs *A* to *G* for: a. North, b. East, c. South and d. West solar orientations

The application of SCFs to the original window decreases the daylighting availability in the office room above 3 000 lux in all solar orientations, reducing the risk of visual discomfort due to glare occurrences. The UDI values between 300-3 000 lux (useful daylighting) also decreased as the daylight availability below 300 lux and 100 lux increased, which according to the UDI metric, can contribute to increasing the energy needs with artificial lighting as it may require artificial lighting to perform office work activities. Some exceptions can be found for the South orientation with SCFs *C* to *G* solutions and West orientation with SCF *F*, as the UDI values between 300-3 000 lux are the same or higher than those obtained for the *original* window and the UDI values above 3 000 lux decreased. In sum, the use of SCFs decrease the risk of glare occurrences and may increase the energy needs of the office room due to low UDI values.

Figure 87 and Figure 88 show the Daylight Glare Index, DGI, for the window without SCF, *original*, and with SCFs *A* to *G* for North, East, South, and West solar orientations.

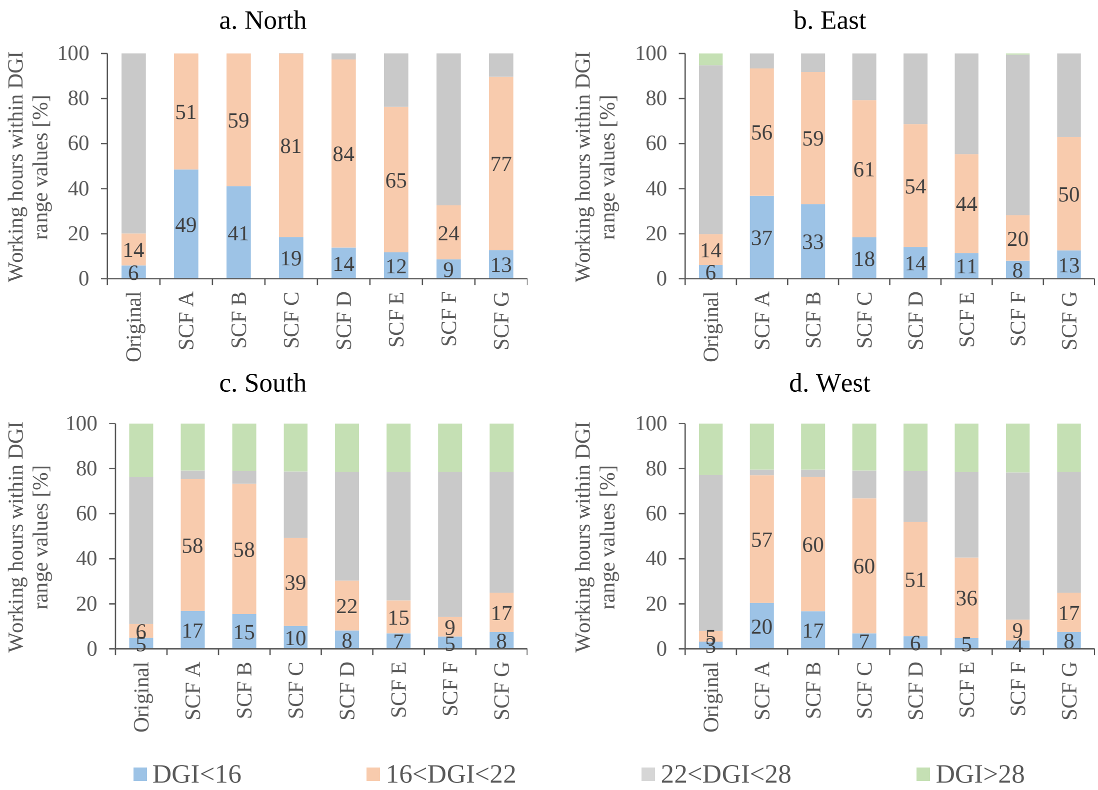

Figure 87. Annual percentage of working hours of different DGI values in the office space for a viewer's direction perpendicular to glazing for the window without SCF, *Original*, and with SCFs *A* to *G* for all solar orientations

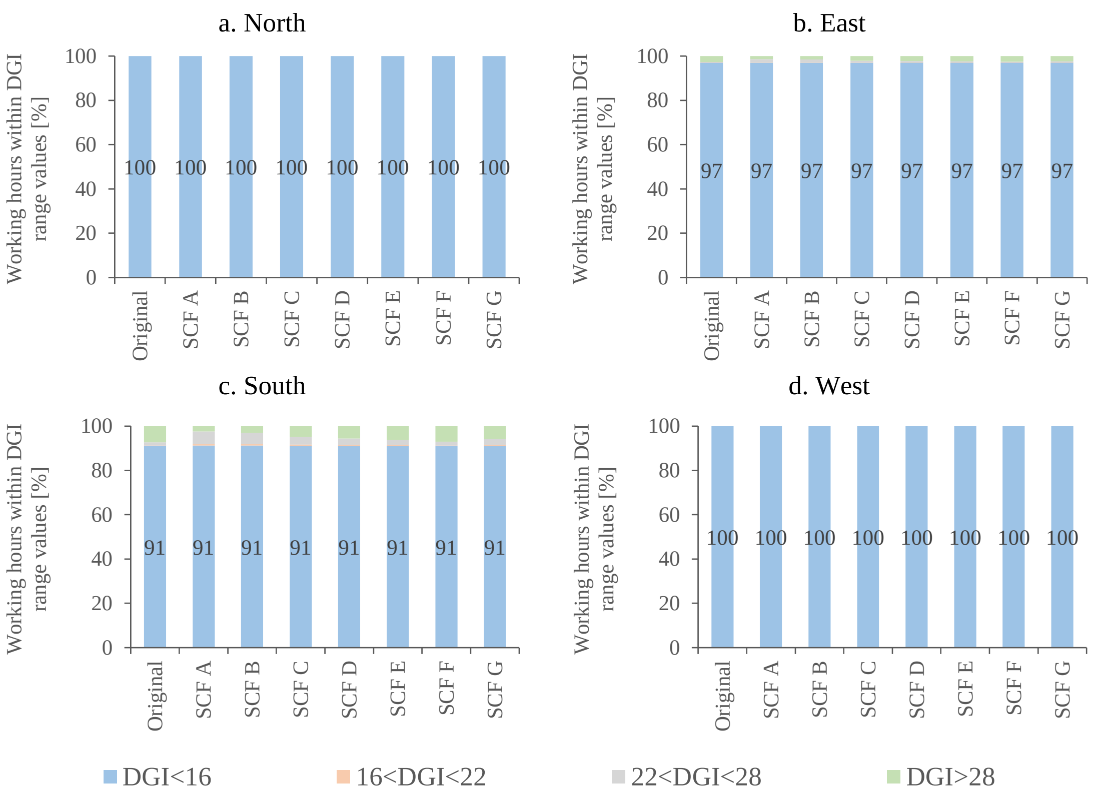

Figure 88. Annual percentage of working hours of different DGI values in the office space for a viewer's direction perpendicular to glazing for the window without SCF, *Original*, and with SCFs *A* to *G* for all solar orientations

The DGI results indicate that glare occurrences are likely to occur for a viewer's direction perpendicular to the glazing system – when the viewer is working in a position where he faces the window. The *original* glazing shows non-perceptible or perceptible but tolerable in 20% of the annual working hours for the North and East orientation and 11% and 8% for a South and West orientation, respectively. With the application of highly reflective films as is the case of SCFs *A* and *B*, the possibility of glare occurrences decreased, showing values of non-perceptible or perceptible but tolerable glare in almost 100% of the working hours for the North orientation and values greater than 70% in the remaining solar orientations.

For South and West solar orientation, an almost constant value of DGI>28 of 20-24% is observed for all glazing solutions. The application of the different window films on the original glazing for both these solar orientations did not significantly improve the values of DGI>28 (characterized by intolerable glare occurrences).

A comprehensive analysis of the clear and overcast sky condition days (Figure 83 to Figure 85) can justify these results. On summer days closer to the summer solstice (Figure 83), when the sun's path depicts its highest arc (displaying the highest elevation angles of the year), it can be observed values of DGI>28 in the morning period for the East orientation, and in the afternoon period for the West orientation, for all glazing solutions. However, for the East orientation, the values of DGI>28 occur outside the working hours of the day and for the West orientation, the values of DGI>28 occur between 15h00 and 18h00, falling inside the working hours for all glazing solutions and justifying the obtained constant annual values of DGI>28. On the contrary, during winter days closer to the winter solstice (Figure 84), when the sun's path depicts its shortest arc (displaying the lowest elevation angles of the year), it is possible to observe values of DGI>28 in the South orientation for all glazing solutions. These results are observed for both clear and overcast (Figure 85) sky conditions in the winter period.

Altering the seated position to a viewer's direction parallel to the glazing system reduces the annual percentage of the working hours above the maximum recommended value of 22, decreasing the risk of visual discomfort due to glare occurrences. In this seated position, the risk of glare occurrences in one year for North and West solar orientation approximates zero, and for East and South solar orientation approximate ~2-3% and ~8-9%, respectively, for all glazing solutions without and with SCFs.

5.6.2.3 Energy needs

A generic HVAC template was included in the simulations to analyse the energy needs in the office space without and with different SCFs. The thermostat temperature was defined according to the thermal comfort range of temperatures for Portugal (18 ºC to 25 ºC). The HVAC efficiency values of COP=3.0 and EER=3.4 expressed in Portuguese regulations were assumed to the Portuguese Regulation of the Energy Performance of Buildings [82]. The annual energy use was calculated as shown below:

$$EN = \left(\frac{EN_{heat}}{COP} + \frac{EN_{cool}}{EER} + EN_{light}\right) \tag{5.3}$$

where

EN_{heat}: energy needs with heating;

EN_{cool}: energy needs with cooling;

EN_{light}: energy needs with lighting.

Simulations without SCF were also carried out for comparison purposes. The annual energy use for cooling, heating, and lighting and the total energy use per square meter of floor area is presented in Figure 89 and the annual energy use savings (%) in Figure 90, for the original window without SCF, *Original*, and with SCFs *A* to *G* for North, East, South and West solar orientation.

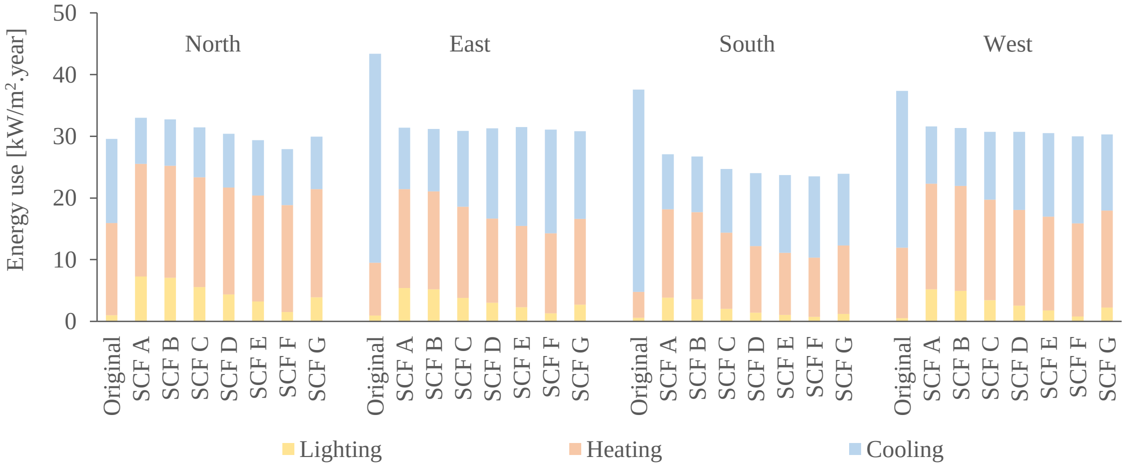

Figure 89. Annual energy use of the original window without SCF, *Original*, and with SCFs *A* to *G* for North, East, South, and West solar orientation

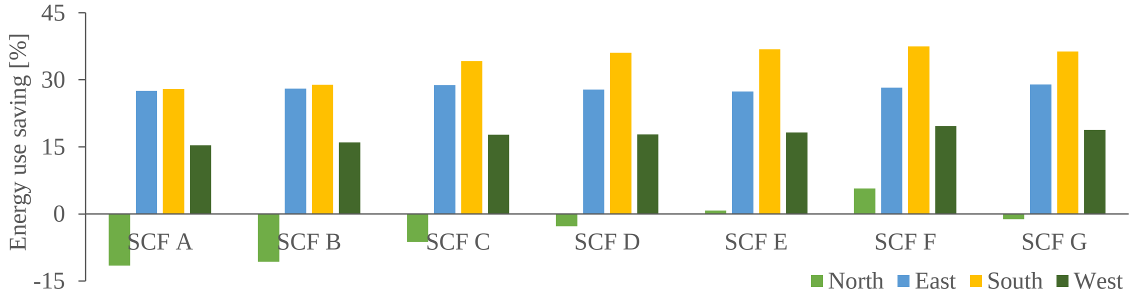

Figure 90. Annual energy savings of the original window without SCF, *Original*, and with SCFs *A* to *G* for North, East, South, and West solar orientation

The results of Figure 89 show that all SCF reduce the cooling energy use and increase the heating and lighting energy use compared to the solution of the *original* window without SCFs, for all solar orientations. The cooling energy use represents the major share of the total energy use of the office rooms (46% for North, 78% for East, 87% for South, and 68% for West orientation) due to Lisbon's Mediterranean climate characteristics of dry and hot summers and mild to cool wet winters, according to the Köppen-Geiger climate classification. As expected, the highly reflective SCFs *A* and *B* show the highest reduction of the cooling energy use for all solar orientations, showing reductions of 45% for North, 70% for East, 73% for South, and 63% for West. Despite the high cooling reductions, an increase in heating and lighting energy use is observed compared to the solution of the *original* window. In fact, the results of Figure 90 show that the highly reflective films *A* and *B* show the lowest overall energy savings of all the SCFs due to the higher increase of the heating and lighting loads compared to the other films.

In terms of energy use savings (Figure 90), the spectrally selective film *F* shows the highest reduction of the total energy use for all solar orientations compared to the other solutions – 6% for North, 28% for East, 37% for South, and 20% for West. This can be explained by the high Light-to-Solar Gain ratio, *LSG*= 1.45, and lowest solar front reflectance $\rho_{f,sol}$= 0.28 when compared to the other solutions, which reduces the cooling energy use at a higher rate than the increase of the lighting and heating energy use, especially during the winter season. SCF *A* shows one of the lowest performances in reducing the total energy use for East, South, and West orientations and shows an increase of the total energy use when applied to a North orientation – energy increase of 12% for North, and energy savings of 28% for East, 28% for South, and 15% for West. This can be justified by the low visible transmittance, τ_{vis}= 0.10, and the high solar (front) reflectance, $\rho_{f,sol}$= 0.56, coefficients of this film, increasing the lighting and the heating energy use (especially during the winter season) at higher rates than the other solutions.

Based on the previous results, Table 27 shows a decision-making framework based on different performance criteria, cooling (C), heating (H), lighting (L) and combinations deriving therefrom (C+H, C+L, H+L, and C+H+L) for all façade orientations (N+E+S+W). Figure 91 shows the corresponding solar transmittance, solar (front) reflectance, and absorption coefficients of the glazing system without SCF (*Original*) and with SCFs *A* to *G*.

Table 27. Decision-making framework based on energy performance criteria for different solar orientations

Performance criteria	Orientation				
	North (N)	East (E)	South (S)	West (W)	N+E+S+W
Cooling (C)	A	A	A	A	A
Heating (H)	Original	Original	Original	Original	Original
Lighting (L)	Original	Original	Original	Original	Original
C+H	B	A	D	A	B
C+L	F	B	B	B	F
H+L	Original	Original	Original	Original	Original
C+H+L	F	F	F	F	F

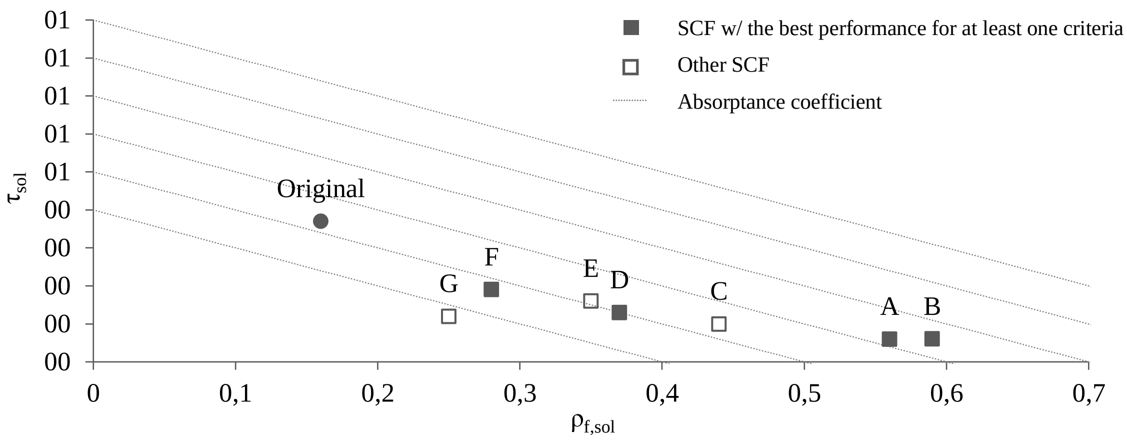

Figure 91. Optical properties of the original window without SCF, *Original*, and with SCFs *A* to *G*

From Table 27 it is can be concluded that SCFs *A* has the best performance for cooling and the *original* window for heating and lighting performance criteria for all solar orientations. For the C+H+L combination, SCF *F* has the best energy performance considering all solar orientations, which can be explained by the high value of the visible transmittance, τ_{vis}= 0.42, and the medium value of the solar (front) reflectance, $\rho_{f,sol}$= 0.28 compared to the other SCFs.

Comparing the optical properties of the SCFs with the best performance for at least one criteria, it can be observed that films with high (front) reflectance coefficients – located on the right side of the graph in

Figure 91 – show better performance when considering the cooling criteria (C, C+H, and C+H+L) and the films with high solar transmittance coefficients – located on the left side of the graph in Figure 91 – show better performance when considering the heating and lighting criteria (H, L, and H+L). SCFs with medium values of (front) reflectance and solar transmittance – located on the centre of the graph in Figure 91 – such as the spectrally selective film, SCF *F*, show better performance when considering C+H+L for all solar orientations. The balanced combination of the optical properties results in a combined reduction of the three performance criteria – cooling (C), heating (H), and lighting (L) – which explains the lower value of the annual energy use.

5.7 Conclusions and perspectives

In this current section, an extensive experimental investigation and a simulation study of existing office rooms located in Lisbon were described to evaluate the thermal and visual comfort and the energy performance of the offices for different scenarios of the glazing system: with the original double-glazed windows without and with different SCFs with external application.

The experimental analysis was carried out on four similar office rooms, two offices with SCFs (offices I and II), one office with the original window without any film (office III), and one office with the original window and a damaged film (office IV). Office III (original window) shows the lowest thermal, luminous, and energy performance for the summer period, reaching indoor temperature maximum values of 35.82ºC and presenting the highest indoor average temperature of 27.18ºC. This office shows the highest indoor illuminance, reaching maximum values of 29 619 lx in summer and 50 219 lx in winter, increasing the need of activating the shading device to control the transmitted solar radiation. However, it does not prevent excessive solar gains and the consequent risk of indoor overheating. These conditions are very likely to induce thermal and visual discomfort in the occupants and reduce the satisfaction with the working space, especially during high insolation periods. Also, the daily range of indoor temperature throughout the days is very high in this office – with temperature varying between 21.88ºC and 35.82ºC in the summer period and between 15.89ºC and 27.81ºC in the winter season, which contributes to occupants' thermal perception and awareness and increasing thermal discomfort in the office.

When comparing the results of the retrofitted offices, it can be observed that the glazing system of office II is more effective in reducing the indoor temperature. In fact, SCFs *G* (office I) and *B* (office II) are both solar control films that alter the windows' properties by decreasing the solar gains through the absorption (office I: $\rho_{f,sol}$= 0.25; α_1= 0.62) and reflection (office II: $\rho_{f,sol}$= 0.59; α_1= 0.35) process, respectively [104]. These properties explains the higher external surface temperatures of the outer pane of the glass in office I compared to office II.

From the existing literature of SCFs, the thermal performance observed of offices I and II was expected since office II has a higher reflective coefficient than office I. Also, it should be noted that the minimum value registered during the winter campaign is very close to the minimum comfort temperature of 18 ºC for the winter period, according to the Portuguese regulation [82]. From a thermal standpoint, different studies emphasize that the application of SCFs is usually beneficial in summer and disadvantageous in winter due to the reduction of the solar gains [55], [57]. In the experimental study developed in section 4 [43], it was concluded that the application of a low reflective coefficient film in single glass windows with an East solar orientation resulted in a short and insufficient decrease of the indoor temperature (less than 1 °C on average on a daily sun-hours basis during the summer days). In the same study, a further investigation through a simulation study concluded that highly reflective films could decrease the discomfort hours above 25 °C by ~35% in the cooling season and increase the annual percentage of comfort hours by ~12%. Another study [57] compared two office areas in a Mediterranean climate with double glazing units without and with a highly reflective external SCF with a Southeast solar orientation. In this study, the authors concluded that a higher reduction of the indoor temperature in the cooling than in the heating season resulted in an increase in annual working hours within the comfort temperature range, according to the Portuguese regulations [82]. In terms of energy performance and aligned with literature findings, office II shows the highest irradiance reduction on vertical plane in relation to the outdoor environment (~96% for summer and winter) and in relation to the reference office III (75.6% for summer and 81.5% for winter), showing maximum irradiance values of 25 W/m^2. The results indicate that this glazing is the most energy effective solution in reducing the solar gains in the summer and winter seasons (highest reduction in relation to the outdoor environment and the reference office).

The luminous performance analysis revealed that office I show the lowest indoor illuminance peak value on vertical plane and consequently the highest illuminance reduction in relation to the outdoor environment and the reference office in both seasons, and office II the second-highest reduction. Even though the illuminance reduction levels are high, the absolute values of indoor illuminance indicate that offices I and II still present daylight illuminance values above the recommended ones to perform office activities during working hours (0.5 lx according to [74]).

A comprehensive analysis of the results obtained in office IV with the damaged SCF, which is a highly reflective film comparable to SCF *B*, showed that the level of deterioration of the film (tears, cracks, blistering, lack of transparency, detachment, and deterioration of external layers) seriously affected its optical and thermal properties. The calculated optical properties showed a variation of 70% of the visible and solar transmittance, having a high impact on the thermal and visual performance of the office space with this film.

6. Energy, environmental, and economic analysis of windows' retrofit with solar control films

Incorporating or replacing materials in buildings may decrease the energy use during the operational stage but increase the embodied energy in a building's life cycle. In this section, three different solar control films from those analysed previously (SCFs *B, F*, and *G*), applied to the existing windows of a building are investigated through energy, environmental and economic perspectives over a defined life cycle period as potential retrofitting solutions of the building glazed area. The complete replacement of the existing window with a new one is also analysed as an alternative retrofitting solution. SCFs *B* and *F* were selected to be further studied in this section as they correspond to the films that showed higher performances in section 5 (see Table 27). This study also included SCF *G* because it corresponds to a spectrally selective film recently introduced in the Portuguese market, and a further analysis of this film's performance can provide a holistic view and more informed decisions for glazing retrofitting. The LCA approach (Life Cycle Analysis) carried out in this section, involves the study of different retrofitting scenarios and, for their implementation, the second case study building described previously (section 5.1) was used. The work developed in this section was published in [58].

6.1 Materials and methods

6.1.1 Goal and scope of the LCA study

Regarding energy rehabilitation of buildings-related projects, the decision-making process on alternative strategies is essentially based on the operational energy savings that can be achieved and the economic costs involved. Although other factors such as environmental sustainability and the life cycle of products are particularly important in decision-making today, their effective consideration has been far from desirable. In this context, it is expected that LCA can give a useful input in the decision-making process since it gives numerous life cycle outcomes of a product, consequence of human activities, with potential impact on the environment and therefore can be used for product comparison over the whole life cycle period.

The present LCA approach uses, as basis of the various analyses, the second case study building of this thesis and comprises the products and processes included in the life cycle of the following three scenarios: *Sc1*) original window; *Sc2*) retrofitting of the existing window using a solar control film (SCF) for three films (SCFs *B*, *F*, and *G*); *Sc3*) retrofitting through full replacement with a new window (NW). *Sc1* is considered the base case scenario – no intervention is done to the building – and *Sc2 and Sc3* are the two alternative retrofitting scenarios. Operational and embodied energy and the carbon footprint are the LCA outcomes used in this study for comparative evaluation and supporting decision-making in retrofitting options of the building glazed area. Further, a more holistic overview of the system performance considers the economic costs incurred in the life cycle of the three SCFs and the NW, which represent another performance measure and provide more comparison information upon the different solutions for the building glazing area.

6.1.2 Databases and calculation tools

The LCA study was carried out using the SimaPro Life Cycle Assessment tool, which is a well-recognized sustainability software package with which complex life cycles can be modelled and analyzed according to the ISO 14040 principles [107]. The LCA process's core is the life cycle inventory (LCI). To build the LCI dataset regarding the materials and activities involved in the retrofitting works, the Ecoinvent database [108] was employed.

In this study, the bill of quantities and works' information of the construction project of the second case study building, on which the LCA of the different scenarios was conducted, and that are essential to perform the corresponding LCI, were not available, whereas in the case of the glazing retrofitting scenarios, they did not exist at all. Measuring the layout elements concerned and using the Andalusia Construction Cost Database (ACCD) to obtain work items and schedule quantities that allow compiling the final inventory were a way of bypassing the problem [109]. The applicability of this Spanish database ACCD to Portuguese buildings has been previously assessed using the Carbon Footprint indicator [110].

Complementary to the tools used specifically for the LCA approach, the popular building energy simulation program EnergyPlus [78] is employed in this study to predict the OE use based on the required heating, cooling and artificial lighting demand to maintain indoor thermal and visual comfort. The calibrated simulation model previously described in section 5 was used.

Since this study involves a comparison between three scenarios – existing window (*Sc1*), different SCFs (*Sc2*) and a new window (*Sc3*) – using the LCA methodology for its evaluation, the life cycle period is considered to start when retrofitting takes place. Given that the useful life of windows is established around

30-50 years [111], to enable a comparable timeline between SCFs and NW, a life cycle period of 40 years was considered. As the useful life of the SCFs selected for this study is estimated around 10 years [112] and given the building life cycle of 40 years, the film will be installed three times after the first retrofitting.

Since retrofitting is a process that occurs after the building has been completed, the life cycle stages of the LCA methodology do not involve the building itself. However, they only encompass the new competing construction solutions, with the building (second case study building) being regarded as a previously finished and consolidated system. Thus, the following stages are the focus of the present work: *Product stage*, associated with raw material supply, transport and manufacturing only referring to the retrofitting construction products; *Construction stage*, associated with transport to workplace and installation construction process only of the retrofitting products; and *Use stage*, related with the impacts during the life-cycle only of the implemented retrofitting solutions. Finally, the *End-of-Life* stage, which includes the disposal, recycle and reuse stages, was not considered particularly interesting because the destiny of most products after use is uncertain; as such, it was not included in the study.

The life cycle of the proposed study is shown schematically in Figure 1. As *Sc1* is related to the original glazing, no major intervention is required besides regular maintenance during the life cycle period in this scenario.

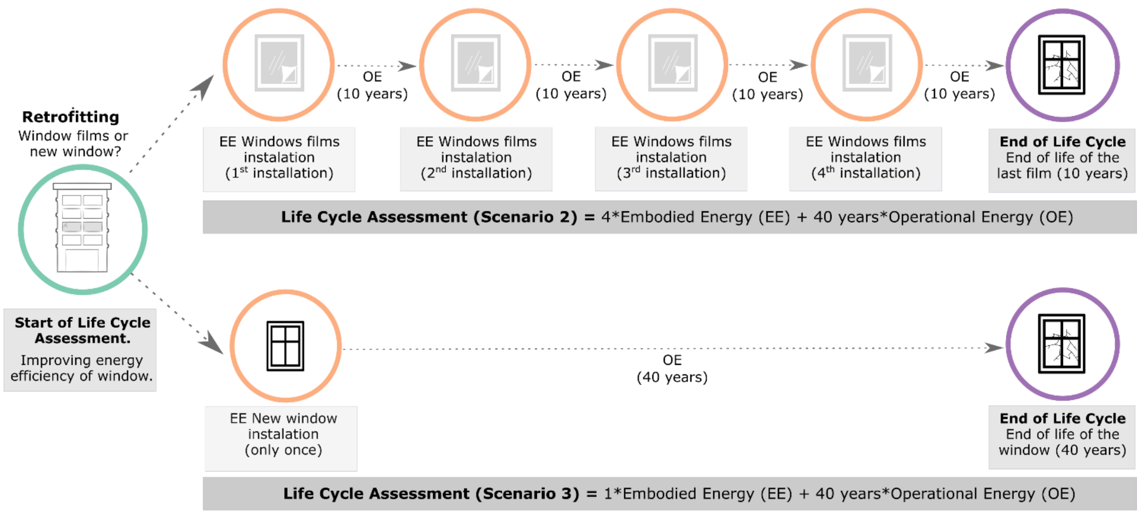

Figure 92. Timeline of events in the life cycle period for retrofitting scenarios *Sc2* and *Sc3*

6.1.3 Organization of the study

The methodology proposed in this study, for investigating the life cycle performance of the fenestration solutions under study, is shown in Figure 93 and comprises the following steps:

a. definition of the three analysed case scenarios: *Sc1*) original glazing of the base case study; *Sc2*) original window for three alternative SCF solutions applied on the external surface of the glazing; and *Sc3*) replacement of the original window by one alternative new window;

b. building energy simulation (BES) with the same model calibration of section 5.6.1, but now extended to the whole building, and again based on the EnergyPlus, SketchUp, Window and Optics programs, so as to assess the building operational energy (*OE*) of the three analysed scenarios;

c. assessment of embodied energy (*EE*), carbon footprint (*CF*) and economic costs (*EC*) for the three analysed case scenarios, when implemented in the building, through an LCA approach; in correspondence with the type of element installed in the fenestration area – NW or SCF – the bill of quantities can be prepared from the work units concerned, taken from the Andalusia Construction Cost Database (ACCD), and the surface area that the fenestration occupies in the building envelope. With the total amount of resources consumed (materials consumption in the retrofitting solutions) and the Ecoinvent database [108] implemented in the SimaPro software, it is possible to obtain the energy and greenhouse gas emissions involved in the production (materials extraction, transport and manufacture) of the retrofitting elements and determine the environmental indicators: Embodied Energy (*EE*) and Carbon Footprint (*CF*). Likewise, the good execution of the budget associated with materials and construction works, from data provided by ACCD, and the operational energy costs provided by PORDATA [113], allows to perform the economic evaluation of the analysed scenarios.

d. finally, a comparison of the operational energy, environmental impacts and economic costs of the base case and the retrofitting strategies for the glazing area of the façade is carried out.

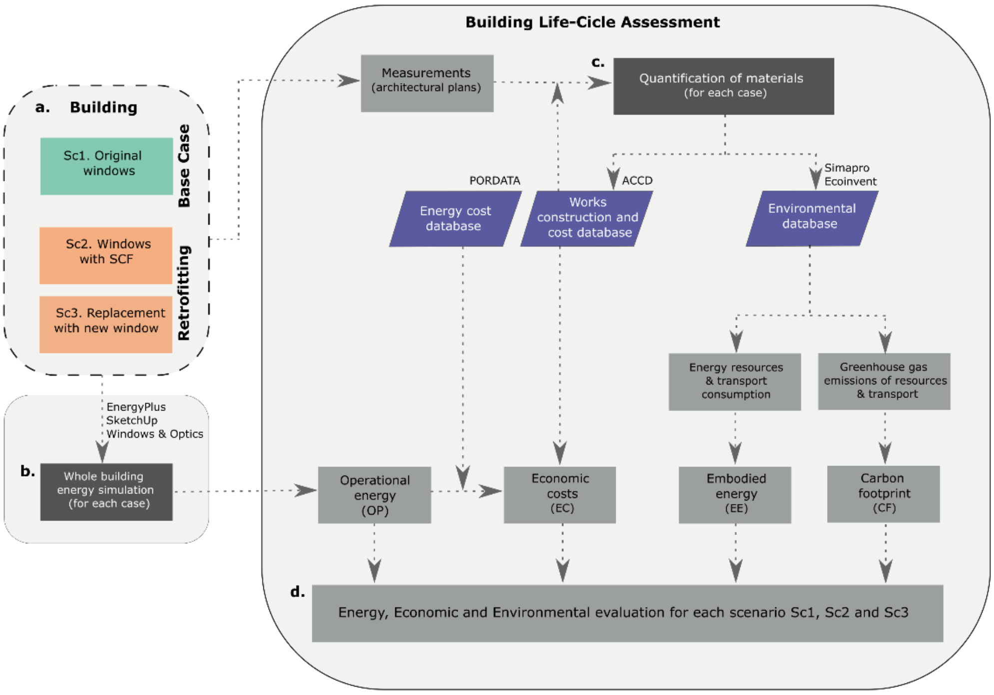

Figure 93. Methodology flowchart

6.2 LCA calculation process

6.2.1 Operational energy

Building energy modelling has become a preferred method to predict energy demand and evaluate different retrofitting scenarios based on energy performance and other metrics in recent years [114]. In this study, the operational energy (*OE*) is considered in the LCA approach as the primary energy required to maintain the thermal and visual comfort in the case study building and was assessed through a whole building energy simulation (BES) using both the EnergyPlus and the SketchUp 3D modelling software over the defined 40 years life cycle. BES models allow to predict the energy use under the influence of external inputs (e.g. weather, occupancy and infiltration) to maintain specified performance criteria, such as indoor temperature and humidity. The simulation model described and calibrated in section 5.6, concerning the office area without SCF, was used as a basis for executing the office areas in a BES model applied to the whole building.

The building energy simulation (BES) model, as showed in Figure 94, was designed in the SketchUp and EnergyPlus software by using the complete architectural plans, detailed construction descriptions, and the materials' properties tuned through the calibration process for the reference office the building carried out in section 5.6.1.

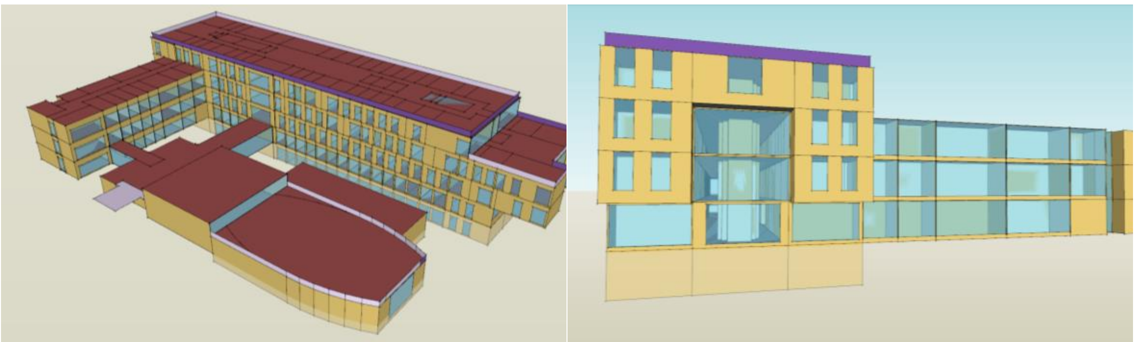

Figure 94. Geometrical model of the building executed on a SketchUp 3D modelling program

The annual *OE* of the building was calculated as shown below (6.1):

$$OE = \left(\frac{EN_{heat}}{COP} + \frac{EN_{cool}}{EER} + EN_{light}\right) \times P_{EF} \qquad (6.1)$$

where

EN_{heat}: energy needs with heating;

EN_{cool}: energy needs with cooling;

EN_{light}: energy needs with lighting.

These indicators were obtained from BES for the three alternative scenarios of the glazing. The efficiency ratios of the HVAC equipment considered in the equation (6.1) are: the coefficient of performance (*COP)* and the energy efficiency ratio (*EER*) used to convert the energy needs into energy use and the primary energy factor of electricity generation, P_{EF}, used to convert energy use into primary energy.

It must be noted that the *OE* considered in the calculations only accounts for the share of the building energy charged to the windows, to be coherent with the embodied energy calculation, which relates solely to the window systems. The *COP* and *EER* used to convert the energy needs into energy use were 3.0 and 3.4 [105], respectively, and a primary energy factor, P_{EF}, of 2.5 kWh_{EP}/kWh [105] was considered.

6.2.2 Embodied energy and carbon footprint

To estimate the embodied energy and the economic and environmental impacts related to the glazing retrofitting operations, it is necessary to quantify all the resources involved in the *Product stage* (raw material extraction, transport to factory and manufacture of retrofitting products), the *Construction stage* (transport to site, assembly and installation of retrofitting products), and in the maintenance operations (concerned to retrofitting products) during the *Use stage* and make the subsequent conversion into energy and carbon emissions by multiplying the resource quantities by proper coefficients representing the energy consumed and the CO_2 equivalent per resource unit (kg, litres, m^2, m^3) [115].

To obtain the consumed resources of the retrofitting works for the different analyzed scenarios, a methodology that incorporates an internal economic and environmental cost database, based on ACCD, was employed in the analyzed case study [116], [117]. This cost database uses a hierarchical classification system whereby each group is divided into subgroups of similar characteristics [109]. The unitary costs representing the group of materials necessary to complete a unit of traditional construction work (work unit) are included at the lower level of the hierarchic structure. Once the work units corresponding to the envisaged retrofit solutions are identified in the database and the involved glazing areas are measured, it is possible to quantify the resources broken down into materials, manpower and machinery. For the inventory, associated with the retrofitting systems, only materials are accounted for computing *EE* and *CF* of the building life cycle.

To obtain both the *EE* and the *CF* of a particular product or building component, the mass of the constitutive materials (kg) is first obtained. Then, the Cumulative Energy Demand (CED) and the International Panel of Climate Change 100a (IPCC 100a) impact indicators are applied not only to respectively estimate the primary energy use to calculate the *EE* but also to measure the total GHG emissions expressed in CO_2 equivalent to calculate the *CF*, per kg of manufactured material. The environmental database used in both indicators is Ecoinvent, implemented in SimaPro, and developed by the Swiss Center for Life cycle Inventories, due to its transparency in the development of processes, consistency, references, and the outstanding fact that it fuses information from several international databases of the construction industry.

The procedure which is applied in the retrofit of a building window for each scenario formerly analysed is shown in the following equations (6.2) and (6.3):

$$EE_M = \sum_i M_i \times \left(E_{mat_i} + E_{trans_i}\right) \tag{6.2}$$

$$CF_M = \sum_i M_i \times \left(I_{mat_i} + I_{trans_i}\right) \tag{6.3}$$

where

EE_M and CF_M: embodied energy and CO_2 equivalent associated with the material resources involved in the retrofitting alternatives;

M : mass of a basic constitutive material of the retrofitting work;

E_{mat} and E_{trans}: primary energy consumption of manufacture and transport of the material;

I_{mat} and I_{trans}: CO_2 equivalent of manufacture and transport of the material.

The life cycle energy (LCE) for each retrofitting solution, throughout the 40 years life-cycle is given by the following formula extended to the number of retrofitted windows:

$$LCE = \sum_i EE_{M_i} + OE \tag{6.4}$$

where

EE_M (equation 6.2) = embodied energy during the *Product* and *Construction* stages;

OE (equation 6.1) = operational energy during the *Use stage.*

On the other hand, the carbon footprint, *CF*, associated with all the retrofit windows for each scenario throughout the 40 years life-cycle is shown below:

$$CF = \sum_i CF_{M_i} + I_{OE} \times \frac{OE}{P_{EF}} \tag{6.5}$$

where

CF_M (equation 6.3): *CF* during the *Product* and *Construction* stages and the CO_2 equivalent associated with the energy use during the *Use stage*;

I_{OE}: conversion factor from electricity to carbon emissions in Portugal (0.28271 $kgCO_2eq/kWh$ [118]).

The environmental and economic impacts associated with the maintenance and cleaning operations were assessed by using data from [115], by built surface (11.42 m^2), as provided in Table 28.

Table 28. Economic (*EC*) and environmental costs (*EE*, embodied energy and *CF*, carbon footprint, respectively), for the maintenance and cleaning operations during the life cycle [115]

Item	*EC* [€/m²/y]	*EC_TOTAL* [€/m²/40y]	*EE* [MJ/m²/y]	*EE_TOTAL* [MJ/m²/40y]	*CF* [kgCO₂eq/m²/y]	*CF_TOTAL* [kgCO₂eq/m²/40y]
Cleaning	42.2300	19 294.04	0.916	418 416.10	0.259	118 286.23
Maintenance	0.0104	4 755.06	4.563	2 084 756.20	1.290	589360.58

6.2.3 Economic costs

The economic costs. *EC*. associated with the different retrofitting solutions of the glazing system were determined for all the window area of the building of the case study and for a 40 years life-cycle period according to the following equation (6.6):

$$EC = EC_{ini} + \sum_{k=1}^{k=\frac{N}{R}-1} \frac{EC_{ini} \times (1+a')^{k\times R}}{(1+a)^{k\times R}} + \sum_{k=0}^{k=N-1} \frac{C_e \times OE \times (1+a')^k}{(1+a)^k} \qquad (6.6)$$

where

EC: economic cost associated with each retrofitting solution;

EC_{ini}: initial cost with production and construction works of the retrofitting solution;

C_e: current value of the electricity cost for domestic consumers;

α': harmonized index of consumer prices;

α: discount rate based on a 10year government treasury yield;

N: life cycle period (*N*=40);

R: periodicity of the retrofitting scenario (*R*=10 in *Sc2* and *R*=40 in *Sc3*).

The first sum of Equation 6.6 represents the net present value of economic costs with product and construction works of the retrofitting solution during its life cycle; the second sum represents the net present value of economic costs with the annual operational energy imputed to the glazing systems (*OE*). Through the LCA methodology used in this study, the initial costs, EC_{ini}, associated with the retrofitting works, cleaning and maintenance tasks were calculated considering the bill of quantities and the work specifications taken from the ACCD. For the calculation of the net present value of periodic and periodic fixed annual costs that occur in different periods of time, the harmonized index of consumer prices obtained through the macroeconomic projections for the euro area by the European Central Bank [119], α', as well as the discount rate based on a 10 year government treasury yield [120], α, were considered. Regarding the electricity cost for domestic consumers, C_e, the current value of 0.215 €/kWh was assumed [113].

6.3 Results and discussion

In this study, two alternative retrofitting scenarios for double-glazing systems were studied on the second building case study of this thesis: the application of SFC on the external surface of the glass and the replacement of the existing window by a new one as shown in Table 29. SCF *B* is a reflective film with silver colour, 0.050mm thickness, and is manufactured through several layers of metallized polyester attached with a pressure sensitive acrylic adhesive and a siliconized Polyethylene Terephthalate (PET) protective liner as a finishing layer. SCFs *F* and *G* are less reflective than SCF *A* due to the metal-free manufacturing process consisting of multi-layers of Polymethyl Methacrylate (PMMA) and PET with a pressure sensitive acrylic adhesive a siliconized PET protective liner as finishing layer. Both films *F* and *G* are spectrally selective with 0.05mm thickness and different solar transmittances (higher for SCF *F*) and while SCF *B* shows a tinted dark-yellow appearance when installed, SCF *B* shows a clear appearance and does not affect the colour of existing glazing.

Table 29. Retrofitting scenarios

Scenario (Sc_i.)	Description
Sc2 Solar control films (SCFs)	Application on the external layer of the original window without the damaged SCF
Sc2.1 SCF *B*	Application of a reflective SCF
Sc2.2 SCF *G*	Application of a spectrally selective SCF (lower solar transmittance)
Sc2.3 SCF *F*	Application of a spectrally selective SCF (higher solar transmittance)
Sc3 New window (NW)	With an air gap
Sc3.1 NW	Increase the thickness of the glass layer and decrease the solar and visible transmittance

Window program has a broad database of glasses, applied films, coatings, and frames that calculate total window thermal performance indices. Nonetheless, it is not always straightforward to select and analyse different films due to the extensive available data. Optics complements the Window program since it provides access to a database of various applied films organized in a specific list, simplifying the process of selecting the films to be investigated. Table 30 shows the optical and thermal properties considering the different scenarios calculated through Window and Optics programs [73].

Table 30. Thermal and optical characteristics of the existing window and the alternative retrofitting scenarios: solar transmittance, τ_{sol}, solar (front) reflectance, $\rho_{f,sol}$, absorptance (front), α_1, visible transmittance, τ_{vis}, visible (front), $\rho_{f,vis}$, and (back), $\rho_{b,vis}$, reflectance, thermal transmittance, U [W/m^2.K], and solar factor, g

Scenario (Sc_i.)	mm	τ_{sol} [%]	$\rho_{f.sol}$ [%]	α_1 [%]	τ_{vis} [%]	$\rho_{f.vis}$ [%]	$\rho_{b.vis}$ [%]	U [W/m^2.K]	g [%]
Sc1 Existing window (*EW*)	32	36.6	16.6	40.9	56.4	14.2	9.82	1.4	48.0
Sc2 Solar control films (SCFs)									
Sc2.1 SCF *B*	32	5.9	58.5	29.8	10.6	57.8	30.4	1.4	12.1
Sc2.2 SCF *G*	32	11.9	25.4	52.5	24.5	8.35	11.5	1.4	23.4
Sc2.3 SCF *F*	32	19.4	28.1	37.2	41.5	15.1	12.1	1.4	29.3
Sc3 New window (NW)									
Sc3.1 NW	38	12.0	25.6	48.6	28.4	23.3	26.4	1.1	29.6

The *OE* for the different scenarios of the glazing system was calculated, using the BES model with the original synthetic weather data of Lisbon's city [78], considering the lighting, heating and cooling energy use, from Monday to Friday and from 8h00 to 18h00. The energy consumption with water heating and appliances was considered independent of the type of the window system used on the façade and therefore was not considered in the OE calculation. The HVAC system was set to turn on when the indoor temperature exceeds the thermal comfort range of temperatures for Portugal (18 ºC to 25 ºC), according to [82].

6.3.1 Operational energy

Figure 95 shows the lighting, heating, cooling, and the total variation of the operational energy, *ΔOE*, between the retrofitting solution and the original glazing calculated per m^2 of floor area during the 40 years life-cycle, for: *Sc2.1* retrofitting using SCF *B*, *Sc2.2* retrofitting using SCF *G*, *Sc2.3* retrofitting using SCF *F*, *Sc3.1* replacement with a NW.

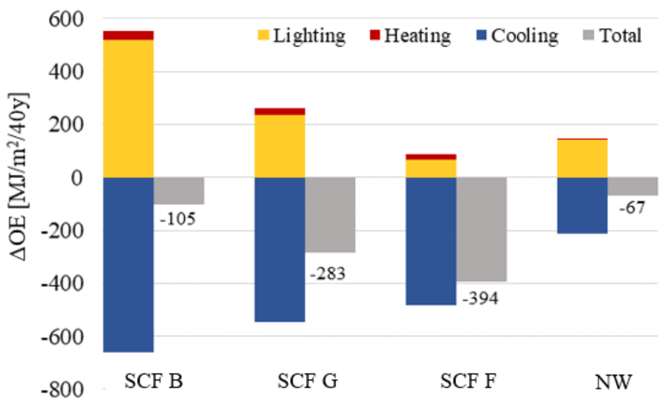

Figure 95. Lighting, heating, cooling, and total variation of the operational energy, *ΔOE*, per m^2 of floor area

When comparing the retrofitting scenarios for the glazing area of the building (Figure 8), it is possible to observe that:

- all retrofitting solutions are feasible to increase the energy efficiency of the building under consideration during the operational stage since they all show negative values of the ΔOE when compared to the original scenario of the glazing system without SCF, *Sc1*;
- SCF *G* (ΔOE= -283 MJ/m^2/40years) and SCF *F* (ΔOE = -394 MJ/m^2/40years) show a higher ΔOE when compared to SCF *B* (ΔOE= -105 MJ/m^2/40years). These differences can be explained by the higher visible transmittance coefficient and solar factor of SCF *G* (τ_{vis}= 24.5; g= 23.4) and SCF *F* (τ_{vis}= 41.5; *g*= 29.3) compared to SCF *B* (τ_{vis}= 10.6; *g*= 12.1). In fact, previous studies [25], [57] show that the application of SCFs on glazing systems decrease the cooling energy use and increase the heating and lighting energy use of glazing systems. For the building under consideration, the cooling energy use represents ~62% of the total *OE*, and the lighting is about ~29%. Therefore, retrofitting solutions with higher light-to-solar gain ratios (τ_{vis}/g) as SCF *G* (τ_{vis}/g= 1.05) and SCF *F* (τ_{vis}/g= 1.42) show a higher variation of the operational energy by decreasing the solar gains in a higher proportion than the decrease of the visible transmittance;
- SCFs show higher ΔOE when compared to the alternative scenario of full replacement of the EW, especially in the variation of the cooling energy. The higher insulation of the NW (1.1W/m^2.K vs 1.4W/m^2.K, see Table 30) decreased the heat losses during the night periods when compared to the other 3 SCFs, trapping heat during the night and requiring more cooling load in the summer periods and less heating load in the winter periods in the first hours of the working hours. These results are in accordance with O'Neill et al. [121] who concluded that the combination of low U values and high solar factor in windows allows the entry of more solar radiation during the day and less heat escapes during the night, increasing the energy needs with HVAC consumption.

It is worth highlighting that a preliminary study that considered 3 NWs with comparable optical and thermal properties to the 3 SCFs applied in the existing glazing was performed. It was concluded that the results of the 3 NWs were very similar due to their similar optical and thermal characteristics, and therefore only one of the NW is presented in this study for comparison purposes.

6.3.2 Carbon footprint and economic costs

Following the methodology described in section 6.2.2, Table 31 and Table 32 show the list and the quantity of resources (materials consumed and total hours of labor) and corresponding disaggregated basic prices involved in *Sc3.1* and *Sc2.3* scenarios for a single building window unit (1.012 m^2). The single unit economic cost of the retrofit work of a window is equal to the sum of the products of the quantities and the respective basic prices.

EE and *CF* were obtained by converting the original measure unit of each basic price (meters, square meters, tons, cubic meters) into cubic meters so that the established density available in supporting documents can be applied. Then, equations (6.2) to (6.5) are applied to obtain *EE* and *CF* of each resource and the respective totals of the retrofit work of the window.

Table 31. Disaggregated resources and basic prices, economic and environmental costs, and carbon dioxide emissions for the replacement of a window unit

Price code	Qu.	Un.	Resource Description	Economic Cost *EC* [€/un]	*EC* [€]	Environmental Cost *EE* [MJ/un]	*EE* [MJ]	*CF* [110] [kgCO_2eq/un]	*CF* [kgCO_2eq]
01KLV90001	1.012	m^2	Labor in selective demolition of window with aluminum profiles						
TP00100	0.3	h	Special labor	18.28	5.55	0.00	0.00	0.00	0.00
06WWR80060	1.012	m^2	Received from received from façade fences.						
WW80010	0.09	kg	TIPS 20x100 cm	7.42	0.68	0.00	0.00	0.00	0.00
AGM00500	0.03	m^3	Cement mortar M5 (1:6) CEM II / A-L 32.5 N						
GW00100	0.263	m^3	Water	0.55	0.00	31.06	0.25	7.40	0.06
GC00200	0.258	t	Cement II / A-L 32.5 N in sacks	92.54	0.72	3778.06	29.59	786.09	53.34
AA00300	1.102	m^3	Gross sand	6.53	0.22	141.43	4.73	15.29	4.35
TP00100	1.030	h	Special labor	18.28	0.57	0.00	0.00	0.00	0.00
TP00200	0.350	h	Professional workmanship	19.23	6.81	0.00	0.00	0.00	0.00
TA00100	0.350	h	Assistant	18.42	6.52	0.00	0.00	0.00	0.00
11LVA80050	1.012	m^2	Window folding aluminum lacquer type IV with TBB (>3m^2)						
TO01600	0.15	h	Workmanship carpentry	19.23	2.92	0.00	0.00	0.00	0.00
TP00100	0.17	h	Special labor	18.28	3.14	0.00	0.00	0.00	0.00
KA01100	3	m	Pre-fence tube steel galvanized fixed or fixed	3.11	9.44	18.43	55.95	1.16	0.59
KL80300	1	m^2	White lacquered aluminum folding window with TBB	230.00	232.76	1 595.96	1 615.11	99.09	297.27
RW01900	3	m	Sealing gasket	1.30	3.95	6.12	18.59	0.13	0.40
WW00300	1	u	Complementary material or specials pieces.	0.55	0.56	2.65	2.68	0.16	0.48
12LTI80016	0.533	m^2	Thermoacoustic lighting colorless polished lenses 8+14+8+8mm. air chamber 14mm.						
VL04650	1	m^2	Double reflective and colorless under emissive and solar control 8+14+8+8mm (air chamber)	43.22	23.04	138.74	73.95	1.58	0.84
VW01500	3	m	Neoprene "U" profile	0.40	0.64	91.09	145.65	2.62	7.85
TO01700	0.85	h	Glass worker	19.23	8.71	0.00	0.00	0.00	0.00
Total (*EC*. *EE*. and *CF*)					306.24		1946.50		365.17

Table 32. Disaggregated resources and basic prices, economic and environmental costs and carbon dioxide emissions for a window retrofitted with SCF *F*

Price code	Qu.	Un.	Resource Description	Economic Cost		Environmental Cost		Carbon Footprint	
				EC [€/un]	*EC* [€]	*EE* [MJ/un]	*EE* [MJ]	*CF* [110] [$kgCO_2eq$/un]	*CF* [$kgCO_2eq$]
20FCL90026	1.012	m^2	Outdoor window cleaning						
TP00100	0.08	h	Special labor	18.28	1.48	0.00	0.00	0.00	0.00
JL00100	0.08	h	Cleaning materials	0.70	0.06	2.87	0.23	0.23	0.00
12WWW00001	1.012	m^2	Installation of outdoor window protection film						
TP00300	0.3	h	Special labor	19.23	5.77	0.00	0.00	0.00	0.00
HW01000	3	m^2	Scaffolding for sale in façade	0.40	1.20	0.00	0.00	0.00	0.00
090	1	m^2	Sheet for windows. exterior placement.	58.00	58.70	48.58	49.16	3.90	11.70
WW00300	2	u	Complementary material or pzas. specials	0.30	0.61	2.65	5.37	0.16	0.32
Total (*EC*, *EE* and *CF*)					67.81		54.76		12.02

Table 33 shows the economic costs (*EC*), embodied energy (*EE*) and carbon footprint (*CF*) obtained for the retrofitting scenarios normalized per m^2 of building floor area without considering the contribution of the operational energy. The values of *EC*, *EE*, and *CF* for *Sc2* are indicated for each installation of the films as well as for the four necessary installations in the life cycle studied. *Sc3* comprehends only one replacement in the starting point of the life cycle under scope, so the values of *EC*, *EE*, and *CF* in the beginning and end of the life cycle are the same.

Table 33. Economic costs, *EC*, and embodied energy, *EE*, and carbon footprint, *CF*, excluding the contribution of operational energy for the 4 retrofitting solutions, per m^2 of floor area

Scenario (Sc_i.)	EC_{ini} [€/m^2/10y]	EE_M+EE_P [MJ/m^2/10y]	CF_M [$kgCO_2eq/m^2$/10y]	*EC (w/o OE)* [€/m^2/40y]	EE_M+EE_P [MJ/m^2/40y]	CF_M [$kgCO_2eq/m^2$/40y]
Sc2 SCFs	One installation in 10 years			Four installations in 40 years		
Sc2.1 SCF *B*	2.69	4.64	1.06	11.72	18.57	4.26
Sc2.2 SCF *G*	6.57	5.85	1.30	28.65	23.39	5.20
Sc2.3 SCF *F*	6.67	5.39	1.18	29.08	21.54	4.73
Sc3 NW	One replacement in 40 years					
Sc3.1 NW	30.12	191.46	35.93	30.12	191.46	35.93

The results show that during the life cycle period, the *EC* of SCFs *F* and *G* are very similar to that of the NW and the *EC* of these 3 retrofitting solutions are, in turn, ~2.5 times higher than the *EC* of SCF *B*. The EE of retrofitting scenario *Sc2* shows the lowest value for the reflective film SCF *B* (18.57 MJ/m^2/40y) and the highest one for the spectrally selective film SCF *G* (23.39 MJ/m^2/40y). The average of the *EE* of the three films is ~89% lower than the *EE* of the NW and the *CF* of the retrofitting scenarios *Sc2* and *Sc3* is

4.4 to 5.3 times higher than the value of the *EE* of the retrofitting solutions, evidencing a high relationship between these two indicators during the *Product* and *Construction* stages.

6.3.3 Energy, economic and environmental analysis

Table 34 shows the operational, *OE*, and embodied, *EE*, energy, and the life cycle energy, *LCE*, associated with the retrofitting scenarios per m^2 of building floor area. The following calculation gives the ratio of the embodied energy to the life cycle energy: *EE/LCE*.

Comparing the values of the *OE* of the retrofitting solutions, it can be concluded that the *OE* varies between 420.84 and 551.66 MJ/m^2/40y, and SCF *F* shows the lowest value of *OE* because of the higher light-to-solar gain ratio (τ_{vis}/g= 1.42) compared to the other solutions. On the other hand, comparing the *LCE* results for the four retrofitting solutions, it can be noticed that the *LCE* is lower using SCFs mainly due to the lower values of *EE* when compared with the total replacement of the window. Observing the proportion of embodied energy to life cycle energy, the embodied energy shows the highest and the lowest percentage of *LCE* for NW (25.8%) and for the reflective SCF *B* (3.3%), respectively.

Table 34. Life cycle energy for the 4 retrofitting solutions: operational, *OE*, and embodied,. *EE*, energy, life cycle energy, *LCE*, and the ratio of the embodied energy to the LCE, *EE/LCE*

Scenario (Sc_i.)	*EE* [MJ/m^2/40y]	*OE* [MJ/m^2/40y]	*LCE* [MJ/m^2/40y]	*EE/LCE* [%]
Sc2 SCFs				
Sc2.1 SCF *B*	18.57	536.63	555	3.3
Sc2.2 SCF *G*	23.39	465.19	489	4.8
Sc2.3 SCF *F*	21.54	420.84	442	4.9
Sc3 NW				
Sc3.1 NW	191.46	551.66	743	25.8

Table 35 shows the economic, *EC*, and environmental, *CF*, costs related to the retrofitting solutions during the 40 years life-cycle. SCF *B* and NW show the lowest (48 €/m^2/40y) and the highest (1046 €/m^2/40y) economic costs of the 4 retrofitting solutions, respectively. It is worth noticing that although SCF *B* shows the highest operational energy costs (35.83 €/m^2/40y) of the three films, the total economic cost is the lowest of the retrofitting solutions due to the lower production and construction works' economic costs associated with this film (11.72 €/m^2/40y).

Observing the results of the CF_M, it can be concluded that the three SCFs generate almost the same amount of CO_2 equivalent per m^2 of floor area (average of 4.73 kgCO_2eq/m^2/40y). In terms of the NW, the CF_M

(35.93 $kgCO_2eq/m^2/40y$) is almost eight times higher than the average of the three films. The total *CF* of the four retrofitting solutions shows that the three SCFs analysed produce almost half of the amount of CO_2 equivalent per m^2 compared to a new window replacement during the 40 years life cycle (which corresponds to the useful life of windows).

Table 35. Economic and environmental costs, *EC* and *CF*, respectively, for the 4 retrofitting solutions: inicial, C_i, and operational, EC_{OE}, economic costs; material, CF_M, and operational, CF_{OE}, carbon footprint

Scenario (Sc_i.)	EC_{OE} [€/m²/40y]	*EC* [€/m²/40y]	CF_M [$kgCO_2eq/m^2/40y$]	CF_{OE} [$kgCO_2eq/m^2/40y$]	*CF* [$kgCO_2eq/m^2/40y$]
Sc2 SCFs					
Sc2.1 SCF *B*	35.83	48	4.26	42.14	46
Sc2.2 SCF *G*	31.06	60	5.20	36.53	42
Sc2.3 SCF *F*	28.10	57	4.73	33.05	38
Sc3 NW					
Sc3.1 NW	36.84	67	35.93	43.32	79

Figure 96 shows the combined embodied, *EE*, and operational, *cooling*, *heating* and *lighting*, energy results and the economic and environmental costs that allow identifying the best solution from a multi-criteria decision analysis for window retrofitting of non-residential buildings in temperate Mediterranean climates. The combined operational and embodied energy results identify the lowest life cycle energy and carbon footprint retrofitting scenario – SCF *F* (*LCE*= 442 $MJ/m^2/40y$, *CF*= 38 $kgCO_2eq/m^2/40y$) and SCF *B* shows the lowest *EC* (48 €/m²/40y) and the highest *LCE* and *CF* (*LCE*= 555 $MJ/m^2/40y$, *CF*= 46 $kgCO_2eq/m^2/40y$) among the three SCFs, resulting in the best SCF investment from an economic point of view, and the least effective from an energy and environmental standpoint.

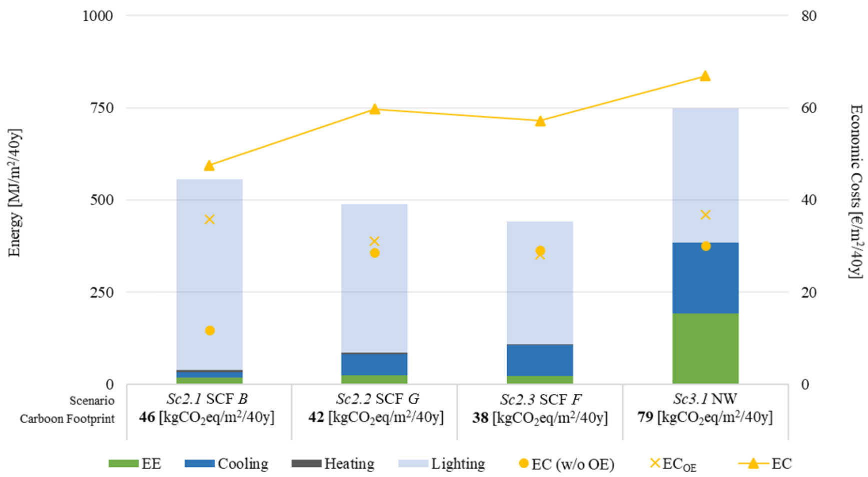

Figure 96. Operational energy with *cooling*, *heating*, and *lighting*, embodied energy, *EE*, economic costs, *EC*, and carbon footprint for the retrofitting solutions per m² of floor area during the life cycle period

6.4 Conclusions

The purpose of this section was to describe and assess the energy, environmental and economic impacts for alternative retrofitting scenarios for glazing areas of existing non-residential buildings using a LCA comparative approach and to quantify the relative importance of embodied and operational energy associated with solar control films (SCFs). The scenario of three SCFs (SCFs *B*, *F* and *G*) with different thermal and optical properties and the scenario of a new window (NW) replacement were the retrofitting scenarios considered in this study to improve the energy efficiency of an existing office building located in Lisbon, considered as the case study. The methodology used consider the building as a previously finished and consolidated system and therefore the life cycle stages of the LCA do not involve the building itself but only the new construction solutions and the economic and environmental costs associated with one of the four retrofitting solutions (three SCFs and one NW). The established life cycle period was set in 40 years (useful life of windows) to enable a comparable timeline between the two alternative retrofitting scenarios.

This study showed that different retrofitting scenarios such as SCFs and NWs can reduce the total operational energy while meeting the current thermal and visual comfort requirements standards in the work environment. The operational energy results showed that retrofitting solutions with higher light-to-solar gain ratios (τ_{vis}/g), such as SCFs *F* and *G*, exhibit higher operational energy savings by decreasing the solar gains in a higher proportion than the decrease of the visible transmittance. Therefore, the reduction in cooling energy needs is much higher than the increase in lighting and heating energy needs. The higher insulation of the new window (U=1.1 W/m^2.K) was also a factor that contributed to the lowest operational energy savings of this solution when compared to those obtained for SCFs (U=1.4W/m^2.K), since it lowered the heat losses during the night periods, trapping heat during the night, and requiring more cooling load in the morning periods.

As expected, all retrofitting solutions increased the embodied energy of the building since retrofitting interventions have impacts associated with the production and transportation of the new components related to each retrofitting solution. The found embodied energy for the four retrofitting solutions revealed that the NW shows the highest value in the life cycle period compared to the three SCFs (~9 times higher than the average of the embodied energy of the films). In fact, the lower values of the life cycle energy of SFCs are related to the lower values of *EE* and *OE* of the 3 SCFs compared to that of the NW.

The Carbon Footprint results showed that the carbon equivalent generated to produce the films is between 38-46 $kgCO_2eq$ per m^2 of building floor area for 40 years, whereas manufacturing NW is 2 times higher than those of the films.

Window retrofitting solutions such as SCF *B* with lower production and construction costs can be economically advantageous. However, while this film was the best investment from an economic point of view compared to the other three retrofitting solutions, it also yielded the highest operational and environmental costs.

Retrofitting solutions with higher light-to-solar gain ratios showed higher energy savings during the operational stage by decreasing the solar gains in a higher proportion than the decrease of the visible transmittance. The best retrofitting solution, SCF *G*, showed a life cycle energy (LCE) (embodied plus operational energy) and a carbon footprint of 4447 $MJ/m^2/40y$ and 380 $kgCO_2eq/m^2/40y$, respectively, whereas the least performant solution, new window, showed a LCE 1.5 times higher than the average of the three SCFs. The higher LCE value of the new window was related to the higher value of the embodied energy compared to those of the three SCFs (~9 times higher than the average of the films).

The results of this section show the importance of a combined operational and embodied energy analysis for retrofitting solutions of existing glazing systems and present valuable information to support the decision-making process towards more efficient and sustainable buildings. Comprehensive studies of retrofitting scenarios should be thoughtfully investigated before retrofitting interventions to promote accurate estimations on the life cycle energy and awareness of possible environmental impacts during their life cycle.

7. Thermal, daylighting and energy performance of glazing with SCFs – aggregated performance indicators

To consolidate and unify all the experimental and numerical conclusions compiled in the execution of the present thesis, a parametric analysis was carried out to evaluate the performance of single and double glazing units of office rooms without and with two high-performing solar control films for different façade conditions and different locations on the mainland Portugal. SCFs *B* and *F* were considered, as these films presented the highest energy performance in sections 4, 5 and 6, according to at least one criteria (cooling, heating and lighting) for clear single and double glass panes.

The embodied energy (EE) was not considered in the study of this section since it was concluded that during the life cycle of a window, the EE of a SCF is negligible as it represents 3% to 5% of the total life cycle energy (see EE/LCE, Table 34 in section 6).

This last section provides a conclusion of the work developed, based on the results obtained in previous sections, as well as valuable information for decision-makers and professionals from the building industry regarding the application of window films in existing buildings in Portugal.

7.1 Methodology

In this section, a parametric analysis to investigate the thermal and visual comfort as well as the energy performance of glazing units in office areas without and with two window films for different façade scenarios is described. Single and double clear glazed units were adopted as reference substrates, representative of two transparent components of building façades. On the other hand, spectrally selective and highly reflective films that showed higher performances (see results and conclusions in sections 5 and 6) were selected as the representative films to be considered. In this section, the office rooms (2.4x6.0m^2) studied in sections 5 and 6, which correspond to the office areas of the building of the second case study, were considered.

Table 36 shows the thermal and optical properties of each of the representative window scenarios investigated in this section.

Table 36. Thermal and optical characteristics of single and double-glazed windows with SCFs *B* and *F* applied to the external side of the back pane glass: solar (front) reflectance, $\rho_{f,sol}$, solar transmittance, τ_{sol}, visible transmittance, τ_{vis}, (front) absorptance, α_1, thermal transmittance, *U* [W/m^2.K], and solar factor, *g*

Glazing scenario	Nomenclature	τ_{sol} [%]	$\rho_{f.sol}$ [%]	α_1 [%]	α_2 [%]	τ_{vis} [%]	$\rho_{f.vis}$ [%]	$\rho_{b,vis}$ [%]	U [W/m^2.K]	g [%]
Single-glazed window (*SG*)	*SG*	77	7	16	-	88	8	8	5.7	83
SG window with SCF *B*	*SG_SCF B*	10	58	30	-	16	58	57	5.6	23
SG window with SCF *F*	*SG_SCF F*	33	27	36	-	65	12	14	5.6	50
Double glazed window (*DG*)	*DG*	61	11	17	11	79	14	14	2.8	72
DG window with SCF *B*	*DG_SCF B*	9	59	30	2	15	58	54	2.7	18
DG window with SCF *F*	*DG_SCF F*	28	28	37	4	58	15	19	2.7	34

Due to the large number of simulations required and amount of results involved in the parametric analysis, the *jEPlus* tool for EnergyPlus was used. This tool was developed to perform complex parametric analysis using EnergyPlus files (.idf) and manage several simulation runs while gathering the results in single output files (e.g .csv), simplifying the analysis for several building design parameters. In this study, the adopted methodology includes the following steps (Figure 97):

a. The development of two Energyplus models (.idf file): the first model (office area of the building of the second case study) was created considering a free float scenario (i) – without climatization and electric lights – to assess the thermal and visual comfort conditions without resorting to energy consumption, whereas the second was designed considering a generic HVAC template and electric lights (ii) to evaluate the energy needs to maintain the indoor thermal and visual comfort conditions, according to the Portuguese and international regulations;

b. the selection of three different climate regions (.epw files) on mainland Portugal located in the south, centre and north regions of Faro, Lisbon and Braganza;

c. the definition of different façade scenarios using the *jEPlus* tool (.jar file) for the parametric analysis, that include the variation of the solar orientation of the façade: North, East, South, and West; the window type: single and double glass units, without and with two SCFs; and the window-to-wall ratio (WWR) that varies between 20% and 100% in increments of 20%.

d. the definition of output variables in RVIs file format using the *jEPlus* tool, for both the Energyplus models:

d(i). indoor temperature, and daylighting in two reference points at different heights to calculate the useful daylight availability at the work desk height and the daylight glare index at the occupants' eyes height;

d(ii). energy consumption and carbon footprint related to the heating, cooling, and lighting energy needs.

According to the Köppen-Geiger climate classification, on the mainland Portugal the climate is divided into two regions with Mediterranean climate conditions [44]: one with short, mild winters, and being characterised by dry and hot summers (Csa), and another with rainy winters, dry and mild summers (Csb). According to the Köppen-Geiger climate classification, Lisbon and Faro are characterized by having a Csa climate, whereas Braganza has a Csb climate. The mean temperatures vary in each region, Lisbon shows monthly average temperatures between 11-22ºC, Faro between 13-24 ºC, and Braganza between 4-21ºC.

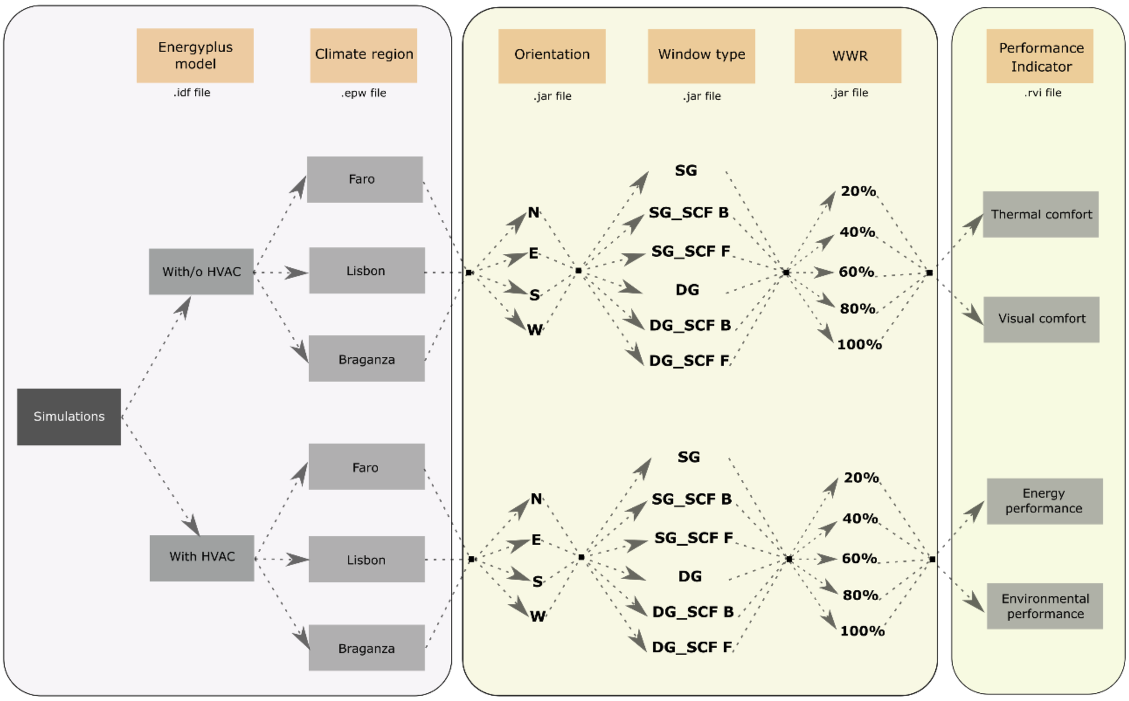

Figure 97. Methodology flowchart: parametric simulations, software, and respective files

To analyse the data obtained using the parametric analysis from a thermal, visual, energy, and environmental performance standpoints, a multi-criteria analysis proposed by Dıáz-Balteiro & Romero [122] was used and adapted to the context of the current study. This method considers an aggregated indicator, IS_i, allowing for a direct comparison of the global performance of $i= 1, 2, \ldots, n$ façade scenarios, which are evaluated according to $j= 1, 2, \ldots, m$ performance indicators, as shown in equation (7.1):

$$IS_i = \sum_{j=1}^{m} W_j . \bar{R}_{ij} \ , \forall i \tag{7.1}$$

where

IS_i: aggregated indicator for the *i* façade scenario;

n: total number of façade scenarios;

m: total number of performance indicators *j* for the façade scenario *I*;

W_j: weight or relative importance of the performance indicator *j*;

$\bar{R}_{ij}$: normalised value of the *j* indicator for the façade scenario *i*.

To compare the performance of the different façade scenarios, four aggregate indicators were estimated and the weights, W_j, were evenly distributed according to several categories. This method estimates a global indicator assembled through a weighting process allowing for a direct comparison between the performances of each strategy for different façades and solar orientations. Consequently, and according to this methodology, the best window solution is the weighted sum of the normalised *j* indicator for the façade scenario *i*, which yields a maximum result. The worst window solution is the weighted sum of the normalised *j* indicator for the façade scenario *i*, which yields a minimum result.

Figure 98 shows the aggregated indicators of performance and Table 37 the adopted weight distribution for the calculation of the aggregate indicators: thermal, visual, energy, and environmental aggregate indicators, and global aggregate indicator.

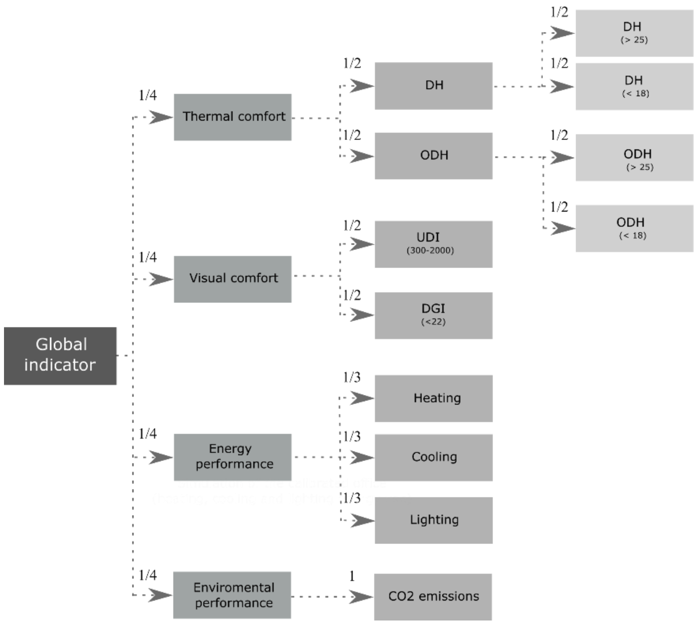

Figure 98. Aggregate indicators, *j*, and weight distribution: discomfort hours above 25ºC, $DH_{>25}$, and below 18ºC, $DH_{<18}$, overheating, $ODH_{<25}$, and overcooling, $ODH_{<18}$, degree hours, useful daylight illuminance, $UDI_{300\text{-}2000}$, daylight glare index, $DGI_{<22}$

Table 37. Attributed weights for each *j* aggregate indicator

j aggregate indicator	$DH_{>25}$	$DH_{<18}$	$ODH_{<25}$	$ODH_{<18}$	$UDI_{300\text{-}2000}$	$DGI_{<22}$	Consumption			CO_2
							H	C	L	
Thermal	1/4	1/4	1/4	1/4						
Visual					1/2	1/2				
Energy							1/3	1/3	1/3	
Environmental										1
Global	1/16	1/16	1/16	1/16	1/8	1/8	1/12	1/12	1/12	1/4

The value of the thermal aggregate indicator depends on the annual discomfort hours above 25ºC and below 18ºC as well as the overheating and overcooling degree hours. These are commonly used metrics to evaluate the thermal discomfort due to the low and high temperatures in indoor spaces. The quality and quantity of daylight was evaluated by the visual aggregate indicator considering values between 300lx and 2000lx as useful daylighting illuminance values and values below 22 as desirable daylight glare index values. As regards the energy aggregate indicator, the energy consumption with heating, cooling, and lighting per square metre was calculated considering the following values of COP=3.4 and EER=3.0 to turn the energy needs into energy consumption values and per area of the office room. To determine the environmental aggregate indicator, the annual CO_2 emissions factor was estimated considering the primary energy associated with the energy consumption (heating and cooling) during the working hours. The considered energy mix and CO_2 emission factors, EF, for the calculation of the annual CO_2 emissions are described in Table 38.

Table 38. Energy mix [%] and emission factors, *EF*, [gCO_2/kWh]

	Energy mix [%]	EF [g_{CO2}/kWh]
Nuclear	2.03	0.00
Renewable cogeneration	3.99	0.00
Other renewables	6.68	0.00
Hydro	7.04	0.00
Fossil cogeneration	8.13	327.00
Natural gas	8.59	386.00
Coal	13.99	970.00
Wind	47.59	0.00
Municipal solid waste	1.96	1.96

It should be noted that the estimated CO_2 emission values are proportional to the obtained energy consumption values for each i façade scenario as the acclimatization and lighting systems have the same energy source – electricity – for heating, cooling and lighting.

In this study, the global indicator comprises the analysis of the thermal and visual comfort, and the energy and environmental performances, for each façade scenario, through the calculation of the different adopted metrics, as shown in Figure 98; however, aggregate indicators take into account different variables and their absolute values are usually in different scales or units (e.g. the calculation of the DH is in hours whereas the energy consumption is in kW.h.m^{-2}). For these reasons, the first step required for the calculation of any aggregate indicator consists of normalising the m indicators to the same scale, for comparison purposes. Dıáz-Balteiro & Romero [122] proposes a normalisation procedure when the indicator is of the type “higher values are better”, as given by equation 7.2 and of the type “lower values are better”, as given by equation 7.3:

$$\bar{R}_{ij} = 1 - \frac{R_j^* - R_{ij}}{R_j^* - R_{*j}} \;, \forall i, j \tag{7.2}$$

$$\bar{R}_{ij} = 1 - \frac{R_{ij} - R_j^*}{R_{*j} - R_j^*} \;, \forall i, j \tag{7.3}$$

where

R_{ij}: simulation result of façade scenario i^{th} when is evaluated according to the j^{th} indicator;

R_j^*: optimum value of the j^{th} indicator of performance (ideal value);

R_{*j}: worst value achieved by the j^{th} indicator of performance (anti-ideal value).

7.2 Results and discussion

After the simulation of different scenarios using the *jEPlus* tool, as shown in Figure 97 and considering the weight distribution of the different indicators as mentioned in Table 37, the results of the global performance indicator was estimated for single and double glazed units without and with two different SCFs applied to façades orientated North, East, South, and West for Lisbon, Faro, and Braganza including five different Window-to-Wall Ratios (WWR) as described in Figure 99, Figure 100, and Figure 101. Second, the thermal and visual comfort and the energy performance aggregate indicators for a south orientated façade located in Lisbon, Faro, and Braganza for a value of WWR=60% was estimated for the same single and double-glazed units without and with SCFs. The final results are shown below.

From the analysis of Figure 99, Figure 100, and Figure 101, the global performance indicator, *IS*, shows that for North oriented façades, the glazing solutions without and with the spectrally selective film, SCF F, show similar *IS* values varying between 0.69 and 0.76, for Lisbon, Faro and Braganza. On the other hand, glazing solutions with the reflective film, SCF B, present lower *IS* values (0.58< *IS* <0.65), indicating that highly reflective films for existing glazing of office rooms with a North solar orientation have worst performances from a thermal and visual comfort and energy and environmental point of views than the glazing without films or with the spectrally selective film. The same conclusions can be drawn for façades oriented to East or West with WWR=20% and WWW=40% and to South with WWR=20% for the three studied cities of Lisbon, Faro, and Braganza. These results indicate that for lower values of incident solar radiation (as it is the case of façades oriented to the North or with lower areas of glass in the façade), glazing rehabilitation through the application of window films is only advantageous if the applied film is in the spectrum of spectrally selective films to ensure high levels of daylight and reduce the energy needs with lighting while reducing the solar heat gains and the cooling energy needs.

In façades with high glazed areas (WWR≥60%) oriented to the East, South, and West, glazing without films or with the spectrally selective film show lower *IS* values than the glazing with the reflective film. According to the results obtained for the 3 cities, the single – and double – glazed windows show the worst global performance, due to the high daylighting values above 2000lx and the discomfort hours above 25ºC, which consequently increase the cooling energy needs and the CO_2 emissions. For the two window solutions without any applied film, the higher the WWR is, the lower values of *IS* were found. The single – and double – glazed windows with the reflective film showed the highest results of the global indicator. The high performance of the glazing with this film is related with the lower values of solar and visible gains due to the reduction of the solar (front) reflectance coefficient, which reduced the discomfort hours above 25ºC, increasing the thermal comfort without resorting to the acclimatisation system, and the cooling energy needs.

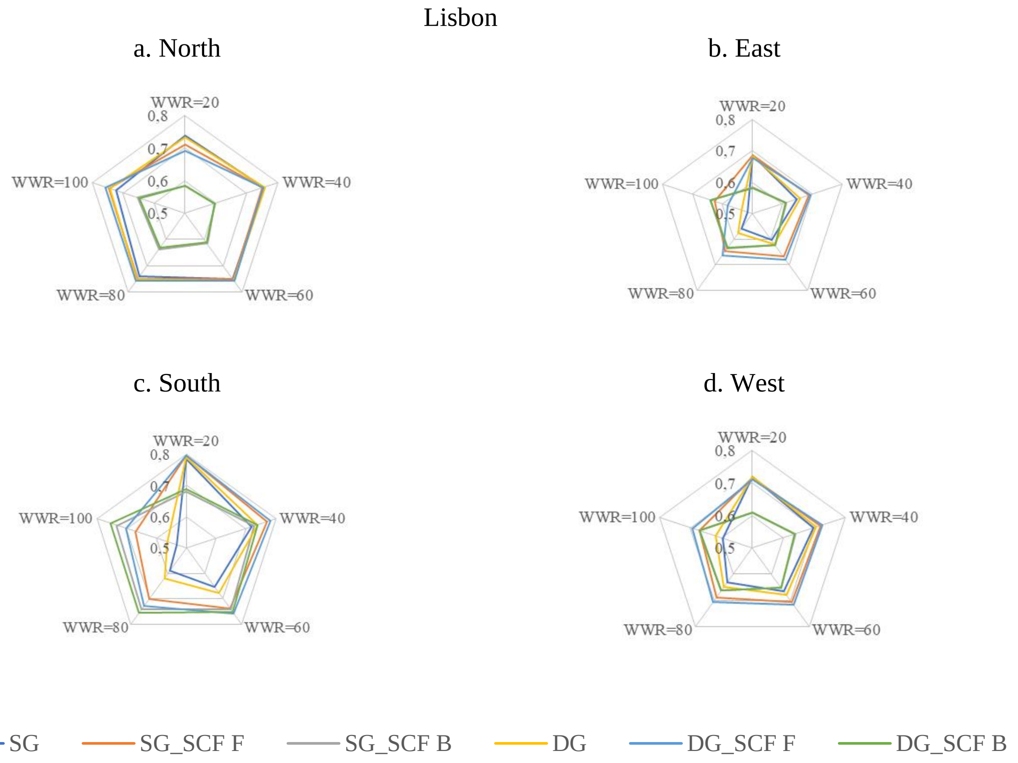

Figure 99. Global performance indicator for single and double glazed units without and with SCFs in a façade orientated to: a. North, b. East, c. South and, d. West in Lisbon's city for different Window-to-Wall Ratios (WWR)

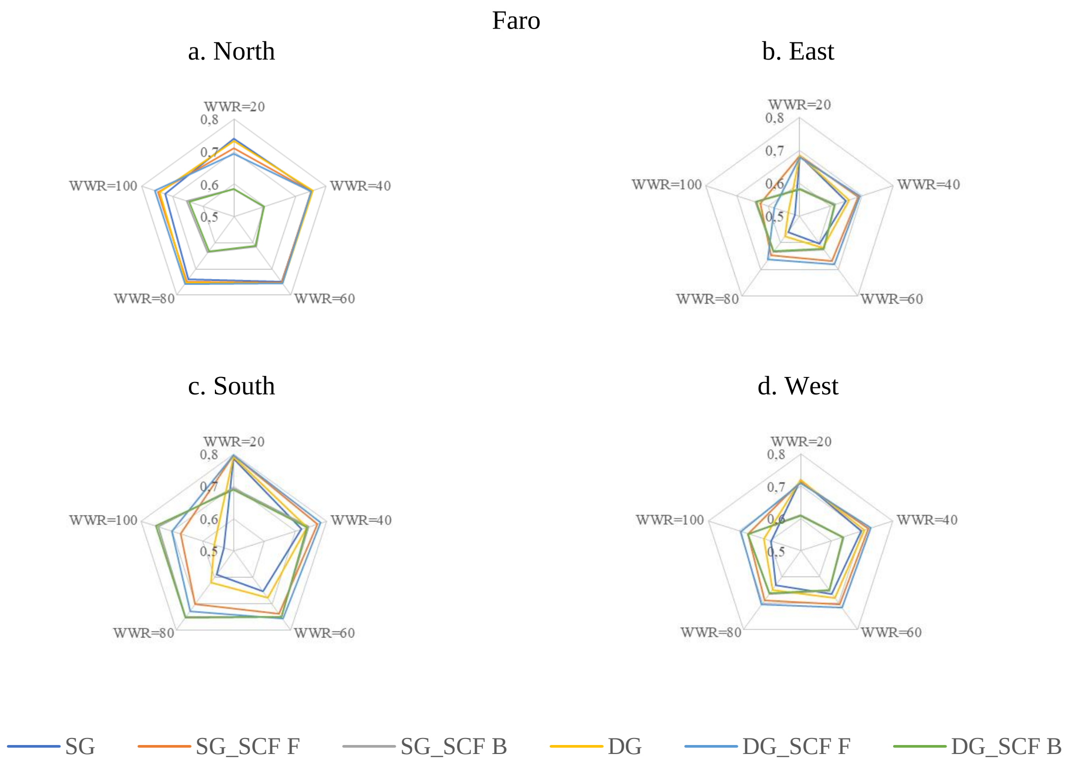

Figure 100. Global performance indicator for single and double glazed units without and with SCFs in a façade orientated to: a. North, b. East, c. South and, d. West in Faro's city for different Window-to-Wall Ratio (WWR)

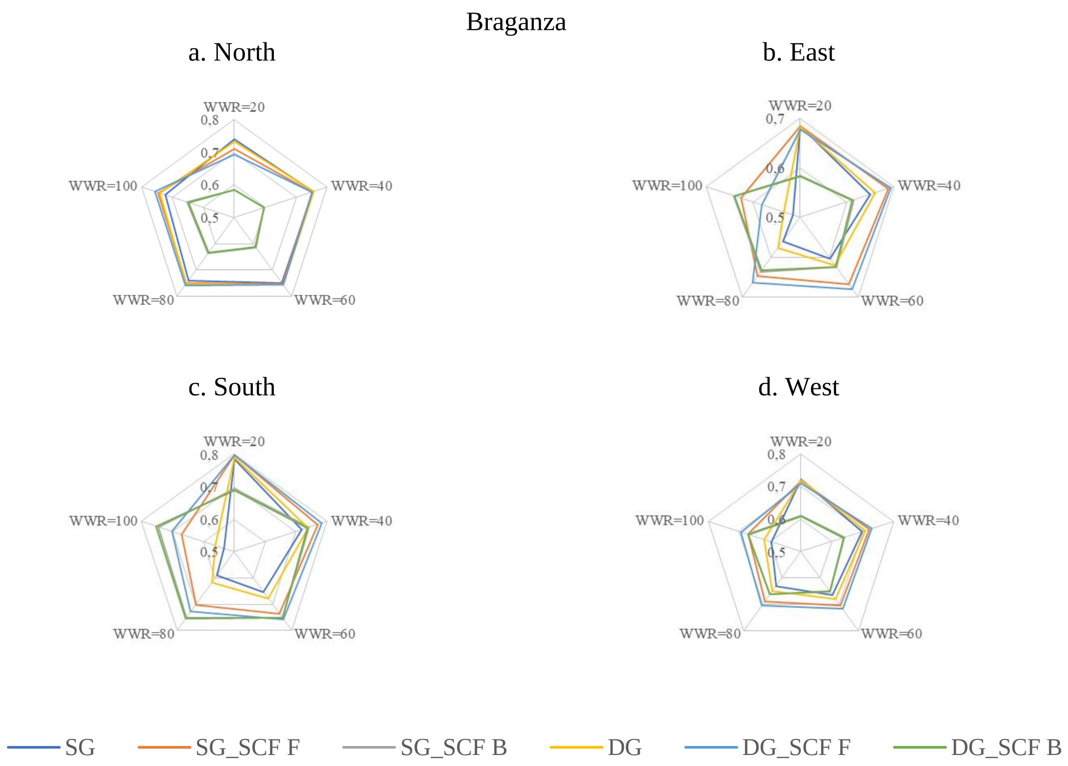

Figure 101. Global performance indicator for single and double glazed units without and with SCFs in a façade orientated to: a. North, b. East, c. South and, d. West in Braganza's city for different Window-to-Wall Ratio (WWR)

To perform a more thorough analysis of the thermal and visual comfort and the energy performance of the glazing systems without and with SCFs, the individual aggregated indicators for a South orientated façade with a WWR of 60% located in Lisbon, Faro, and Braganza was investigated. The results are shown in Figure 102. According to the obtained results, it is possible to conclude that South oriented façades of office rooms with large areas of glazing in the façade (WWR=60%) show higher thermal, visual, and energy related indicators for glazing with highly reflective films.

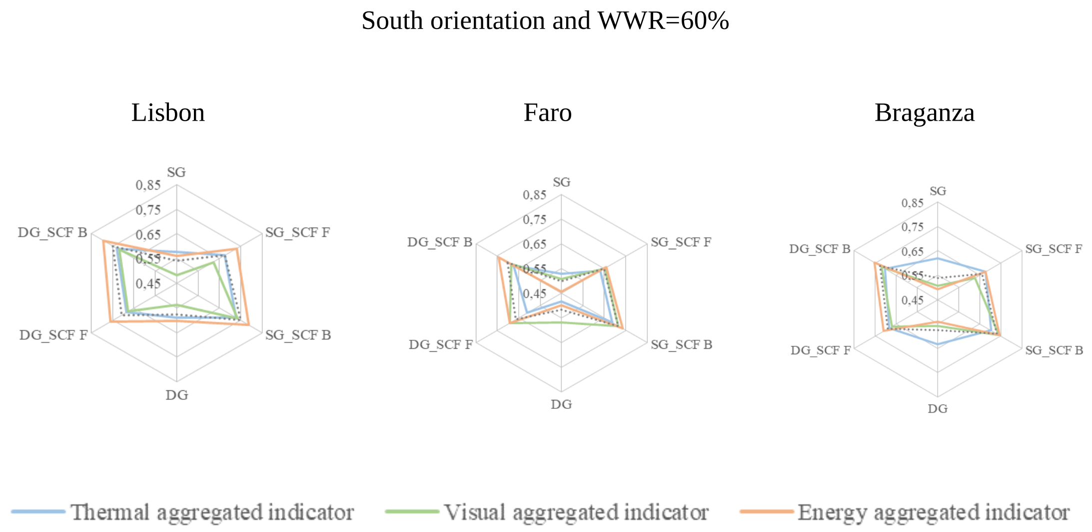

Figure 102. Thermal, visual, and energy aggregated indicators for a South oriented façade with a WWR of 60% for single and double glazed units without and with SCFs

8. Conclusions and perspectives for future research

8.1 General remarks

In the buildings' rehabilitation context, decision-makers often face challenges in selecting materials or construction solutions as, on the one hand, rehabilitation decisions must consider thermal and visual comfort requirements, energy efficiency and environmental sustainability, and on the other hand, consider users' preferences, economic availability and even personal preferences. Moreover, the relationship between comfort conditions and energy and environmental sustainability in selecting the best retrofitting scenario is not straightforward, since solutions that increase the thermal conditions may decrease visual comfort or daylighting availability, and result in an increase of energy needs. Also, incorporating or replacing materials in buildings may increase energy efficiency but also increase the embodied energy in a building's life cycle.

To address the first question of the thesis, "is there reliable information for decision-makers and building professionals regarding the retrofit potential of SCFs regarding the differences in type and application, and advantages and disadvantages", an extensive literature review was conducted (chapter 2). Even though SCFs are not a new material in what concerns their use in windows systems of buildings, the existing studies and available information are somewhat scarce and scattered (Table 2), making it challenging to identify the best film to apply in order to tackle thermal and/or visual comfort issues and increase the overall energy efficiency.

A comprehensive investigation allowed to enumerate the typical composition, main types and main thermal and optical properties of SCFs. Clear and consistent information regarding the performance of SCFs, specifically the variation in the thermal and optical properties, was calculated for commonly used types of glass in Portugal. This calculation allowed to answer the second question, "how do SCFs influence glass's thermal and optical properties in a window system". After reviewing the extensive libraries of both *Optics* and *Windows* tools, it was possible to identify 156 films from leading manufacturers and estimate the full range of the main thermal and optical properties for eight types of glass with the films.

To address the third question of the thesis, "how do Solar Control Films (SCF) influence the thermal and visual conditions and the energy performance of existing office buildings", a combined experimental and modelling analysis that focused on two buildings located in Lisbon, capital of Portugal, one with single (chapter 4) and the other with double-glazed (chapter 5) windows was performed. The proposed methodology involved the following steps:

- experimental field analyses of office areas with similar characteristics – geometry, materials, solar exposition and orientation, and internal gains –, wherein one office area was monitored without any film applied and taken as a reference scenario, and in the other office area(s) SCFs were applied to the glazing system. This experimental analysis helped identifying the film and respective thermal and optical properties that could better improve the indoor comfort conditions and decrease the energy demand. Also, the experimental data allowed to compare the differences in terms of thermal and visual comfort of similar offices without and with SCFs under real usage conditions;
- use the experimental data to calibrate simulation models in EnergyPlus by comparing the experimental measured values of different variables with the predicted data of the simulation model. The generic climate file of Lisbon's city was used and variables, such as, outdoor temperature, and global and diffuse radiation were replaced with the measured outdoor corresponding variables when executing the verification procedure;
- estimate the comfort indexes based on an annual performance using the calibrated models of the office areas of the two buildings of case study – one with single and the other with double glazing –, and extend the analysis for different SCFs and solar orientations.

In order to understand the "environmental and economic impacts of SCFs in the life cycle of a building", an examination using a LCA process, comprising the products and processes included in the life cycle of three different scenarios of the glazing system – original window, retrofitting with SCFs, and retrofitting through full replacement with a new window – was performed (chapter 6). The second building, corresponding to the second case study of this thesis, was considered for this investigation and the calibrated models of the office's rooms were taken into consideration when defining building parameters in the simulation model of the building. An energy, economic and environmental study was achieved that allowed to compare spectrally selective and reflective films and compare films as a refurbishment solution with the replacement of the glazing areas by a full new window.

A final study that allowed to determine a global performance indicator and that estimates, for single and double glazed units, without and with two different SCFs applied on façades with different orientations for three different climates in Portugal and five different Window-to-Wall Ratios of façades was also performed using the *jEPlus* tool (chapter 7). This chapter concludes the thesis and provides valuable information for decision-makers and professionals in the building industry regarding the application of window films in existing Portuguese buildings.

8.2 Final conclusions

This thesis enhances the knowledge of the thermal, daylight, and energy performance of solar control films (SCFs) as a retrofitting solution for glazing areas of existing buildings to improve their energy efficiency and contribute to decarbonizing the building sector. In this context, this research is a contribution in the retrofit decision-making process in what concerns the application of SCFs in existing glazing. In chapter 2, it was concluded that:

- despite the existing documentation and the several studies on window films' properties and performance, the information is still limited and scattered;
- SCFs are composed of several membranes of intercalated materials, and one film can reach up to eight different layers and undergo seven different manufacturing procedures. A standard structure of a SCF comprises the following layers: scratch-resistant coating, polyester layers, lamination adhesive(s), metals, high-performance UV resin, and protective release liners;
- extensive research identified the main types of window films: solar control (the focus of the current study), low emissivity, protection against ultraviolet (UV) radiation, privacy, decorative, protection, safety, and radio and electromagnetic frequencies' protection, and anti-grafitti.
- the optical and thermal properties by type of film (reflective, dual reflective, neutral, low emissivity, spectrally selective, ceramic, and protection and safety) applied to different types of glass (clear and tinted single glass, clear, and tinted, reflective, low emissivity for low, medium and high solar gains) were estimated. The range value (minimum and maximum) of each optical and thermal property was estimated, which allows understanding the full potential of window films in varying the properties of different glazing systems.

The experimental and computational work performed in office areas with single and double glazed systems without and with SCFs in chapters 4 and 5 allowed to conclude:

- the application of SCF in single glass reduced the average indoor temperature during working hours (from 9h00 to 18h00) both in the winter and summer days, with the maximum reduction in the summer days being approximately the double of the winter days;
- all SCFs increased the heating and lighting energy use but reduced the cooling energy use of the typical office for East, South and West solar orientations;
- SCFs with low solar transmittance and high solar (front) reflectance induced higher reductions of the cooling energy use and higher increases of the heating and lighting energy use;
- SCFs with high solar (front) reflectance and low solar and visible transmittance led to the best energy performance for the criterion accounting for the cooling, heating, and lighting energy use for all solar orientations (N, E, S and W);
- retrofitting solutions with higher light-to-solar gain ratios (τ_{vis}/g) exhibit higher operational energy savings by decreasing the solar gains in a higher proportion than the decrease of the visible transmittance. Therefore, the reduction in cooling energy needs is much higher than the increase in lighting and heating energy needs;
- higher insulation of windows (U below 1.1W/m^2.K) lead to higher energy needs since it lowers the heat losses during the night periods, trapping heat inside during the night, and requires more cooling load during the morning periods;
- incorrect applications of SCF result in unsatisfactory performances that unfairly contribute to product discredit.

The LCA analyses performed in chapter 6 indicated that the embodied energy is not significant compared to the operational energy since it only represents 3% to 5% of the total life cycle energy of the building.

In chapter 7, several simulation analyses were performed for a typical office room considering the variation of the following parameters: single and double glazing, two SCFs, different façade orientations, three different cities in mainland Portugal, and different WWR. For each simulation, the thermal and visual comfort and the energy performance aggregate indicators were calculated. The results indicate that for lower values of incident solar radiation (as it is the case of North oriented façades or with lower WWR), glazing rehabilitation through the application of window films is only advantageous if the applied film is in the spectrum of spectrally selective films to ensure high levels of daylight availability and reduce the energy needs with lighting while reducing the solar heat gains and the cooling energy needs. In façades with large glazed areas (WWR≥60%) oriented to the East, South, and West, glazing with reflective films exhibit higher aggregated performance values than glazing without films or with spectrally selective films.

8.3 Future work

Future development of the research work initiated with this thesis can be composed of many research streams. The ones considered by the author to be the most promising, and that can be initiated immediately, are:

- develop a numerical model to assess the optical properties of window films independently, without considering the substrate where the film is applied;
- perform experimental measurements on a building scale and develop calibrate building energy simulation models using sensitivity analysis to identify the optical parameters that most influence SCFs performance, for different temperature and global radiation ranges;
- regarding the calibration of the simulation models, the work developed in this thesis can be further improved by calibrating other variables that also contribute to approximate experimental and simulated values, such as energy consumption and air infiltration rates. Other types of sensors, to monitor occupancy of office areas and sensor that indicate when shading devices were activated or when the windows were opened and closed, can contribute to an added value when analysing experimental data and better estimate energy consumption profiles;
- perform an experimental and computed study on thermochromic and electrochromic films;
- develop a national energy label for SCF that support the decision making of glazing retrofitting considering the thermal, daylight and energy performance of each film.

Bibliography

[1] “Climate change 2021 Synthesis Report (AR6): The physical science basis summary for policymakers. Intergovernmental Panel on Climate Change (IPCC).”

[2] “Global climate change, vital signs of the planet. NASA. Available on <https://climate.nasa.gov/> [consulted in August 2020].” .

[3] “Paris Agreement, United Nations. Availabe on <https://unfccc.int/sites/default/files/english_paris_agreement.pdf> [consulted in August 2020],” 2015.

[4] “Climate Change 2014 Synthesis Report (AR 5): Summary Chapter for Policymakers, International Protocol on Climate Change. Intergovernmental Panel on Climate Change (IPCC),” 2014, doi: 10.1017/CBO9781107415324.

[5] J. P. Kevin A. Baumert, Timothy Herzog, *Navigating the Numbers Greenhouse Gas Data and International Climate Policy. [consulted in August 2021].* .

[6] “Climate watch data. Available on <https://www.climatewatchdata.org/> [consulted in August 2021].” .

[7] “Energy Technology Perspectives, International Energy Agency (EIA), 2020, Paris,” 2020. doi: 10.1787/ab43a9a5-en.

[8] “Directive 2010/31/EU of the European Parliment and of the Council of 19 May 2010 on the energy performance of buildings,” *Off. J. Eur. Union*, no. 19 May 2010, pp. 13–35, 2010.

[9] “Directive 2018/844/EU of the European Parliament and of the Council of 30 May 2018 amending Directive 2010/31/EU on the energy performance of buildings and Directive 2012/27/EU on energy efficiency,” 2018.

[10] “Material efficiency in clean energy transitions, 2019, International Energy Agency,” 2019. [Online]. Available: https://www.iea.org/reports/global-status-report-for-buildings-and-construction-2019.

[11] Buildings Performance Institute Europe (BPIE), “Europe ’ s buildings under the microscope - A country-by-country review of the energy performance of buildings Buildings Performance Institute Europe,” 2011. doi: ISBN: 9789491143014.

[12] P. Europeu, “Estratégia de longo prazo para a renovação dos edifícios (ELPRE),” 2020. [Online]. Available: https://participa.pt/contents/consultationdocument/ELPREconsultapublica.pdf.

[13] “Plano Nacional de Energia e Clima 2021-2030.”

[14] *Estatísticas da construção e habitação, Instituto Nacional de Estatística*. 2019.

[15] L. G. Bakker and H. Visser, “Impact of Solar Control Glazing on energy and CO2 savings in Europe,” 2007.

[16] *Censos 2011. XV recenseamento geral da populaçao, V recenseamento geral da habitaçao. Instituto Nacional de Estatistica, 2011*. .

[17] “PLANO NACIONAL ENERGIA E CLIMA 2021-2030 (PNEC 2030),” 2019.

[18] Republica Portuguesa, “Road map for cabon neutrality 2050 (RNC2050) - Long-term strategy for carbon neutrality of the Potuguese economy by 2050,” *DESCARBONIZAR 2050*, vol. 2050, 2018, [Online]. Available: https://www.portugal.gov.pt/download-ficheiros/ficheiro.aspx?v=aa27c4c9-dac3-47c3-96ae-4ca86183635d.

[19] M. Ferreira and M. Almeida, “Benefits from energy related building renovation beyond costs, energy and emissions,” *Energy Procedia*, vol. 78, pp. 2397–2402, 2015, doi: 10.1016/j.egypro.2015.11.199.

[20] “EN 15752-1 Glass in building - Adhesive backed polymeric film - Part 1: Definitions and requirements,” *Eur. Comm. Stand.*, pp. 1–36, 2014.

[21] CEN, “EN 410:2011 Glass in building - Determination of luminous and solar characteristics of glazing.” 2011.

[22] “Window Glazing Types | Efficient Windows Collaborative.” .

[23] C. R. Faustino, “Influência dos Vãos Envidraçados no Desempenho Energético de Edifícios,” Dissertação para a obtenção do Grau de Mestre em Engenharia Civil, DECivil, Instituto Superior Técnico, Universidade de Lisboa, 2012.

[24] “Optics | Windows and Daylighting.” .

[25] J. Pereira, M. Glória Gomes, A. Moret Rodrigues, and M. Almeida, “Thermal, luminous and energy performance of solar control films in single-glazed windows: Use of energy performance criteria to support decision making,” *Energy Build.*, vol. 198, 2019, doi: 10.1016/j.enbuild.2019.06.003.

[26] J. Pereira, H. Teixeira, M. Glória Gomes, and A. Moret Rodrigues, “Assessment of an early degradation of glazing systems with damaged solar control films.”

[27] “European Window Film Association. Available on <https://iwfa.com/ewfa> [consulted in January 2021].” .

[28] J. Pereira, M. G. Gomes, A. M. Rodrigues, H. Teixeira, and M. Almeida, “Small-scale field study of window films ’ impact on daylight availability under clear sky conditions,” *J. Façade Des. Eng.*, 2020.

[29] “Window & Daylighting. International Glazing Data Base. Available on <https://windows.lbl.gov/software/igdb> [consulted in September 2020].” .

[30] NFRC, “National Fenestration Rating Council.” .

[31] National Fenestration Rating Council Incorporated, *NFRC 303-2017 User’s Guide for Submitting a Laminate Interlayer to be Approved and Used in OPTICS*. 2017.

[32] “EN 12898:2019 Glass in building - Determination of the emissivity.” 2019.

[33] “BS EN 410:1998 Glass in building - Determination of luminous and solar characteristics of glazing.” pp. 1–24, 1998.

[34] CEN, “EN 15755-1:2014 Glass in building - Adhesive backed polymeric glass - Part 1: Definitions and requirements.” pp. 1–29, 2014.

[35] Parlamento Europeu e o Conselho da União Europeia, “DIRETIVA 2012/27/UE DO PARLAMENTO EUROPEU E DO CONSELHO de 25 de outubro de 2012 relativa à eficiência energética, que altera as Diretivas 2009/125/CE e 2010/30/UE e revoga as Diretivas 2004/8/CE e 2006/32/CE,” *J. Of. da União Eur.*, pp. 1–56, 2012.

[36] European Comission, “Energy performance of buildings | Energy.” .

[37] R. Yin, P. Xu, and P. Shen, “Case study: Energy savings from solar window film in two commercial buildings in Shanghai,” *Energy Build.*, vol. 45, pp. 132–140, 2012, doi: 10.1016/j.enbuild.2011.10.062.

[38] J. Xamán, C. Pérez-Nucamendi, J. Arce, J. Hinojosa, G. Álvarez, and I. Zavala-Guillén, “Thermal analysis for a double pane window with a solar control film for using in cold and warm climates,” *Energy Build.*, vol. 76, pp. 429–439, 2014, doi: 10.1016/j.enbuild.2014.03.015.

[39] J. Xamán, Y. Olazo-Gómez, I. Zavala-Guillén, I. Hernández-Pérez, J. O. Aguilar, and J. F. Hinojosa, “Thermal evaluation of a Room coupled with a Double Glazing Window with/without a solar control film for Mexico,” *Appl. Therm. Eng.*, vol. 110, pp. 805–820, 2017, doi: 10.1016/j.applthermaleng.2016.08.156.

[40] S. Chaiyapinunt, B. Phueakphongsuriya, K. Mongkornsaksit, and N. Khomporn, “Performance rating of glass windows and glass windows with films in aspect of thermal comfort and heat

transmission," *Energy Build.*, 2005, doi: 10.1016/j.enbuild.2004.10.008.

[41] T. Nagahama, T. Sato, T. Harima, and J. Shimizu, "Optical properties and field test results of spectrally-selective solar control window film that enables not increasing downward reflection," *Energy Build.*, 2017, doi: 10.1016/j.enbuild.2017.01.037.

[42] E. Moretti and E. Belloni, "Evaluation of energy, thermal, and daylighting performance of solar control films for a case study in moderate climate," *Build. Environ.*, vol. 94, pp. 183–195, 2015, doi: 10.1016/j.buildenv.2015.07.031.

[43] C. Li, J. Tan, T. T. Chow, and Z. Qiu, "Experimental and theoretical study on the effect of window films on building energy consumption," *Energy Build.*, vol. 102, pp. 129–138, 2015, doi: 10.1016/j.enbuild.2015.04.025.

[44] F. R. M. Kottek, J. Grieser, C. Beck, B. Rudolf, "World map of the Köppen-Geiger climate classification updated," *Meteorol. Zeitschrift*, vol. 15, no. 3, pp. 259–263, 2006, doi: 10.1127/0941-2948/2006/0130.

[45] S. Debusk, "Creating an Energy-Efficient Building Envelope Using Solar-Control Window Films," pp. 1–14, [Online]. Available: http://w3.llumar.com/pdf/en/EnergyEncyclopediaDOE2StudyandSolar-ControlWindowFilms.pdf.

[46] D. H. W. Li, T. N. T. Lam, S. L. Wong, and E. K. W. Tsang, "Lighting and cooling energy consumption in an open-plan office using solar film coating," *Energy*, vol. 33, no. 8, pp. 1288–1297, Aug. 2008, doi: 10.1016/J.ENERGY.2008.03.002.

[47] Y. Chen, G. Hou, H. Xie, and W. Chan, "In-site experimental measurement of energy-saving performance for solar-control film on single window glass," *IAQVEC 2007 Proc. - 6th Int. Conf. Indoor Air Qual. Vent. Energy Conserv. Build. Sustain. Built Environ.*, vol. 1, pp. 47–53, 2007.

[48] W. W. Chan *et al.*, "Energy saving and tourism sustainability: Solar control window film in hotel rooms," *J. Sustain. Tour.*, vol. 16, no. 5, pp. 563–574, 2008, doi: 10.2167/jost803.0.

[49] F. Noh-Pat, J. Xamán, G. Álvarez, Y. Chávez, and J. Arce, "Thermal analysis for a double glazing unit with and without a solar control film (SnS-CuxS) for using in hot climates," *Energy Build.*, vol. 43, no. 2–3, pp. 704–712, 2011, doi: 10.1016/j.enbuild.2010.11.015.

[50] J. Currie, J. B. Williamson, J. Stinson, and M. Jonnard, "Historic Scotland Technical Paper 23 - Thermal assessment of internal shutters and window film applied to traditional single glazed sash and case windows," *Hist. Scotland's Tech. Pap.*, 2014.

[51] E. Moretti, E. Belloni, and E. Lascaro, "The Influence of Solar Control Films on Energy and Daylighting Performance by Means of Experimental Data and Preliminary Unsteady Simulations," *Energy Procedia*, vol. 78, pp. 340–345, Nov. 2015, doi: 10.1016/J.EGYPRO.2015.11.660.

[52] A. Bahadori-Jahromi, A. Rotimi, A. Mylona, P. Godfrey, and D. Cook, "Impact of window films on the overall energy consumption of existing UK hotel buildings," *Sustain.*, vol. 9, no. 5, pp. 1–23, 2017, doi: 10.3390/su9050731.

[53] S. Amirkhani, A. Bahadori-Jahromi, A. Mylona, P. Godfrey, and D. Cook, "Impact of Low-E window films on energy consumption and CO2 emissions of an existing UK hotel building," *Sustain.*, vol. 11, no. 16, 2019, doi: 10.3390/su11164265.

[54] K. M. Yousif, "Solar gain in buildings in hot climatic zones: case study of a selected Iraqi building using window solar control film," *ISESCO J. Sci. Technol.*, vol. 11, no. 19, pp. 43–50, 2015.

[55] J. Pereira, M. Glória Gomes, A. Moret Rodrigues, and M. Almeida, "Thermal, luminous and energy performance of solar control films in single-glazed windows: Use of energy performance criteria to support decision making," *Energy Build.*, vol. 198, pp. 431–443, Sep. 2019, doi: 10.1016/J.ENBUILD.2019.06.003.

[56] C. M. Calama-González, Á. L. León-Rodríguez, and R. Suárez, "Daylighting performance of solar control films for hospital buildings in a Mediterranean climate," *Energies*, vol. 12, no. 3, 2019, doi: 10.3390/en12030489.

[57] H. Teixeira, M. Glória Gomes, A. Moret, and J. Pereira, "Thermal and visual comfort, energy use and environmental performance of glazing systems with solar control films," *Build. Environ.*, vol. 168, p. 106474, Oct. 2020, doi: 10.1016/J.BUILDENV.2019.106474.

[58] J. Pereira, C. C. Rivero, M. G. Gomes, A. M. Rodrigues, and M. Marrero, "Energy, environmental and economic analysis of windows' retrofit with solar control films: A case study in Mediterranean climate," *Energy*, vol. 233, p. 121083, Oct. 2021, doi: 10.1016/J.ENERGY.2021.121083.

[59] J. Potočnik and M. Košir, "Influence of commercial glazing and wall colours on the resulting non-visual daylight conditions of an office," *Build. Environ.*, vol. 171, p. 106627, 2019, doi: 10.1016/j.buildenv.2019.106627.

[60] C. Aghemo, A. Pellegrino, and V. R. M. Lo Verso, "The approach to daylighting by scale models and sun and sky simulators: A case study for different shading systems," *Build. Environ.*, vol. 43, no. 5, pp. 917–927, 2008, doi: 10.1016/j.buildenv.2007.01.020.

[61] M. B. Cruz, G. Pereira, Júlia, Maria da Glória, and M. S. M. Kong, “Comparative analysis of the luminous performance of fenestration with Japanese paper and glazing with a polymeric film in meditation rooms,” *Intell. Creat. Fantasy*, no. September, pp. 555–562, 2020, doi: 10.1201/9780429297755-92.

[62] N. E. Klepeis *et al.*, “The National Human Activity Pattern Survey (NHAPS): A resource for assessing exposure to environmental pollutants,” *J. Expo. Anal. Environ. Epidemiol.*, vol. 11, no. 3, pp. 231–252, 2001, doi: 10.1038/sj.jea.7500165.

[63] M. Ayoub, “A review on light transport algorithms and simulation tools to model daylighting inside buildings,” *Sol. Energy*, vol. 198, no. February, pp. 623–642, 2020, doi: 10.1016/j.solener.2020.02.018.

[64] C. Reinhart and A. Fitz, “Findings from a survey on the current use of daylight simulations in building design,” *Energy Build.*, vol. 38, no. 7, pp. 824–835, 2006, doi: 10.1016/j.enbuild.2006.03.012.

[65] O. Boccia and P. Zazzini, “Daylight in buildings equipped with traditional or innovative sources: A critical analysis on the use of the scale model approach,” *Energy Build.*, vol. 86, pp. 376–393, 2015, doi: 10.1016/j.enbuild.2014.10.003.

[66] D. Kesten, S. Fiedler, F. Thumm, A. Löffler, and U. Eicker, “Evaluation of daylight performance in scale models and a full-scale mock-up office,” *Int. J. Low-Carbon Technol.*, vol. 5, no. 3, pp. 158–165, 2010, doi: 10.1093/ijlct/ctq023.

[67] K.-S. Kim, L. Boyer, and L. Degelman, “Daylighting analysis through scale model, fullscale measurements and computer analysis for Texas A&M University campus building,” *Second Annu. Symp. Improv. Build. Energy Effic. Hot Humid Clim.*, no. February, pp. 16–21, 1985.

[68] J. A. Love and M. Navvab, “Daylighting estimation under real skies: A comparison of full-scale photometry, model photometry, and computer simulation,” *Illum. Eng.*, vol. 20, no. 1, pp. 140–156, 1991, doi: 10.1080/00994480.1991.10748933.

[69] S. W. A. Cannon-Brookes, “Simple scale models for daylighting design: Analysis of sources of error in illuminance prediction,” *Light. Res. Technol.*, vol. 29, no. 3, pp. 135–147, 1997.

[70] T. Silva, R. Vicente, F. Rodrigues, A. Samagaio, and C. Cardoso, “Development of a window shutter with phase change materials: Full scale outdoor experimental approach,” *Energy Build.*, vol. 88, pp. 110–121, 2015, doi: 10.1016/j.enbuild.2014.11.053.

[71] M. G. Gomes, A. M. Rodrigues, and J. A. Bogas, “Numerical and experimental study of the optical properties of venetian blinds,” *J. Build. Phys.*, vol. 36, no. 1, pp. 7–34, 2012, doi: 10.1177/1744259112444022.

[72] “CIE S003 Spatial distribution of daylight - CIE standard overcast sky and clear sky, Commission International de l’Eclairage.” 2004.

[73] C. Curcija, S. Vidanovic, R. Hart, J. Jonsson, and R. Mitchell, “WINDOW Technical Documentation,” *Wind. Envel. Mater. Group, Lawrence Berkeley Natl. Lab.*, 2018.

[74] CEN, “EN 12464-1 Light & Lighting – Lighting of Indoor Workplaces - Part 1 : Indoor work,” *European Committee for Standardization*. pp. 1–43.

[75] A. Nabil and J. Mardaljevic, “Useful daylight illuminance: A new paradigm for assessing daylight in buildings,” *Light. Res. Technol.*, vol. 37, no. 1, pp. 41–59, 2005, doi: 10.1191/1365782805li146ed.

[76] A. J. C. dos Santos, “Desenvolvimento de um método para a caracterização dinâmica da iluminação natural nos edifícios aplicável a climas mediterrânicos. Tese especialmente elaborada no Laboratório Nacional de Engenharia Civil para obtenção do Grau de Doutor em Engenharia Civil.” 2011.

[77] A. Roos, P. Polato, P. A. van Nijnatten, M. G. Hutchins, F. Olive, and C. Anderson, “Angular-dependent optical properties of low-e and solar control windows—: Simulations versus measurements,” *Sol. Energy*, vol. 69, pp. 15–26, Jul. 2001, doi: 10.1016/S0038-092X(01)00019-6.

[78] U.S. Department of Energy, “EnergyPlus™ Version 9.0.1 Documentation,” *U.S. Dep. Energy*, vol. Input Outp, p. 2691, 2018.

[79] ASHRAE, “ASHRAE Guideline 14-2002: Measurement of Energy Demand and Savings,” *Am. Soc. Heating, Refrig. Air-Conditioning Eng. Atlanta, GA, USA*, 2002, doi: 10.1111/jsr.67_12618.

[80] IPMVP New Construction Subcommittee, “International Performance Measurement & Verification Protocol: Concepts and Options for Determining Energy Savings in New Construction - Volume III,” *Washington, DC, USA*, vol. III, no. April, pp. 1–249, 2003.

[81] FEMP, “M&V Guidelines: Measurement and Verification for Performance-Based Contracts Version 4.0,” no. November, pp. 1–306, 2015, doi: 10.1016/j.radmeas.2006.01.002.

[82] 1.ª série — N.º 159 — 20 de agosto de 2013 Diário da República, “Decreto-Lei n.º 118/2013,” *Diário da República*, pp. 4988–5005, 2013.

[83] J. Karlsson and A. Roos, “Modelling the angular behaviour of the total solar energy transmittance of windows,” *Sol. Energy*, vol. 69, no. 4, pp. 321–329, Jan. 2000, doi: 10.1016/S0038-092X(00)00083-9.

[84] “ASHRAE Fenestrations, chapter 30 in ASHRAE Fundamentals 2000,” *A*, pp. 631–638, 2010, doi: 10.1111/j.1752-1688.1982.tb00078.x.

[85] M. G. Gomes, A. J. Santos, and A. M. Rodrigues, “Solar and visible optical properties of glazing systems with venetian blinds: Numerical, experimental and blind control study,” *Build. Environ.*, vol. 71, pp. 47–59, Jan. 2014, doi: 10.1016/J.BUILDENV.2013.09.003.

[86] ANSI/ASHRAE/IES, “Standard 90.1-2013 Determination of Energy Savings : Quantitative Analysis,” no. August, 2014.

[87] Navigant Consulting, “2010 U .S. Lighting Market Characterization,” no. January, p. 100, 2012, [Online]. Available: http://dl.dropbox.com/u/16546920/2010-lmc-final-jan-2012.pdf.

[88] I. Korolija, L. Marjanovic-Halburd, Y. Zhang, and V. I. Hanby, “UK office buildings archetypal model as methodological approach in development of regression models for predicting building energy consumption from heating and cooling demands,” *Energy Build.*, vol. 60, pp. 152–162, May 2013, doi: 10.1016/J.ENBUILD.2012.12.032.

[89] ECG019, “Energy Consumption Guide 019: Energy Use in Offices,” *Carbon Trust*, pp. 1–24, 2003, [Online]. Available: http://www.cibse.org/getmedia/7fb5616f-1ed7-4854-bf72-2dae1d8bde62/ECG19-Energy-Use-in-Offices-(formerly-ECON19.

[90] ANSI/ASHRAE, “Standard 90. 1-2007 Energy Standard for Buildings Except Low- Rise Residential Buildings,” Atlanta, GA, 2007.

[91] U. S. D. of E. Pacific Northwest National Laboratory, “Spectrally Selective Glazings,” no. DOE/EE-0173, pp. 1–47, 1998.

[92] “ISO 15469/CIE S003 (1996), Spatial distribution of daylight - CIE standard overcast sky and clear sky.” .

[93] D. Piccoli, B., D’Orso, M., Polselli, G., Leka, I., Pisaniello, “Luminance In the Occupational Visual Field : An Evaluation of Office Workstations Luminance In the Occupational Visual Field : An Evaluation of Office Workstations,” vol. 7, no. 1, pp. 23–28, 2015.

[94] M. Velds, “Assessment of lighting quality in office rooms with daylighting systems,” 2000.

[95] A. D. Galasiu and J. A. Veitch, “Occupant preferences and satisfaction with the luminous

environment and control systems in daylit offices: a literature review," *Energy Build.*, vol. 38, no. 7, pp. 728–742, 2006, doi: 10.1016/j.enbuild.2006.03.001.

[96] C. L. Robbins, *Daylighting: Design and Analysis. New York: Van Nostrand Reinhold Company*. 1986.

[97] N. Z. Occupational Safety & Health Service, *Approved Code of Practice for the Use of Visual Display Units*. 1996.

[98] J. Y. Suk, "Luminance and vertical eye illuminance thresholds for occupants' visual comfort in daylit office environments," *Build. Environ.*, vol. 148, pp. 107–115, 2019, doi: 10.1016/j.buildenv.2018.10.058.

[99] J. Christoffersen and J. Wienold, "Monitoring Procedure for assessment of user reaction to glare (Report ECCO-DBUR- 0303-01). European Community.," 2004.

[100] Y. Sutter, D. Dumortier, and M. Fontoynont, "The use of shading systems in VDU task offices: A pilot study," *Energy Build.*, vol. 38, no. 7, pp. 780–789, 2006, doi: 10.1016/j.enbuild.2006.03.010.

[101] A. S. Linney, "Maximum Luminances and Luminance Ratios and their Impact on Users ' Discomfort Glare Perception and Productivity in Daylit Offices," 2008.

[102] K. Van Den Wymelenberg, M. Inanici, and P. Johnson, "The effect of luminance distribution patterns on occupant preference in a daylit office environment," *LEUKOS - J. Illum. Eng. Soc. North Am.*, vol. 7, no. 2, pp. 103–122, 2010, doi: 10.1582/LEUKOS.2010.07.02003.

[103] L. B. N. Laboratory, "Commissioning and Verification Procedures for the Automated Roller Shade System at The New York Times Headquarters, New York, New York," 2007.

[104] J. Pereira, M. Glória Gomes, A. M. Rodrigues, and H. Teixeira, "Small-scale field experimental study on the impact of window films on the indoor illuminance levels."

[105] "Regulamento de Desempenho Energético dos Edifícios de Habitação (REH), Decreto-Lei 118/2013 de 20 de Agosto 2013," *Diário da República*, vol. 159, pp. 4988–5005, 2013.

[106] R. G. Hopkinson, "Glare from daylighting in buildings," *Appl. Ergon.*, vol. 3, no. 4, pp. 206–215, 1972, doi: 10.1016/0003-6870(72)90102-0.

[107] I. 14040:2006; I. O. for Standardization, "ISO. Environmental Management — Life Cycle Assessment — Principles and Framework." Geneve, [Online]. Available: https://www.iso.org/standard/37456.html.

[108] G. Wernet, C. Bauer, B. Steubing, J. Reinhard, E. Moreno-Ruiz, and B. Weidema, "The ecoinvent

database version 3 (part I): overview and methodology," *International Journal of Life Cycle Assessment*, vol. 21, no. 9. pp. 1218–1230, 2016, doi: 10.1007/s11367-016-1087-8.

[109] M. Marrero and A. Ramirez-De-Arellano, "The building cost system in andalusia: Application to construction and demolition waste management," *Constr. Manag. Econ.*, vol. 28, no. 5, pp. 495–507, 2010, doi: 10.1080/01446191003735500.

[110] C. Rivero Camacho, J. Pereira, M. G. Gomes, and M. Marrero, "Huella de carbono como instrumento de decisión en la rehabilitación energética. Películas de control solar frente a la sustitución de ventanas," *Rev. Hábitat Sustentable*, vol. 8, no. 2, pp. 20–31, 2018, doi: 10.22320/07190700.2018.08.02.02.

[111] M. Asif, T. Muneer, and J. Kubie, "Sustainability analysis of window frames," *Build. Serv. Eng. Res. Technol.*, vol. 26, no. 1, pp. 71–87, 2005, doi: 10.1191/0143624405bt118tn.

[112] "The 3M Quality Promise. Energy Products Distribution. Available online in December 2020 <https://epdwindowfilm.com/warranty/>." .

[113] PORDATA - Base de Dados Portugal Contemporâneo, "Preços eletricidade para utilizadores domésticos e industriais (Euro/ECU)," 2019. https://www.pordata.pt/Europa/Preços+da+electricidade+para+utilizadores+domésticos+e+industriais+(Euro+ECU)-1477-313029.

[114] T. L. Garwood, B. R. Hughes, M. R. Oates, D. O'Connor, and R. Hughes, "A review of energy simulation tools for the manufacturing sector," *Renew. Sustain. Energy Rev.*, vol. 81, no. August 2017, pp. 895–911, 2018, doi: 10.1016/j.rser.2017.08.063.

[115] A. Martínez-Rocamora, J. Solís-Guzmán, and M. Marrero, "Ecological footprint of the use and maintenance phase of buildings: Maintenance tasks and final results," *Energy Build.*, vol. 155, pp. 339–351, 2017, doi: https://doi.org/10.1016/j.enbuild.2017.09.038.

[116] J. Solís-Guzmán, M. Marrero, and A. Ramírez-De-Arellano, "Methodology for determining the ecological footprint of the construction of residential buildings in Andalusia (Spain)," *Ecol. Indic.*, vol. 25, pp. 239–249, 2013, doi: 10.1016/j.ecolind.2012.10.008.

[117] M. Marrero, A. Fonseca, R. Falcon, and A. Ramirez-de-Arellano, "Schedule and Cost Control in Dwelling Construction Using Control Charts," *Open Constr. Build. Technol. J.*, vol. 8, no. 1, pp. 63–79, 2014, doi: 10.2174/1874836801408010063.

[118] Department of Energy & Climate Change, "Greenhouse gas reporting - Conversion factors 2015,"

2015, doi: 10.1017/CBO9781107415324.004.

[119] E. C. B. (ECB), "Eurosystem staff macroeconomic projections for the euro area," no. December 2009, pp. 1–19, 2019.

[120] E. C. B. (ECB), "Mercados financeiros," no. 1, p. 2020, 2020.

[121] R. O'Neill, A. Window, S. Kenway, and P. Dargusch, "Integrated operational and life-cycle modelling of energy, carbon and cost for building façades," *J. Clean. Prod.*, vol. 286, p. 125370, 2021, doi: 10.1016/j.jclepro.2020.125370.

[122] L. Díaz-Balteiro and C. Romero, "Modeling timber harvest scheduling problems with multiple criteria: An application in Spain," *For. Sci.*, vol. 44, no. 1, pp. 47–57, 1998, doi: 10.1093/forestscience/44.1.47.

Annexes

Annex A – Thermal and optical properties of the analysed glazing without and with different SCF

Table 39. Thermal and optical properties of the analysed SCF in a clear single glazing with 6mm: solar transmittance, τ_e ; visible light transmittance, τ_v; visible exterior reflectance, $\rho_{v,e}$; visible interior reflectance, $\rho_{v,i}$; external emissivity, ε_e; internal emissivity, ε_i; solar factor, g; and thermal transmission coefficient, U [W/m^2.K]

Type of SCFs	P[1]	Man.[2]	SCF	τ_e	τ_v	$\rho_{v,e}$	$\rho_{v,i}$	ε_e	ε_i	g	U
Low-e	i	HC	Silver 20 Low-E	0.11	0.16	0.54	0.63	0.84	0.39	0.22	4.42
		LL	LEP 35 SR CDF	0.20	0.34	0.42	0.25	0.84	0.05	0.26	3.26
			LEP70SRCDF	0.43	0.68	0.08	0.04	0.84	0.09	0.50	3.41
			VE35SRCDF	0.19	0.30	0.40	0.39	0.84	0.38	0.29	4.38
			VE50SRCDF	0.33	0.48	0.24	0.23	0.84	0.45	0.42	4.62
		SG	Silver AG 25 Low-E	0.14	0.21	0.39	0.48	0.84	0.33	0.24	4.23
			Silver AG 50 Low-E	0.33	0.50	0.23	0.27	0.84	0.37	0.43	4.36
Ceramic	i	3M	CM 30	0.23	0.36	0.17	0.15	0.84	0.84	0.42	5.80
			CM 40	0.30	0.44	0.14	0.12	0.84	0.86	0.48	5.86
			CM 50	0.38	0.53	0.11	0.10	0.84	0.87	0.54	5.89
		JWF	PD 25	0.21	0.24	0.26	0.24	0.84	0.90	0.40	5.98
			PD 35	0.27	0.41	0.16	0.14	0.84	0.90	0.45	5.97
			PD 45	0.34	0.48	0.13	0.11	0.84	0.91	0.50	6.01
			PD 55	0.42	0.57	0.11	0.09	0.84	0.93	0.57	6.06
Dual-reflective	e	HC	Titan 07 Xtra	0.07	0.08	0.57	0.18	0.75	0.84	0.18	5.77
			Titan 20 Xtra	0.17	0.19	0.34	0.13	0.92	0.84	0.31	5.80
			Titan 35xtra	0.29	0.35	0.22	0.13	0.88	0.84	0.43	5.80
			Titan 50 xtra	0.38	0.52	0.18	0.18	0.84	0.84	0.50	5.79
	i	3M	NV 15	0.12	0.15	0.37	0.11	0.84	0.76	0.29	5.56
			NV 25	0.21	0.24	0.19	0.07	0.84	0.80	0.40	5.67
			NV 35	0.31	0.36	0.12	0.07	0.84	0.86	0.49	5.85
		HC	Optitune 15 SR WA	0.11	0.13	0.53	0.25	0.84	0.76	0.24	5.56
			Optitune 22 SR WA	0.17	0.21	0.30	0.14	0.84	0.80	0.34	5.68
			Optitune 30 SR WA	0.24	0.32	0.31	0.26	0.84	0.81	0.38	5.71
			Optitune 05 SR WA	0.05	0.06	0.60	0.15	0.84	0.75	0.19	5.54
			Optitune 40 SR WA	0.31	0.40	0.20	0.18	0.84	0.83	0.46	5.77
			Optitune 55 SR WA	0.47	0.59	0.12	0.10	0.84	0.87	0.60	5.88
		JWF	Night Scape 05%	0.15	0.07	0.10	0.10	0.84	0.80	0.35	5.67
			Night Scape 15%	0.26	0.16	0.13	0.06	0.84	0.85	0.45	5.81
			Night Scape 25%	0.29	0.27	0.15	0.08	0.84	0.84	0.47	5.79
			Night Scape 35%	0.32	0.35	0.17	0.11	0.84	0.81	0.48	5.70
			SV 10	0.07	0.09	0.51	0.24	0.84	0.88	0.23	5.90
			SV 30	0.24	0.32	0.30	0.21	0.84	0.83	0.39	5.76
			SV 40	0.38	0.48	0.15	0.12	0.84	0.75	0.54	5.96
		LL	V 14 SR CDF	0.08	0.11	0.50	0.24	0.84	0.88	0.24	5.92
			V 18 SR CDF	0.14	0.20	0.38	0.20	0.84	0.88	0.31	5.92
			V 28 SR CDF	0.20	0.27	0.31	0.19	0.84	0.87	0.36	5.90
			V 38 SR CDF	0.29	0.39	0.22	0.16	0.84	0.87	0.45	5.90
			V 48 SR CDF	0.36	0.45	0.14	0.10	0.84	0.92	0.53	6.03
			V 50 SR CDF	0.36	0.50	0.08	0.08	0.84	0.71	0.50	5.42
		SG	Slate 10	0.08	0.12	0.43	0.21	0.84	0.82	0.23	5.74
			Slate 20	0.15	0.22	0.30	0.17	0.84	0.84	0.32	5.80
			Slate 30	0.21	0.29	0.23	0.14	0.84	0.84	0.38	5.80
			Slate 40	0.33	0.44	0.17	0.12	0.84	0.81	0.47	5.71
			Slate 50	0.33	0.47	0.24	0.24	0.84	0.82	0.47	5.73

[1] Position of the film: i – interior; e – exterior
[2] Manufacturer: 3M – 3M; HC – Hanita Coatings; JWF – Johnson Window Films; LL – Llumar; SG – Solar Gard

Table 40. (cont.) Thermal and optical properties of the analysed SCF in a clear single glazing with 6mm: solar transmittance, τ_e ; visible light transmittance, τ_v; visible exterior reflectance, $\rho_{v,e}$; visible interior reflectance, $\rho_{v,i}$; external emissivity, ε_e; internal emissivity, ε_i; solar factor, g; and thermal transmission coefficient, U [W/m^2.K]

Type of SCFs	P[1]	Man.[2]	SCF	τ_e	τ_v	$\rho_{v,e}$	$\rho_{v,i}$	ε_e	ε_i	g	U
Dual-reflective	i	SG	True Vue 15	0.08	0.12	0.43	0.23	0.84	0.75	0.23	5.54
			True Vue 30	0.25	0.31	0.21	0.13	0.84	0.75	0.40	5.54
			True Vue 40	0.34	0.38	0.14	0.10	0.84	0.75	0.48	5.54
			True Vue 05	0.05	0.05	0.43	0.08	0.84	0.75	0.21	5.54
Spectrally-selective	e	3M	PR 40 EXT	0.23	0.42	0.06	0.05	0.87	0.84	0.40	5.80
			PR 70 EXT	0.37	0.71	0.07	0.07	0.87	0.84	0.48	5.80
			PR 90 EXT	0.61	0.88	0.09	0.09	0.89	0.84	0.65	5.80
	i	3M	PR 40	0.22	0.39	0.06	0.07	0.84	0.78	0.41	5.63
			PR 50	0.28	0.50	0.08	0.07	0.84	0.78	0.45	5.63
			PR 60	0.32	0.60	0.08	0.08	0.84	0.78	0.48	5.63
			PR 70	0.37	0.69	0.08	0.09	0.84	0.78	0.51	5.63
		HC	E-Lite 70	0.34	0.65	0.15	0.15	0.84	0.73	0.48	5.48
		LL	VS 42 SR CDF	0.21	0.42	0.10	0.12	0.84	0.83	0.38	5.77
			VS 60 SR CDF	0.32	0.60	0.08	0.09	0.84	0.68	0.45	5.33
			VS 61 SR CDF	0.43	0.62	0.17	0.18	0.84	0.76	0.54	5.55
			VS 70 SR CDF	0.37	0.69	0.08	0.08	0.84	0.66	0.48	5.26
		SG	Sterling 20	0.14	0.22	0.44	0.42	0.84	0.67	0.26	5.30
			Sterling 40	0.27	0.41	0.32	0.30	0.84	0.68	0.38	5.33
			Sterling 50	0.33	0.49	0.25	0.24	0.84	0.69	0.44	5.36
			Sterling 60	0.46	0.63	0.17	0.16	0.84	0.76	0.56	5.57
			Sterling 70	0.56	0.73	0.12	0.12	0.84	0.80	0.65	5.70
Neutral	e	JWF	DN 20 EXT	0.20	0.22	0.26	0.25	0.92	0.84	0.37	5.80
			DN 35 EXT	0.36	0.36	0.16	0.18	0.95	0.84	0.51	5.81
			DN 50 EXT	0.42	0.48	0.11	0.13	0.95	0.84	0.56	5.81
	i	3M	RE 20 NEAR	0.12	0.15	0.20	0.19	0.84	0.78	0.33	5.63
			RE 35 NEAR	0.28	0.35	0.19	0.18	0.84	0.77	0.45	5.60
			RE 50 NEAR	0.43	0.52	0.12	0.11	0.84	0.85	0.57	5.84
			RE 70 NEAR	0.59	0.69	0.09	0.08	0.84	0.85	0.69	5.84
		JWF	DN 15	0.15	0.17	0.18	0.16	0.84	0.92	0.38	6.02
			DN 20	0.20	0.22	0.25	0.26	0.84	0.92	0.40	6.01
			DN 25	0.23	0.26	0.15	0.12	0.84	0.94	0.44	6.08
			DN 35	0.36	0.36	0.18	0.16	0.84	0.95	0.52	6.12
			DN 50	0.42	0.48	0.13	0.11	0.84	0.95	0.57	6.11
			DN 60	0.53	0.61	0.10	0.09	0.84	0.96	0.66	6.13
		LL	N 1020 B SR CDF	0.12	0.19	0.36	0.35	0.84	0.70	0.25	5.38
			N 1020 SR CDF	0.20	0.23	0.28	0.26	0.84	0.90	0.38	5.96
			N1035BSRCDF	0.24	0.36	0.24	0.23	0.84	0.71	0.37	5.43
			N 1040 SR CDF	0.33	0.39	0.17	0.15	0.84	0.93	0.50	6.05
			N 1050 B SR CDF	0.41	0.54	0.14	0.12	0.84	0.77	0.53	5.60
			N 1050 SR CDF	0.41	0.48	0.14	0.12	0.84	0.94	0.56	6.08
			V 33 SR CDF	0.28	0.33	0.21	0.19	0.84	0.92	0.45	6.02
			V 45 SR CDF	0.36	0.42	0.16	0.14	0.84	0.94	0.53	6.06
			V 58 SR CDF	0.50	0.58	0.12	0.09	0.84	0.95	0.63	6.10
		SG	Stainless Steel 10	0.08	0.09	0.42	0.42	0.84	0.79	0.26	5.65
			Stainless Steel 20	0.20	0.23	0.27	0.25	0.84	0.84	0.39	5.80
			Stainless Steel 30	0.29	0.33	0.19	0.17	0.84	0.86	0.46	5.86
			Stainless Steel 35	0.36	0.41	0.15	0.12	0.84	0.88	0.53	5.91
			Stainless Steel 50	0.41	0.47	0.13	0.11	0.84	0.89	0.57	5.94

[1] Position of the film: i – interior; e – exterior

[2] Manufacturer: 3M – 3M; HC – Hanita Coatings; JWF – Johnson Window Films; LL – Llumar; SG – Solar Gard

Table 41. (cont.) Thermal and optical properties of the analysed SCF in a clear single glazing with 6mm: solar transmittance, τ_e ; visible light transmittance, τ_v; visible exterior reflectance, $\rho_{v,e}$; visible interior reflectance, $\rho_{v,i}$; external emissivity, ε_e; internal emissivity, ε_i; solar factor, g; and thermal transmission coefficient, U [W/m^2.K]

Type of SCFs	P[1]	Man.[2]	SCF	τ_e	τ_v	$\rho_{v,e}$	$\rho_{v,i}$	ε_e	ε_i	g	U
Protection and safety	e	HC	Silver 20 5 mil Xtra	0.12	0.17	0.63	0.59	0.81	0.84	0.19	5.77
		SG	Sentinel 4 mil Clear	0.74	0.87	0.09	0.09	0.90	0.84	0.80	5.79
	i	HC	Silver 20 4 mil	0.13	0.18	0.57	0.61	0.84	0.74	0.25	5.49
		LL	V 28 SR PS8	0.20	0.27	0.30	0.22	0.84	0.94	0.37	6.04
			V 38 SR PS8	0.27	0.37	0.25	0.19	0.84	0.94	0.44	6.04
		SG	10 mil Clear	0.73	0.85	0.11	0.11	0.84	0.96	0.79	6.09
			10 mil Silver 20	0.11	0.17	0.55	0.56	0.84	0.70	0.24	5.36
			11 mil Clear	0.72	0.86	0.11	0.11	0.84	0.96	0.78	6.09
			14 mil Clear	0.71	0.84	0.12	0.12	0.84	0.94	0.77	6.03
			2 mil Clear	0.74	0.87	0.09	0.09	0.84	0.95	0.80	6.12
			4 mil Clear	0.74	0.86	0.10	0.10	0.84	0.96	0.79	6.12
			4 mil Silver 20	0.10	0.15	0.57	0.60	0.84	0.71	0.23	5.41
			4 mil Solar Bronze 35	0.18	0.31	0.28	0.27	0.84	0.68	0.31	5.32
			4 mil Stainless Steel 20	0.19	0.22	0.26	0.25	0.84	0.85	0.38	5.82
			4 mil Stainless Steel 50	0.40	0.46	0.13	0.11	0.84	0.90	0.56	5.96
			4 mil Sterling 60	0.43	0.61	0.19	0.18	0.84	0.72	0.53	5.44
			7 mil Clear	0.74	0.86	0.10	0.10	0.84	0.96	0.79	6.11
			8 mil Clear	0.72	0.85	0.10	0.10	0.84	0.96	0.79	6.10
			8 mil Silver 20	0.10	0.14	0.56	0.59	0.84	0.70	0.22	5.37
			8 mil Silver 35	0.24	0.35	0.34	0.33	0.84	0.71	0.38	5.40
			8 mil Slate 40	0.33	0.45	0.20	0.13	0.84	0.83	0.47	5.74
			8 mil Stainless Steel 20	0.18	0.21	0.26	0.24	0.84	0.86	0.38	5.83
			8 mil Stainless Steel 35	0.33	0.38	0.15	0.13	0.84	0.88	0.50	5.89
			8 mil Stainless Steel 50	0.37	0.43	0.13	0.11	0.84	0.88	0.54	5.89
Reflective	e	HC	Silver 20 Xtra	0.11	0.17	0.62	0.59	0.80	0.84	0.19	5.79
			Silver 35 Xtra	0.23	0.32	0.41	0.40	0.76	0.84	0.33	5.78
			Silver 50 Xtra	0.34	0.47	0.27	0.27	0.84	0.84	0.45	5.79
			Solar Bronze 20 Xtra	0.24	0.33	0.41	0.36	0.78	0.84	0.33	5.78
			Solar Bronze 35 Xtra	0.20	0.32	0.30	0.26	0.70	0.84	0.28	5.77
		JWF	SS 20 EXT	0.15	0.22	0.50	0.48	0.73	0.84	0.25	5.77
			SS 35 EXT	0.28	0.39	0.32	0.32	0.76	0.84	0.39	5.78
		SG	Sentinel Silver 20 OSW	0.11	0.16	0.61	0.56	0.76	0.84	0.18	5.78
			Sentinel Silver 35 OSW	0.24	0.33	0.41	0.36	0.78	0.84	0.33	5.78
	i	3M	P 18 AR	0.11	0.17	0.55	0.58	0.84	0.66	0.23	5.28
		HC	Silver 20 SR WA	0.12	0.17	0.59	0.62	0.84	0.71	0.24	5.42
			Silver 35 SR WA	0.24	0.33	0.40	0.40	0.84	0.72	0.36	5.45
			Solar Bronze 20	0.09	0.17	0.38	0.45	0.84	0.69	0.22	5.36
			Solar Bronze 35	0.19	0.32	0.28	0.29	0.84	0.70	0.32	5.39
			Solar Bronze 50	0.34	0.49	0.18	0.17	0.84	0.71	0.45	5.42
		JWF	MBL 20	0.22	0.23	0.15	0.31	0.84	0.77	0.39	5.59
			MBL 35	0.31	0.34	0.11	0.18	0.84	0.83	0.48	5.78
			MBL 50	0.47	0.51	0.09	0.10	0.84	0.93	0.61	6.05
			MG 05	0.14	0.06	0.10	0.09	0.84	0.80	0.35	5.67
			MG 10	0.09	0.07	0.13	0.53	0.84	0.72	0.28	5.45
			MG 20	0.21	0.23	0.14	0.31	0.84	0.77	0.39	5.60
			MGD 20	0.15	0.21	0.41	0.49	0.84	0.73	0.29	5.47
			MGD 35	0.28	0.37	0.26	0.30	0.84	0.77	0.42	5.59
			MGN 20	0.22	0.24	0.13	0.28	0.84	0.78	0.40	5.62
			MGN 35	0.32	0.34	0.09	0.15	0.84	0.86	0.49	5.85

[1] Position of the film: i – interior; e – exterior

[2] Manufacturer: 3M – 3M; HC – Hanita Coatings; JWF – Johnson Window Films; LL – Llumar; SG – Solar Gard

Table 42. (cont.) Thermal and optical properties of the analysed SCF in a clear single glazing with 6mm: solar transmittance, τ_e ; visible light transmittance, τ_v; visible exterior reflectance, $\rho_{v,e}$; visible interior reflectance, $\rho_{v,i}$; external emissivity, ε_e; internal emissivity, ε_i; solar factor, g; and thermal transmission coefficient, U [W/m^2.K]

Type of SCFs	P[1]	Man.[2]	SCF	τ_e	τ_v	$\rho_{v,e}$	$\rho_{v,i}$	ε_e	ε_i	g	U
Reflective	i	JWF	SB 20	0.12	0.19	0.35	0.33	0.84	0.70	0.26	5.39
			SB 30	0.21	0.32	0.26	0.24	0.84	0.72	0.35	5.45
			SB 50	0.38	0.52	0.15	0.14	0.84	0.76	0.51	5.57
			SS 20	0.15	0.22	0.48	0.50	0.84	0.73	0.28	5.47
			SS 35	0.28	0.39	0.32	0.32	0.84	0.76	0.41	5.57
		LL	R 20 SR CDF	0.11	0.16	0.57	0.59	0.84	0.71	0.24	5.43
			R 35 SR CDF	0.20	0.28	0.44	0.45	0.84	0.74	0.32	5.50
			R 50 SR CDF	0.34	0.47	0.27	0.27	0.84	0.79	0.46	5.63
		SG	Silver 20	0.11	0.16	0.56	0.58	0.84	0.70	0.23	5.39
			Silver 35	0.24	0.34	0.36	0.36	0.84	0.73	0.37	5.48
			Silver 50	0.37	0.52	0.22	0.22	0.84	0.77	0.50	5.60
			Solar Bronze 20	0.12	0.22	0.36	0.36	0.84	0.66	0.24	5.27
			Solar Bronze 35	0.20	0.34	0.28	0.27	0.84	0.68	0.32	5.33
			Solar Bronze 50	0.28	0.44	0.22	0.21	0.84	0.69	0.39	5.36

[1] Position of the film: i – interior; e – exterior

[2] Manufacturer: 3M – 3M; HC – Hanita Coatings; JWF – Johnson Window Films; LL – Llumar; SG – Solar Gard

Annex B – Mean and standard deviation of the main thermal and optical properties of clear and tinted glass with SCFs

Table 43. Mean, $\bar{x}$, and coefficient of variation, C_v, of the main thermal and optical properties of the analysed SCFs applied in a clear and tinted single glazing with 6mm: solar transmittance, τ_e; visible light transmittance, τ_v; visible exterior reflectance, $\rho_{v,e}$; visible interior reflectance, $\rho_{v,i}$; external emissivity, ε_e; internal emissivity, ε_i; solar factor, g; and thermal transmission coefficient, U [W/m^2.K]

Type of glass substrate			τ_e		τ_v		$\rho_{v,e}$		$\rho_{v,i}$		ε_e		ε_i		g		U	
Type of SCFs	P[1]	n	$\bar{x}$	C_v	$\bar{x}$	C_v	$\bar{x}$	C_v	$\bar{x}$	C_v	$\bar{x}$	C_v	$\bar{x}$	C_v	$\bar{x}$	C_v	$\bar{x}$	C_v
Clear single glass																		
Low-emissivity	i	7	0.25	0.48	0.38	0.48	0.33	0.47	0.33	0.59	0.84	0.00	0.29	0.54	0.34	0.33	4.10	0.13
Ceramic	i	7	0.31	0.25	0.43	0.26	0.15	0.34	0.14	0.37	0.84	0.00	0.89	0.04	0.48	0.13	5.94	0.02
Dual-reflective	e	4	0.23	0.60	0.29	0.67	0.33	0.54	0.16	0.19	0.85	0.09	0.84	0.00	0.35	0.40	5.79	0.00
Dual-reflective	i	31	0.22	0.51	0.28	0.54	0.27	0.53	0.15	0.42	0.84	0.00	0.81	0.06	0.38	0.29	5.74	0.03
Spectrally-selective	e	3	0.40	0.48	0.67	0.35	0.07	0.21	0.07	0.29	0.88	0.01	0.84	0.00	0.51	0.25	5.80	0.00
Spectrally-selective	i	14	0.33	0.33	0.55	0.27	0.16	0.71	0.16	0.66	0.84	0.00	0.74	0.07	0.46	0.20	5.51	0.03
Neutral	e	3	0.33	0.34	0.35	0.38	0.18	0.43	0.19	0.33	0.94	0.02	0.84	0.00	0.48	0.20	5.81	0.00
Neutral	i	24	0.31	0.44	0.37	0.43	0.19	0.42	0.17	0.49	0.84	0.00	0.87	0.09	0.48	0.24	5.89	0.04
Protection and safety	e	2	0.43	1.02	0.52	0.95	0.36	1.06	0.34	1.04	0.86	0.07	0.84	0.00	0.49	0.86	5.78	0.00
Protection and safety	i	22	0.39	0.64	0.49	0.58	0.25	0.68	0.24	0.76	0.84	0.00	0.85	0.12	0.51	0.42	5.80	0.05
Reflective	e	9	0.21	0.37	0.30	0.34	0.43	0.30	0.40	0.30	0.77	0.05	0.84	0.00	0.31	0.29	5.78	0.00
Reflective	i	30	0.22	0.45	0.29	0.44	0.29	0.53	0.34	0.45	0.84	0.00	0.74	0.08	0.36	0.28	5.51	0.03
Tinted single glass																		
Low-emissivity	i	7	0.16	0.50	0.21	0.49	0.13	0.36	0.31	0.63	0.84	0.00	0.29	0.54	0.31	0.25	4.27	0.18
Ceramic	i	7	0.20	0.25	0.24	0.26	0.08	0.20	0.13	0.42	0.84	0.00	0.89	0.04	0.43	0.09	5.94	0.02
Dual-reflective	e	4	0.14	0.60	0.16	0.67	0.32	0.55	0.08	0.10	0.85	0.09	0.84	0.00	0.30	0.37	5.79	0.00
Dual-reflective	i	31	0.14	0.58	0.15	0.62	0.12	0.39	0.15	0.43	0.84	0.00	0.82	0.06	0.37	0.20	5.74	0.03
Spectrally-selective	e	3	0.25	0.51	0.37	0.35	0.06	0.10	0.05	0.10	0.88	0.01	0.84	0.00	0.41	0.21	5.80	0.00
Spectrally-selective	i	14	0.20	0.29	0.29	0.26	0.08	0.44	0.14	0.74	0.84	0.00	0.75	0.09	0.40	0.13	5.53	0.04
Neutral	e	3	0.21	0.34	0.19	0.37	0.17	0.45	0.09	0.21	0.94	0.02	0.84	0.00	0.41	0.18	5.81	0.00
Neutral	i	24	0.20	0.44	0.20	0.43	0.09	0.27	0.17	0.50	0.84	0.00	0.86	0.10	0.42	0.17	5.86	0.04
Protection and safety	e	2	0.28	1.04	0.29	0.97	0.35	1.14	0.13	0.80	0.86	0.07	0.84	0.00	0.39	0.83	5.78	0.00
Protection and safety	i	22	0.25	0.65	0.27	0.59	0.11	0.48	0.23	0.82	0.84	0.00	0.85	0.12	0.45	0.30	5.80	0.05
Reflective	e	9	0.12	0.46	0.15	0.40	0.43	0.30	0.16	0.23	0.76	0.05	0.84	0.00	0.24	0.32	5.78	0.00
Reflective	i	30	0.13	0.48	0.16	0.45	0.12	0.40	0.35	0.46	0.84	0.00	0.74	0.08	0.35	0.18	5.52	0.03

[1] Position of the film: i – interior; e – exterior

Table 44. Mean, $\bar{x}$, and coefficient of variation, C_v, of the main thermal and optical properties of the analysed SCFs applied in a clear double glazing: solar transmittance, τ_e; visible light transmittance, τ_v; visible exterior reflectance, $\rho_{v,e}$; visible interior reflectance, $\rho_{v,i}$; external emissivity, ε_e; internal emissivity, ε_i; solar factor, g; and thermal transmission coefficient, U [W/m²·K]

Type of glass substrate			τ_e		τ_v		$\rho_{v,e}$		$\rho_{v,i}$		ε_e		ε_i		g		U	
Type of SCFs	P[1]	n	$\bar{x}$	C_v	$\bar{x}$	C_v	$\bar{x}$	C_v	$\bar{x}$	C_v	$\bar{x}$	C_v	$\bar{x}$	C_v	$\bar{x}$	C_v	$\bar{x}$	C_v
Clear double-glazing																		
Low-emissivity	i	7	0.23	0.53	0.36	0.48	0.34	0.42	0.32	0.61	0.84	0.00	0.28	0.52	0.43	0.28	2.21	0.14
Ceramic	i	7	0.26	0.24	0.39	0.26	0.20	0.20	0.15	0.29	0.84	0.00	0.89	0.04	0.57	0.07	2.72	0.01
Dual-reflective	e	4	0.19	0.60	0.26	0.67	0.34	0.50	0.21	0.10	0.85	0.09	0.84	0.00	0.27	0.47	2.69	0.00
Dual-reflective	i	31	0.20	0.48	0.27	0.60	0.30	0.41	0.16	0.38	0.84	0.00	0.83	0.06	0.50	0.20	2.68	0.02
Spectrally-selective	e	3	0.34	0.47	0.60	0.35	0.11	0.36	0.14	0.10	0.88	0.01	0.84	0.00	0.42	0.33	2.69	0.00
Spectrally-selective	i	14	0.28	0.32	0.48	0.26	0.22	0.41	0.19	0.51	0.84	0.00	0.75	0.07	0.53	0.13	2.59	0.03
Neutral	e	3	0.27	0.34	0.32	0.37	0.19	0.36	0.23	0.21	0.94	0.02	0.84	0.00	0.37	0.25	2.69	0.00
Neutral	i	24	0.26	0.43	0.33	0.42	0.24	0.28	0.19	0.41	0.84	0.00	0.87	0.09	0.56	0.14	2.71	0.02
Protection and safety	e	2	0.36	1.01	0.47	0.94	0.39	0.86	0.36	0.82	0.86	0.07	0.84	0.00	0.42	0.91	2.68	0.00
Protection and safety	i	22	0.33	0.62	0.45	0.57	0.28	0.51	0.26	0.64	0.84	0.00	0.84	0.13	0.55	0.26	2.68	0.03
Reflective	e	9	0.17	0.44	0.26	0.39	0.43	0.28	0.42	0.24	0.76	0.06	0.84	0.00	0.23	0.37	2.68	0.00
Reflective	i	30	0.19	0.44	0.27	0.44	0.32	0.40	0.35	0.43	0.84	0.00	0.74	0.08	0.45	0.19	2.61	0.02

[1] Position of the film: i – interior; e – exterior

Low-emissive high solar gain
Low-emissive moderate solar gain
Low-emissive reduced solar gain

Table 45. Mean, $\bar{x}$, and coefficient of variation, C_v, of the main thermal and optical properties of the analysed SCFs applied in tinted double glazing: solar transmittance, τ_e; visible light transmittance, τ_v; visible exterior reflectance, $\rho_{v,e}$; visible interior reflectance, $\rho_{v,i}$; external emissivity, ε_e; internal emissivity, ε_i; solar factor, g; and thermal transmission coefficient, U [W/m^2.K]

Type of glass substrate			τ_e		τ_v		$\rho_{v,e}$		$\rho_{v,i}$		ε_e		ε_i		g		U	
Type of SCFs	P[1]	n	$\bar{x}$	C_v	$\bar{x}$	C_v	$\bar{x}$	C_v	$\bar{x}$	C_v	$\bar{x}$	C_v	$\bar{x}$	C_v	$\bar{x}$	C_v	$\bar{x}$	C_v
Tinted double-glazing																		
Low-emissivity	i	7	0.13	0.47	0.19	0.47	0.14	0.28	0.34	0.54	0.84	0.00	0.29	0.54	0.31	0.16	2.15	0.09
Ceramic	i	7	0.16	0.24	0.21	0.26	0.09	0.14	0.14	0.32	0.84	0.00	0.89	0.04	0.41	0.06	2.72	0.01
Dual-reflective	e	4	0.12	0.60	0.14	0.67	0.33	0.54	0.14	0.05	0.85	0.09	0.84	0.00	0.21	0.43	2.69	0.00
Dual-reflective	i	31	0.11	0.51	0.14	0.54	0.12	0.30	0.15	0.40	0.84	0.00	0.82	0.06	0.36	0.15	2.67	0.02
Spectrally-selective	e	3	0.21	0.50	0.33	0.35	0.07	0.19	0.12	0.04	0.88	0.01	0.84	0.00	0.31	0.30	2.69	0.00
Spectrally-selective	i	14	0.17	0.33	0.27	0.27	0.09	0.30	0.17	0.58	0.84	0.00	0.74	0.07	0.39	0.10	2.61	0.02
Neutral	e	3	0.18	0.34	0.17	0.37	0.18	0.43	0.15	0.10	0.94	0.02	0.84	0.00	0.29	0.22	2.69	0.00
Neutral	i	24	0.16	0.44	0.18	0.42	0.10	0.19	0.18	0.43	0.84	0.00	0.87	0.09	0.41	0.12	2.71	0.02
Protection and safety	e	2	0.23	1.04	0.26	0.96	0.36	1.07	0.19	0.46	0.86	0.07	0.84	0.00	0.31	0.90	2.68	0.00
Protection and safety	i	22	0.20	0.64	0.24	0.58	0.12	0.37	0.26	0.67	0.84	0.00	0.85	0.12	0.41	0.21	2.69	0.03
Reflective	e	9	0.10	0.46	0.14	0.40	0.43	0.30	0.21	0.14	0.76	0.06	0.84	0.00	0.17	0.36	2.68	0.00
Reflective	i	30	0.11	0.46	0.14	0.46	0.13	0.31	0.34	0.44	0.84	0.00	0.74	0.08	0.34	0.15	2.61	0.02
Reflective double-glazing																		
Low-emissivity	i	7	0.11	0.44	0.14	0.41	0.58	0.04	0.42	0.31	0.84	0.00	0.29	0.54	0.25	0.16	2.15	0.09
Ceramic	i	7	0.14	0.24	0.14	0.24	0.55	0.01	0.23	0.09	0.84	0.00	0.89	0.04	0.35	0.06	2.72	0.01
Dual-reflective	e	4	0.11	0.58	0.10	0.68	0.38	0.34	0.54	0.01	0.85	0.09	0.84	0.00	0.20	0.40	2.69	0.00
Dual-reflective	i	31	0.11	0.49	0.10	0.50	0.57	0.04	0.20	0.34	0.84	0.00	0.82	0.06	0.31	0.16	2.67	0.02
Spectrally-selective	e	3	0.18	0.59	0.22	0.35	0.30	0.53	0.52	0.00	0.88	0.01	0.84	0.00	0.26	0.31	2.69	0.00
Spectrally-selective	i	14	0.14	0.38	0.18	0.25	0.55	0.03	0.31	0.29	0.84	0.00	0.74	0.07	0.32	0.11	2.60	0.02
Neutral	e	3	0.18	0.32	0.12	0.34	0.25	0.13	0.54	0.01	0.94	0.02	0.84	0.00	0.29	0.21	2.69	0.00
Neutral	i	24	0.15	0.43	0.13	0.40	0.56	0.02	0.25	0.23	0.84	0.00	0.87	0.09	0.35	0.12	2.71	0.02
Protection and safety	e	2	0.22	1.01	0.18	0.85	0.55	0.23	0.56	0.09	0.86	0.07	0.84	0.00	0.28	0.85	2.68	0.00
Protection and safety	i	22	0.19	0.64	0.17	0.54	0.57	0.04	0.39	0.36	0.84	0.00	0.85	0.12	0.35	0.23	2.68	0.03
Reflective	e	9	0.10	0.43	0.11	0.35	0.48	0.21	0.57	0.03	0.76	0.06	0.84	0.00	0.17	0.34	2.68	0.00
Reflective	i	30	0.11	0.44	0.11	0.41	0.57	0.04	0.39	0.34	0.84	0.00	0.74	0.08	0.29	0.16	2.60	0.02
Low-emissive (high solar gain)																		
Low-emissivity	i	7	0.18	0.46	0.34	0.47	0.32	0.39	0.34	0.55	0.05	0.00	0.29	0.54	0.37	0.18	1.44	0.08
Ceramic	i	7	0.20	0.25	0.38	0.26	0.18	0.22	0.14	0.32	0.05	0.00	0.89	0.04	0.47	0.05	1.74	0.01
Dual-reflective	e	4	0.15	0.62	0.25	0.67	0.33	0.52	0.18	0.12	0.85	0.09	0.84	0.00	0.20	0.52	1.70	0.00
Dual-reflective	i	31	0.15	0.50	0.24	0.53	0.27	0.42	0.15	0.40	0.05	0.00	0.82	0.06	0.41	0.15	1.71	0.01
Spectrally-selective	e	3	0.29	0.38	0.59	0.35	0.09	0.30	0.11	0.13	0.88	0.01	0.84	0.00	0.33	0.30	1.70	0.00
Spectrally-selective	i	14	0.24	0.28	0.48	0.27	0.18	0.47	0.17	0.58	0.05	0.00	0.74	0.07	0.46	0.10	1.68	0.01
Neutral	e	3	0.19	0.35	0.31	0.37	0.18	0.39	0.20	0.24	0.94	0.02	0.84	0.00	0.25	0.28	1.70	0.00
Neutral	i	24	0.19	0.42	0.33	0.42	0.21	0.30	0.18	0.44	0.05	0.00	0.87	0.09	0.45	0.10	1.73	0.02
Protection and safety	e	2	0.27	0.96	0.46	0.95	0.37	0.96	0.32	0.87	0.86	0.07	0.84	0.00	0.31	0.90	1.70	0.00
Protection and safety	i	22	0.25	0.59	0.43	0.58	0.25	0.53	0.25	0.68	0.05	0.00	0.85	0.12	0.44	0.19	1.72	0.02
Reflective	e	9	0.14	0.42	0.25	0.40	0.43	0.29	0.38	0.25	0.76	0.06	0.84	0.00	0.17	0.38	1.70	0.00
Reflective	i	30	0.15	0.42	0.26	0.44	0.29	0.42	0.34	0.44	0.05	0.00	0.74	0.08	0.40	0.16	1.68	0.01
Low-emissive (moderate solar gain)																		
Low-emissivity	i	7	0.14	0.46	0.30	0.47	0.38	0.10	0.34	0.54	0.04	0.00	0.29	0.54	0.27	0.18	1.43	0.08
Ceramic	i	7	0.15	0.25	0.34	0.26	0.34	0.03	0.15	0.31	0.04	0.00	0.89	0.04	0.33	0.06	1.72	0.01
Dual-reflective	e	4	0.11	0.65	0.22	0.67	0.38	0.38	0.18	0.09	0.85	0.09	0.84	0.00	0.15	0.51	1.70	0.00
Dual-reflective	i	31	0.10	0.51	0.22	0.53	0.37	0.10	0.16	0.40	0.04	0.00	0.82	0.06	0.29	0.15	1.70	0.01
Spectrally-selective	e	3	0.23	0.36	0.53	0.35	0.31	0.30	0.12	0.09	0.88	0.01	0.84	0.00	0.28	0.26	1.70	0.00
Spectrally-selective	i	14	0.19	0.27	0.43	0.27	0.34	0.08	0.17	0.56	0.04	0.00	0.74	0.07	0.33	0.10	1.67	0.01
Neutral	e	3	0.14	0.36	0.28	0.37	0.22	0.19	0.20	0.19	0.94	0.02	0.84	0.00	0.19	0.26	1.70	0.00
Neutral	i	24	0.14	0.42	0.29	0.42	0.35	0.06	0.18	0.43	0.04	0.00	0.87	0.09	0.32	0.10	1.71	0.02
Protection and safety	e	2	0.20	0.94	0.41	0.95	0.48	0.50	0.30	0.76	0.86	0.07	0.84	0.00	0.23	0.86	1.70	0.00
Protection and safety	i	22	0.18	0.58	0.38	0.58	0.36	0.12	0.26	0.66	0.04	0.00	0.85	0.12	0.31	0.20	1.70	0.02
Reflective	e	9	0.10	0.41	0.22	0.40	0.52	0.21	0.34	0.23	0.76	0.06	0.84	0.00	0.14	0.36	1.70	0.00
Reflective	i	30	0.11	0.43	0.23	0.44	0.38	0.10	0.34	0.44	0.04	0.00	0.74	0.08	0.28	0.16	1.67	0.01

[1] Position of the film: i – interior; e – exterior

Table 46. (cont.) Mean, $\bar{x}$, and coefficient of variation, C_v, of the main thermal and optical properties of the analysed SCFs applied in a double glazing: solar transmittance, τ_e; visible light transmittance, τ_v; visible exterior reflectance, $\rho_{v,e}$; visible interior reflectance, $\rho_{v,i}$; external emissivity, ε_e; internal emissivity, ε_i; solar factor, g; and thermal transmission coefficient, U [W/m^2.K]

Type of glass substrate			τ_e		τ_v		$\rho_{v,e}$		$\rho_{v,i}$		ε_e		ε_i		g		U	
Type of SCFs	P[1]	n	$\bar{x}$	C_v	$\bar{x}$	C_v	$\bar{x}$	C_v	$\bar{x}$	C_v	$\bar{x}$	C_v	$\bar{x}$	C_v	$\bar{x}$	C_v	$\bar{x}$	C_v
Low-emissive (low solar gain)																		
Low-emissivity	i	7	0.11	0.45	0.26	0.46	0.28	0.27	0.35	0.51	0.04	0.00	0.29	0.54	0.22	0.17	1.43	0.08
Ceramic	i	7	0.12	0.25	0.29	0.26	0.19	0.12	0.16	0.27	0.04	0.00	0.89	0.04	0.26	0.05	1.72	0.01
Dual-reflective	e	4	0.08	0.65	0.19	0.67	0.34	0.49	0.20	0.06	0.85	0.09	0.84	0.00	0.13	0.48	1.70	0.00
Dual-reflective	i	31	0.08	0.52	0.19	0.53	0.25	0.28	0.16	0.38	0.04	0.00	0.82	0.06	0.23	0.14	1.70	0.01
Spectrally-selective	e	3	0.18	0.36	0.45	0.35	0.12	0.38	0.16	0.05	0.88	0.01	0.84	0.00	0.23	0.24	1.70	0.00
Spectrally-selective	i	14	0.15	0.26	0.37	0.26	0.20	0.26	0.19	0.50	0.04	0.00	0.74	0.07	0.26	0.10	1.67	0.01
Neutral	e	3	0.10	0.36	0.24	0.37	0.19	0.34	0.22	0.13	0.94	0.02	0.84	0.00	0.16	0.24	1.70	0.00
Neutral	i	24	0.10	0.42	0.25	0.42	0.21	0.18	0.19	0.39	0.04	0.00	0.87	0.09	0.25	0.09	1.71	0.02
Protection and safety	e	2	0.15	0.92	0.36	0.94	0.40	0.81	0.30	0.58	0.86	0.07	0.84	0.00	0.18	0.82	1.70	0.00
Protection and safety	i	22	0.14	0.57	0.33	0.57	0.24	0.34	0.27	0.59	0.04	0.00	0.85	0.12	0.25	0.19	1.70	0.02
Reflective	e	9	0.08	0.40	0.20	0.39	0.44	0.28	0.33	0.18	0.76	0.06	0.84	0.00	0.12	0.34	1.70	0.00
Reflective	i	30	0.08	0.43	0.20	0.43	0.26	0.28	0.35	0.42	0.04	0.00	0.74	0.08	0.23	0.15	1.67	0.01

[1] Position of the film: i – interior; e – exterior

Annex C – Illuminance levels according to UDI metric scale

Figure 103. Digital photos and illuminance levels on a horizontal plane at 0.8 m height at 09h00, 12h00 and 15h00 in the summer solstice under clear sky conditions for: a) clear glass; b) SCF A; c) SCF B; d) SCF C and; e) SCF D

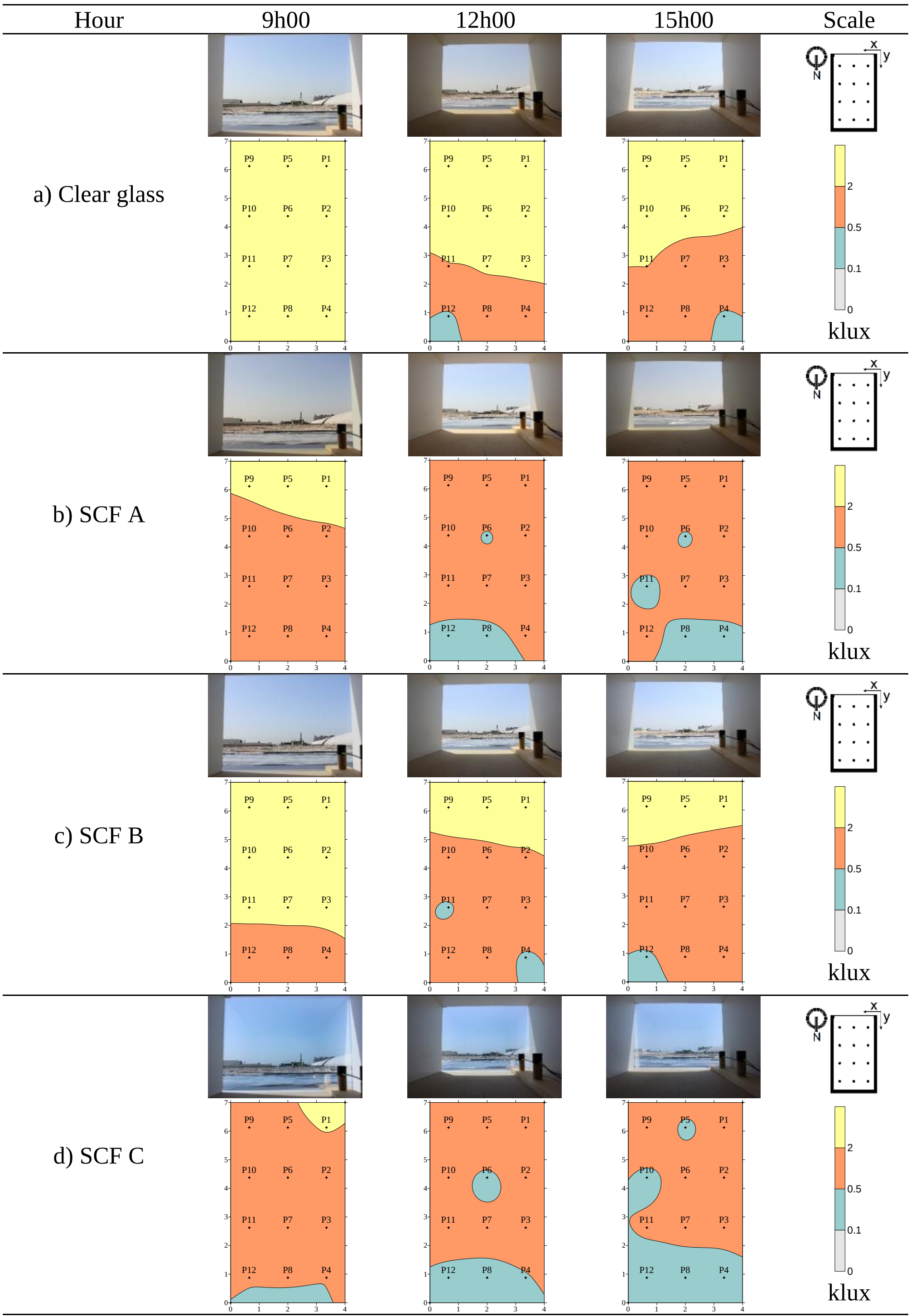

Figure 104. (cont.) Digital photos and illuminance levels on a horizontal plane at 0.8 m height at 09h00, 12h00 and 15h00 in the summer solstice under clear sky conditions for: a) clear glass; b) SCF A; c) SCF B; d) SCF C and; e) SCF D

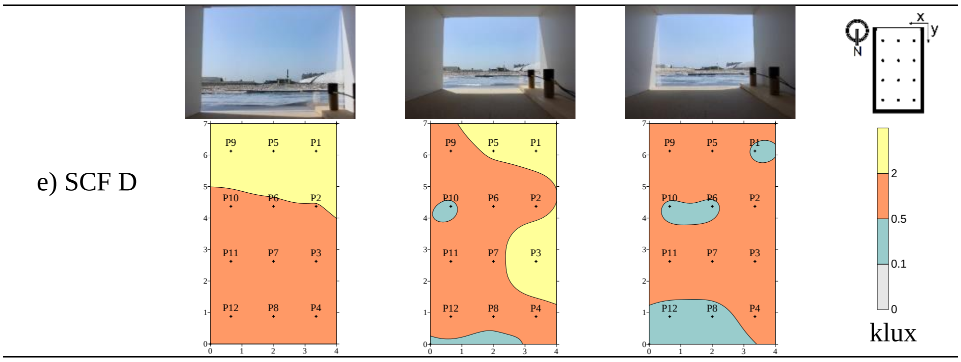

Figure 105. Digital photos and illuminance levels on a horizontal plane at 0.8 m height at 09h00, 12h00 and 15h00 in the winter solstice under clear sky conditions for: a) clear glass; b) SCF A; c) SCF B; d) SCF C and; e) SCF D

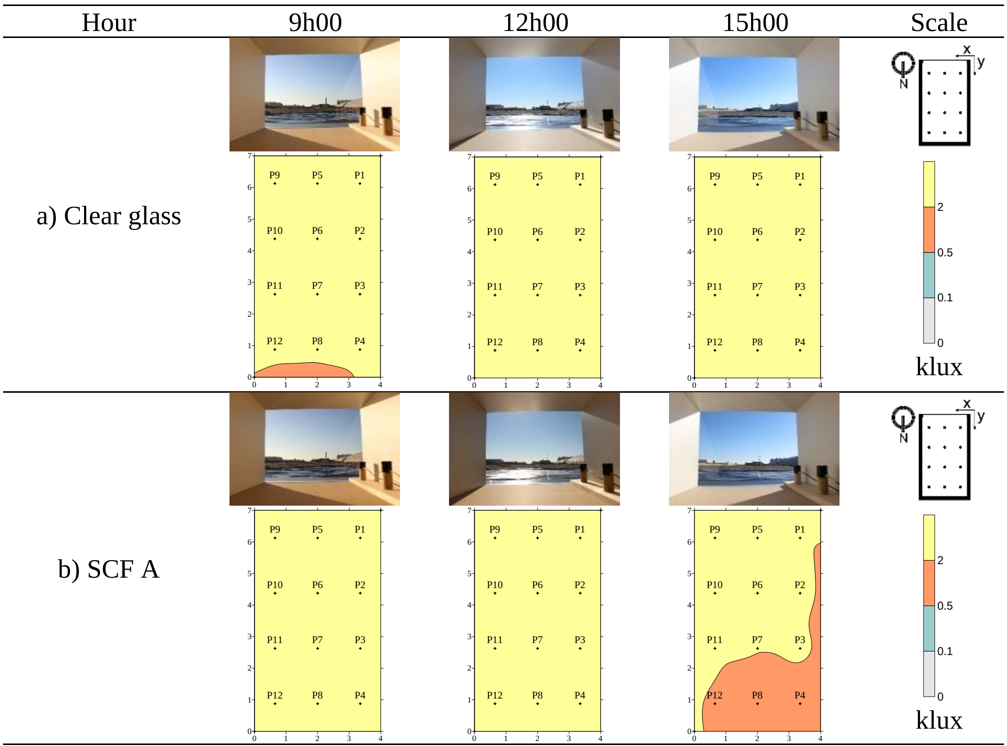

Figure 106. (cont.) Digital photos and illuminance levels on a horizontal plane at 0.8 m height at 09h00, 12h00 and 15h00 in the winter solstice under clear sky conditions for: a) clear glass; b) SCF A; c) SCF B; d) SCF C and; e) SCF D

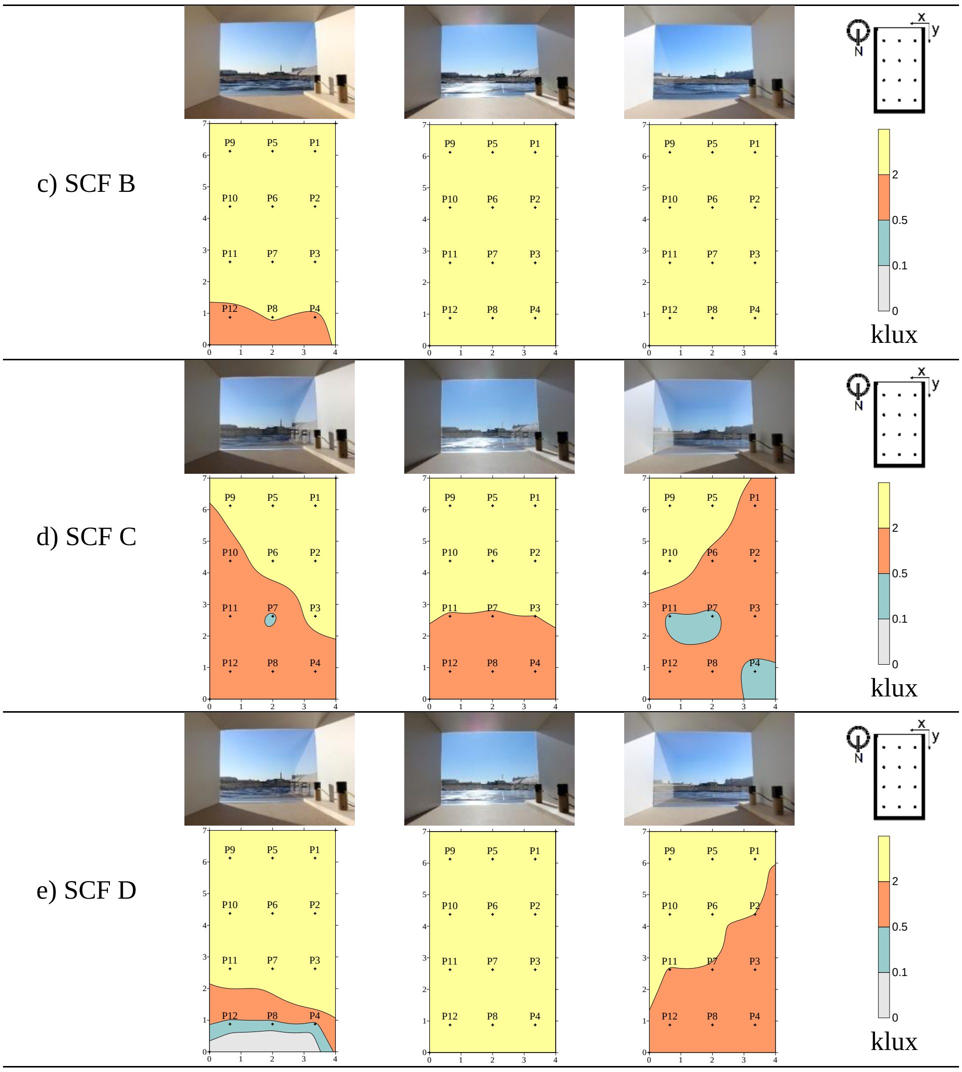

Figure 107. Digital photos and illuminance levels on a horizontal plane at 0.8 m height under overcast sky conditions for: a) clear glass; b) SCF A; c) SCF B; d) SCF C and; e) SCF D

Annex D – Model calibration

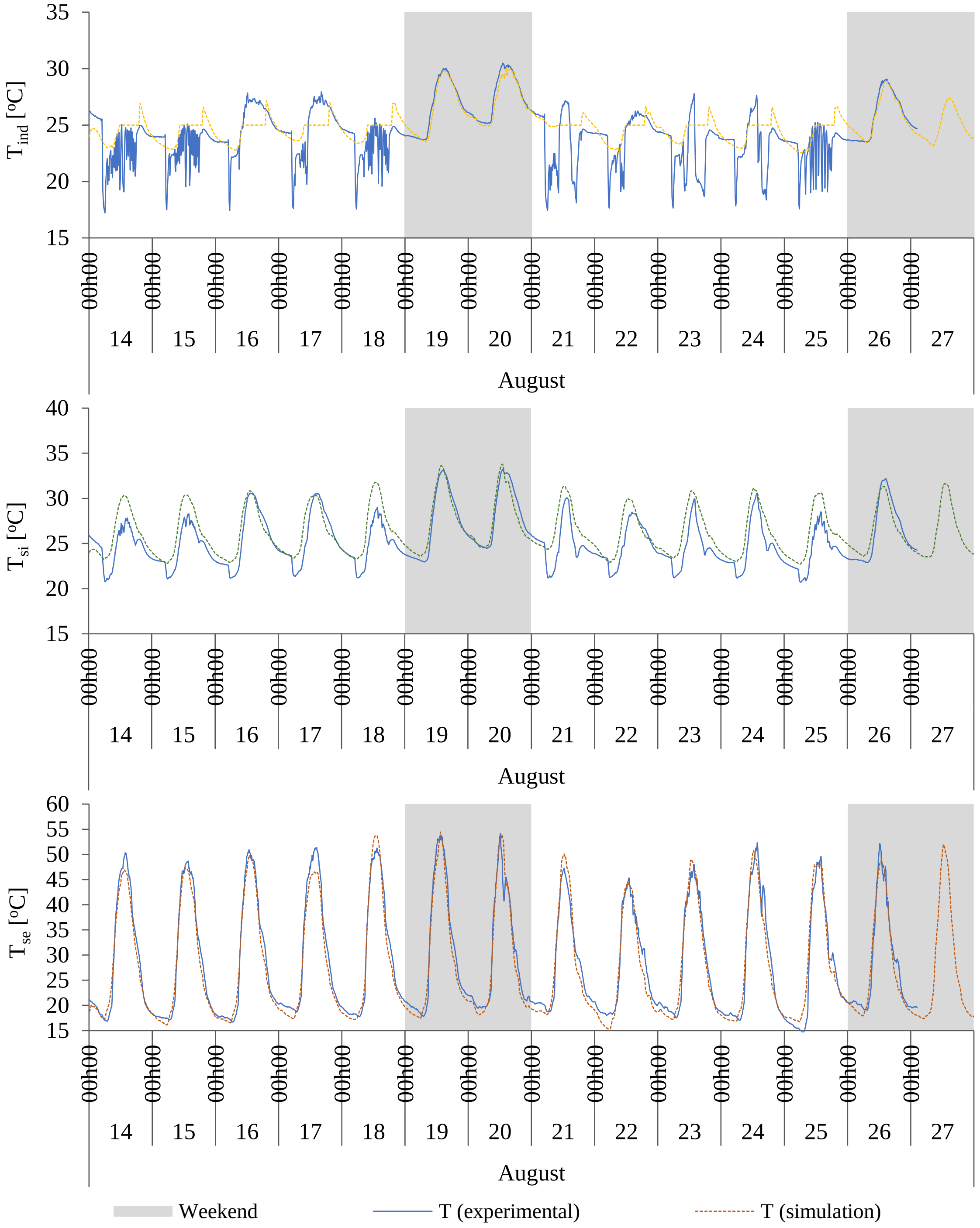

Figure 108. Experimental (plain lines) and simulated (dashed lines) values of indoor temperature. T_{ind}. and internal. T_{si}. and external. T_{se}. surface temperatures of office I in the summer period

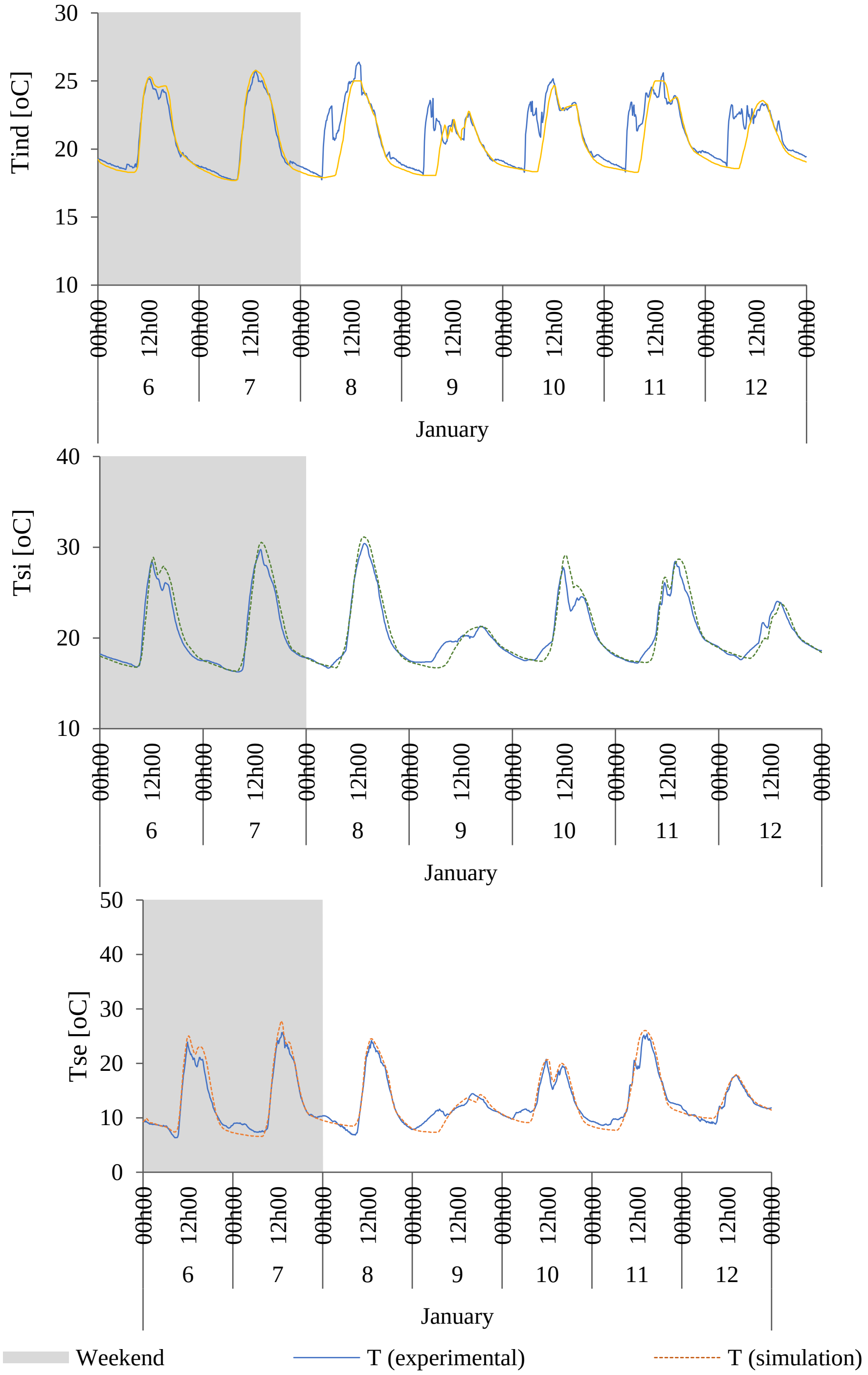

Figure 109. Experimental (plain lines) and simulated (dashed lines) values of indoor temperature. T_{ind}. and internal. T_{si}. and external. T_{se}. surface temperatures of office I in the winter period

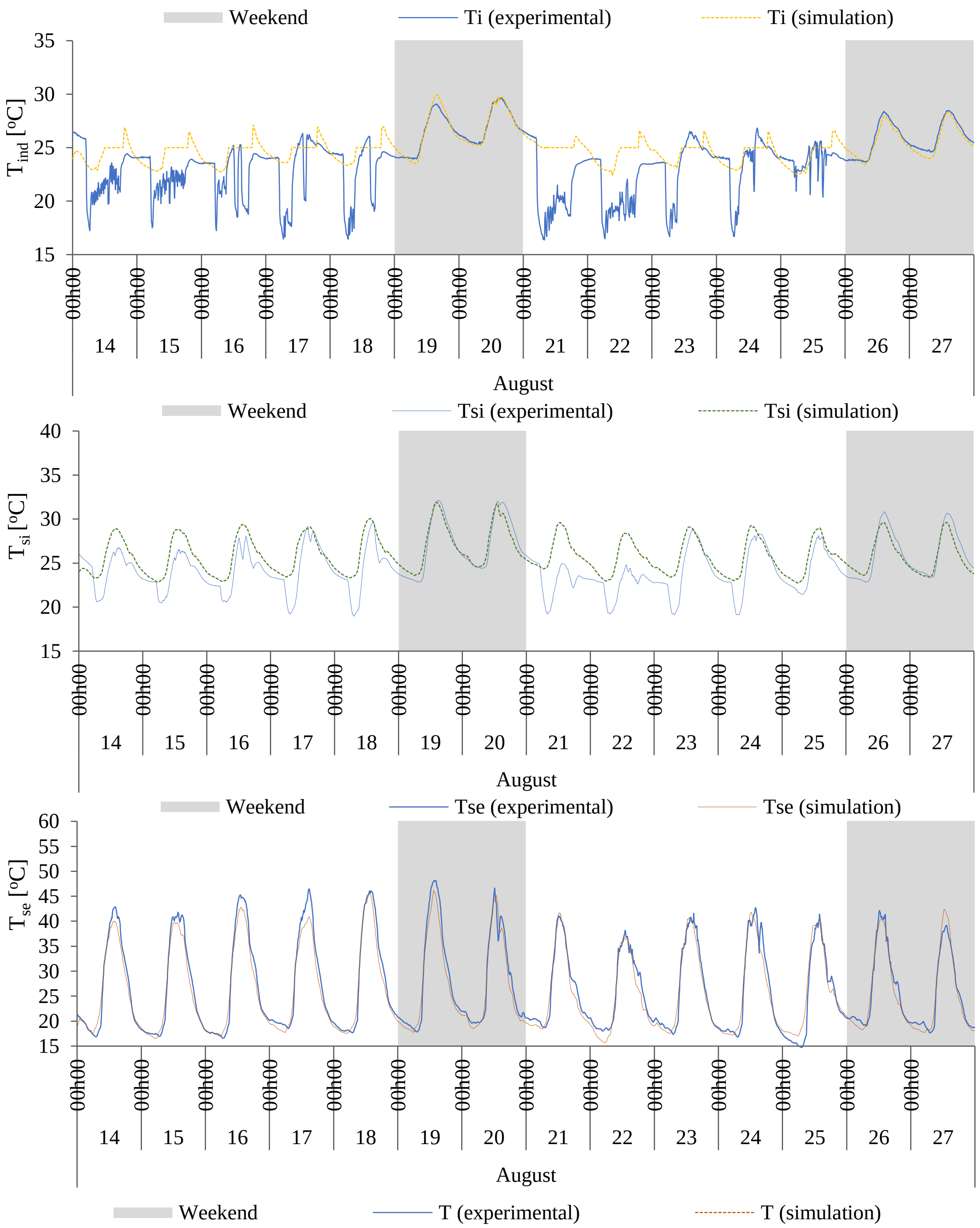

Figure 110. Experimental (plain lines) and simulated (dashed lines) values of indoor temperature. T_{ind}. and internal. T_{si}. and external. T_{se}. surface temperatures of office II in the summer period

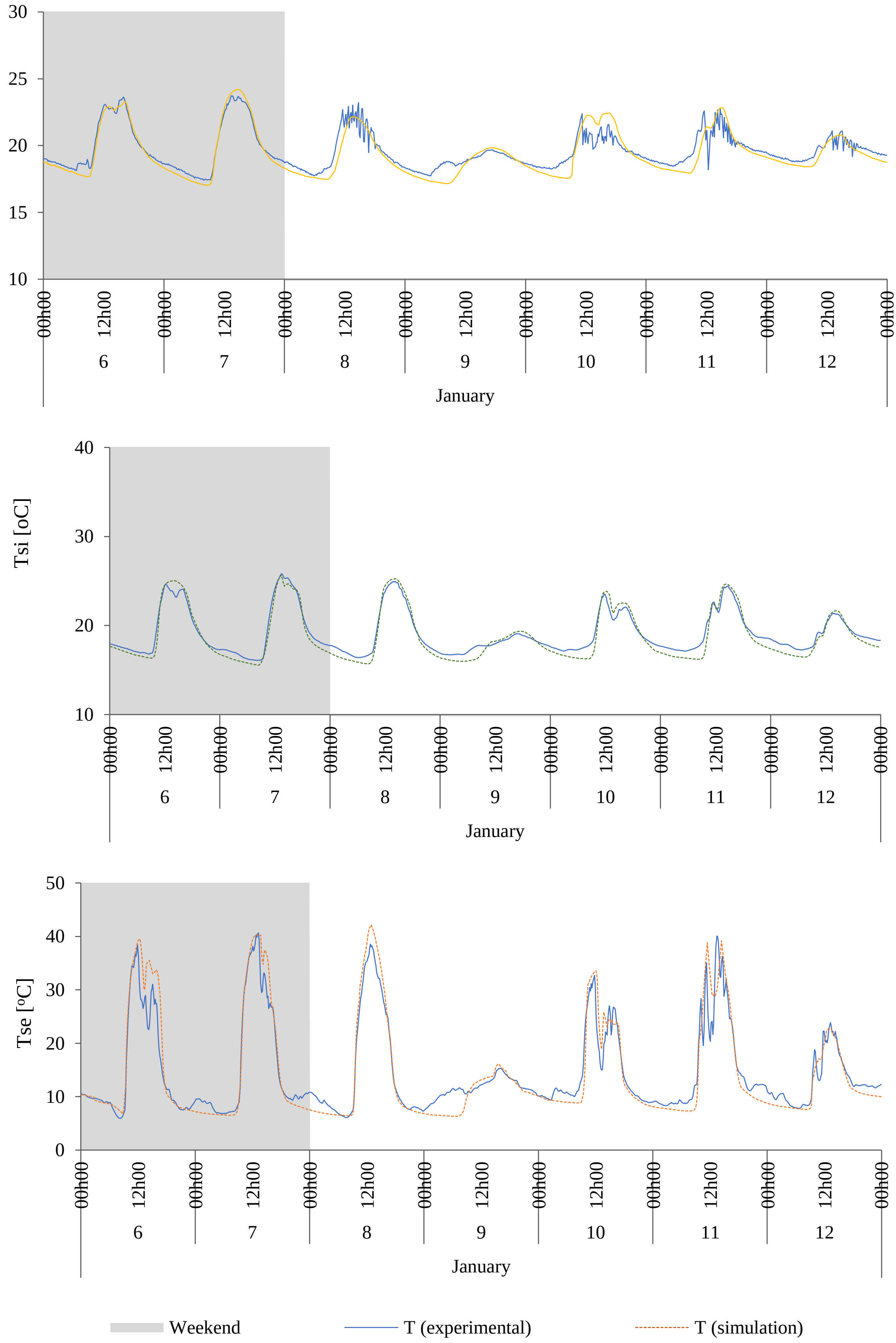

Figure 111. Experimental (plain lines) and simulated (dashed lines) values of indoor temperature. T_{ind}. and internal. T_{si}. and external. T_{se}. surface temperatures of office II in the winter period